University of São Paulo
Physics Institute

Conformal Dissipative Relativistic Hydrodynamics

Hugo Cangussu Marrochio

Dissertation presented to the Physics Institute of University of São Paulo as a requirement to the title of Master in Science

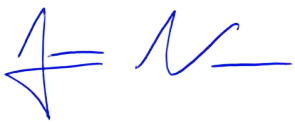

Adviser: Prof. Dr. Jorge Noronha

São Paulo
2015

Universidade de São Paulo
Insituto de Física

Hidrodinâmica Relativística Dissipativa Conforme

Hugo Cangussu Marrochio

Dissertação apresentada ao Instituto de Física da Universidade de São Paulo como requisito para o título de Mestre em Ciências

Orientador: Prof. Dr. Jorge Noronha

São Paulo
2015

Resumo

Marrochio, H. **Hidrodinâmica Relativística Dissipativa Confome** 2014. Dissertação (Mestrado) - Instituto de Física, Universidade de São Paulo, São Paulo, 2014.

Nesta tese investigamos construções de hidrodinâmica relativística dissipativa e suas regiões de validade através de vínculos associados a simetrias, perturbação linear e apresentamos algumas de suas descrições holográficas duais.

Primeiramente, estudamos vínculos de simetria em hidrodinâmica relativística conforme para construir soluções analíticas e semi-analíticas que evoluem no tempo e espaço de fluidos dissipativos. Encontramos uma descrição simples mas não-trivial semi-analítica de um fluído dissipativo causal (Israel-Stewart). Nós também investigamos o papel da produção de entropia como um teste do comportamento físico destas soluções.

Nós investigamos a influência do coeficiente de transporte de 2ª ordem na propagação de ondas não-lineares sob um método perturbativo não linear em $(1+1)$, e encontramos uma generalização de segunda ordem da conhecida equação de Burger's.

Em seguida, exploramos abordagens distintas de hidrodinâmica dissipativa sob perturbação linear. Nós apresentamos nossa construção de forma covariante, que expõe a estrutura da correções de ordem superior, assim como a dependência da velocidade de fundo. Encontramos que teorias construídas com expansão em gradientes das variáveis de um fluido perfeito sempre possuem números diferentes de modos entre um fundo estático e um em movimento, o que associamos com a presença de causalidade e instabilidades. Nós também mostramos que Israel-Stewart é bem comportada sob perturbações lineares.

Por fim, revisamos a literatura básica sobre a correspondência Fluido-Gravidade, que é a versão holográfica do método de Chapman-Enskog, construída por uma expansão em gradientes. Nós revisamos como construir a métrica dual a Navier-Stokes, que resolve a equação de Einstein até primeira ordem nas derivadas das variáveis na fronteira. Finalmente, exploramos construções que podem levar a uma truncarem consistente de hidrodinâmica além da expansão em gradientes, e esboçamos investigações futuras.

Palavras-chave: Hidrodinâmica relativística conforme, estabilidade linear, dualidade *fluid-gravity*.

Abstract

Marrochio, H. **Conformal Dissipative Relativistic Hydrodynamics**. 2014. Dissertation (Master's) - Instituto de Física, Universidade de São Paulo, São Paulo, 2014.

In this thesis we investigate dissipative relativistic hydrodynamics constructions and their regime of validity, through symmetry constraints, linear perturbation and overview some of their holographic duals.

First, we study symmetry constraints on conformal relativistic hydrodynamics to construct spatial and time evolving non-trivial analytic and semi-analytic solutions of different dissipative theories of hydrodynamics. We find a simple yet non-trivial semi-analytic description of causal (Israel-Stewart theory) dissipative fluids. In addition, we investigate the role of entropy production as a consistency check on the physical behavior of solutions.

We also investigate the influence of the second order transport coefficient on nonlinear wave propagation. We use the perturbative nonlinear method RPM in a simple $(1 + 1)$ construction to find a second order extension of the well known Burger's equation.

Next, we explore different approaches of dissipative hydrodynamics under linear perturbation. We present our construction in a covariant notation, which exposes the general structure of higher order corrections on dispersion relations, as well as the dependence on the background velocity. We find that theories constructed with gradient expansion of the perfect fluid dynamical variables always have different number of modes between a static background and a moving one, which we associate with acausal behavior and the presence of instabilities. Also, we show that the Israel-Stewart formalism is well-behaved under linear perturbations.

We then overview some aspects of the Fluid-Gravity correspondence, which is the holographic realization of Chapman-Enskog's theory, constructed via gradient expansion. We review how to reconstruct the metric dual to Navier-Stokes equations, which solves Einstein equation up to first order in the derivatives of the fluid variables. Finally, we explore constructions that might lead to a consistent non-equilibrium truncation of hydrodynamics beyond the gradient expansion formalism, and outline future investigations.
Keywords: Conformal relativistic hydrodynamics, linear stability, *fluid-gravity* duality.

Contents

List of Figures

List of Publications

This thesis is based on the following papers,

1. H. Marrochio, D. A. Fogaça, J. Noronha, G. S. Denicol, *Breakdown of Gradient Expansion in Relativistic Hydrodynamics?*, In preparation, to appear soon on arXiv.

2. S. I. Finazzo, R. Rougemont, H. Marrochio and J. Noronha, *Hydrodynamic transport coefficients for the non-conformal quark-gluon plasma from holography*, Accepted for publication in JHEP. [arXiv:1412.2968 [hep-ph]]

3. D. A. Fogaça, H. Marrochio, F. S. Navarra, J. Noronha, *Nonlinear waves in second order conformal hydrodynamics*, Nuclear Phys. A **934**, no. 0, 18-40. (2015). [arXiv:1402.5508 [nucl-th]].

4. H. Marrochio, J. Noronha, G. S. Denicol, M. Luzum, S. Jeon and C. Gale, *Solutions of Conformal Israel-Stewart Relativistic Viscous Fluid Dynamics*, Phys. Rev. C **91**, 014903 (2015). [arXiv:1307.6130 [nucl-th]].

Chapter 1

Overview

1.1 Theoretical overview of heavy-ion collisions

In the first chapter of this thesis we overview the main developments and ideas that will be further explored in the subsequent chapters.

Hydrodynamics has been a subject of interest for centuries [2]. Recently, it has been employed as a description of collective behavior of the hottest state of matter produced in laboratories, the Quark Gluon Plasma (QGP) [3, 4]. The Quark Gluon Plasma produced at RHIC [5, 6] and LHC [7, 8] should be a highly energetic near perfect fluid, which features very small dissipative effects, and naturally since the velocities are close to the speed of light, the hydrodynamical formalism should be relativistic [9]. Also, from microscopical arguments, such as the mean free path l_{mfp} in the quasiparticle picture, the strongly coupled nature of Quantum Chromodynamics (QCD) interaction leads to small but nonzero dissipative effects [10]. Therefore, it seems appropriate that the correct framework to study the low energy, long wavelength evolution of the QGP is relativistic dissipative hydrodynamics. We represent a heavy ion collision in Fig. 1.1.

The argument that heavy ion collisions should produce an almost perfect relativistic fluid is far from obvious and there are often many conceptual obstacles to surpass. For one, it has been understood that the correct framework to study strong interactions is QCD [11–14]. QCD is a very non-trivial quantum field theory with a rich phenomenology. A major property arises from its negative beta function; as a consequence, QCD is asymptotic free in the regime of high energies, ultraviolet (UV), but strongly coupled in the low energy limit, infrared (IR) [15, 16]. Perturbative quantum field theory is generally well-understood, but there is not a unique framework to approach the full theory when it is in the strongly coupled regime. One interesting physical consequence of IR nonperturbative effects in QCD is confinement [17]. Quarks and gluons are not measured directly; in fact, at low energies the theory organizes itself in hadronic degrees of freedom, which

are widely investigated theoretically and experimentally [14, 18].

If the collision only involves two protons, the underlying dynamics can already be very complicated, as quarks and gluons interact in a very non-perturbative regime. Understanding these collisions is already a complicated task. However, in heavy-ion collisions, one is usually colliding gold and lead nuclei, which contain around 200 nucleons! Therefore, it is very nontrivial to understand initial conditions in heavy-ion collisions, i.e., the initial $< T_{\mu\nu} >$ that comes from initial condition and eventually becomes dissipative hydrodynamics. The geometric properties of scattering of nuclei can be studied using the Glauber model [19], and the input energy density is usually parameterized by a Woods-Saxon distribution with some experimental input for the parameters. There is also a different model for the initial energy density, related to the idea of color-glass-condensate (CGC) [20], and the collision of CGC sheets resulting in glasma [21], an amorphous precursor of the QGP phase.

One very powerful tool to analyze the properties of a strongly coupled gauge theory is the lattice formalism. The community of lattice QCD has already achieved great results, such as the calculation of the proton mass from first principles [22]. Also, lattice QCD is a very successful framework for computing the thermodynamical equilibrium properties of the gauge theory but it still lacks a more efficient method for calculating dynamical non-equilibrium quantities. For instance, lattice QCD results for the QCD equation of state are very reliable [23, 24], as the error bars involved in the lattice formalism are generally small for such studies. However, reliable calculations of shear viscosity and relaxation times are still absent because these quantities involve the calculation of real-time correlation functions, which are not computed directly on the lattice [25].

It is natural then to look for an effective theory that describes the collective behavior for quarks and gluons. Instead of solving the complicated gauge theory, one may solve the relativistic Boltzmann equation [26, 27]. Naturally, this formalism has its own complications and subtleties, but the advantage is that the convoluted QCD dynamics can be represented by simple models in the interaction between the quasi-particles. Such approach has been very success describing the evolution of a hadronic gas, with realistically good estimation of the transport coefficients [28–30]. It is also possible to use coarse graining techniques in relativistic Boltzmann Equation to obtain an IR effective theory, which ends up being relativistic dissipative hydrodynamics. There are different coarse graining methods, and later in this thesis we will discuss the consequences of such to the effective hydrodynamical theory.

Despite its success in the description of the hadronic gas, the relativistic Boltzmann equation is not the appropriate tool to study the QGP at all temperatures. Firstly, the reliable techniques involve the existence of quasiparticles, which is a perturbative concept.

Since the QGP may be strongly coupled, there is no guarantee that the transport coefficients calculated in this formalism are useful. Also, experiments suggest a small shear viscosity to entropy ratio [31], which is generally not achieved by simple models within kinetic theory.

1.2 Brief discussion about holography and hydrodynamics

A possibility to describe from first principles nearly perfect fluids came from string theory. The gauge/gravity duality, known in its most famous realization as AdS/CFT (Anti-de Sitter/Conformal Field Theory) [32], is a conjecture relating two apparent different theories: Type-IIB string theory in $AdS_5 \times S^5$ background and a conformal field theory $\mathcal{N} = 4$ Supersymmetric Yang-Mills (SYM) theory in 4 dimensions. In most applications, the ten dimensional spacetime reduces to a fixed background of AdS_5 (the compact sphere S^5 acts as a phase space configuration). The duality is usually employed in the large N_c regime, where the number of colors of the Yang-Mills gauge theory $SU(N_c)$ is very large. Holography becomes a useful tool because of the inverse coupling relations. The t'Hooft coupling of the large-N field theory is $\lambda = g_{YM}^2 N_c$. A careful analysis (see for instance [33–35]) of the string theory properties of the duality indicates that quantum gravity effects should be taken under consideration as the ratios of the string length l_s, l_P planck length and the AdS radius L are small. These ratios are

$$\left(\frac{l_s}{L}\right)^2 = \frac{1}{\sqrt{\lambda}}\,, \qquad\qquad \left(\frac{l_P}{L}\right)^8 = \frac{\pi^4}{2N_c^2}\,. \tag{1.1}$$

Therefore, the theory in AdS_5 is classical and absent of quantum and stringy fluctuations in the limit $N_c \gg 1$ and $\lambda \gg 1$. Therefore, solving the classical gravitational theory in AdS_5 bulk should correspond to the infinitely strongly coupled quantum field theory at the boundary. The low energy background should then be Einstein's equation in the presence of a negative cosmological constant for AdS_5

$$R_{MN} - \frac{R}{2} g_{MN} + \Lambda g_{MN} = 0\,, \qquad\qquad \Lambda \equiv -\frac{10}{L^2}\,, \tag{1.2}$$

where the cosmological constant Λ can be related to the AdS radius for AdS_5 via the above formula.

If the boundary field theory is thermal, then the bulk description becomes of a black

hole in asymptotically Anti-de Sitter spacetimes. Since the full picture involves degrees of freedom of string theories, these objects are often called black branes, which are black hole solutions in extended spatial dimensions. It is known that black objects not only radiate semi-classically Hawking radiation, but also that their entropy scales as the area of the black object. This is a realization of the holographic principle [36]: In a gravitational theory, the degrees of freedom scale with the area, while in a quantum field theory, these degrees of freedom scale with the volume. In this light, the correspondence between theories existing in different dimensions gets a stronger evidence. In more practical terms, one can write the black brane metric in AdS_{d+1} in Fefferman-Graham coordinates, which makes manifest the conformal factor at each position in the fifth dimension z [33–35]

$$ds^2 = \frac{L^2}{z^2}\left(-f(z)dt^2 + d\vec{x}^{\,2} + \frac{dz^2}{f(z)} \right). \tag{1.3}$$

It follows from holography then that the thermal properties of the boundary field theory is encoded in the dynamics of the bulk. One great advantage holography has compared to other methods at this moment is that it can access real time dynamics of the strongly coupled gauge theory. For this reason, holography is widely explored in understanding transport coefficients and non-equilibrium dynamics [31, 37]. One early result of great importance has been the calculation of the shear viscosity over entropy ratio for $\mathcal{N} = 4$ SYM [10], which turns out to be the general ratio for isotropic two derivative theories of gravity. The resulting ratio is

$$\frac{\eta}{s} = \frac{1}{4\pi}\,, \tag{1.4}$$

which is in better agreement with the experimental data than calculations from kinetic theory, for instance [28–30]. Of course, $\mathcal{N} = 4$ SYM in the large N_c limit is very different from QCD, which contains only three colors, no supersymmetry, confinement and a running beta function just to mention a few. Interestingly enough, QCD at finite temperature and above its critical temperature associated to the confining scale seems to share some properties with $\mathcal{N} = 4$ SYM at finite temperature, such as broken supersymmetry and scale symmetry. There are bottom-up holographic models that mimic the thermodynamical properties of QCD calculated by lattice methods, and therefore these more "realistic" models can be used to derive transport coefficients from holography [38].

However, the question remains on how a consistent dissipative theory of hydrodynamics arises from holography. One example of such is encoded in the so called fluid-gravity correspondence [39]. This duality relates perturbative black brane metrics in asymptotically spacetimes in d dimensions to nonlinear fluid dynamics at the $(d-1)$ dimensional boundary. One simple interpretation is that the fluid-gravity correspondence is the ex-

treme IR and classical limit in the thermal AdS/CFT, where the excitations should be the ones in hydrodynamics. Despite its rich structure and successes, one immediate problem is that the fluid-gravity correspondence is the holographic realization of the well known Chapman-Enskog construction used in Kinetic theory (see for instance [40]), which consists of order-by-order truncations in the gradients of the fluid dynamical variables. We will often refer to this construction, whether in holography or in kinetic theory, as the gradient expansion. The Chapman-Enskog construction is plagued with linear instabilities and acausality issues [41–43], and throughout this thesis we will review the literature on such topic, as well as expose our new results regarding the mathematical inconsistencies of such formalism. The effective low energy theory that fixes these problems and is obtained from gravity in AdS spacetimes is still an open problem. In this thesis we briefly discuss these issues and point out that numerical relativity might be the correct framework to study these problems [44, 45].

1.3 Symmetries, Hydrodynamics, Instabilities

Much effort in developing theoretical physics for the past decades has been related to the role of symmetries in our universe. One remarkable example is the application of group theory in the Standard Model of Particle Physics [46], as well as constructing simpler effective field theories in a regime where certain symmetries are approximately valid [47].

Conformal symmetry is a very special type of symmetry, which preserves angles under relativistic transformations, i.e., an extension of the Poincaré group to include scale transformations and special conformal transformation, which is related to inversion and translation ([48] and Appendix A). It is not expected that realistically many theories will obey such a symmetry, as the existence of scale seems to be very fundamental in most of the low energy physics of classical and quantum phenomena. Despite these shortcomings, conformal theories are useful as toy models for their relative simplicity, and some phase transition phenomena should involve approximate conformal invariance near a critical temperature [48].

This is the leading argument in most examples where conformal theories are employed in this thesis: it is not supposed to be a detailed description of the physical system, but instead a first approximation to understand some universal physical properties. In this spirit, in Chapter 2 we present the first analytic and semi-analytic solutions of causal dissipative relativistic hydrodynamics, within the Israel-Stewart(IS) formulation [49, 50] , where the flow is boost invariant, but time evolving, and radially expanding in the transverse plane perpendicular to the colliding direction (Gubser Flow [51, 52]). We also

analyse how different dissipative approaches lead to ill-defined solutions. This chapter is an expansion upon on our paper [53].

Next, we investigate the influence of the relaxation time parameter found in most dissipative second order theories, such as Israel-Stewart theory, in solitonic behavior and nonlinear phenomena. Chapter 3 covers the use of the Reductive Perturbative Method (RPM) [54–56] to find an extension of the Burger's Equation to include second order corrections. We found that the relaxation time contributes to the solitonic stable propagation, and found that the nonlinear perturbative method fails to address the correct dynamics of very irregular initial conditions. This chapter is heavily based on our paper [57].

In Chapter 4 we investigate the structure of dissipative relativistic hydrodynamics under linear perturbations. We present a more general covariant structure of dispersion relation than found in the recent literature [58, 59]. Also, we expand the original investigation of linear instability and acausality in relativistic Navier-Stokes theory [41–43] to higher order gradient theories, and we conclude that the gradient expansion approach not only fails to address these issues but may actually add new inconsistencies. This chapter is based on a small part of our paper [38], and the majority of it is based on a paper in preparation [60].

Finally, in Chapter 5 we review the Fluid-Gravity formalism [39, 61, 62], which is the holographic construction of the gradient expansion that leads to dissipative fluid dynamics. We briefly review some basic knowledge about black hole geometries and the holographic construction of thermal theories. The goal of this chapter is to review the relevant literature and investigate how a more general effective dissipative theory at strong coupling might emerge from gravity, in analogy to the derivation of Israel-Stewart hydrodynamics from Boltzmann equation in kinetic theory [30]. In contrast to the other chapters in this thesis, there are no new results presented in this chapter. We finish in Chapter 6 with conclusion, and an outlook to future work directions.

There are several appendices in this thesis. In Appendix A we review the relevant properties of the conformal group. Next, we review the behavior of hydrodynamics under Weyl transformations in Appendix B, and we check that the hydrodynamical theories studied in this thesis transform appropriately under such transformation. In Appendix C, we review the geometric properties of the de Sitter space in order to gain intuition of the Gubser flow discussed in Chapter 2. We provide a detailed calculation of the RPM method employed in Chapter 3 in Appendix D, and finally in Appendix E we analyze linear stability properties of a second order gradient expansion theory with bulk and shear viscosity.

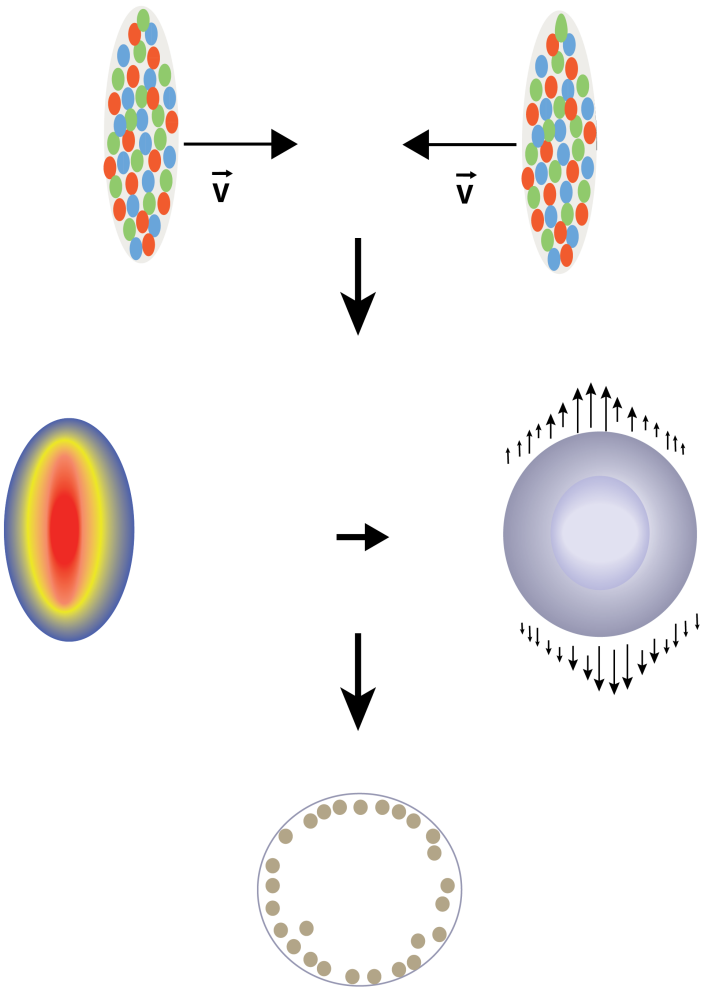

Figure 1.1: *Representation of a heavy ion collision. First, two relativistic nuclei approach each other. Then, the system approximately thermalizes and a very hot fluid expands. Spatial anisotropy is translated to momentum space anisotropy through hydrodynamic evolution. Later, the fluid cools and the degrees of freedom become hadronic.*

Chapter 2

Gubser flow for causal dissipative relativistic hydrodynamics

The first chapter of this thesis deals with what is called Gubser flow of hydrodynamics [51, 52]. We discuss and show how one can use symmetry arguments to find analytical and semi-analytical solutions of dissipative relativistic hydrodynamics. We explore both Bjorken [63] and Gubser symmetries. We also study entropy production and the role of initial conditions for the Gubser flow, and we show that a second-order theory constructed using the gradient expansion displays problems for both solutions constructed upon these symmetry constraints. Our investigation is the first to find a non-trivial semi-analytical solution to a causal dissipative hydrodynamics theory, which can then be used to test the consistency of the various computer schemes used in simulations of QGP dynamics. We show an example of such comparison to the numerical simulation of MUSIC [64–66].

This chapter is based on our paper [53], but expanded to include the analysis of Bjorken solutions and entropy production. We adopt the metric signature $g_{\mu\nu} = \text{diag}(-1, 1, 1, 1)$ and natural units for this chapter.

2.1 An introduction to Relativistic Hydrodynamics

We follow the spirit of the review [67], but notice that our metric signature in this chapter is different than theirs. Fluid dynamics is an effective nonlinear theory for the low energy excitations that describe collective behavior near local equilibrium. We usually define the thermodynamic properties to be the energy density and the pressure of the medium. In non-relativistic hydrodynamics, one is usually concerned to solve for the mass density and pressure, which is natural since mass is generally conserved in the the non-relativistic regime [9]. The situation is already different in simple relativistic interactions, since the kinetic energy is comparable to the rest mass energy contribution. Therefore,

one needs to work with energy density instead of mass density in a consistent theory of relativistic fluid flow.

Another vital ingredient for the description of fluids is the velocity of a local fluid cell. In a relativistic theory, the usual concept of spatial euclidian vector needs to be extended to the 4-vector structure, including a time-like component. These are the fundamental ingredients for a relativistic hydrodynamical theory without conserved charges: two numbers related to energy density (ε) and pressure (p), at least in some reference frame, a four-velocity and the metric tensor itself. Therefore, one can argue that the most general tensor structure for the stress-energy tensor should be built-up from these quantities, at least in equilibrium and assuming isotropy. We can summarize this argument noticing that

$$T^{\mu\nu} = x\, g^{\mu\nu} + y\, u^{\mu} u^{\nu} \,, \tag{2.1}$$

where $T^{\mu\nu}$ is the stress-energy tensor, $g^{\mu\nu}$ is the metric, $u^{\mu} \equiv dx^{\mu}/dt^{'}$, and $dt^{'} = \gamma^{-1} dt$ is the four-velocity with property $u^{\mu} u_{\mu} = -1$ (in our signature), as the Lorentz factor is $\gamma = (1 - \vec{v}^{\,2})^{-1/2}$. The variables x and y are just numbers that should be related to the energy density and pressure somehow, which are the two relevant thermodynamical variables of the problem. Suppose that the metric is the Minkowski flat $3+1$ spacetime, with mostly plus signature, $g_{\mu\nu} = \mathrm{diag}(-1, 1, 1, 1)$. In the rest frame, the four-velocity has a very simple form $u^{\mu} = (1, 0, 0, 0)$. Therefore, the isotropic stress-energy tensor in Minkowski spacetime and in the local rest frame has the following structure

$$T_0^{\mu\nu} = \begin{pmatrix} (y-x) & 0 & 0 & 0 \\ 0 & x & 0 & 0 \\ 0 & 0 & x & 0 \\ 0 & 0 & 0 & x \end{pmatrix} . \tag{2.2}$$

The time-like component $(y - x)$ should be the energy density, and the x components should be identified as pressure. Therefore, the most general tensor for ideal fluid dynamics, which satisfies the right quantities in the rest frame, is

$$T^{\mu\nu}_{\mathrm{ideal}} = p g^{\mu\nu} + (\varepsilon + p) u^{\mu} u^{\nu} \,. \tag{2.3}$$

There is a more convenient way to write the tensor components in hydrodynamics, since there is a natural four-vector in the theory, the four-velocity. We define the operator

$$\Delta^{\mu\nu} = g^{\mu\nu} + u^{\mu} u^{\nu} \,, \tag{2.4}$$

where the plus sign is consistent with our metric signature. This projector is by con-

struction orthogonal to the four-velocity flow, and it is useful to separate the degrees of freedom in the conservation equations, for example. With the orthogonal operator, the stress-tensor can then be written as

$$T^{\mu\nu}_{\rm ideal} = (\varepsilon + p)\Delta^{\mu\nu} - \varepsilon g^{\mu\nu} = \varepsilon u^{\mu}u^{\nu} + p\Delta^{\mu\nu}\,. \tag{2.5}$$

We denote the covariant derivative ∇_μ with the proper definition of connection in that specific spacetime, which satisfies the property $\nabla_\alpha g_{\mu\nu} = 0$. For ideal fluid-dynamics, one just needs to impose conservation of momentum and energy, i.e., $\nabla_\mu T^{\mu\nu}_{\rm ideal} = 0$. These constraints can then be written as the following projections of the divergence of the stress-energy tensor,

$$\begin{aligned} u_\nu \nabla_\mu T^{\mu\nu}_{ideal} &= D\,\varepsilon + (\varepsilon + p)\,\theta = 0\,, \\ \Delta^\alpha_\nu \nabla_\mu T^{\mu\nu}_{ideal} &= (\varepsilon + p) Du^\alpha - \nabla^\alpha_\perp p = 0\,, \end{aligned} \tag{2.6}$$

where we defined the comoving derivative $D \equiv u^\mu \nabla_\mu$, θ is the four-divergence of the four-velocity $\theta \equiv \nabla_\mu u^\mu$ and $\nabla^\alpha_\perp \equiv \Delta^{\alpha\mu}\nabla_\mu$ is the transverse derivative. Notice that the non-relativistic limits of Eqs. (2.6) are the Euler equations [9]. There seems to be effectively five independent equations, because the range of the index alpha is $0 - 3$. However, the equation is orthogonal to the four-velocity, which is a constraint and then effectively there are only 4 independent equations, as it should be. If one knows the equation of state, i.e. how the energy density and pressure are related for a specific medium, then these equations are complete and therefore can be solved using some powerful integration method.

Eqs. (2.6), as there are energy losses due to the second law of thermodynamics, which are associated to dissipation. The usual method to write dissipation is by adding exactly what is lost in terms of energy and momentum in the stress-energy tensor. Therefore, the four-divergence of this general energy-momentum tensor, $T^{\mu\nu}$ will still be zero, $\nabla_\mu T^{\mu\nu}$. The recipe is then to add [9]

$$T^{\mu\nu} = T^{\mu\nu}_{ideal} + \Pi^{\mu\nu} = (\varepsilon + p)\Delta^{\mu\nu} - \varepsilon g^{\mu\nu} + \Pi^{\mu\nu}\,, \tag{2.7}$$

where $\Pi^{\mu\nu}$ is precisely the dissipative contribution. There is a "gauge" choice in defining the coordinates of this tensor, we adopt the so called Landau frame [9], where the energy density is at rest in the local rest frame. This condition implies that the dissipative tensor is orthogonal to the four-velocity, i.e., $u_\mu \Pi^{\mu\nu} = 0$. If one takes this general form under consideration, the equations of hydrodynamics take the form

$$u_\nu \nabla_\mu T^{\mu\nu} = D\,\varepsilon + (\varepsilon + p)\,\theta + \Pi^{\mu\nu}\nabla_{\perp(\mu}u_{\nu)} = 0\,,$$
$$\Delta^\alpha_\nu \nabla_\mu T^{\mu\nu} = (\varepsilon + p)Du^\alpha + \nabla^\alpha_\perp\, p + \Delta^\alpha_\nu \nabla_\mu \Pi^{\mu\nu} = 0\,, \tag{2.8}$$

with the symmetrization of the indicesis denoted by $A_{(\mu\nu)} = (A_{\mu\nu} + A_{\nu\mu})/2$. This is a general construction of the dissipative fluid dynamics laws. The intricate details of what exactly the dissipative theory is depend on the evolution equation for the symmetric tensor $\Pi^{\mu\nu}$, which has in general 10 independent coordinates in four dimensions.

We can separate out the degrees of freedom of the dissipative tensor by separating its trace in the irreducible representation, which results in

$$\Pi^{\mu\nu} = \pi^{\mu\nu} + \Pi\Delta^{\mu\nu}\,, \tag{2.9}$$

where $\Pi \equiv g_{\mu\nu}\Pi^{\mu\nu}/3$ is a fraction of the trace of the full $\Pi^{\mu\nu}$ and $\pi^{\mu\nu}$ is the traceless symmetric dissipative tensor. If the dissipative tensor were not defined in the Landau gauge, there would necessarily be a non-zero four vector part in Eq. (2.9) associated to particle density flow.

There is a simplest generalization involving the lowest order of derivatives of the thermodynamical variables that matches the Navier-Stokes equations in the non-relativistic limit - this is called the relativistic Navier-Stokes (NS) theory. When we mention NS, we refer to the relativistic theory, unless explicitly said the contrary. There is one simple argument to "derive" the NS theory. First, the equilibrium entropy current is given by

$$s^\mu = s\,u^\mu\,, \tag{2.10}$$

where from thermodynamics we have the equilibrium entropy density (at zero chemical potential) $s = (\varepsilon + p)/T$, and $Tds = d\varepsilon$. Notice that the four-divergence $\nabla_\mu u^\mu$ is a source equation, and from the second law we should expect $\nabla_\mu s^\mu \geq 0$. If we evaluate explicitly the derivative $\nabla_\mu s^\mu$ and make usage of the conservation equations Eqs (2.8), one finds

$$\nabla_\mu s^\mu = Ds + s\theta = -\frac{1}{T}\Pi^{\mu\nu}\nabla_{\perp(\mu}u_{\nu)}\,. \tag{2.11}$$

For such manipulations, is is useful to define a projector that is symmetric, traceless and orthogonal to four-velocity. We then define

$$\Delta^{\mu\nu\alpha\beta} \equiv \frac{1}{2}\left(\Delta^{\mu\alpha}\Delta^{\nu\beta} + \Delta^{\mu\beta}\Delta^{\nu\alpha}\right) - \frac{1}{3}\Delta^{\mu\nu}\Delta^{\alpha\beta}\,,$$
$$\sigma^{\mu\nu} \equiv \Delta^{\mu\nu\alpha\beta}\nabla_\alpha u_\beta\,, \tag{2.12}$$

where we call the tensor $\sigma^{\mu\nu}$ the shear tensor. We also define the operation $A^{<\mu\nu>}$ as $A^{<\mu\nu>} \equiv \Delta^{\mu\nu\alpha\beta}A_{\alpha\beta}$. Now, rewriting Eq. (2.11) with the dissipative tensor separated as Eq. (2.9), we have

$$\nabla_\mu s^\mu = -\frac{1}{T}\left(\pi^{\mu\nu}\,\sigma_{\mu\nu} + \Pi\,\theta\right) \geq 0\,. \tag{2.13}$$

Therefore, the usual definition relativistic definition that reduces to the correct Navier-Stokes equations in the non-relativistic regime is

$$\pi^{\mu\nu} = -2\eta\sigma^{\mu\nu}\,, \quad \Pi = -\zeta\theta\,, \tag{2.14}$$

with η being the shear and ζ the bulk viscosity coefficients. Notice that with these definitions for the dissipative tensor, the divergence of the equilibrium entropy is always positive if the temperature is also positive. Although this statement seems obvious, we will see that the Gubser flow in Navier-Stokes theory has a regime with negative temperature, and one of the consequences for such is the violation of the second law of thermodynamics. For most of the analysis in this thesis, we consider only shear contributions, unless explicitly stated the opposite. Conformal theories have zero bulk contribution.

To summarize, the simplest conformal dissipative theory that only includes the lowest order gradient corrections [1], without heat flow and chemical potential, and that contain the non-relativistic Navier-Stokes limit is [9, 67] :

$$D\,\varepsilon + (\varepsilon + p)\,\theta + \pi^{\mu\nu}\sigma_{\mu\nu} = 0\,,$$
$$(\varepsilon + p)Du^\alpha + \nabla_\perp^\alpha\, p + \Delta_\nu^\alpha\nabla_\mu\pi^{\mu\nu} = 0\,,$$
$$\pi^{\mu\nu}_{NS} = -2\eta\,\sigma^{\mu\nu}\,. \tag{2.15}$$

Despite its success in describing a large range of phenomenology in non-relativistic physics, the relativistic Navier-Stokes is not a full satisfactory theory. In this thesis alone, we show that the relativistic Navier-Stokes equations lead to exact solutions with negative

[1] Otherwise, Eq. (2.13) would not be guaranteed to hold for different values of velocity flow. Since in the Navier-Stokes theory it assumes a squared value, it is always a positive quantity.

temperature [52], besides being linearly unstable and displaying violation of causality (Chapter 4) [41–43].

The usual lore is that dissipative theories which contain higher order derivatives in the form of a Taylor expansion should fix these problems of NS; however, there is not a unique procedure to generalize it and include second order gradient terms. Ideally, these theories should be derived from first principles, but even that procedure might be flawed from its initial assumptions. We will study two classes of dissipative relativistic hydrodynamics; one constructed truncating in a derivative series of the ideal fluid variables, the Chapman-Enskog construction, which we also refer as the gradient expansion approach [40]. One example of such constructions, which we only write the terms relevant for the Gubser flow in flat spacetime, is the second order gradient expansion conformal theory [68],

$$\pi^{\mu\nu} = -2\eta\sigma^{\mu\nu} + 2\eta\tau_\pi \left(D\sigma^{<\mu\nu>} + \frac{\theta}{3}\sigma^{\mu\nu} \right) + 4\lambda_1 \, \sigma_\lambda^{<\mu}\sigma^{\nu>\lambda} \,, \tag{2.16}$$

where we define the tensor $DA^{<\mu\nu>} = \Delta^{\mu\nu\alpha\beta} DA^{\alpha\beta}$. We will show that this theory also contains instabilities and acausality under linear perturbation in Chapter 4 [38, 60], as well as an inconsistent descriptions in the Bjorken and Gubser flows.

Another approach is the phenomenologically inspired Israel-Stewart theory [49, 50], which is known to be derived from the Boltzmann equation using the moments method [30]. This theory involves a differential equation for the dissipative tensor instead of an algebraic one, such as the NS. The conformal theory we use to compare with Eq. (2.16) is [69]

$$\tau_\pi \left(D\pi^{<\mu\nu>} + \frac{4}{3}\theta\pi^{\mu\nu} \right) + \pi^{\mu\nu} = -2\eta\sigma^{\mu\nu} - 2\frac{\lambda_1}{\eta}\pi_\lambda^{<\mu}\sigma^{\nu>\lambda} \,, \tag{2.17}$$

Notice that, as argued in [68], if the asymptotic value of the dissipative tensor is approximately $\pi^{\mu\nu} \approx -2\eta\sigma^{\mu\nu}$, in this very specific regime these two theories are approximately equivalent. However, we will argue in which limits this is a reasonable approximation, and in which regimes the gradient expansion approach fails to be a consistent theory. For these second order theories, there is a correction to the equilibrium entropy. We will explore the influence of the initial conditions on Israel-Stewart for the entropy production [53], for instance.

There is an even more interesting way to write the hydrodynamic equations for a conformal theory. There is only one scale in a thermal conformal theory, which is the temperature. Therefore, every thermodynamical variable and transport coefficient contain a specific power of temperature dictated by simple dimensional analysis. For instance, the energy density scales as the fourth power, the entropy and the shear viscosity as the cubic power, while the relaxation time as the inverse of the temperature, and so on. Of

course the exact coefficient that relates energy density and temperature, for instance, is given by the specific microscopic model under consideration. For a conformal theory some simplifications occur. Suppose that the energy density is related to the temperature as

$$\varepsilon = \alpha T^4 \,, \tag{2.18}$$

in which α is a constant. For a conformal theory in flat space, the tracelessness condition implies that $3p - \varepsilon = 0$, and then the speed of sound is $c_s = 1/\sqrt{3}$. Therefore, we can also associate the entropy density with the constant α using the first law of thermodynamics,

$$s = \frac{(\varepsilon + p)}{T} = \frac{4}{3}\alpha T^3 \,. \tag{2.19}$$

The conservation equations (2.8) then become (for a conformal theory $\Pi = 0$)

$$\begin{aligned} DT + \frac{T}{3}\theta + \frac{\pi^{\mu\nu}\sigma_{\mu\nu}}{3s} &= 0 \,, \\ \nabla_\perp^\mu T + TDu^\mu + \frac{\Delta^\mu_\nu \nabla_\alpha \pi^{\alpha\nu}}{s} &= 0 \,, \end{aligned} \tag{2.20}$$

As usual the dissipative contributions are encoded in $\pi^{\mu\nu}$ and are specific to each theory of hydrodynamics and the definition of the dissipative shear tensor. In the next sections we will show analytical and semi-analytical methods to solve these nonlinear coupled PDEs.

2.2 Bjorken Flow and Hydrodynamics

Before discussing Bjorken symmetry, we first need to introduce the coordinate system in which this symmetry is mostly manifest. We are defining the so called Milne coordinate system, which is a hyperbolic coordinate relating one of the spatial directions to the time coordinate. Therefore, in terms of applications to heavy ion physics, one can think of the longitudinal spatial direction as the colliding direction of the beam axis, for instance the z direction. It is possible then to relate these two coordinates through hyperbolic mapping, such as the proper time $\tau = \sqrt{t^2 - z^2}$ and the rapidity $\xi = 1/2 \times \ln\left[(t+z)\,/\,(t-z)\right]$. For most central collisions, boost invariance[2] is a reasonable approximation, which motivates the use of such system. We choose to parametrize the transverse plane to be the usual polar coordinates, $r = \sqrt{x^2 + y^2}$ and $\phi = \tan^{-1}\left(\frac{y}{x}\right)$. The Milne coordinate is then $x^\mu =$

[2] In a Lorentz boost in the z direction, $(t^{'} + z^{'}) = \gamma(1-v)(t+z)$ and $(t^{'} - z^{'}) = \gamma(1+v)(t-z)$, and then the rapidity transforms as a translation $\xi = \xi^{'} + \frac{1}{2}\ln\frac{1-v}{1+v} = \xi^{'} + a$.

(τ, r, ϕ, ξ) and the line element is

$$ds^2 = -d\tau^2 + dr^2 + r^2 d\phi^2 + \tau^2 d\xi^2 \,, \tag{2.21}$$

which covers the future wedge of $\mathbb{R}^{3,1}$. The Bjorken symmetry is a scaling symmetry. In the Milne coordinates, the four-velocity is simply $u^\mu = (1, 0, 0, 0)$. However, notice that such four-velocity in cartesian coordinates has two non-zero components. The Bjorken scaling solution assumes that all thermodynamical variables depend only on proper time τ, since the full isometry group is the rotation group in the plane, the radial symmetry, as well as boost invariance. In terms of real applications, the Bjorken scaling solution is very simple, as it does not account for any evolution on the transverse directions and it relies on boost invariance. It is nonetheless instructive to learn about the properties of different dissipative theories: we will study the ideal case, Navier-Stokes theory and the two second order theories, gradient expansion and Israel-Stewart shown in Eqs. (2.16) and (2.17).

The conformal group is reviewed in Appendix A. It is a generalization of the Poincaré group ISO(3,1) to SO(4,2), with the inclusion of scale transformations and special conformal transformations (SCT). In Appendix B, we show that the equations of conformal hydrodynamics are invariant under a Weyl transformation.

The Bjorken symmetry contains boost invariance in one spatial direction, the symmetry group SO(1,1). It also contains a Z_2, as there is a symmetry under a parity transformation for the rapidity ξ. Also, there is no dependence on the transverse plane variables, which implies rotational symmetry as well as a translation radial symmetry. These are contained in the Poincaré group on two dimensions, ISO(2). The Bjorken symmetry is then the direct product of these 3 groups, $SO(1,1) \otimes ISO(2) \otimes Z_2$ [51]. These symmetries imply that the static flow in Milne coordinates is the only possible flow consistent with the symmetries. One explicit and more rigorous way to prove such is by using the Lie derivative along the four-velocity for each of these symmetries, i. e.,

$$\mathcal{L}_{\psi_i} u = 0 \,, \tag{2.22}$$

where ψ_i is the vector field associated with each of these symmetries above. The condition that such operator equals zero is the symmetry constraint for the symmetries of Poincaré group.

There are some useful quantities that can be calculated right away. The expansion rate θ is

$$\theta = \nabla_\mu u^\mu = \frac{1}{\sqrt{-g}} \partial_\mu (\sqrt{-g} u^\mu) = \frac{1}{\tau} \,. \tag{2.23}$$

Also, the non-zero Christoffel symbols are [3]

$$\Gamma^{\tau}_{\xi\xi} = \tau\,, \qquad \Gamma^{\xi}_{\tau\xi} = \Gamma^{\xi}_{\tau\xi} = \frac{1}{\tau}\,. \tag{2.24}$$

Therefore, the only non-zero derivative of the four-velocity is

$$\begin{aligned} \nabla_\mu u_\nu = -\Gamma^{\lambda}_{\mu\nu} u_\lambda = \Gamma^{\tau}_{\mu\nu}\,, \\ \nabla_\xi u_\xi = \tau \end{aligned} \tag{2.25}$$

The shear tensor can be constructed right away from its definition, $\sigma^{\mu\nu} = \Delta^{\mu\nu\alpha\beta}\nabla_\alpha u_\beta$ and the flow velocity. The non-zero components are then

$$\sigma^x_x = \sigma^y_y = -\frac{1}{3\tau}\,, \qquad \sigma^\xi_\xi = \frac{2}{3\tau}\,, \tag{2.26}$$

which results in a traceless tensor, and also orthogonal to u^μ, as it should be.

2.2.1 Bjorken, Ideal and Navier-Stokes

The Bjorken solution for ideal hydrodynamics has been known for quite some time in the literature [63]. The equations of motion are very simple for the ideal case. The dissipative tensor is zero in Eqs. (2.20), and the energy conservation simply becomes

$$\partial_\tau T + \frac{1}{3}\frac{T}{\tau} = 0\,, \tag{2.27}$$

with solution

$$T_{\text{ideal}}(\tau) = \frac{T_0}{\tau^{1/3}}\,, \tag{2.28}$$

the solution is simply a scaling solution

If we include just he first dissipative corrections, which is the Navier-Stokes equation with $\pi^{\mu\nu} = -2\eta\sigma^{\mu\nu}$, the differential equation can still be solved exactly in the conformal limit. So, with Eq. (2.26), the Navier-Stokes differential equation is

$$\partial_\tau T + \frac{1}{3}\frac{T}{\tau} - \frac{4}{9\tau^2}\frac{\eta}{s} = 0\,, \tag{2.29}$$

[3] Notice that even though the space has non-zero Christoffel symbols, it is still flat.

with solution

$$T_{\rm NS}(\tau) = \frac{T_0}{\tau^{1/3}} - \frac{2}{3\tau}\frac{\eta}{s}\,. \tag{2.30}$$

Notice already an unusual feature of the exact Bjorken solution of Navier-Stokes theory. Once the initial condition is determined at $\tau_0 \neq 0$, there is always an earlier time where the negative term dominates, which is independent of the initial condition! Therefore, this solution is unphysical for early times. Nevertheless, in this Bjorken case, since $\theta = 1/\tau$, early times is equal to large gradients, which is outside the scope of NS theory.

2.2.2 Gradient Expansion and Bjorken Flow

It has been suggested that if one takes second order corrections to Navier-Stokes theory, the mathematical inconsistencies of NS should vanish. We argue that second order gradient theory is not enough to circumvent such problems and in some cases it might even aggravate them.

Let us now investigate the second order gradient expansion theory in Eq. (2.16), originally studied in [68, 70]. There are two extra terms to be calculated: the comoving derivative of the shear tensor and a tensor related to the square of the shear tensor. Since the Milner metric has non-zero connection, the comoving derivative of the shear tensor has the following form

$$D\sigma_{\mu\nu} = u^\lambda \partial_\lambda \sigma_{\mu\nu} = u^\lambda \left(\partial_\lambda \sigma_{\mu\nu} - \Gamma^\alpha_{\mu\lambda}\sigma_{\alpha\nu} - \Gamma^\alpha_{\nu\lambda}\sigma_{\mu\alpha}\right)\,, \tag{2.31}$$

so with the non-zero Christoffel symbols Eq. (2.24) and the shear tensor non-zero components Eq. (2.26), it is straightforward to compute Eq. (2.31). The tracelessness condition permits to calculate only the contribution to $\pi^{\xi\xi}$, as the dissipative contribution to the energy equation, $\pi^{\mu\nu}\sigma_{\mu\nu}$, is simply $\frac{3}{2}\pi^{\xi\xi}\sigma_{\xi\xi}$. The second term that is related to the derivative of the shear tensor is then

$$\left(D\sigma^{<\xi\xi>} + \frac{\theta\sigma^{\xi\xi}}{3}\right) = -\frac{4}{9}\frac{1}{\tau^4}\,. \tag{2.32}$$

The other term is more straightforward since it involves only operations with the shear tensor but not its derivatives. This contribution is just then

$$\sigma^{<\xi}_\lambda \sigma^{\xi>\lambda} = \Delta^{\xi\xi}_{\alpha\beta}\sigma^\mu_\lambda \sigma^{\nu\lambda} = \frac{2}{9}\frac{1}{\tau^4}\,. \tag{2.33}$$

Finally, the equation for the temperature of the conformal fluid in the second order

gradient expansion approach is [68, 70]

$$\partial_\tau T + \frac{1}{3}\frac{T}{\tau} - \frac{4}{9}\frac{\eta}{s}\frac{1}{\tau^2} - \frac{8}{27}\frac{\eta}{s}\tau_\pi T\frac{1}{T\tau^3} + \frac{8}{27}\frac{\lambda_1 T}{s}\frac{1}{\tau^3 T} = 0\,. \tag{2.34}$$

The transport coefficients have been purposely left with the usual combinations of the thermodynamical values that compensate the temperature contributions, so they are just a pure number. For example, in a conformal fluid, η/s, $\tau_\pi T$ and $\lambda_1 T/s$ are just pure numbers. This differential equation does not have an analytical solution, but one can easily solve it with standard numerical routines available for instance in Wolfram's Mathematica [4]. In order to numerically solve this, we need to give values for the transport coefficients, which is then dependant on which microscopic theory is under analysis. For the quark-gluon plasma, so far holographic methods have been successful in order to describe the general hydrodynamic behavior of the theory, so we will for simplicity consider the coefficients for strongly coupled $\mathcal{N} = 4$ SYM, as calculated in [68],

$$\frac{\eta}{s} = \frac{1}{4\pi}\,, \qquad \tau_\pi T = \frac{2 - \ln[2]}{2\pi}\,, \qquad \frac{\lambda_1 T}{s} = \frac{1}{2\pi}\frac{\eta}{s}\,. \tag{2.35}$$

One general feature of holography is that these transport coefficient ratios are considerably smaller than than those calculated from simple kinetic theory models [28–30]. In weak coupling QCD calculations, $\eta/s \approx 1/(g^4 \ln g^1)$, which makes $\eta/s >> 1$ if the coupling g is $g \to 0$ [71, 72].The initial condition is that at proper time $\tau = 1$ fm, we have a temperature of $T(1) = 1.2\,\mathrm{fm}^{-1}$. We also adopt the usual conversion in natural units, $1\,\mathrm{fm} = \frac{1}{197.3}\,\mathrm{MeV}^{-1}$. The non-equilibrium entropy of the second order theory is given by [73]

$$s_{neq} = s - \frac{\tau_\pi \eta}{T}\sigma^{\alpha\beta}\sigma_{\alpha\beta} + \mathcal{O}(3)\,, \tag{2.36}$$

and the full entropy production up to second order in the gradient expansion Eq. (2.16) is

$$\begin{aligned}\nabla_\mu(s_{neq}\,u^\mu) = {} & \frac{\eta}{s}\frac{s}{2T}\sigma_{\mu\nu}\sigma^{\mu\nu} - \frac{1}{2}\frac{\lambda_1}{Ts}\frac{s}{T^2}\sigma_{\mu\nu}\sigma^\mu_\lambda\sigma^\lambda_\nu \\ & - \frac{\eta}{s}\tau_\pi T\frac{s}{T^2}\sigma_{\mu\nu}\left(D\sigma^{<\mu\nu>} + \frac{1}{3}\theta\sigma^{\mu\nu}\right)\,.\end{aligned} \tag{2.37}$$

The computation of how the entropy density and the temperature are related in

[4] In this thesis we use Wolfram's Mathematica version 10

strongly coupled $\mathcal{N}=4$ SYM is [10] (we also derive this equation in Chapter 5)

$$s = \frac{N_c^2 \pi^2}{2} T^3 \,, \tag{2.38}$$

and we set $N_c = 3$. The results are displayed in Fig. 2.1. As in the Navier-Stokes theory, it is not possible to properly define the temperature at early times. The Navier-Stokes theory has temperature equals to zero at time $\tau = \frac{2\sqrt{2}\tau_0}{(2\eta/s+3T_0\tau_0)^{3/2}} (\eta/s)^{3/2}$. In the second order gradient expansion theory we are solving, with initial condition $T(\tau_0 = 1) = 1.2$ and coefficients (2.35), the numerical integration stopped at $\tau = 0.134$. In NS under the same conditions, the temperature becomes zero at $\tau = 0.0087$.

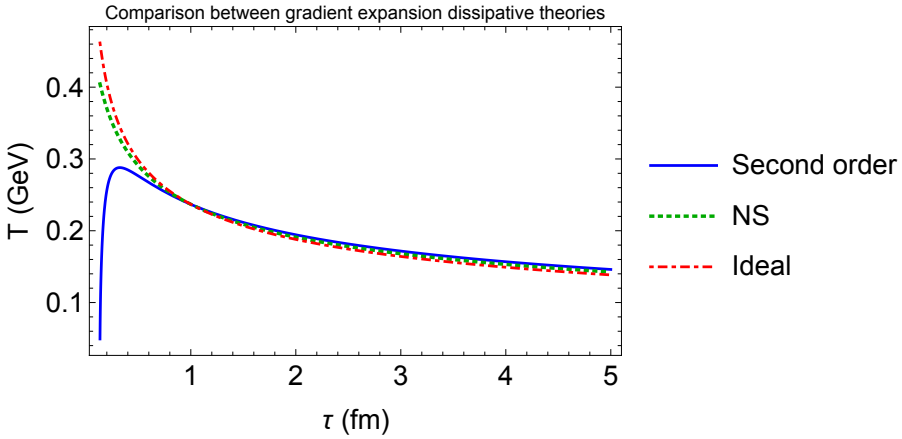

(a)

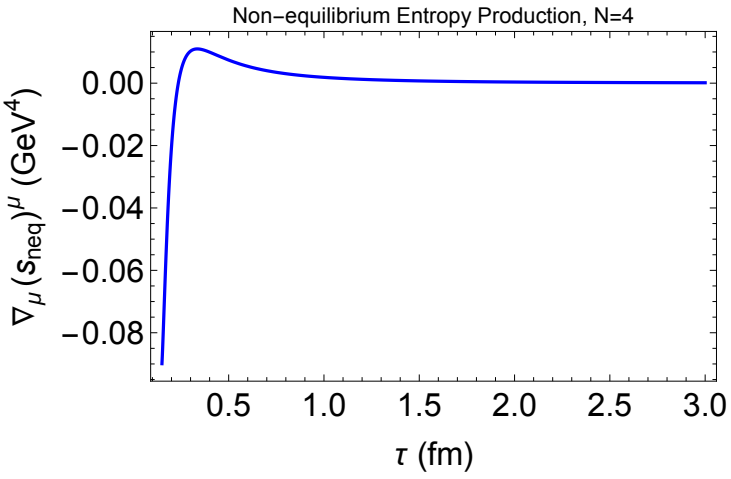

(b)

Figure 2.1: *Comparison between the solutions for the temperature in the three different hydrodynamic theories, ideal, Navier-Stokes and second order constructed via gradient expansion, all using the holographic values of $\mathcal{N}=4$ SYM transport coefficients. In the second figure we plot the non-equilibrium entropy production for the second order theory. Both the temperature and the non-equilibrium entropy production are not well-defined at early times.*

We may also compare the predictions of the exact Bjorken solution for theories de-

rived within kinetic theory, for instance considering a hard sphere interaction microscopic model [28–30]. It is not expected that these transport coefficients describe the strongly coupled QGP regime, but nonetheless it is interesting to understand the scope of such viscous solutions in more viscous scenarios, also because it shows good agreement with the hadronic gas phase. For such, we adopt the coefficients

$$\frac{\eta}{s} = 1\,, \qquad \tau_\pi T = 5\frac{\eta}{s}\,, \qquad \frac{\lambda_1 T}{s} = \frac{5}{7}(\tau_\pi T)\frac{\eta}{s}\,. \tag{2.39}$$

For the kinetic theory transport coefficients, we also use the equation of state of an ideal gas of massless N_F flavors of quarks and gluons

$$\varepsilon = 3\left[2\left(n_C^2 - 1\right) + \frac{7}{2}n_C N_F\right]\frac{\pi^2}{90}T^4\,,$$

where $n_C = 3$ and $N_F = 2.5$.

We repeat the calculations for the temperature and non-equilibrium entropy for the kinetic theory-inspired transport coefficients in Fig. 2.2.

The second order gradient expansion theory did not eliminate the inconsistencies from Navier-Stokes theory. On the contrary, the second order theory violates the second law of thermodynamics in a larger range of proper time.

2.2.3 Israel-Stewart and Bjorken Flow

We now investigate the behavior of IS theory (2.17) undergoing Bjorken flow. The dissipative tensor $\pi^{\mu\nu}$ is symmetric, traceless and orthogonal to the four-velocity. Its co-moving derivative is

$$D\pi_{\mu\nu} = u^\lambda \nabla_\lambda \pi_{\mu\nu} = u^\lambda\left(\partial_\lambda \pi_{\mu\nu} - \Gamma^\alpha_{\mu\lambda}\pi_{\alpha\nu} - \Gamma^\alpha_{\nu\lambda}\pi_{\mu\alpha}\right)\,, \tag{2.40}$$

in analogy to the shear tensor. It is straightforward to show that the contribution $\pi^{\xi\xi}$ can be taken as the only independent variable to Eq. (2.17) (tracelessness and symmetries of transverse plane) undergoing Bjorken flow. We have then

$$D\pi^{<\xi\xi>} + \frac{4}{3}\pi^{\xi\xi}\theta = \frac{\partial_\tau \pi^\xi_\xi}{\tau^2} + \frac{4}{3}\frac{\pi^\xi_\xi}{\tau^3}\,. \tag{2.41}$$

The quadratic term with coefficient λ_1 can be written as

$$\pi^{<\xi}_\lambda \sigma^{\xi\lambda>} = \frac{1}{2}\sigma^{\xi\xi}\pi^\xi_\xi\,. \tag{2.42}$$

We define the following quantity, $f \equiv \pi^{\xi}_{\xi}/sT$, which is an interesting quantity as it is conformal invariant, which is going to be manifestly important in the discussion of the Gubser Flow. Therefore, Eq.(2.17) and the energy equation Eq. (2.20) together for the Bjorken flow have the following structure,

$$\partial_\tau T + \frac{1}{3}\frac{T}{\tau} + \frac{fT}{3\tau} = 0\,, \tag{2.43}$$

$$(\tau_\pi T)\left[\partial_\tau f - \frac{4}{3}\frac{f^2}{\tau}\right] + fT = -\frac{4}{3}\frac{\eta}{s}\frac{1}{\tau} - \frac{2}{3}\frac{\lambda_1 T}{s}\frac{1}{\eta/s}\frac{f}{\tau}\,. \tag{2.44}$$

The main noticeable difference between the second order gradient expansion and Israel-Stewart theory is that now there are two coupled differential equations to solve. We follow the same idea as before, using simple numerical routines to determine solutions with given initial conditions to T and f. The early time complications of the Navier-Stokes and second order gradient expansion theories are eliminated in an interesting way here, through the choice of the initial condition of the dissipative variable f. One should be careful and integrate from small τ for a small choice of initial f. This procedure is necessary in order to assure the smallness of the dissipative quantity even at early times. A similar approach will be needed when we discuss the Israel-Stewart solutions of Gubser Flow. However, notice the advantage over the gradient expansion method: It is possible to find consistent solutions that respect the second law of thermodynamics at all times.

Next, we discuss entropy production in the Gubser flow regime. First of all, it is important to note that in Israel-Stewart theory the thermodynamic entropy, obtained from the equation of state, i.e., $s\,(T) = (\varepsilon + P)/T$, does not satisfy the second law of thermodynamics. As a matter of fact, Israel-Stewart theory is (phenomenologically) derived by generalizing the thermodynamic entropy so that the second law of thermodynamics is satisfied [49, 50] while, simultaneously, the fluid-dynamical equations of motion are causal and linearly stable (Chapter 4). In this approach, the entropy density and current can only be obtained approximately, up to a certain order in powers of the shear-stress tensor (and other dissipative currents, if they are present). Up to second order in $\pi^{\mu\nu}$, the generalized entropy current reads [49, 50],

$$S^\mu = su^\mu - \frac{\tau_\pi}{4\eta T}u^\mu \pi_{\alpha\beta}\pi^{\alpha\beta} + \mathcal{O}\,(3)\ , \tag{2.45}$$

where $\mathcal{O}\,(3)$ denotes terms of third order in the dissipative currents. The nonequilibrium entropy density is then $(-u^\mu S^\mu)$

$$s_{neq} = s - \frac{\tau_\pi}{4\eta T}\pi^{\alpha\beta}\pi_{\alpha\beta} + \mathcal{O}(3)\,. \tag{2.46}$$

Note that here we did not consider contributions that arise from bulk viscous pressure and heat flow. The complete expansion can be found in, e.g. Ref. [50]. In contrast to Navier-Stokes theory, the entropy production in Israel-Stewart theory is not linearly proportional to the shear viscosity coefficient.

Using the fluid-dynamical equations described in the previous sections, Eqs. (2.8), and (2.17), one can show that, up to fourth order in powers of the shear-stress tensor, the entropy production is a positive definite quadratic function of the dissipative currents,

$$\nabla_\mu S^\mu = \frac{1}{2\eta T}\pi_{\mu\nu}\pi^{\mu\nu} - \frac{25}{12T\left(\varepsilon + P\right)^2}\pi_{\alpha\beta}\pi^{\alpha\beta}\pi_{\mu\nu}\sigma^{\mu\nu} = \frac{1}{2\eta T}\pi_{\mu\nu}\pi^{\mu\nu} + \mathcal{O}\left(4\right). \tag{2.47}$$

This is only true since the temperature and shear viscosity are positive definite quantities (as already discussed, negative temperatures do not appear in solutions of Israel-Stewart theory). When fluid dynamics breaks down, the $\mathcal{O}\left(4\right)$ term in the equation above is not necessarily negligible and the entropy production is no longer guaranteed to be positive.

An example of a "good" initial condition and a consistent non-equilibrium entropy can be found in in Fig. 2.3. If one chooses the initial condition at $\tau = 1$ fm of the dissipative tensor to be zero with the same initial temperature, then there would be violation of the second law of thermodynamics. We show this behavior in Fig. 2.4. Therefore, it seems that a consistent behavior of Israel-Stewart theory is dependent on what the initial condition of the dissipative tensor is. In Fig. 2.3, the requirement is that for small proper times the dissipative variable f must remain small. The difference in a gradient expansion theory is that there is no freedom to accomplish that since the dissipation is determined solely by the initial condition on the four-velocity.

For completeness, we also plot the results of the Israel-Stewart theory with coefficients derived from Boltzmann equation in Fig. 2.5. Once more, depending on the initial condition for f, one gets negative s_{neq}.

It is important to state that we do not expect that hydrodynamics should be an appropriate physical description at small τ (which implies large gradients $\theta = 1/\tau$). However, it is very convenient that the hydrodynamic theory is mathematically well-behaved in such regime since many numerical schemes depend on it for stability.

2.3 General considerations about Gubser Flow

Bjorken symmetry was an important analytical and semi-analytic tool to understand the regime of applicability of dissipative relativistic hydrodynamics. In this section we review the derivation of the Gubser flow [51, 52], which is a generalization of Bjorken symmetry, but includes the special conformal symmetry instead of translation invariance

in the transverse plane. The advantage is that the solution depends on both the transverse plane radius r and the proper-time τ, although symmetry constraints only a special combination of both. Since we showed that the equations of conformal hydrodynamics are Weyl invariant (Appendix B), in this approach one performs a conformal transformation to make the symmetry manifest, which includes solving for a static fluid in curved spacetime, $dS_3 \otimes \mathbb{R}$ [52]. The immediate advantage of this solution is that it is both time evolving and radially expanding, which is not only more realistic to approximate heavy ion collisions, but it can also be illuminating to reveal the structure of different dissipative theories of hydrodynamics.

The symmetry assumptions of the Gubser flow include the following: Boost invariance $SO(1,1)$ between the collision direction and the time coordinate, Z_2 parity symmetry under the exchange of rapidity, rotational symmetry on the transverse plane $SO(2)$, which are all similar to Bjorken, and finally SCT in the radial direction, characterized by an energy scale q. This is a subgroup of the bigger conformal group in 4 dimensions, $SO(4,2)$. The additional SCT satisfies a conformal Killing vector condition, which for a conformal symmetry ψ_i reads

$$\mathcal{L}_\psi g_{\mu\nu} = \frac{1}{2}(\nabla_\lambda \psi^\lambda) g_{\mu\nu} \,. \tag{2.48}$$

Therefore, the condition for the flow to be symmetric for the conformal symmetry should be

$$\mathcal{L}_\psi u_\mu = -\frac{w}{4}(\nabla_\lambda \psi^\lambda) u_\mu = -\frac{1}{4}(\nabla_\lambda \psi^\lambda) u_\mu \,, \tag{2.49}$$

where w is the conformal weight (Appendix B).

Under these symmetries the flow is then boost invariant and radially symmetric, i.e., $T = T(\tau, r)$ and $\pi^{\mu\nu} = \pi^{\mu\nu}(\tau, r)$. We note that these conditions are approximately met near mid-rapidity in ultra-central collisions at the LHC, recently measured by the ATLAS and CMS Collaborations [7], [8]. In order to obtain analytical solutions, we will follow [51] and further assume that the conformal fluid flow is actually invariant under $\mathrm{SO}(3) \otimes \mathrm{SO}(1,1) \otimes \mathrm{Z}_2$. The SO(3) piece is a subgroup of the SO(4, 2) conformal group (Appendix A) which describes the symmetry of the solution under rotations around the beam axis and two operations constructed using special conformal transformations that replace translation invariance in the transverse plane. For more details regarding the generators of the SO(3) symmetry group of this solution, see Ref. [51]. In this case, the dynamical variables depend on τ and r through the dimensionless combination [51, 52]

$$\rho = \sinh^{-1}\left(-\frac{1-\tilde{\tau}^2+\tilde{r}^2}{2\tilde{\tau}}\right), \tag{2.50}$$

where $\tilde{\tau} \equiv q\tau$ and $\tilde{r} = qr$. Without loss of generality, we set $q = 1$ fm^{-1} when solving the fluid-dynamical equations. Furthermore, the flow is completely determined by symmetry constraints to be [51, 52]

$$\begin{aligned} u_\tau &= -\cosh\left[\tanh^{-1}\left(\frac{2\tilde{\tau}\tilde{r}}{1+\tilde{\tau}^2+\tilde{r}^2}\right)\right], \\ u_r &= \sinh\left[\tanh^{-1}\left(\frac{2\tilde{\tau}\tilde{r}}{1+\tilde{\tau}^2+\tilde{r}^2}\right)\right], \\ u_\phi &= u_\xi = 0\,. \end{aligned} \tag{2.51}$$

The exact form for this flow can be obtained exactly by solving the appropriate equations for the Lie derivatives in the Killing vector equations for each symmetry. This defines the Gubser flow. Since the flow is known (2.51), the relativistic Euler equation (2.20) is automatically satisfied and, thus, only the equations for the temperature and the shear-stress tensor for the appropriate dissipative theory need to be solved.

In order to solve the remaining equations, it is convenient to go to a different coordinate system in which the flow velocity is zero. In order to do so, one needs to first find a metric conformally connected to the Minkowski spacetime (or at least the future-wedge), and then finally find a coordinate system in which the symmetries of the Gubser flow are manifest. For this purpose, one must first perform a Weyl rescaling of the metric, $ds^2 \to d\hat{s}^2 \equiv ds^2/\tau^2$, which is the metric in $\mathrm{dS}_3 \otimes \mathbf{R}$, with dS_3 corresponding to the 3-dimensional de Sitter space. We show in Appendix B that the hydrodynamics theories under consideration are conformal invariants. Therefore, the map between quantities on each spacetime is determined solely by the conformal weight. One can implement the coordinate transformation introduced in [52]

$$\sinh\rho = -\frac{1-\tilde{\tau}^2+\tilde{r}^2}{2\tilde{\tau}}\,, \qquad \tan\theta = \frac{2\tilde{r}}{1+\tilde{\tau}^2-\tilde{r}^2}\,, \tag{2.52}$$

which takes $d\hat{s}^2$ to

$$d\hat{s}^2 = -d\rho^2 + \cosh^2\rho\, d\theta^2 + \cosh^2\rho \sin^2\theta\, d\phi^2 + d\xi^2\,. \tag{2.53}$$

We explore basic geometric properties of de Sitter space in Appendix C. Notice that the symmetries are manifest: there is a rotational symmetry on the parameters θ and ϕ, although these are not the usual angles in spherical coordinates to represent the sphere, instead they parametrize the de-Sitter spacetime. Boost invariance and parity symmetry of the rapidity ensures that the solution should depend only on ρ in this spacetime.

In this coordinate system the fluid is at rest and, even though spacetime is curved

$dS^3 \otimes \mathbb{R}$. Consequently, the equations of motion for ε and $\pi^{\mu\nu}$ considerably simplify, making it possible to find analytical and semi-analytical solutions of several dissipative theories. However, the complicated systems of partial differential equations now are reduced to solving ordinary differential equations, which are much simpler in practical terms.

In the following, we denote all fluid-dynamical variables in this new coordinate system with a hat. As mentioned, such generalized de Sitter coordinate is extremely convenient since it leads to a static velocity profile, i.e., $\hat{u}_\mu = (-1, 0, 0, 0)$. As already mentioned, the fields are only functions of ρ, i.e, $\hat{T} = \hat{T}(\rho)$ and $\hat{\pi}^{\mu\nu} = \hat{\pi}^{\mu\nu}(\rho)$. Because of the metric rescaling and the coordinate transformation $x^\mu = (\tau, r, \phi, \xi) \to \hat{x}^\mu(\rho, \theta, \phi, \xi)$, the dimensionless dynamical variables in $\mathrm{dS}_3 \otimes \mathbb{R}$ are related to those in Milne as follows

$$u_\mu(\tau, r) = \tau \frac{\partial \hat{x}^\nu}{\partial x^\mu} \hat{u}_\nu \,, \tag{2.54}$$

$$T(\tau, r) = \frac{\hat{T}}{\tau} \,, \tag{2.55}$$

$$\pi_{\mu\nu}(\tau, r) = \frac{1}{\tau^2} \frac{\partial \hat{x}^\alpha}{\partial x^\mu} \frac{\partial \hat{x}^\beta}{\partial x^\nu} \hat{\pi}_{\alpha\beta} \,. \tag{2.56}$$

These conditions are direct consequences of the conformal weight discussed in Appendix B, of how hydrodynamics variables scale under Weyl transformations (see also [52]). This is crucial since in the end one of the goals is to study the results to appropriate Milner coordinates in Minkowski spacetime. We present the exact mapping for convenience if one is interested in using such solutions.

For instance, since $\pi_{\mu\nu} \to \Omega^2 \pi_{\mu\nu}$ under Weyl rescaling $g_{\mu\nu} \to \Omega^{-2} g_{\mu\nu}$ with $\Omega = \tau$, there is a factor of $1/\tau^2$ in (2.56). Given the dictionary between the fields in the different spaces shown above, one can solve the equations (2.16), (2.17) and (2.20) in $\mathrm{dS}_3 \otimes \mathbf{R}$ where the fluid is static and the fields are homogeneous (i.e., they only depend on the de Sitter time coordinate ρ) and plug in the solutions to find the fields in the standard flat space-time. This is the general strategy that we shall follow below to find solutions for the viscous relativistic fluid defined above.

We emphasize that the Gubser flow solution described so far does assume symmetries that are not strictly present in realistic ultracentral heavy ion collisions, such as conformal symmetry. Despite this fact, it can still be useful to understand the solutions of relativistic fluid dynamics on a qualitative level and also, as will be shown in this thesis, to test numerical simulations of relativistic fluid dynamics in a setting similar to that created in a heavy ion collision.

2.3.1 Ideal and Navier-Stokes for Gubser Flow

First, it is of interest to solve simpler scenarios involving Gubser flow. These studies were originally performed in Ref. [52].

The expansion rate in this curved spacetime is

$$\hat{\theta} = \frac{\partial_\mu \left(\sqrt{-g}\, \hat{u}^\mu\right)}{\sqrt{-g}} = 2\tanh(\rho)\,. \tag{2.57}$$

For ideal hydrodynamics, the relevant equation (2.20) is simply

$$\partial_\rho \hat{T} + \frac{\hat{\theta}}{3}\hat{T} = 0\,. \tag{2.58}$$

The analytical solution is the one found in [51, 52]

$$\hat{T}_{\rm ideal}(\rho) = \frac{\hat{T}_0}{\cosh^{2/3}\rho}\,, \tag{2.59}$$

where $\hat{T}_0 \equiv \hat{T}_{\rm ideal}(0)$ is a positive constant (so then $\hat{T}_{\rm ideal}$ is positive-definite). Using the dictionary in (2.55), we see that the temperature in the original Milne is given by

$$T_{\rm ideal}(\tau, r) = \frac{\hat{T}_0 (2q\tau)^{2/3}}{\tau\left[1 + 2q^2(\tau^2 + r^2) + q^4(\tau^2 - r^2)^2\right]^{1/3}}, \tag{2.60}$$

and, at the time $\tau_0 = 1/q$, one finds $T_{\rm ideal}(\tau_0, 0) = \hat{T}_0\, q$.

For Navier-Stokes theory, we need to calculate the shear tensor in this spacetime. Though this is a straightforward calculation, we outline the elements here for completeness. The non-zero Christoffel symbols are

$$\begin{aligned}
\Gamma^\rho_{\theta\theta} &= \cosh\rho \sinh\rho \qquad & \Gamma^\rho_{\phi\phi} &= \sin^2\theta \cosh\rho \sinh\rho\,,\\
\Gamma^\theta_{\rho\theta} &= \Gamma^\theta_{\theta\rho} = \tanh\rho \qquad & \Gamma^\theta_{\phi\phi} &= -\sin\theta\cos\theta\,,\\
\Gamma^\phi_{\rho\phi} &= \Gamma^\phi_{\phi\rho} = \tanh\rho \qquad & \Gamma^\phi_{\theta\phi} &= \Gamma^\phi_{\phi\theta} = \frac{1}{\tanh\rho}\,,
\end{aligned} \tag{2.61}$$

and the shear tensor is $\hat{\sigma}^{\mu\nu} = \hat{\Delta}_{\mu\nu\alpha\beta}\nabla^\alpha \hat{u}^\beta = \Gamma^\rho_{\mu\nu} - \hat{\Delta}_{\mu\nu}\hat{\theta}/3$. The non-zero terms of the shear tensor are then

$$\hat{\sigma}^\xi_\xi = -2\tanh\rho/3\,, \qquad\qquad \hat{\sigma}^\theta_\theta = \hat{\sigma}^\phi_\phi = \tanh\rho/3\,. \tag{2.62}$$

Once more, there is only one independent component of the shear tensor, which we

take to be $\hat{\sigma}^{\xi}_{\xi}$. The dissipative tensor in Navier-Stokes is not a dynamical variable, and the only differential equation left to be solved is the energy conservation equation

$$\frac{d}{d\rho}\hat{T} + \frac{2}{3}\hat{T}\tanh\rho = \frac{4}{9}\frac{\eta}{s}(\tanh\rho)^2 .$$

The analytical solution, previously found in [51, 52], is

$$\hat{T}_{\rm NS}(\rho) = \frac{\hat{T}_0}{\cosh^{2/3}\rho} + \frac{4}{27}\frac{\eta}{s}\frac{\sinh^3\rho}{\cosh^{2/3}\rho}\,{}_2F_1\left(\frac{3}{2},\frac{7}{6};\frac{5}{2};-\sinh^2\rho\right), \tag{2.63}$$

where ${}_2F_1$ is a hypergeometric function. From the equation of motion, the condition $\lim_{\rho\to\pm\infty}\hat{T}'_{\rm NS}(\rho) = 0$ shows that $\lim_{\rho\to\pm\infty}\hat{T}_{\rm NS}(\rho) = \pm 2\eta/3s$ [51, 52]. In this case, once $\eta/s \neq 0$, for any given τ there is always a value of r beyond which the temperature switches sign and becomes negative (which is very different than the ideal case in which $\lim_{\rho\to\pm\infty}\hat{T}_{\rm ideal} = 0$). This effect may be connected with the well-known causality issue (see, for instance, [58, 74]) of the relativistic Navier-Stokes equations. We shall see below that once the relaxation time coefficient is taken into account one can find a solution where $\hat{T}$ is positive-definite and $\lim_{\rho\to-\infty}\hat{T}(\rho) = 0$. We show these results in Fig. 2.6.

2.3.2 Gubser flow and the gradient expansion

The Navier-Stokes theory contained inconsistencies in the Gubser Flow. In this section, we derive the Gubser flow equation for the second order gradient expansion theory [52], and show that the theory only exists in a limited range of ρ and seems to violate the second law of thermodynamics. Therefore, a second order correction by itself is not sufficient to improve the consistency of NS in the Gubser Flow at negative large values of ρ, in analogy to the result we found in the Bjorken case.

It is a straightforward exercise to calculate the comoving derivative of the shear tensor with the Christoffel symbols and the non-zero shear tensors Eqs. (2.61) and (2.62). Therefore, the dissipative contribution f, derived from Eq. (2.16), is

$$f = \frac{4}{3}\frac{\eta}{s}\frac{\tanh\rho}{\hat{T}} + 2\frac{\eta}{s}\frac{\tau_\pi\hat{T}}{\hat{T}^2}\left(\frac{2}{9}\tanh^2\rho - \frac{2}{3}\right) + \frac{8}{9}\frac{\lambda_1}{\hat{s}\hat{T}}\tanh\rho . \tag{2.64}$$

Since the dissipative contribution is not an independent dynamical degree of freedom, there is only one differential equation, which is the energy conservation

$$\frac{d}{d\rho}\hat{T} + \frac{2}{3}\hat{T}\tanh\rho = \frac{1}{3}\tanh\rho\left(\frac{4}{3}\frac{\eta}{s}\tanh\rho + 2\frac{\eta}{s}\frac{\tau_\pi\hat{T}}{\hat{T}}\left(\frac{2}{9}\tanh^2\rho - \frac{2}{3}\right) + \frac{8}{9}\frac{\lambda_1}{\hat{s}\hat{T}}\hat{T}\tanh\rho\right). \tag{2.65}$$

The asymptotic behavior of this differential equation is problematic. Suppose we solve for the temperature, when its derivative is very small and the tanhρ is close to unity. Solving this equation we find the following dependence on the asymptotic temperature

$$T_f(\rho \pm \infty) = \frac{1}{3}\left(\frac{\eta}{s} \pm \sqrt{\left(\frac{\eta}{s}\right)^2 + 4\frac{\lambda_1 T}{s} - 4\frac{\eta}{s}\tau_\pi T}\right) . \tag{2.66}$$

Notice that not only it is possible to find negative values, but also imaginary! For instance, using the values of $\mathcal{N} = 4$ SYM (2.35), the asymptotic values are $T_F \approx 0.0265 \pm 0.0320\, i$, and for kinetic theory (2.39) $T_F \approx 0.333 \pm 0.724\, i$. Both cases would lead to instabilities in a numerical implementation, which is the reason a numerical routine can only solve these equations in a short range. We show the result for $\mathcal{N} = 4$ coefficients in the region where the solution for T exists and is real.

2.3.3 Gubser Flow for Israel-Stewart theory (non-zero λ_1)

We consider a general Israel-Stewart second order theory that undergoes the dynamics in the Gubser flow, described by Eq. (2.17). We investigated a related solution in Ref. [53], but in our paper we considered $\lambda_1 = 0$. We discuss this solution in the next section, as we compare the results from our paper with numerical simulations.

The procedure for calculating the differential equations is the same as before, one needs to carefully calculate the covariant derivatives through the Chrystoffel symbols in Eq. (2.61), and use the properties that the dissipative tensor is symmetric, traceless and orthogonal to the four-velocity. Another assumption is that the non-diagonal differential equations for the dissipative tensors can always be set to zero, since the off-diagonal terms of the shear tensor are zero as well. The relevant equations of motion are just two coupled ordinary differential equations, one for the temperature $\hat{T}$ and another one for the dissipative contribution $f = \hat{\pi}^\xi_\xi/\hat{s}\hat{T}$. They are

$$\begin{aligned} \frac{d}{d\rho}\hat{T} + \frac{2}{3}\hat{T}\tanh\rho - \frac{1}{3} f \tanh\rho = 0\,, \\ \tau_\pi \hat{T}\left(\frac{d}{d\rho} f + \frac{4}{3} f^2 \tanh\rho\right) + f\hat{T} = \frac{4}{3}\frac{\eta}{\hat{s}}\tanh\rho + \frac{2}{3}\frac{\lambda_1 \hat{T}}{\hat{s}}\frac{1}{\eta/\hat{s}} f \tanh\rho\,, \end{aligned} \tag{2.67}$$

where we write the dissipative transport coefficients with their dimensionless combinations. We solve these differential equations in the same way as last section, we define the inverse length $q = 1\,\mathrm{fm}^{-1}$ and the initial temperature to be $T = 1.2\,\mathrm{fm}^{-1}$. In Israel-Stewart theory the dissipative tensor is an independent dynamical degree of freedom, and thus one needs to give initial conditions. There is a rich physical consequence in the choice

of initial conditions, and in this section we argue for it and show explicit calculations that may help to define a initial condition choice to be "physical". In this case, we investigate the behavior of Eq. (2.67) for asymptotically large values of ρ. For an asymptotic value T_F of the temperature, the solutions of f are

$$f(\rho \to \pm\infty) = \frac{2\,\lambda_1 - 3\,T_F\,\eta/\hat{s} \pm \sqrt{(3\,T_F\,\eta/\hat{s} - 2\,\lambda_1)^2 + 64\hat{T}\,\tau_\pi\,\eta^3/\hat{s}^3}}{8\hat{T}\tau_\pi\,\eta/\hat{s}}\,. \tag{2.68}$$

Notice that f is always a real number. One of the inconsistencies of the second order gradient expansion we found before was that asymptotic values of temperature for known transport coefficients are imaginary. The Israel-Stewart approach has the freedom of defining a positive temperature at all ρ, and for the parameter space of consistent η, τ_π and λ_1, f is always a real number. This choice of initial condition, despite not providing a matching with Navier-Stokes at $\rho = 0$, seems to be the physical relevant description. There are no inconsistencies such as negative or imaginary temperature, and the second law of thermodynamics seems to always be preserved.

Since proper-time and radius are connected through the only degree of freedom, the de-Sitter time ρ, it is instructive to plot our results as a function of such. In Fig. 2.8 we plot both the temperature and the dissipative term f as functions of ρ. For this plot we numerically integrated from large values of ρ, following the asymptotic values in Eq. (2.68). The asymptotic temperature T_F was adjusted to give $\hat{T}(0) = 1.2$, which is the initial condition we have been using.

One useful quantity to investigate is the entropy production of this dissipative theory. We truncate the corrections of the non-equilibrium entropy of IS theory to second order as in Eq. (2.46). The four-divergence of the non-equilibrium entropy current (2.47) is then rewritten as

$$\nabla_\mu\left(s_{\rm neq}u^\mu\right) = \frac{\pi_{\alpha\beta}\pi^{\alpha\beta}}{2\eta T}\left[1 - \frac{25}{12}\frac{\pi_{\mu\nu}}{(\varepsilon+p)}\frac{2\eta\sigma^{\mu\nu}}{(\varepsilon+p)}\right] + \mathcal{O}(6)\,, \tag{2.69}$$

where the higher corrections are beyond the dynamics of Israel-Stewart. If the right hand side of Eq. (2.69) is always positive for every value of the coordinate ρ, then the non-equilibrium entropy always increases, which is necessary for the second law of thermodynamics to be valid. Throughout this section we use the value Eq. (2.2.2) for an equation of state of massless quarks and gluons. This is exactly what is shown in Fig. 2.9, for the "good" initial conditions integrated from asymptotic values of ρ.

It is also illustrative to show the temperature profile evolution in Milner coordinates r and τ. We just need to perform the coordinate and Weyl transformations exemplified

in the dictionaries Eqs. (2.55) and (2.56).

The explicit map of the dissipative tensor is a straightforward map from Eq. (2.56), but for completeness we write here the exact maps. If one solves for the dissipative term f, the dissipative tensor component is related as $\hat{\pi}^{\xi}_{\xi} = f\,\hat{s}\hat{T}$. Therefore, in the de-Sitter spacetime, we have simply

$$\hat{\pi}_{\xi\xi}(\rho) = \hat{\pi}^{\xi}_{\xi}(\rho)\,, \quad \hat{\pi}_{\theta\theta}(\rho) = -\frac{1}{2}\cosh^2\rho\,\hat{\pi}^{\xi}_{\xi}(\rho)\,, \quad \hat{\pi}_{\phi\phi}(\rho,\theta) = -\frac{1}{2}\sin^2\theta\cosh^2\rho\,\hat{\pi}^{\xi}_{\xi}(\rho)\,. \tag{2.70}$$

Then, we have to do the inverse Weyl scaling and a coordinate transformation. The components of the dissipative tensor and the temperature are then ($q = 1\,\mathrm{fm}^{-1}$)

$$\begin{aligned}
T(\tau\rho) &= \frac{1}{\tau}\hat{T}[\rho(\tau,r)]\,,\\
\pi_{rr}(\tau,r) &= \frac{1}{\tau^2}\left(\frac{2(1+r^2+\tau^2)}{\tau^4+2\tau^2(1-r^2)+(1+r^2)^2}\right)^2\hat{\pi}_{\theta\theta}[\rho(\tau,r)]\,,\\
\pi_{\tau\tau}(\tau,r) &= \frac{1}{\tau^2}\left(\frac{4r\tau}{\tau^4+2\tau^2(1-r^2)+(1+r^2)^2}\right)^2\hat{\pi}_{\theta\theta}[\rho(\tau,r)]\,,\\
\pi_{r\tau}(\tau,r) &= -\frac{1}{\tau^2}\left(\frac{1}{\tau^4+2\tau^2(1-r^2)+(1+r^2)^2}\right)^2\left(8r\tau(1+r^2+\tau^2)\right)\hat{\pi}_{\theta\theta}[\rho(\tau,r)]\,,\\
\pi_{\phi\phi}(\tau,r) &= \frac{1}{\tau^2}\,\hat{\pi}_{\phi\phi}[\rho(\tau,r),\theta(\tau,r)]\,,\\
\pi_{\xi\xi}(\tau,r) &= \frac{1}{\tau^2}\,\hat{\pi}_{\xi\xi}[\rho(\tau,r)]\,.
\end{aligned} \tag{2.71}$$

We plot the results in the Milne coordinates in Fig. 2.10. In the next section, for the case where $\lambda_1 = 0$, we compared the semi-analytical results to full numerical simulations perfumed by the McGill group in order to check the accuracy of such simulations, as well as to fix some free-parameters needed to develop the numerical code. Also, for phenomenological heavy ion applications, knowing how the solution behaves in Milne coordinates is very convenient.

It is important to check if the entropy production and the second law of thermodynamics are consistent in the Milne space. For such, we multiply s_{neq} with the volume factor ($r \times \tau$) and the gamma factor u^{τ}. If the second law of thermodynamics holds, we expect that for large integrated values, the resulting integral should increase with time. We checked this in two different scenarios: For Fig. 2.11(a) we calculated the effect of increasing the integrated volume. The expected result is that once the whole relevant space is integrated, i. e., there is no flux of entropy leaving the integrated volume, the

second law holds. Also, we tested if the solution would not breakdown at small values of proper time, and we found that the agreement holds in Fig. 2.11(b). The large integrated value of radius is to ensure that this increase is a physical feature, and not a geometrical artefact due to the finite integration range.

It is crucial that the initial conditions of the Israel-Stewart equations are consistent. We turn our attention to the features of the semi-analytical solution if an initial condition matching Navier-Stokes at $\rho = 0$, i.e., matching $f(0) = 0$, in addition to the usual $\hat{T}(0) = 1.2$ is used. There seems to be a fine tuning problem with this initial condition; we noticed that for many transport coefficients, there were unphysical results or divergences in some regions of ρ. In order to illustrate the unphysical results even when there is a well-defined temperature profile, we chose the shear viscosity coefficient to be $\eta/s = 0.2$, and then τ_π and λ_1 with values from the Boltzmann kinetic theory calculations of (2.39).

Compare Fig. 2.13 and Fig. 2.9. The non-physical initial conditions imply a region of ρ where the non-equilibrium entropy production is negative. On the other hand, for asymptotic consistent initial conditions, such inconsistency is absent.

It is also interesting to investigate if the integrated non-equilibrium entropy decreases with time. In Fig. 2.14 we show that this is exactly the situation for "bad" initial conditions. The integrated value not only becomes smaller, it actually changes sign with increasing proper time. Therefore, if one imposes that the dissipative tensor resembles the one from Navier-Stokes at $\rho = 0$, the resulting theory is not well-defined and unphysical at early times.

This concludes our investigation of the consistency and properties of the Israel-Stewart second order dissipative theory undergoing Gubser flow. It is interesting how a careful analysis of the Bjorken and Gubser solutions shed new light on the inconsistencies of the gradient expansion approach for dissipative hydrodynamics, as well as the importance of the initial conditions in Israel-Stewart theory. In Chapter 4, we will investigate further this problem through the light of linear perturbations around equilibrium situations.

We show the results of our original motivation in the next section, i.e., how one can test the accuracy of numerical hydrodynamic codes using our analytical and semi-analytical solutions.

2.4 Testing Fluid dynamics

In this section, we follow our Ref. [53] in order to test numerically the Gubser solution of hydrodynamics. For simplicity, we consider only the relaxation effect ($\lambda_1 = 0$) and for the most part we compare the solutions for the initial condition, $f(0) = 0$. This is still a valid approach since the solutions are only compared in regions where the second law of

thermodynamics holds. We also present a limit of Israel-Stewart that has an analytical solution, which we call the "cold plasma limit", and also its comparison to numerical simulations.

We warn the reader that we do not expect the results in this section to be appropriate to describe realistic heavy ion collisions for the following reasons: the Gubser symmetry is a rather restrictive symmetry, we do not consider the effects of the parameter λ_1, and most importantly because the initial condition employed for f is not valid for all space and time. Also, the energy density is not homogeneous [4]. However, for the sake of comparing numerical solutions and fixing free parameters in numerical codes, the previous concerns are not important.

The equations of motion for $\hat{T}(\rho)$ and $\hat{\pi}^{\mu}_{\nu}(\rho)$ are simply Eq. (2.67) with $\lambda_1 = 0$,

$$\begin{aligned} \frac{d}{d\rho}\hat{T} + \frac{2}{3}\hat{T}\tanh\rho - \frac{1}{3}f\tanh\rho = 0\,, \\ \tau_\pi\hat{T}\left(\frac{d}{d\rho}f + \frac{4}{3}f^2\tanh\rho\right) + f\hat{T} = \frac{4}{3}\frac{\eta}{\hat{s}}\tanh\rho\,, \end{aligned} \tag{2.72}$$

Note that for any nonzero τ, the value of ρ decreases with r, while for a fixed r the value of ρ increases with τ. Thus, when $\rho \ll 0$ and negative one probes regions in which $r \gg 1$, and when $\rho \gg 1$ one has $\tau \gg 1$. In this sense, we expect that physically meaningful solutions behave as $\lim_{\rho\to\pm\infty}\hat{T}(\rho) = 0$, i.e., at an infinite radius or time the temperature should go to zero. On the other hand, given the definition of f, it is consistent to have $\lim_{\rho\to\pm\infty} f(\rho)$ finite and nonzero (f is a ratio between two quantities that should vanish when $\rho \to \pm\infty$). In this section we write the parametrization of the relaxation time with respect to the shear viscosity, as follows

$$\tau_\pi = (\eta/s) \times (c/T)\,. \tag{2.73}$$

In analogy to the discussions in the past sections, it is possible to find one qualitative difference between the asymptotic solutions ($\lim_{\rho\to\pm\infty}$) of Navier-Stokes and Israel-Stewart theories. If one imposes that $\lim_{\rho\to\pm\infty}\hat{T}(\rho) = 0$ and, simultaneously, $\lim_{\rho\to\pm\infty} df(\rho)/d\rho = 0$, one can find the asymptotic solution for $f(\rho)$, $\lim_{\rho\to\pm\infty}|f| = \sqrt{1/c}$ (note that the parameter c appeared in the definition of the relaxation time, see Eq. (2.73). Therefore, in contrast to Navier-Stokes theory, solutions in which $\lim_{\rho\to\pm\infty}\hat{T}(\rho) = 0$ are possible in Israel-Stewart and do happen in practice as long as τ_π is nonzero.

There is a limit in which one can find analytical solutions for $\hat{T}$ and f. This becomes possible when the fluid is very viscous or when the temperature is very small, i.e., when $\eta/(s\hat{T}) \gg 1$. In this case, called here the *cold plasma limit*, the term f becomes negligible

in comparison to all the other terms in Eq. (2.72), which are all linear in $\eta/(s\hat{T})$. In this limit, one can directly solve the equation for f to find

$$f(\rho) = \sqrt{\frac{1}{c}} \tanh\left[\sqrt{\frac{1}{c}}\left(\frac{4}{3}\ln\cosh\rho - f_0 c\right)\right], \tag{2.74}$$

where $\bar{\pi}_0$ is a constant and, substituting this into Eq. (2.72), we obtain

$$\hat{T}(\rho) = \hat{T}_1 \frac{\exp\left(c f_0/2\right)}{(\cosh\rho)^{2/3}} \cosh^{1/4}\left[\sqrt{\frac{1}{c}}\left(\frac{4}{3}\ln\cosh\rho - f c\right)\right]. \tag{2.75}$$

where $\hat{T}_1$ is a constant. These analytical solutions are even in ρ, $\hat{T}$ is positive-definite, and $\lim_{\rho\to\pm\infty}\hat{T}(\rho) = 0$ if $4c > 1$. Moreover, note that as long as $c > 1$, f is always smaller than 1 for any value of ρ, i.e, the dissipative correction to the energy-momentum tensor is always smaller than the ideal fluid contribution. In the next section, the analytical solutions in Eqs. (2.74) and (2.75) will be compared to numerical solutions of fluid dynamics obtained with MUSIC. Also, for completeness, we remark [75] found analytical solutions of a different set of IS equations undergoing Gubser flow.

We show in Fig. 2.15 a comparison between $\hat{T}$ and f computed for an ideal fluid, Navier-Stokes theory, and Israel-Stewart theory for $\eta/s = 0.2$, which is a value in the ballpark of that normally used in hydrodynamic simulations of the QGP in heavy ion collisions [76], and $c = 5$, which is the typical value obtained from approximations of the Boltzmann equation [28–30]. The equation of state employed is that of an ideal gas of massless quarks and gluons, Eq. (2.2.2).

We have chosen the initial conditions for the equations such that $\hat{T}(0) = 1.2$, for all the cases, and, for the Israel-Stewart case, $f(0) = 0$. We solve Eqs. (2.72) numerically using MATHEMATICA's NDSolve subroutine. The Israel-Stewart theory results are shown in solid black, the Navier-Stokes results in dashed blue, and the ideal fluid result in the dashed-dotted red curve. One can see that the Israel-Stewart solution for $\hat{T}$ is positive-definite and $\lim_{\rho\to\pm\infty}\hat{T}(\rho) = 0$. Moreover, viscous effects break the parity of the solutions with respect to $\rho \to -\rho$. Note that, as mentioned before, f goes to $\sqrt{1/c}$ when $\rho \to \pm\infty$ in Israel-Stewart theory while for the Navier-Stokes solution this quantity diverges at $\rho \approx -4.19$, which is the value of ρ at which $\hat{T}_{NS} = 0$. We also checked that the analytical limit in Eqs. (2.74) and (2.75) matches the numerical solution for $\eta/s = 1/(4\pi)$ [10] and $c = 5$ when $\hat{T}(0) \leq 0.001$, i.e., when the temperature is extremely small.

In order to study the space-time dependence of the Israel-Stewart solutions we define $q = 1$ fm^{-1} so that $\rho = 0$ corresponds to $\tau = 1$ fm and $r = 0$. Therefore, in standard hyperbolic coordinates, $T\left(r = 0, \tau_0 = 1\text{ fm}\right) = 1.2$ fm^{-1} and $\bar{\pi}^{\xi}_{\xi}\left(r = 0, \tau_0 = 1\text{ fm}\right) = 0$. In

Fig. 3.1 we show a comparison between the temperature profiles for Israel-Stewart theory at the times $\tau = 1.2,\ 1.5,\ 2$ fm, with $\eta/s = 0.2$, $c = 5$. Also, in the same figure we show $\tau^2\pi^{\xi\xi}$ as a function of the radius for the same times. The other components of the shear-stress tensor can be obtained using the dictionary in Eq. (2.56).

Note that the system is expanding in the transverse plane. It appears to be imploding because of the energy flowing out in the longitudinal direction. A larger viscosity might change this effect quantitatively, but the qualitatively features will remain the same.

In Fig. 2.17(a) we plot the generalized entropy current multiplied by $\tau r u^\tau$ as a function of the radius, r. We multiply the entropy density by the relevant phase space factors $r \times \tau$ and by the gamma factor u^τ (the factor τ is taken out from the integration in the longitudinal direction, which should be made in $\tau\xi$ and not just ξ). Due to the symmetries assumed when deriving the Gubser flow solution, s and u^τ are constant in ϕ and ξ and, hence, the integration in these variables is trivial. Thus, the total entropy is proportional to the area under the curves in Fig. 2.17(a).

In Fig. 2.17(b), we further show the entropy production, $Q = \pi_{\mu\nu}\pi^{\mu\nu}/(2\eta T)$, as a function of the radius, for several time steps. One can see that the entropy production in Gubser flow solutions is not very large, even though the system is far away from the Navier-Stokes regime. In Fig. 2.17(c), we show the total entropy production of the theory $Q_{\text{total}} = \pi_{\mu\nu}\pi^{\mu\nu}/(2\eta T) - 25\pi_{\alpha\beta}\pi^{\alpha\beta}\pi_{\mu\nu}\sigma^{\mu\nu}/\left[12T\left(\varepsilon + P\right)^2\right]$, Eq. (2.69), which does not neglect the term of order 4, as is usually done in Israel-Stewart theory. We see that the order 4 term is not necessarily small and does affect the entropy production significantly. At late times and small values of radius, it appears as just a correction. However, at early times and large radius, the $\mathcal{O}(4)$ term is large and can even drive the entropy production term to negative values. For example, when $\tau = 1$ fm, the entropy production becomes negative when $r \gtrsim 3.5$. On the other hand, at $\tau = 2$ fm, the entropy production is always positive between $r = 0$ and 5 fm. We note that, at any time, there will always be a value of the radius for which the entropy production becomes negative. The larger the time, the larger this value of radius will be.

Even though 1 fm of time evolution might appear to be small, in Gubser flow solutions it is enough time for the energy density in the center of the system to decrease by a factor 16 (and for the temperature to decrease by a factor 2). So we consider that the time interval chosen, even though apparently small when compared to evolution times in heavy ion collisions, is more than enough for the purposes of this thesis. Note that such rapid expansion is a feature of conformal symmetry and may not be present in realistic simulations of heavy ion collisions. For this reason, we do not think that additional time steps are needed. For the comparison with numerical simulations, performed in the next sections, running additional time steps would be numerically (extremely) expensive and

the addition of such plots would not change the conclusions shown here.

2.4.1 Numerical Comparison

While there are analytical and semi-analytical solutions of relativistic ideal fluid dynamics [63, 77–79], the same is not the case for Israel-Stewart theory. This makes testing numerical algorithms that solve the equations of relativistic fluid dynamics rather problematic. Procedures such as fixing the numerical viscosity, choosing appropriate parameters for flux limiters, etc, which strongly rely on trial and error, become then highly nontrivial. Furthermore, most algorithms used to numerically solve the equations of Israel-Stewart theory were not developed for this purpose: they were developed to solve conservation laws or even Navier-Stokes theory, usually in the non-relativistic limit. In practice, most simulation codes used in heavy ion collisions have to adapt such algorithms to also solve Israel-Stewart theory. In this sense, the set of parameters that were found optimal to solve certain problems in the non-relativistic regime, such as the Riemann problem [80–82], might not be optimal to solve Israel-Stewart theory in the conditions produced in heavy ion collisions.

In this section, we compare numerical solutions of dissipative fluid dynamics obtained via the Kurganov-Tadmor (KT) algorithm [83, 84] using MUSIC [64–66], with semi-analytical solutions of (conformal) Israel-Stewart theory in the Gubser flow scenario. We show how this can be used to probe not only the quality and accuracy of the dynamical simulation but also to find the optimal value for some of the (numerical) parameters that exist in the algorithm. The numerical hydrodynamics results were done by the McGill group as part of our collaboration in our paper [53]. We include these results in this thesis as an evidence of the potential uses of the solutions of IS Gubser Flow for the heavy ion community.

In the standard version of MUSIC, the evolution equations that are solved are already those listed in Eqs. (2.8), and (2.17). Therefore, the solutions calculated with MUSIC can already be compared with those of Gubser flow obtained in the previous section.

The numerical implementation is very similar to the one discussed in the last section, for instance the initial temperature is $\hat{T}(0) = 1.2$ fm^{-1}. The shear-stress tensor at $\rho = 0$ is initialized to be $\pi^{\mu\nu} = 0$. The viscosity in MUSIC is set to $\eta/s = 0.2$ while the relaxation time is fixed to $\tau_\pi = 5\eta/(\varepsilon + P)$, i.e., $c = 5$. This parametrization for the relaxation time guarantees that the fluid dynamical evolution is causal [74]. The time step and grid spacing used in the numerical simulation are $\delta\tau = 0.005$ fm and $\delta x = \delta y = 0.05$ fm, respectively ($\delta\tau$, δx, and δy are small enough to achieve the continuum limit). We remark that in Gubser flow the values of the transport coefficients actually affect the initial condition of the fluid, since in this scheme the initial condition in hyperbolic coordinates must also be

constructed by actually solving the fluid-dynamical equations in the generalized de Sitter space.

Note that MUSIC was originally designed to solve Israel-Stewart theory in 3+1–dimensions, while the Gubser flow solution assumes boost invariance (and radial symmetry in the transverse plane). In a numerical simulation in 3+1–dimensions, boost invariance can be trivially obtained by providing an initial condition that is also boost invariant. In this situation, the solutions of fluid dynamics should maintain exact boost invariance, remaining trivial in the longitudinal direction. We checked that this does occur in the solutions obtained with MUSIC: the temperature and $\pi^{\mu\nu}$ profiles remain (exactly) constant in the ξ–direction (e.g., $\pi^{\xi x}$, $\pi^{x\xi}$, $\pi^{\xi y}$, $\pi^{y\xi}$ are exactly zero) while the longitudinal component of the velocity field is exactly zero. This is only not the case at the boundary of the grid where boost invariance is not exactly maintained due to finite size effects.

2.4.2 Comparison to semi-analytical solution

In the following we compare the numerical solutions of MUSIC with the semi-analytical solutions of Israel-Stewart theory. Figures 2.18 and 2.19 show the spatial profiles of temperature, T, velocity, u^x, and the $\xi\xi$, yy, and xy components of the shear-stress tensor, $\pi^{\xi\xi}$, π^{yy}, and π^{xy}, respectively. Without loss of generality, T, u^x, $\pi^{\xi\xi}$, π^{yy} are shown as a function of x in the $y = 0$ axis, while the π^{xy} profile is shown as a function of x in the $x = y$ direction. The component π^{xy} vanishes on the x,y–axis, which we verified also happens in MUSIC. Note that all the other components of $\pi^{\mu\nu}$ can be obtained from the 3 components displayed, i.e., $\pi^{\xi\xi}$, π^{yy}, and π^{xy}.

One can see that the agreement between the numerical simulation and the semi-analytical solutions is very good. Only the xy component of the shear-stress tensor displayed some oscillation at late times. However, since this component is small, this oscillation is not enough to spoil the overall agreement.

We remark that such good agreement could only be obtained by adjusting the flux limiter used in the KT algorithm. Flux limiters are employed in MUSCL scheme algorithms, such as the KT algorithm, to control artificial oscillations that usually occur when using higher order discretization schemes for spatial derivatives. Such spurious oscillations are known to appear when resolving shock problems, solutions with discontinuities in density profiles or velocity field, or even when describing systems which display high gradients, such as the system created in relativistic heavy ion collisions. Since dissipative effects originate mainly from space-like gradients of the velocity field, flux limiters are essential in order to obtain a precise numerical solution of dissipative fluid dynamics.

Currently, there are several flux limiter algorithms available and many others still being developed. In MUSIC, the van Leer minmod filter is used [64–66]. In this case, the

gradients of currents and fluxes are controlled according to a free parameter χ, which may vary from $\chi = 1$ (most dissipative) to $\chi = 2$ (least dissipative). The optimal value of χ can vary case by case and is usually fixed by trial and error; in previous work, MUSIC was run with $\chi = 1.1$. However, the agreement displayed in Figs. 2.18 and 2.19 is only obtained by choosing a larger value, $\chi = 1.8$, corresponding to the less diffusive case. The solutions of the temperature and velocity fields are not very sensitive to changes in the flux limiter scheme. On the other hand, the solutions of the shear-stress tensor do depend on the choice of this numerical parameter. In Fig. 2.20 we show the numerical solutions of MUSIC obtained with $\chi = 1.1$ (open circles) for the xx and yy components of the shear-stress tensor, which are the components most sensitive to this parameter. These solutions are compared with those of $\chi = 1.8$ (full circles) and the semi-analytical solutions (solid line). One can see that when $\chi = 1.1$ the agreement becomes worse, demonstrating the usefulness of the semi-analytic solution found in this paper in testing the algorithm. It should be noted that, if a flux limiter is not employed at all, it is not possible to properly describe the Gubser flow solutions of Israel-Stewart theory.

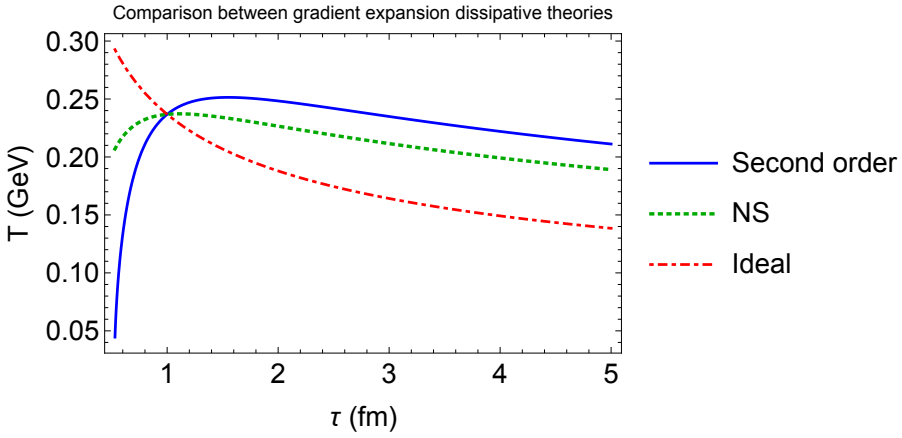

(a)

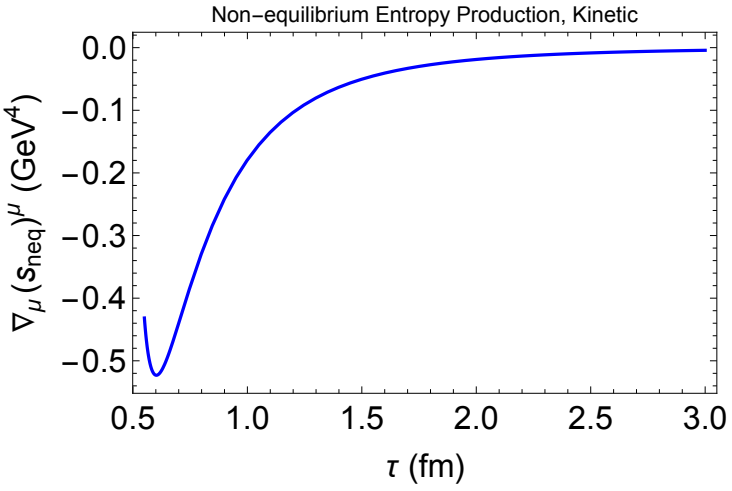

(b)

Figure 2.2: *Comparison between the solutions for the temperature in the three different hydrodynamic theories, ideal, Navier-Stokes and second order constructed via gradient expansion, all using the kinetic theory values of massless ideal gas. In the second figure we plot the non-equilibrium entropy production for the second order theory. Both the temperature and the non-equilibrium entropy are not well-defined at early times.*

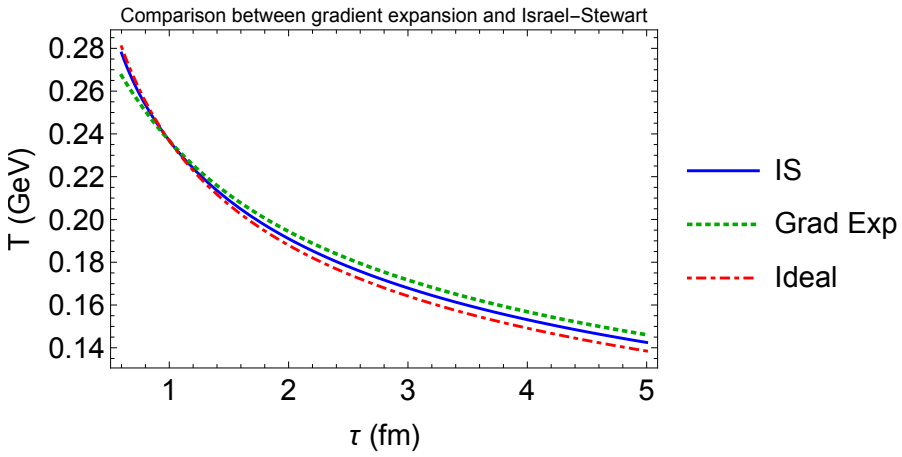

(a)

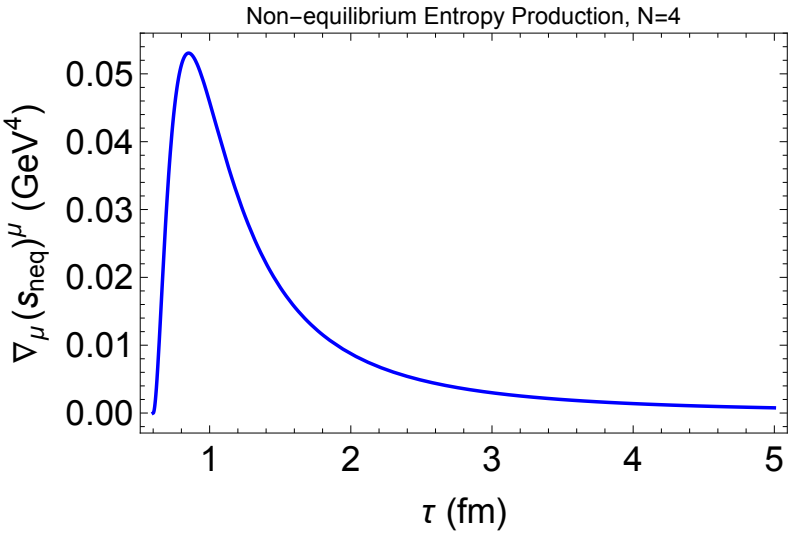

(b)

Figure 2.3: *Comparison between the solutions for the temperature in the three different hydrodynamic theories, ideal, second order gradient expansion and Israel-Stewart, all using the holographic values of $\mathcal{N} = 4$ SYM transport coefficients. In the second figure we plot the non-equilibrium entropy production for Israel-Stewart theory. The initial conditions are $T(1) = 1.2\,fm^{-1}$ and $f(1) = -0.082$.*

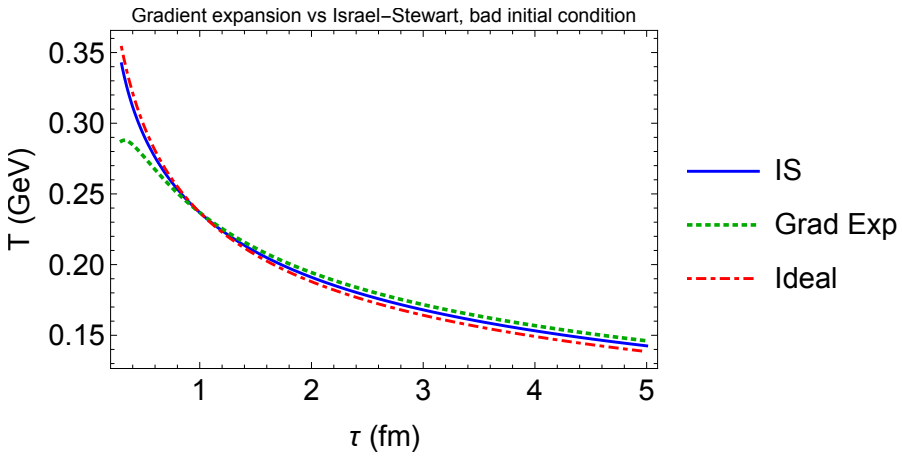

(a)

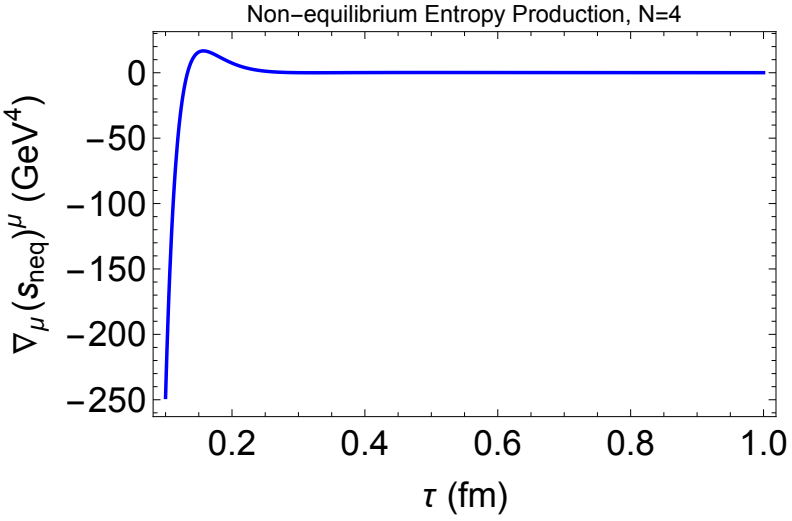

(b)

Figure 2.4: *Comparison between the solutions for the temperature in the three different hydrodynamic theories, ideal, second order gradient expansion and Israel-Stewart, all using the holographic values of $\mathcal{N} = 4$ SYM transport coefficients. In the second figure we plot the non-equilibrium entropy for Israel-Stewart theory. The initial conditions are $T(1) = 1.2\, fm^{-1}$ and $f(1) = \frac{-4\eta/s}{3T(\tau_0)\tau_0} = \frac{-4\eta/s}{3\times 1.2}$, which is the Navier-Stokes value of the dissipative tensor at $\tau = 1$. Notice the negative entropy production at early times due to "bad" initial conditions.*

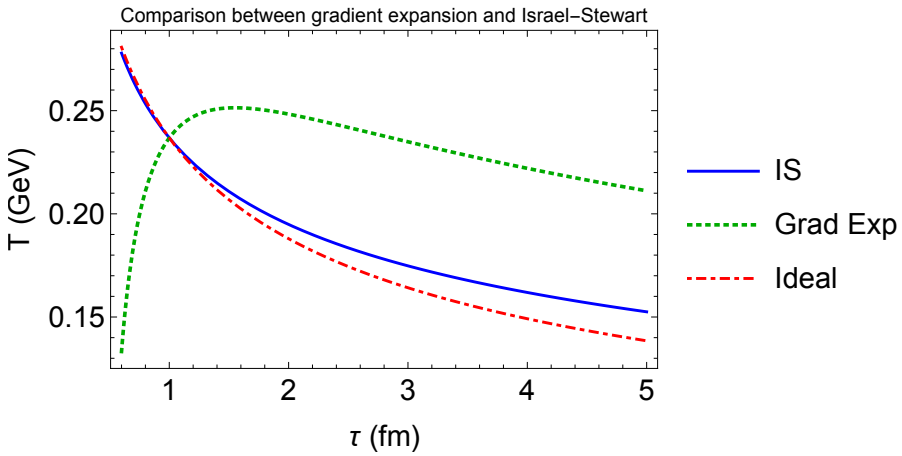

(a)

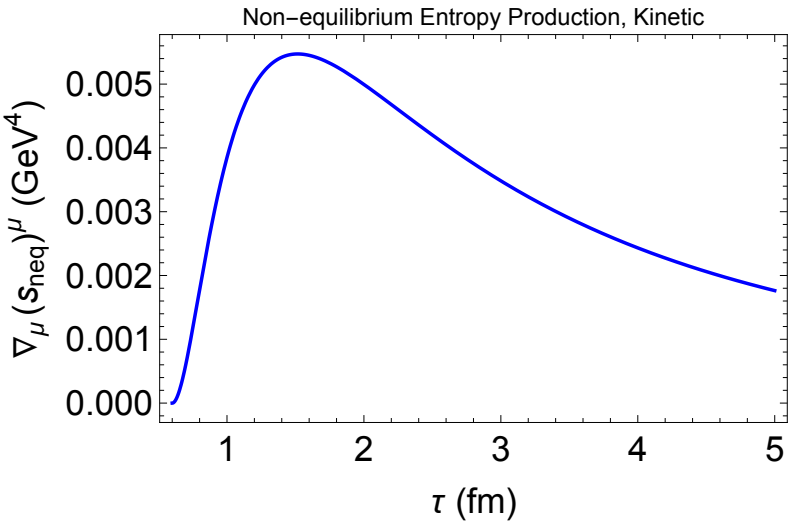

(b)

Figure 2.5: *Comparison between the solutions for the temperature in the three different hydrodynamic theories, ideal, second order gradient expansion and Israel-Stewart, all using the coefficients from kinetic theory. In the second figure we plot the non-equilibrium entropy production for Israel-Stewart. The initial conditions are* $T(1) = 1.2\,fm^{-1}$ *and* $f(1) = -0.112$*. Notice that the solution is well-behaved, in contrast to Fig. 2.2.*

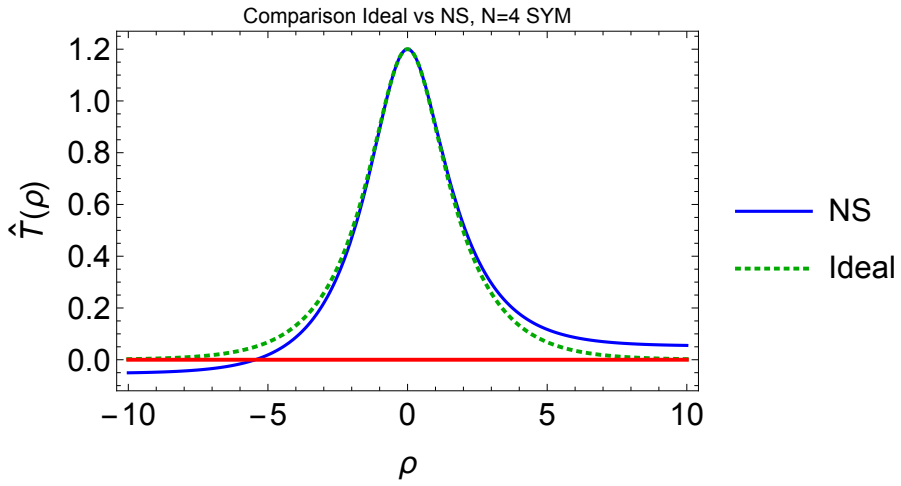

Figure 2.6: *Comparison between ideal and Navier-Stokes theories in Gubser flow, in de-Sitter time, N=4 SYM transport coefficients. Notice the negative temperature regime for NS at large negative ρ. The red solid line delimitates negative and positive temperatures.*

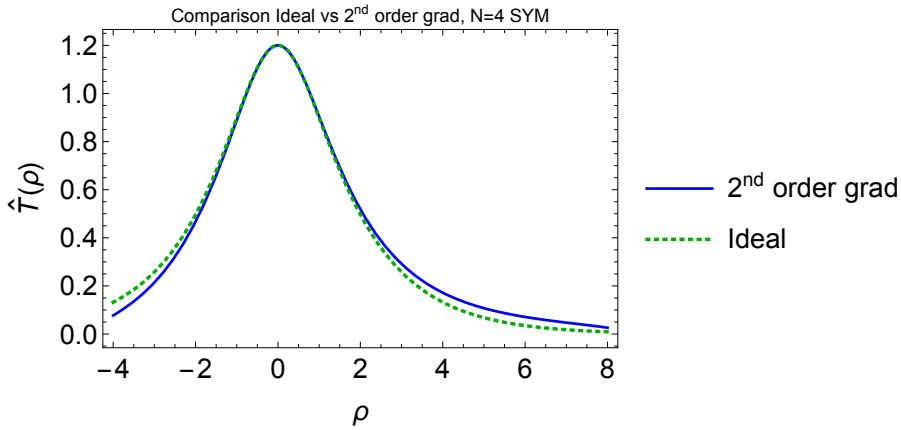

Figure 2.7: *The second order gradient expansion theory, in de-Sitter time, N=4 SYM transport coefficients. The solution is unstable and unphysical in other regions of ρ, therefore the limited plot range.*

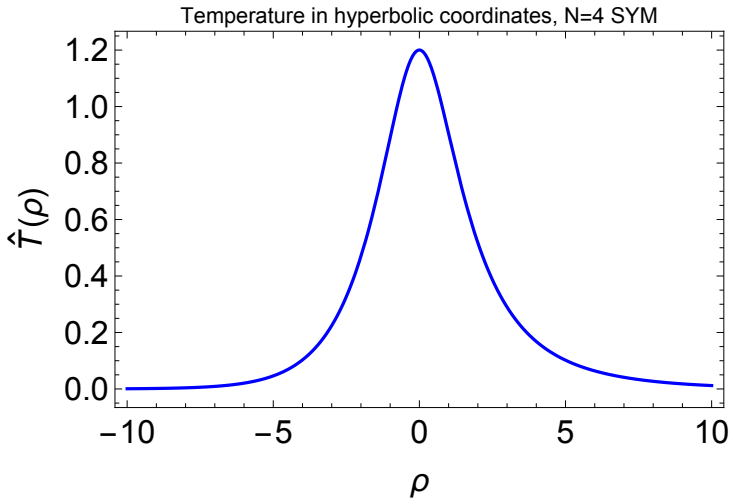

(a)

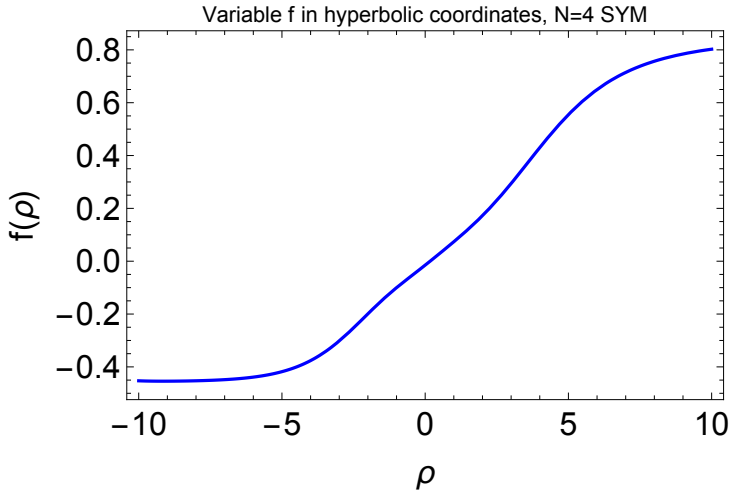

(b)

Figure 2.8: *Gubser flow for Israel-Stewart theory, N=4 SYM transport coefficients. Initial conditions were such that the asymptotic behavior (2.68) was obtained, and* $\hat{T}(0) = 1.2$. $\hat{T}(-20) \approx 3.305 \times 10^{-6}$ *and* $f(-20) \approx 0.839$.

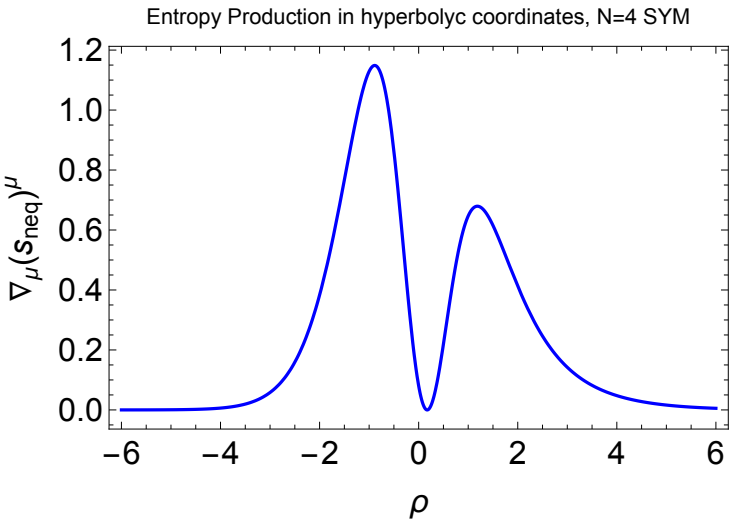

Figure 2.9: *Entropy production in Israel-Stewart theory, see the right hand side of Eq. (2.69). This is the "good" set of initial conditions, integrated from an asymptotic large value of ρ, using $\mathcal{N} = 4$ SYM transport coefficients. Notice that this is always positive quantity, which respects the second law of thermodynamics for any ρ.*

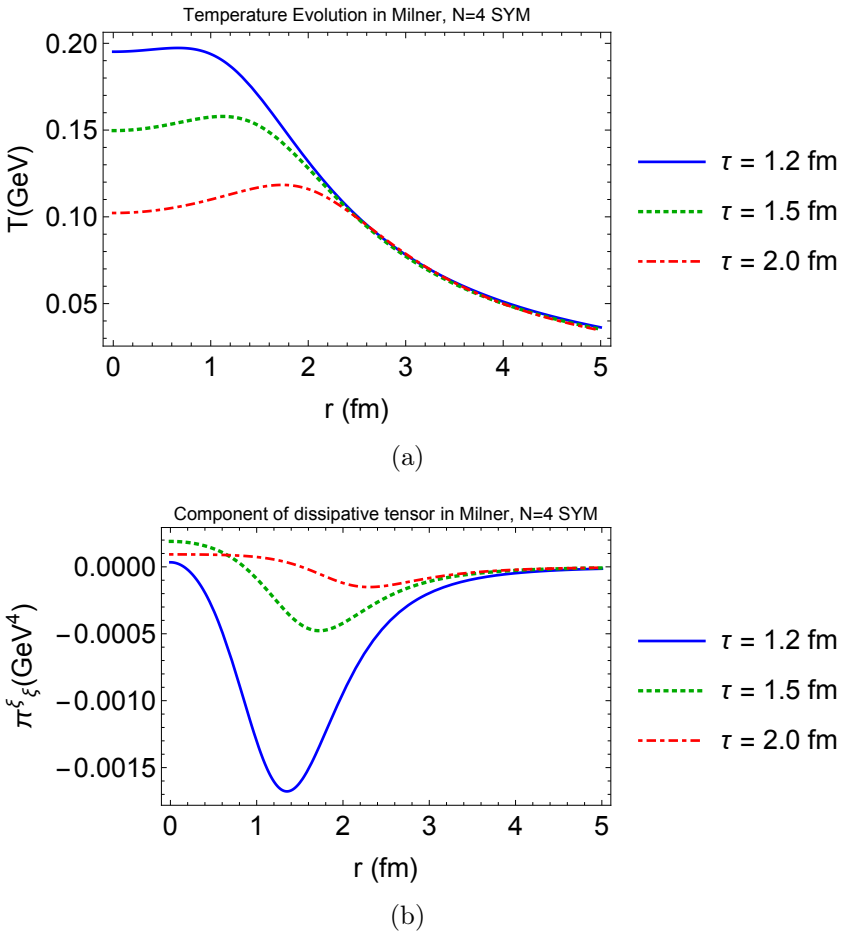

Figure 2.10: *Gubser flow in Milne coordinates for Israel-Stewart theory, with N=4 SYM transport coefficients. This solution has"good" set of initial conditions, integrated from an asymptotic large value of* ρ

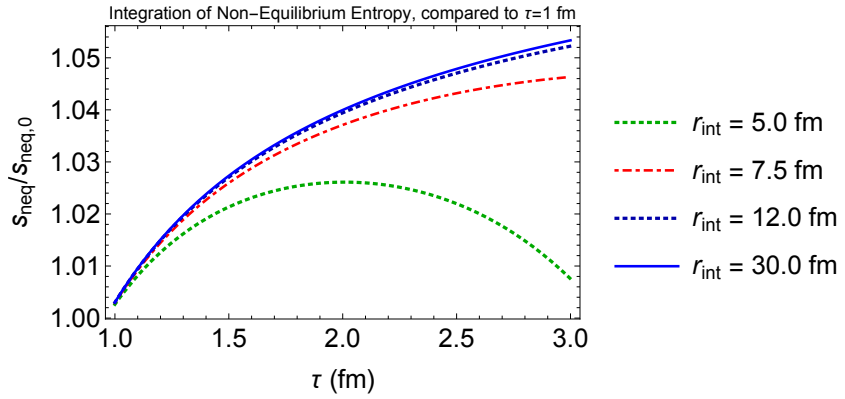

(a)

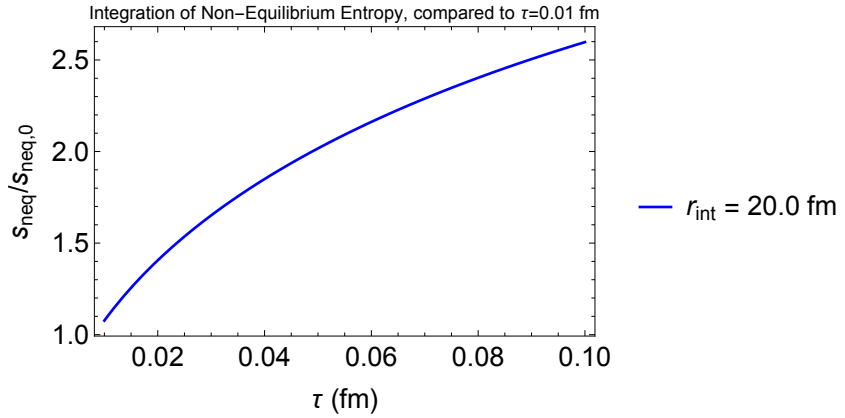

(b)

Figure 2.11: *Normalized entropy production for $\mathcal{N} = 4$ SYM, with consistent asymptotic initial conditions. Fig. 2.11(a) investigates the influence of a limited volume integral, and it saturates once the whole space is taken under consideration. Fig. 2.11(b) illustrates consistency with the second law of thermodynamics for short proper time.*

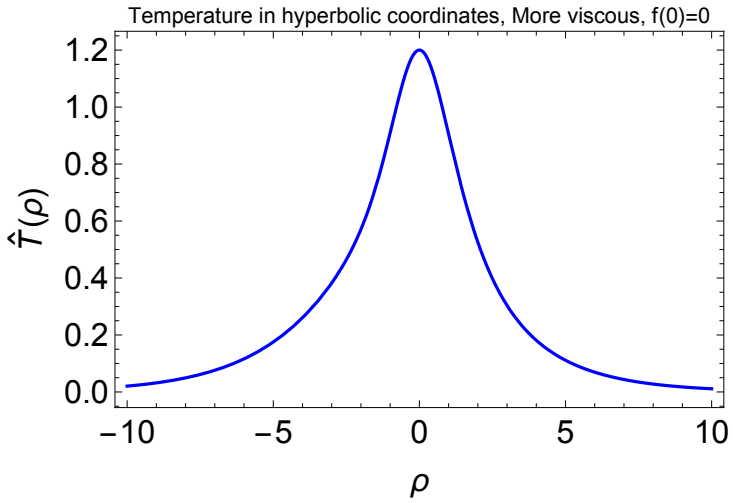

(a)

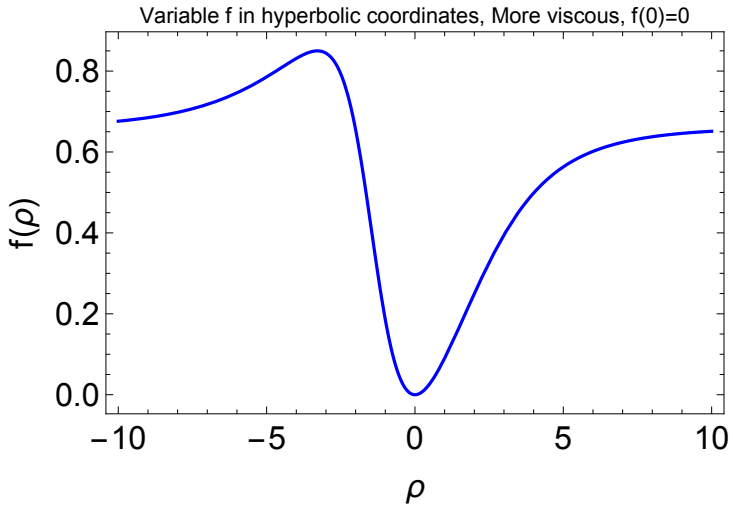

(b)

Figure 2.12: *Gubser flow for Israel-Stewart theory with kinetic theory transport coefficients (2.39) with* $\eta/s = 0.2$. *Initial conditions were* $\hat{T}(0) = 1.2$ *and* $\hat{f}(0) = 0$.

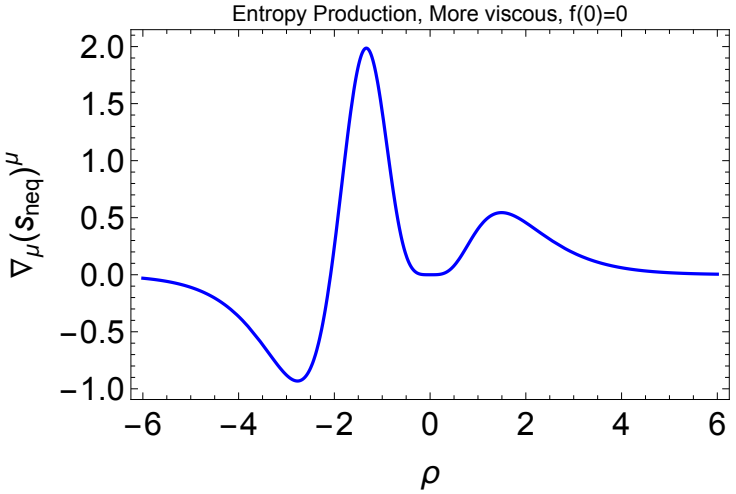

Figure 2.13: *Entropy production in IS theory with kinetic theory transport coefficients (2.39) with $\eta/s = 0.2$. Notice the region where it becomes a negative quantity, which is a unphysical behavior due to the bad initial condition for the dissipative factor f.*

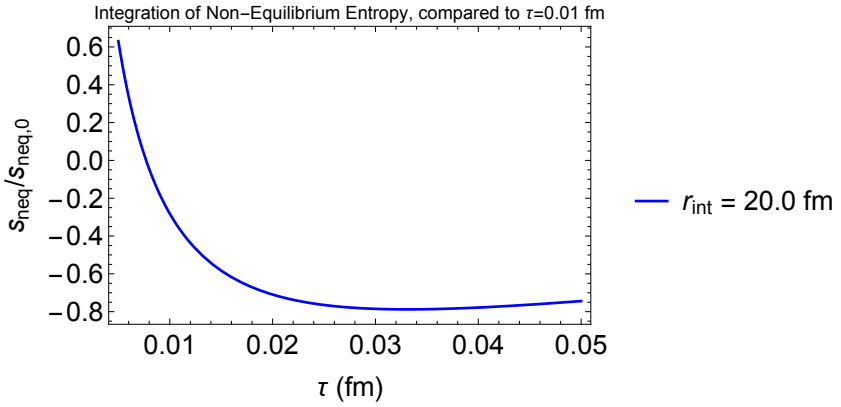

Figure 2.14: *Integrated non-equilibrium entropy with kinetic theory transport coefficients (2.39) with $\eta/s = 0.2$. Notice that it decreases with time, and even becomes negative for short proper time.*

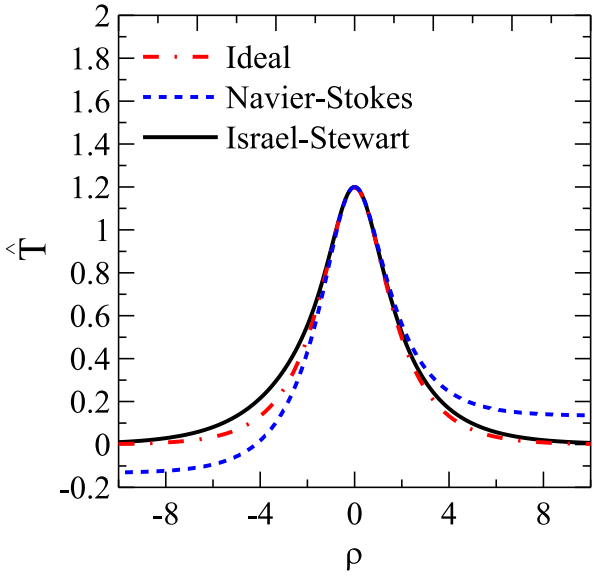

(a)

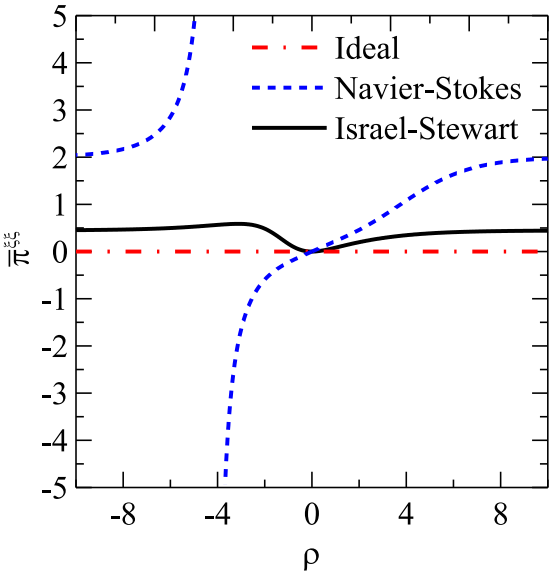

(b)

Figure 2.15: *Comparison between the solutions for* $\hat{T}$ *and* $\bar{\pi}^{\xi}_{\xi}$ *for* $\eta/s = 0.2$, $c = 5$, $\hat{T}(0) = 1.2$ *and* $f(0) = 0$ *found using different versions of the relativistic fluid equations. The solid black lines denote solutions of Israel-Stewart theory, results from relativistic Navier-Stokes theory are in dashed blue, while the dashed-dotted red curves correspond to the ideal fluid case. We recall that* $\bar{\pi}^{\xi\xi}$ *is equivalent to* f *in our notation.*

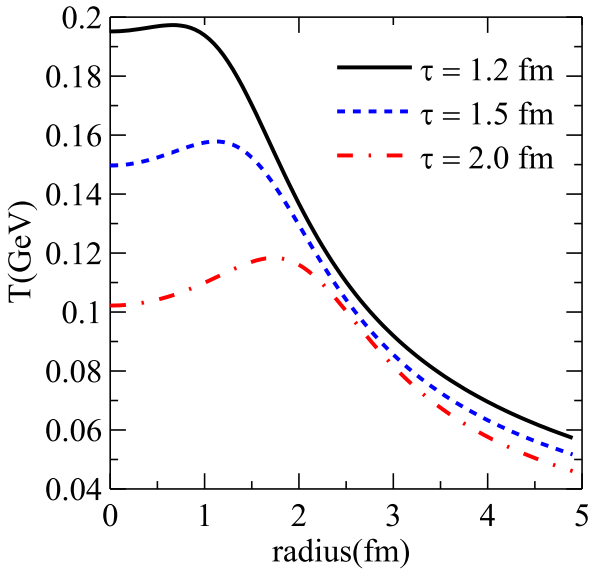

(a)

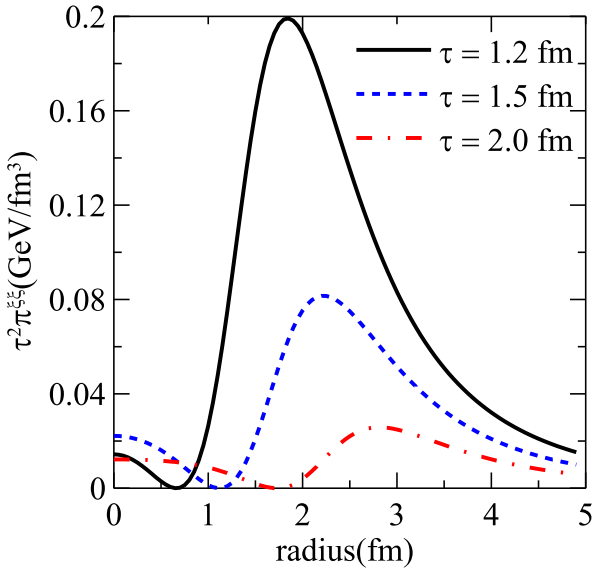

(b)

Figure 2.16: *Temperature and $\tau^2\pi^{\xi\xi}$ profiles in Israel-Stewart theory for $\tau = 1.2$ fm (solid black curves), $\tau = 1.5$ fm (dashed blue curves), and $\tau = 2$ fm (dashed-dotted red curves) with $q = 1$ fm^{-1}, $\eta/s = 0.2$, $c = 5$, $\hat{T}(0) = 1.2$ and $f(0) = 0$.*

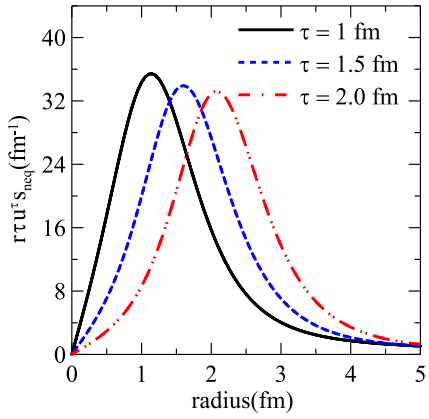

(a)

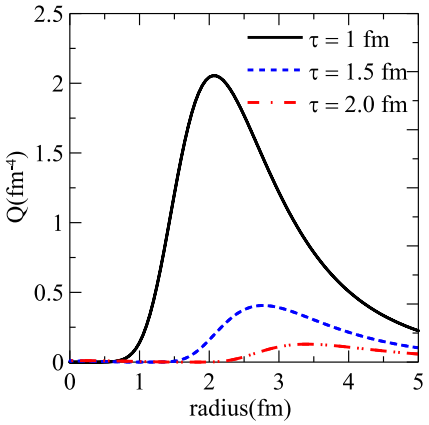

(b)

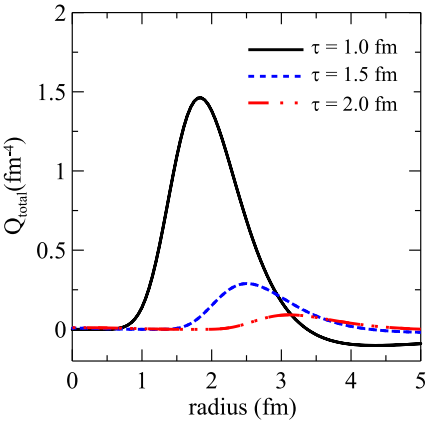

(c)

Figure 2.17: *$\tau r u^\tau s_{\rm neq}$, entropy production up to second order, Q, and total entropy production, $Q_{\rm total}$, profiles as a function of the radius in Israel-Stewart theory for $\tau = 1$ fm (solid black curves), $\tau = 1.5$ fm (dashed blue curves), and $\tau = 2$ fm (dashed-dotted red curves) .*

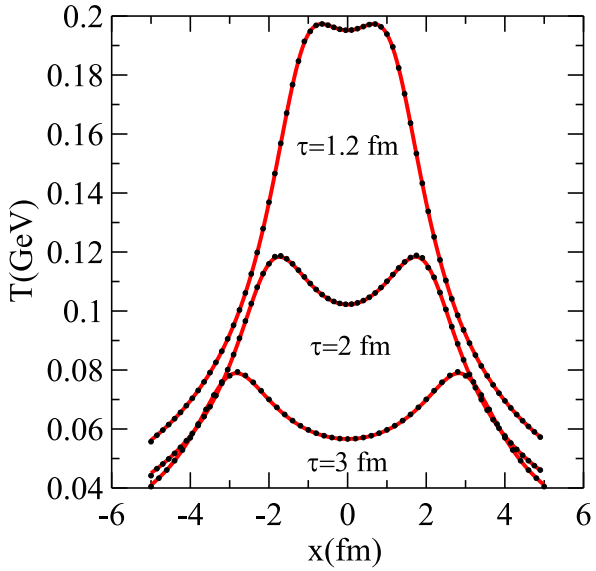

(a)

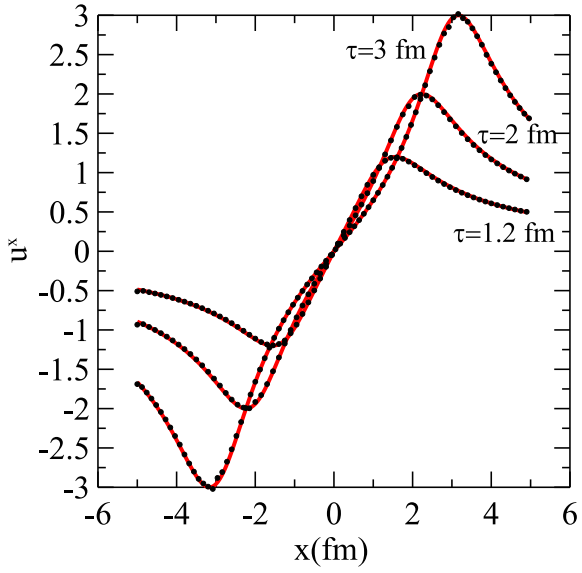

(b)

Figure 2.18: *Comparison between the solutions for temperature (left panel) and the x–component of the 4-velocity (right panel) from Gubser flow and* MUSIC *(numerical), as a function of x. In this plot $\eta/s = 0.2$ and $\tau_\pi T = 5\eta/s$. The solid lines denote the semi-analytic solution while the points denote solutions obtained from* MUSIC.

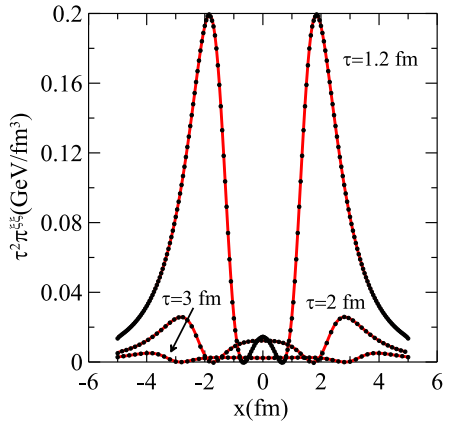

(a)

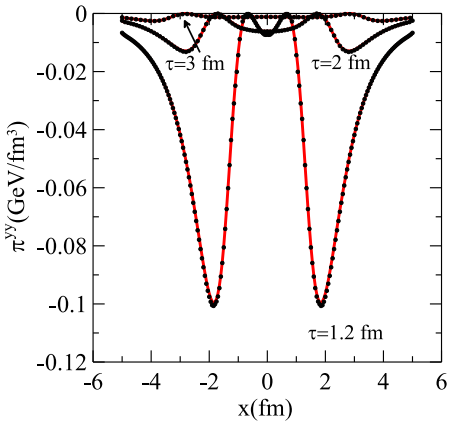

(b)

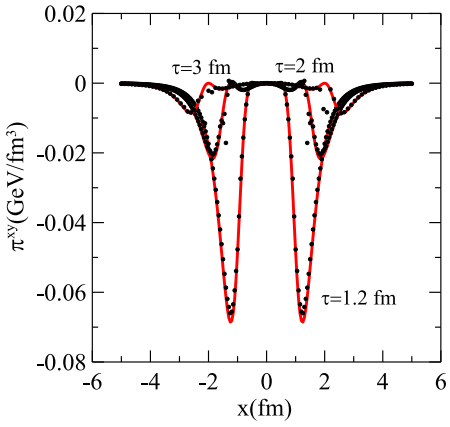

(c)

Figure 2.19: *Comparison between the solutions for the ξξ (left panel), yy (right panel), and xy (lower panel) components of the shear-stress tensor from Gubser flow and* MUSIC *(numerical), as a function of x. In this plot $\eta/s = 0.2$ and $\tau_\pi T = 5\eta/s$. The solid lines denote the semi-analytic solution while the points denote solutions obtained from* MUSIC.

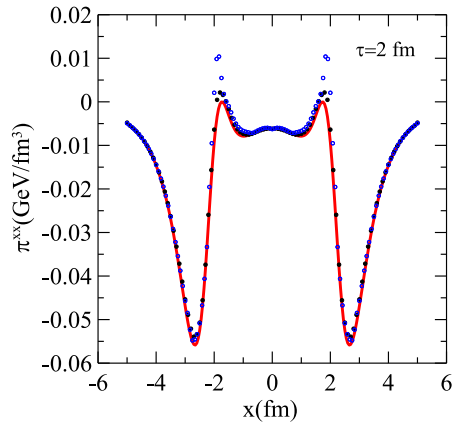

(a)

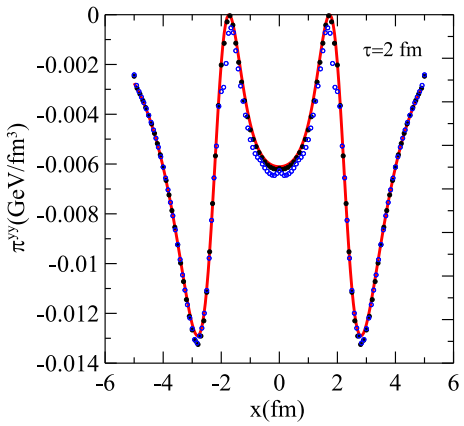

(b)

Figure 2.20: *Numerical solutions of* MUSIC *obtained with* $\chi = 1.1$ *(open circles) for the xx (left panel) and yy (right panel) components of the shear-stress tensor. The full circles correspond to the solutions obtained with* $\chi = 1.8$ *and the solid lines correspond to the semi-analytic solution.*

Figures 2.21(a) and 2.21(b) show the total equilibrium and nonequilibrium entropy (integrated from r =0 to r =5 fm) as a function of time. The entropy is normalized so that its value at $\tau = 1$ fm is equal to 1. The solid (red) line corresponds to the total entropy of the semi-analytical solution, while the circles correspond to the total entropy obtained from our numerical solution. We also included the dashed (blue) and dash-dotted (green) lines in Fig. 2.21(b), which corresponds to the total nonequilibrium entropy integrated over larger volumes, r =0 to r =7.5 fm, and r =0 to r =12 fm, respectively. As one can see, the agreement between the total entropy obtained from the numerical solution and the semi-analytic solution is very good, indicating a negligible amount of numerical entropy production in the simulation. As already mentioned, the equilibrium entropy does not satisfy the second law of thermodynamics, so it does not have to increase with time. On the other hand, the nonequilibrium entropy is expected to increase with time as long as the $\mathcal{O}(4)$ term in Eq. (2.47) remains small. As shown in the previous section, the

overall entropy produced between $r = 0$–5 fm is positive in the semi-analytical solution, at least for times larger than $\tau = 1$ fm. Note that we do not integrate the nonequilibrium entropy density over an infinite volume so, at some point, the integrated nonequilibrium entropy will start to decrease due to the amount of entropy that is leaving the box. This happens for both numerical and semi-analytical solutions around $\tau = 2$ fm. Nevertheless, the agreement between the numerical simulation and the semi-analytical solution remains very good even at these stages.

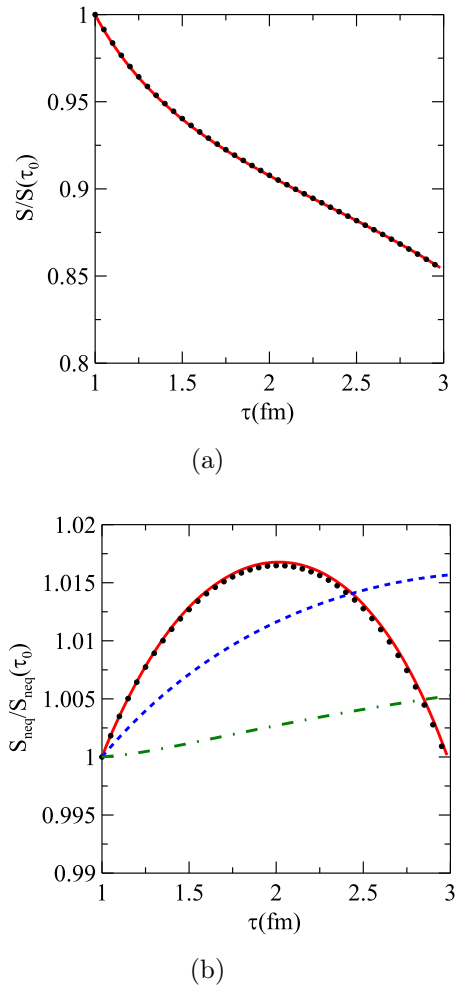

Figure 2.21: *Comparison between the solutions for the total equilibrium entropy (left panel) and total nonequilibrium entropy (right panel) from Gubser flow and* MUSIC *(numerical), as a function of τ. In both plots the total entropy is obtained by integrating corresponding entropy density from $r = 0$ to $r = 5$ fm. The solid lines denote the semi-analytic solution while the points denote solutions obtained from* MUSIC*. On the right panel, we also show the total nonequilibrium entropy obtained by integrating from $r = 0$ to $r = 7.5$ fm (dashed line) and $r = 0$ to $r = 12$ fm (dashed-dotted line).*

2.4.3 Comparison to analytical solution

In the previous section, we showed that an analytical solution for Israel-Stewart theory can be found in the limit of extremely large viscosity or, equivalently, of extremely small temperatures (cold plasma limit). Note that this analytical solution is no longer an approximation if the term $\pi^{\mu\nu}$ is removed from Israel-Stewart theory. That is, if one solves the equation,

$$\frac{\tau_R}{sT}\left(\Delta^{\mu}_{\alpha}\Delta^{\nu}_{\beta}\, D_\tau \pi^{\alpha\beta} + \frac{4}{3}\pi^{\mu\nu}\nabla_\alpha u^\alpha\right) = -\frac{2\eta}{s}\frac{\sigma^{\mu\nu}}{T}, \tag{2.76}$$

instead of Eq. (2.17).

The solution of this equation no longer relaxes to Navies-Stokes theory. However, it can still be used to test algorithms that solve relativistic fluid dynamics. The same algorithm that solves Israel–Stewart theory should also be able to solve the above equation of motion and this can be used as an independent and powerful test of a given numerical approach. Furthermore, the term $\pi^{\mu\nu}$ is rather simple and does not demand much work to be removed.

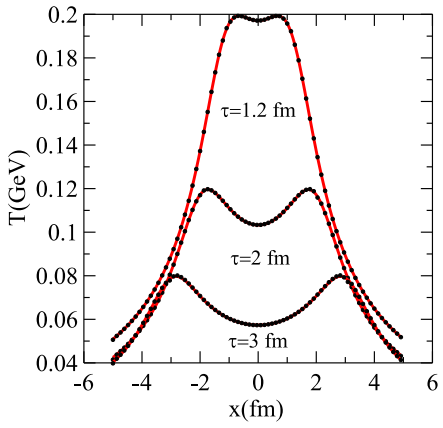

(a)

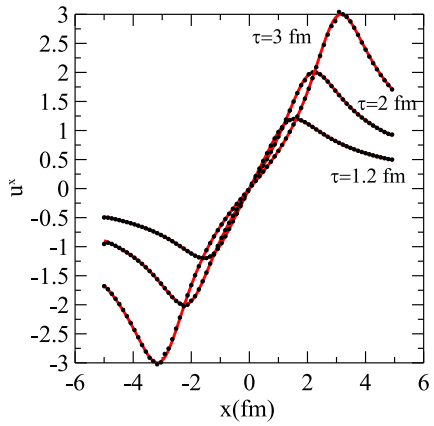

(b)

Figure 2.22: *Comparison between the solutions for temperature (left panel) and the x–component of the 4-velocity from Gubser flow and* MUSIC *(numerical), as a function of x. In this plot $\eta/s = 0.2$ and $\tau_\pi T = 5\eta/s$. The solid lines denote the analytic solution while the points denote solutions obtained from* MUSIC.

As already mentioned, in this case the solution of the theory in de Sitter space can be found analytically, see Eqs. (2.75) and (2.74). We numerically solved Eqs. (2.8) and (2.76) using MUSIC by subtracting the aforementioned term, using the same initial condition described before. The comparison is showed in Figs. 2.22 and 2.23, which show the spatial profiles of T, u^x, $\pi^{\xi\xi}$, π^{yy}, and π^{xy}. The solid lines correspond to the analytical solutions

while the points correspond to the numerical solutions of Eq. (2.76) obtained with MUSIC.

Note that the level of agreement is the same as before. The solutions in hyperbolic coordinate even appear to be qualitatively the same, containing the same general structures as the full solutions. However, from a practical point of view, the above solutions are very convenient to test a code since they are already cast in the form of functions and can be written directly into the code.

2.5 Conclusions of the chapter

We have presented the first analytical and semi-analytical solutions of a radially expanding viscous conformal fluid that follows relaxation-type equations such as the Israel-Stewart equations. The $\mathrm{SO}(3) \otimes \mathrm{SO}(1,1) \otimes \mathrm{Z}_2$ invariant solutions for the temperature, shear stress tensor, and flow discussed here can be used to test the existing numerical algorithms used to solve the equations of motion of viscous relativistic fluid dynamics in ultrarelativistic heavy ion collision applications.

We further demonstrated how the solutions derived in this thesis can be used to optimize the numerical algorithm of a well known hydrodynamical code, fixing numerical parameters that can only be determined by trial and error. The MUSIC simulation code was shown to produce results that are in good agreement with the analytic and semi-analytic solutions of Israel-Stewart theory undergoing Gubser flow.

Also, we showed how entropy production, in both Bjorken and Gubser flows, constraints the set of physical initial conditions for the dissipative tensor, which is a non-trivial test of the validity of the Israel-Stewart approach in comparison to the gradient expansion.

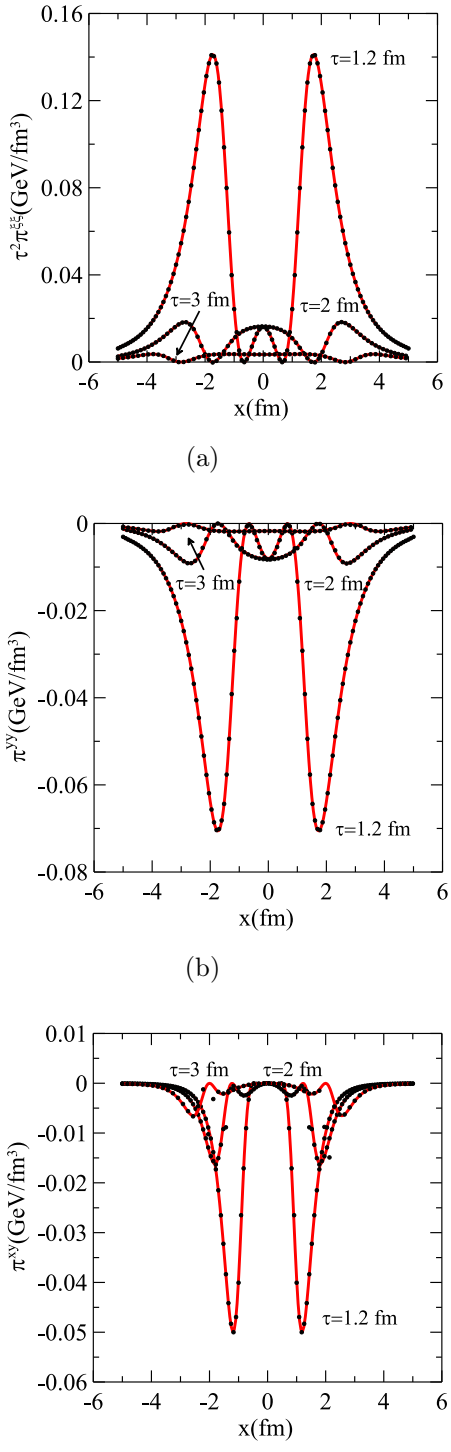

Figure 2.23: *Comparison between the solutions for the $\xi\xi$, yy, and xy components of the shear-stress tensor from Gubser flow and* MUSIC *(numerical), as a function of x. In this plot $\eta/s = 0.2$ and $\tau_\pi T = 5\eta/s$. The solid lines denote the analytic solution while the points denote solutions obtained from* MUSIC.

Chapter 3

Nonlinear Waves in second order relativistic hydrodynamics

In this chapter we shift gears from exact solutions of hydrodynamics to focus on a perturbative nonlinear method in $1+1$ dimensions. We investigate how the presence of a nonzero shear viscosity relaxation time affects wave propagation in relativistic fluids. The majority of this chapter is based on our paper [57].

Waves in a hadronic medium may be caused, for example, by fluctuations in baryon number or energy density. These fluctuations may be produced by inhomogeneous initial conditions which, as pointed out in [85], are the result of quantum fluctuations in the densities of the two colliding nuclei and also in the energy deposition mechanism. These fluctuations and their phenomenological implications have been studied extensively [66, 86–92] because they may be responsible for the angular correlations of particle emission observed in heavy-ion experiments. There are also hydrodynamic fluctuations [85], which are the result of finite particle number effects in a given fluid cell. This generates local thermal fluctuations of the energy density (and flow velocity) which propagate throughout the fluid. Furthermore, there may be fluctuations induced by energetic partons, which have been scattered in the initial collision of the two nuclei and propagate through the medium, losing energy and acting as a source term for the hydrodynamical equations [93–99]. Finally, there may be also freeze-out fluctuations, which may be caused by finite particle number effects during and after the freeze-out of the hydrodynamically expanding fluid.

In non-relativistic fluid dynamics the most successful theory of dissipative systems is the Navier-Stokes (NS) theory [9, 100]. For instance, one can use this theory to investigate the evolution of density perturbations in a non-relativistic hadron gas and in a non-relativistic quark gluon plasma. Perturbations are usually studied with the linearization formalism [67, 101], which is the simplest way to study small deviations from equilibrium

to obtain wave equations, eventually featuring dissipative and relaxation terms. The propagation of perturbations through a QGP has been investigated in several works with the help of a linearized version of the hydrodynamics of perfect fluids and of viscous fluids. In [102] the authors went beyond linearization and considered the effects of shear viscosity on the propagation of nonlinear waves. This study was performed with the help of the well established reductive perturbation method [54–56].

We have already showed inconsistencies in the solutions of the Navier-Stokes equation in Chapter 2. In Chapter 4 we will review and expand the analysis of linear instabilities of NS and higher order gradient expansion theories. As mentioned in the previous chapter, the usual procedure to circumvent such problems is to introduce the Israel-Stewart theory with relaxation type equations of dissipation. One of the motivations for the study outlined in this chapter is to investigate the influence of the relaxation time transport coefficient in solitonic behavior.

We study the propagation of nonlinear waves in relativistic fluids described by (a simplified set of) of the second order conformal IS equations. Solutions of nonlinear equations of motion generally contain nonlinear dispersive and dissipative terms. The relative strength of these different terms depends on microscopic properties of the system, which manifest themselves in the transport coefficients (such as the shear viscosity coefficient, η, and the relaxation time, τ_π) and in the equation of state. Different combinations of these terms generate Korteweg - de Vries solitons, shock waves, strongly damped waves and so on. In principle, given the underlying microscopic theory, one can calculate the transport coefficients and the equation of state to determine the type of waves which can propagate in the system. However, when the underlying theory is QCD this is not an easy task due to the strongly coupled nature of the quark-gluon plasma and one needs to resort to phenomenological models to estimate η and τ_π (the QCD equation of state can be reliably computed on the lattice [23, 24, 103, 104]). The choice of these quantities defines the properties of the solutions of the wave equations. Inconsistent choices may lead to unphysical solutions and this opens the possibility of using waves to put some additional constraints on the values of η and τ_π in the QGP.

Finally, we present how to obtain a system of two coupled differential equations to study nonlinear waves in conformal IS theory. We solve this system numerically, determining the role played by shear viscosity and its relaxation time on wave packet evolution. One of the equations of this system is the Burgers' equation for the first order perturbation in the energy density, which does not contain relaxation effects, and it is, thus, the same equation obtained in the NS-based approach developed in [105]. The other equation describes the second order perturbation in the energy density, where the effects from a nonzero relaxation time coefficient become manifest. Our results indicate the presence

of a "soliton-like", i.e., an approximately solitary wave solution, in IS theory despite the dissipative and relaxation effects. Another motivation to study nonlinear perturbations is the possibility to find an upper bound for the relaxation scale, which is not found in the linear treatment.

Throughout this chapter and the next one we use the mostly minus flat spacetime metric $g_{\mu\nu} = \mathrm{diag}(+,-,-,-)$ and natural units.

3.1 Nonlinear wave equations in Conformal Israel-Stewart theory

The effects from a relaxation timescale τ_π have not yet been studied in the context of nonlinear wave propagation. The RPM was used to study nonlinear waves in relativistic and non-relativistic hydrodynamics in [102, 105–107]. Our goal in this section is to find the nonlinear wave equation that governs the perturbation of the energy density in a hot dissipative and causal fluid described by IS hydrodynamics.

3.1.1 Reductive Perturbation Method

We quickly review the equations of relativistic hydrodynamics when the metric signature is mostly negative. The energy-momentum tensor of a relativistic fluid is

$$T^{\mu\nu} = \varepsilon u^\mu u^\nu - p\Delta^{\mu\nu} + \pi^{\mu\nu} \tag{3.1}$$

where as usual ε is the energy density, p is the pressure, u^μ is the fluid 4-velocity $u^\mu = (\gamma, \gamma\vec{v})$ and γ is the Lorentz factor $\gamma = (1-v^2)^{-1/2}$ (hence, $u^\mu u_\mu = 1$). The connection between ε and p defines the equation of state, which will be taken to be that of a conformal fluid, $\varepsilon = 3p$. The entropy density is then $s = \kappa T^3$, where κ is a numerical coefficient. Furthermore, the projection operator orthogonal to the fluid velocity is given by $\Delta^{\mu\nu} \equiv g^{\mu\nu} - u^\mu u^\nu$. The shear stress tensor $\pi^{\mu\nu}$ is a symmetric (and traceless) tensor that is orthogonal to the flow $u_\mu \pi^{\mu\nu} = 0$ (i.e, the Landau frame [9]). Besides the energy-momentum conservation equations $\partial_\mu T^{\mu\nu} = 0$, or in explicit form,

$$D\varepsilon + (\varepsilon + p)\theta - \pi^{\mu\nu}\,\sigma_{\mu\nu} = 0 \tag{3.2}$$

$$(\varepsilon + p)Du^\alpha - \nabla^\alpha_\perp p + \Delta^\alpha_\nu \partial_\mu \pi^{\mu\nu} = 0 \tag{3.3}$$

the simplified set of the conformal IS equations [68] that defines the dynamics of the shear stress tensor $\pi^{\mu\nu}$ used here are [53]

$$\tau_\pi\left(\Delta^\mu_\alpha\Delta^\nu_\beta D\pi^{\alpha\beta}+\frac{4}{3}\pi^{\mu\nu}\theta\right)+\pi^{\mu\nu}=2\eta\sigma^{\mu\nu} \tag{3.4}$$

With the RPM we can derive the nonlinear wave equation for perturbations in a fluid performing the following set of operations [102, 106] (the majority of the detailed calculation can be found in Appendix D):

(a) Rewrite Eqs. (3.2), (3.3), and (3.4) using the following dimensionless variables

$$\hat{\varepsilon}(x,t)=\frac{\varepsilon(x,t)}{\varepsilon_0}\ ,\ \hat{v}_x(x,t)=\frac{v_x(x,t)}{c_s}=\sqrt{3}\ v_x(x,t)\qquad\text{and}\qquad\hat{\pi}^{xx}(x,t)=\frac{\pi^{xx}(x,t)}{p_0} \tag{3.5}$$

(b) Change the coordinates in Eqs. (3.2), (3.3), and (3.4) from (x,t) to the (X,Y) space defined by the "stretched coordinates" [54–56]

$$X=\sigma^{1/2}\frac{(x-c_st)}{L}=\sigma^{1/2}\frac{1}{L}\left(x-\frac{t}{\sqrt{3}}\right)\qquad\text{and}\qquad Y=\sigma^{3/2}\frac{c_st}{L}=\sigma^{3/2}\frac{t}{\sqrt{3}L} \tag{3.6}$$

where L is a characteristic length scale of the problem, which will be simplified in the final expressions, and σ is a small $(0<\sigma<1)$, dimensionless expansion parameter. We also change the shear viscosity coefficient and the relaxation time to the (X,Y) space in the following way [108, 109]

$$\eta=\sigma^{1/2}\,\tilde{\eta}\qquad\text{and}\qquad\tau_\pi=\sigma^{1/2}\,\tilde{\tau}_\pi\,. \tag{3.7}$$

We refer the reader to the Appendix D for the details. While the scaling of η with σ was known in literature [108, 109], the proposed scaling of τ_π with σ used here is new and it is the simplest choice that is consistent with the sound mode dispersion relation (discussed in Chapter 4).

(c) Expand the variables in Eq. (3.5) around their equilibrium values

$$\hat{\varepsilon}=\frac{\varepsilon}{\varepsilon_0}=1+\sigma\varepsilon_1+\sigma^2\varepsilon_2+\sigma^3\varepsilon_3+\ldots \tag{3.8}$$

$$\hat{v}_x=\frac{v_x}{c_s}=\sigma v_1+\sigma^2 v_2+\sigma^3 v_3+\ldots \tag{3.9}$$

and

$$\hat{\pi}^{xx} = \frac{\pi^{xx}}{p_0} = \sigma\pi_1^{xx} + \sigma^2\pi_2^{xx} + \sigma^3\pi_3^{xx} + \dots . \tag{3.10}$$

After the expansions, we organize the resulting equations in powers of σ, neglecting terms with powers greater than σ^3. In the usual RPM method, only terms proportional to σ and σ^2 are kept. However, the linear hydrodynamical modes (discussed in Chapter 4) show that relaxation effects may appear only in the next order of the usual expansion, i.e., at order $\hat{k}^3$. For this reason we consider the σ expansion up to $\mathcal{O}(\sigma^3)$ terms to study relaxation effects in nonlinear waves.

(d) By solving the system of algebraic equations: $\sigma^{1/2}\{\dots\} = 0$, $\dots$, $\sigma^3\{\dots\} = 0$ obtained in the step (c), it is possible to find the system of wave equations in the (X, Y) space. Such system may be transformed back to the (x, t) coordinates through the stretching transformations (3.6) and (3.7) yielding the final system of nonlinear wave equations for the perturbations in the energy density.

3.1.2 Nonlinear wave equations

The set of differential equations obtained from the RPM method is given by

$$\frac{\partial}{\partial\hat{t}}\hat{\varepsilon}_1 + \frac{1}{\sqrt{3}}\frac{\partial}{\partial\hat{x}}\hat{\varepsilon}_1 + \frac{1}{2\sqrt{3}}\hat{\varepsilon}_1\frac{\partial}{\partial\hat{x}}\hat{\varepsilon}_1 = \frac{\chi}{2}\frac{\partial^2}{\partial\hat{x}^2}\hat{\varepsilon}_1 \tag{3.11}$$

and

$$\begin{aligned}\frac{\partial}{\partial\hat{t}}\hat{\varepsilon}_2 + \frac{1}{\sqrt{3}}\frac{\partial}{\partial\hat{x}}\hat{\varepsilon}_2 + \frac{1}{2\sqrt{3}}\hat{\varepsilon}_1\frac{\partial}{\partial\hat{x}}\hat{\varepsilon}_2 - \frac{\chi}{2}\frac{\partial^2}{\partial\hat{x}^2}\hat{\varepsilon}_2 + \frac{1}{2\sqrt{3}}\hat{\varepsilon}_2\frac{\partial}{\partial\hat{x}}\hat{\varepsilon}_1 + \frac{\chi}{4}\hat{\varepsilon}_1\frac{\partial^2}{\partial\hat{x}^2}\hat{\varepsilon}_1 \\ + \frac{1}{4}\hat{\varepsilon}_1\frac{\partial}{\partial\hat{t}}\hat{\varepsilon}_1 + \frac{1}{4\sqrt{3}}\hat{\varepsilon}_1\frac{\partial}{\partial\hat{x}}\hat{\varepsilon}_1 + \frac{\chi}{2}\left[\frac{\chi\sqrt{3}}{4} - \frac{\hat{\tau}_\pi}{\sqrt{3}}\right]\frac{\partial^3}{\partial\hat{x}^3}\hat{\varepsilon}_1 = 0\,,\end{aligned} \tag{3.12}$$

where $\hat{\varepsilon}_1 \equiv \sigma\varepsilon_1$, $\hat{\varepsilon}_2 \equiv \sigma^2\varepsilon_2$ and $\chi \equiv 4\eta_0/(3s_0)$. The details of the calculations and assumptions needed to derive these equations are presented in the Appendix D. Also, given the solution of (29) and (30), one is also able to study the behavior of $\hat{\pi}^{xx}$. However, in this thesis we shall focus on the energy density disturbance and leave a detailed study of the shear stress tensor in this approach for future work.

We emphasize that the Burgers' equation (3.11) for the first order energy perturbation $\hat{\varepsilon}_1$ does not contain relaxation effects and, thus, it is the same both in Navier-Stokes and in Israel-Stewart theory. This feature has lead us to consider perturbations up to third order in energy density and fluid velocity. This provides the first equation where the relaxation time coefficient appears: Eq. (3.12) for $\hat{\varepsilon}_2$.

3.2 Numerical results and discussion

An analytical solution of the Burgers' equation (3.11) can be obtained by the *hyperbolic tangent expansion method* [102] and its variants. However, it is not possible to find a finite solution after substituting the analytical solution for $\hat{\varepsilon}_1$ into (3.12) to solve it for $\hat{\varepsilon}_2$. We have thus proceeded to solve (3.11) and (3.12) numerically.

3.2.1 Soliton initial profile

Several different sets of parameters and initial profiles are considered in this study. Starting with the following typical strong coupling parameters $3\chi/4 = \eta_0/s_0 = 1/(4\pi)$ and $\hat{\tau}_\pi = [2 - ln2]/(2\pi)$ [68], we show the propagation of nonlinear waves in Fig. 3.1. We start by solving (3.11) with the following initial condition

$$\hat{\varepsilon}_1(\hat{x}, 0) = A_1 \; sech^2\left(\frac{\hat{x}}{B_1}\right) \tag{3.13}$$

and inserting the obtained numerical solution of (3.11) into (3.12) with the initial profile for $\hat{\varepsilon}_2$

$$\hat{\varepsilon}_2(\hat{x}, 0) = A_2 \; sech^2\left(\frac{\hat{x}}{B_2}\right). \tag{3.14}$$

The first case in Fig. 3.1 corresponds to $A_1 = 0.8$, $A_2 = 0.2$ and $B_1 = B_2 = 0.5$. The numerical solution of (3.11), (3.12), and the total energy perturbation given by (3.8), $\hat{\varepsilon} = 1 + \hat{\varepsilon}_1 + \hat{\varepsilon}_2$, are shown in Fig. 3.1. We notice that, in spite of the dissipative and relaxation effects, the perturbations still survive as time increases.

In Fig. 3.2 we show similar calculations as in Fig. 3.1 but now considering large viscosity and relaxation time coefficients given respectively by $\eta_0/s_0 = 1$ and $\hat{\tau}_\pi = 5\eta_0/s_0$, which is in the ballpark of kinetic theory calculations [29, 30]. In Fig. 3.2(a) we obtain the expected result for the Burgers' equation with large viscosity: a strong dissipation of the initial pulse. In Fig. 3.2(b) we also obtain the same dissipation effect but at some intermediate time scales $\hat{t} = 5$ to $\hat{t} = 20$ there is also rarefaction. The total perturbation does not survive for longer times and the perturbed fluid tends to recover the background configuration $\hat{\varepsilon} = 1$ as time increases.

The calculations shown in Fig. 3.1 are repeated in Fig. 3.3 (same transport coefficients) now with different initial conditions, i.e, larger widths $B_1 = B_2 = 3$. Fig. 3.3 shows an intermediate configuration between shock wave formation (wall formation) and an approximately stable soliton propagation for the total perturbation $\hat{\varepsilon}$ in 3.3(c). We note that pulses with larger width are not only more stable but the second order effects become more significant for larger times.

In Fig. 3.4 we considered $A_1 = 0.6$, $A_2 = 0.3$, $B_1 = 0.7$, and $B_2 = 0.5$ for a small viscosity $\eta_0/s_0 = 1/(4\pi)$ and varied the value of the relaxation time coefficient. The values considered were $\hat{\tau}_\pi = 0$ (Navier-Stokes limit) and $\hat{\tau}_\pi = 120\eta_0/s_0$ (where the relaxation time is much more important than the shear viscosity). We only plot the perturbations affected by relaxation: $\hat{\varepsilon}_2$ and consequently $\hat{\varepsilon}$. We notice that the size of the perturbations increase when one increases the relaxation coefficient. This limit is not a very plausible choice but it is interesting to see that the resulting solutions are unstable since they generate values of $\hat{\varepsilon}_2$ which are unacceptably large. If we consider that pulses originate from inhomogeneous density profiles or quantum fluctuations, it is reasonable to assume that the most realistic pulses could be in principle more localized in space and thus they would suffer dissipative, nonlinear, and dispersive effects losing its localized profile.

In Eq. (3.12) the terms with η_0/s_0 (except for the last one) contribute to dissipation. The last term of (3.12) introduces dispersion and involves both η_0/s_0 and the combination $\Delta_3 = \eta_0/s_0 - \hat{\tau}_\pi$. When $\hat{\tau}_\pi$ tends to zero we recover the Navier-Stokes limit, where problems with causality and instability are expected to appear. When $\hat{\tau}_\pi$ becomes very large, in principle, no problem was expected to occur. However the very large amplification of the amplitude $\hat{\varepsilon}_2$ is surprising. It implies that a large amount of energy is transferred from the medium to the wave. We see here evidence that the large value chosen for $\hat{\tau}_\pi$ in this particular configuration may be unphysical. This is a interesting finding since in the linear perturbative limit (discussed before in Section II) there were no apparent inconsistencies associated with large values of $\hat{\tau}_\pi$. The existence of an upper bound for $\hat{\tau}_\pi$ can only be seen in the nonlinear perturbation theory used here. However, one may also interpret this enhancement in the amplitude as an indication that the higher order terms that were neglected in the expansion have become significant and must be taken into account (the initial profile is such that the initial spatial gradients are not very small). It would be interesting to check if this nonlinear instability can appear in the existing numerical hydrodynamic codes.

In Fig. 3.5 for a large viscosity $\eta_0/s_0 = 1$ and small amplitudes and widths, given by $A_1 = 0.1$, $A_2 = 0.01$ and $B_1 = B_2 = 0.5$, we compare the results for two different theories, NS and IS. In this case $\hat{\tau}_\pi = 0$ (Navier-Stokes case) and $\hat{\tau}_\pi = 5\eta_0/s_0$, which is a reasonable estimate for $\hat{\tau}_\pi$ for systems described by the Boltzmann equation. This figure is analogous to Fig. 3.4, as the Israel-Stewart fluid ensures that rarefaction occurs in the tail and there is an enhancement in the front of the pulse.

Using the same parameters as in Fig. 3.5, we summarize the effects of relaxation considering the "soliton-like" configuration for the initial conditions: $A_1 = 0.6$, $A_2 = 0.4$, $B_1 = B_2 = 4$ in Fig. 3.6. Relaxation increases the pulse amplitudes in some regions, as it has a dispersive character. However, this behavior is different from the NS case in which

there is an enhancement of the amplitude in the opposite direction of the pulse.

The pulse in the Israel-Stewart fluid propagates ahead of that from the Navier-Stokes fluid. We clearly notice that IS hydrodynamics favors the wall front formation, while NS disperses the pulse to the opposite direction of motion. This might be the most important feature of relaxation time effects in nonlinear wave perturbation found in this thesis and is both present for strong and weak coupling inspired parameters.

3.2.2 Gaussian initial profile

Again, we consider the strong coupling parameters $3\chi/4 = \eta_0/s_0 = 1/(4\pi)$ and two values for $\hat{\tau}$. We solve (3.11) with the following gaussian initial condition

$$\hat{\varepsilon}_1(\hat{x}, 0) = C_1 \; e^{-(\hat{x}/D_1)^2} \tag{3.15}$$

and insert the obtained numerical solution of (3.11) into (3.12) with the initial gaussian profile for $\hat{\varepsilon}_2$

$$\hat{\varepsilon}_2(\hat{x}, 0) = C_2 \; e^{-(\hat{x}/D_2)^2}. \tag{3.16}$$

The amplitudes C_1, C_2 and the widths D_1, D_2 are chosen to study some stability features.

We consider $\hat{\tau}_\pi = [2 - ln(2)]/(2\pi)$, $C_1 = 0.5$ and $C_2 = 0.3$ in Fig. 3.7. One can see that by increasing the width of the initial profile from $D_1 = D_2 = 2$ to $D_1 = D_2 = 20$ guarantees stability (the gradients are significantly reduced in this case). The solution of the Burgers equation (3.11) for $\hat{\varepsilon}_1$ mimics a soliton when $D_1 = D_2 = 20$.

In Fig. 3.8 we repeat the same calculation for Fig. 3.7, but considering a larger value for the relaxation time $\hat{\tau}_\pi = 200\eta_0/s_0$. In Fig. 3.8(b) with increasing width the solution displays a soliton-like behavior when compared to Fig. 3.8(a). In Fig. 3.8(c) and Fig. 3.8(e) we show the case of small width and instabilities in the propagation of the pulse are found. However, we clearly observe in Fig. 3.8(d) and Fig. 3.8(f) that by increasing the width (or, equivalently, by decreasing the initial spatial gradient) one can find a stable propagating pulse even for a large value of the relaxation time. We conclude that even for large values of the relaxation time one can still find a stable nonlinear propagation of the initial gaussian profile, if the initial gradients are sufficiently small, i.e., if the initial gaussian width is small enough. Therefore, in the hydrodynamic limit we find soliton-like solutions of the nonlinear wave equations in Israel-Stewart theory.

In all figures we notice that the numerical solutions of (3.11) and (3.12) do not diverge for long times, i.e., they are not unstable. The nontrivial study of causality and stability for nonlinear wave equations cannot be performed as simply as it was done in the linear case. Such study is in progress.

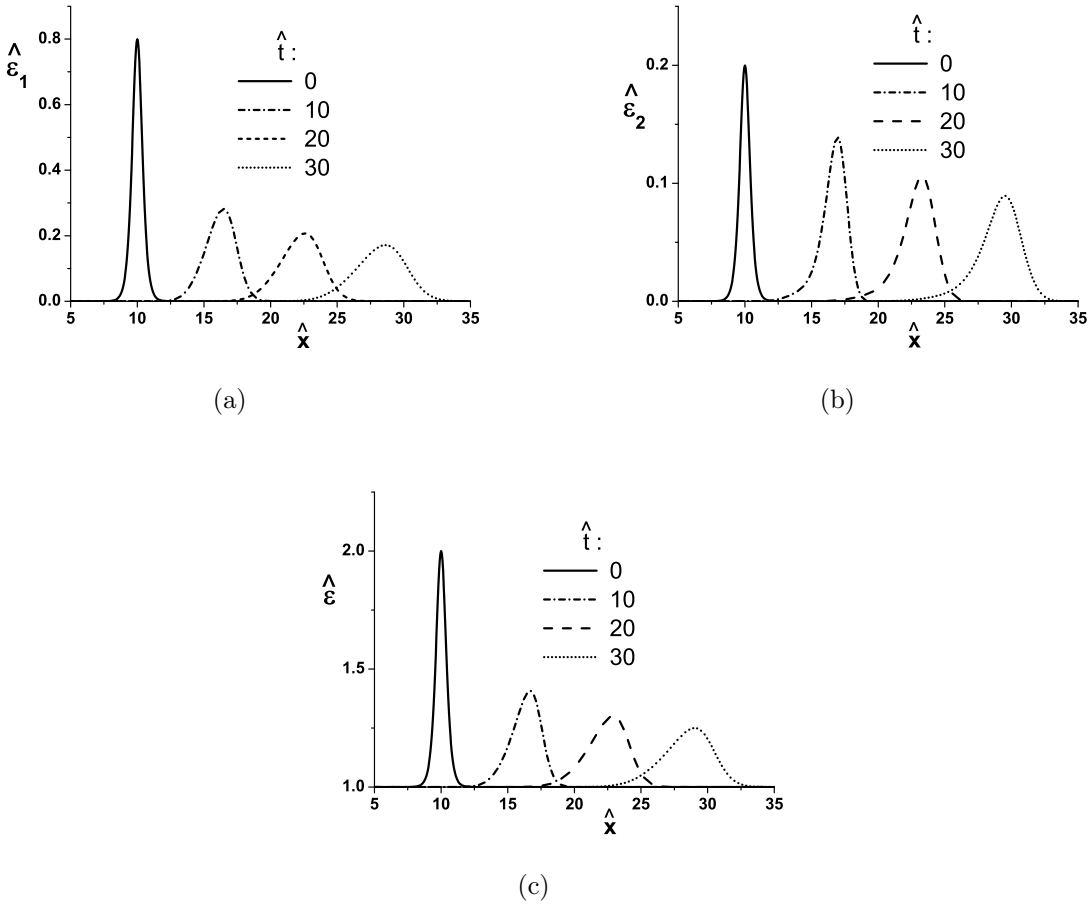

Figure 3.1: *Numerical solutions for the energy density disturbances in the nonlinear regime in Eqs. (3.11) (fig. 3.1(a)) and (3.12) (fig. 3.1(b)) for* $\eta_0/s_0 = 1/(4\pi)$ *and* $\hat{\tau}_\pi = [2 - ln\, 2]/(2\pi)$*. The initial conditions are (3.13) and (3.14) with* $A_1 = 0.8$*,* $A_2 = 0.2$ *and* $B_1 = B_2 = 0.5$ *. The fig. 3.1(c) shows the complete energy density perturbation* $\hat{\varepsilon} = 1 + \hat{\varepsilon}_1 + \hat{\varepsilon}_2$*. The perturbations survive despite the dissipative effects.*

3.3 Conclusions of the Chapter

Our system of differential equations can be easily solved numerically and in certain conditions gives "soliton-like" behavior for the initial wave packet evolution. This investigation may be relevant for the understanding of nonlinear perturbations in viscous relativistic hydrodynamics. For instance, our study of the deep "Israel-Stewart limit" where $\hat{\tau}_\pi = 120\eta_0/s_0$ in Fig. 3.4 and $\hat{\tau}_\pi = 200\eta_0/s_0$ in Fig. 3.8 suggest the existence of an upper bound for $\hat{\tau}_\pi$ (for a given η_0/s_0), which marks the onset of a possible instability in the solutions in this case that involves moderately large initial spatial gradients. While the linearized study of wave propagation shows that $\hat{\tau}_\pi$ cannot be much smaller than η_0/s_0 (due to instabilities), our nonlinear treatment of the wave equation for the energy density

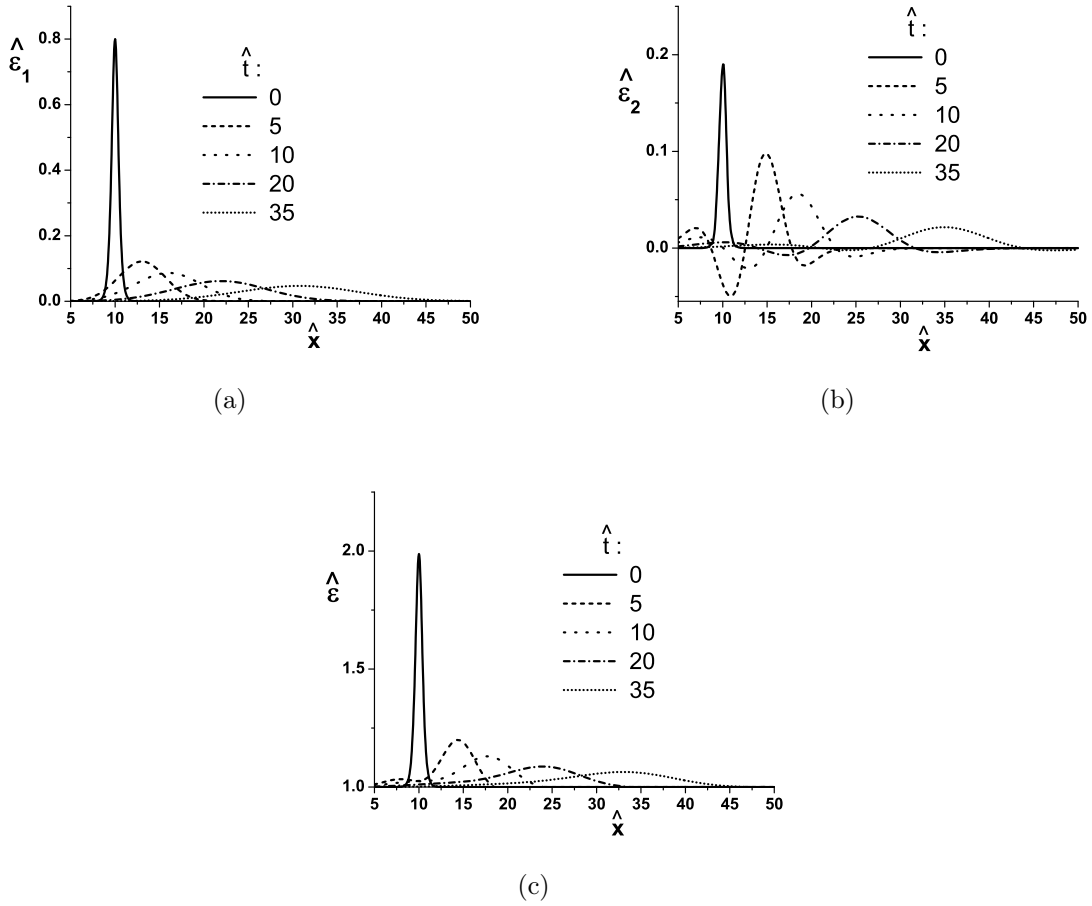

Figure 3.2: *Numerical solutions for the energy density disturbances in the nonlinear regime in Eqs. (29) (fig. 3.2(a)) and (30) (fig. 3.2(b)) for* $\eta_0/s_0 = 1$ *and* $\hat{\tau}_\pi = 5\eta_0/s_0$*. The initial conditions are (3.13) and (3.14) with* $A_1 = 0.8$*,* $A_2 = 0.2$ *and* $B_1 = B_2 = 0.5$ *. The fig. 3.2(c) shows the complete energy density perturbation. The perturbations do not survive due large dissipative effects.*

in hydrodynamics indicates that in a consistent microscopic theory $\hat{\tau}_\pi$ and η_0/s_0 must be of comparable magnitude (this is valid, for instance, in the case of kinetic theory calculations). However, we remark that in the “rigorous" hydrodynamical limit of small spatial gradients, when considering initial gaussian profiles with large widths, it is possible to avoid instabilities in wave propagation, as observed in Fig. 3.8, while still maintaining the soliton-like solution. Therefore, our nonlinear study suggests that in the case of small spatial gradients, Israel-Stewart theory should support soliton-like wave phenomena.

For most of our investigations we found that the influence of $\hat{\tau}_\pi$ did not determine the overall behavior of wave propagation in the nonlinear regime. This conclusion agrees with previous investigations in the literature on the small effect of second order transport coefficients in heavy ion collisions [110]. Our only exceptions were the ones that implied

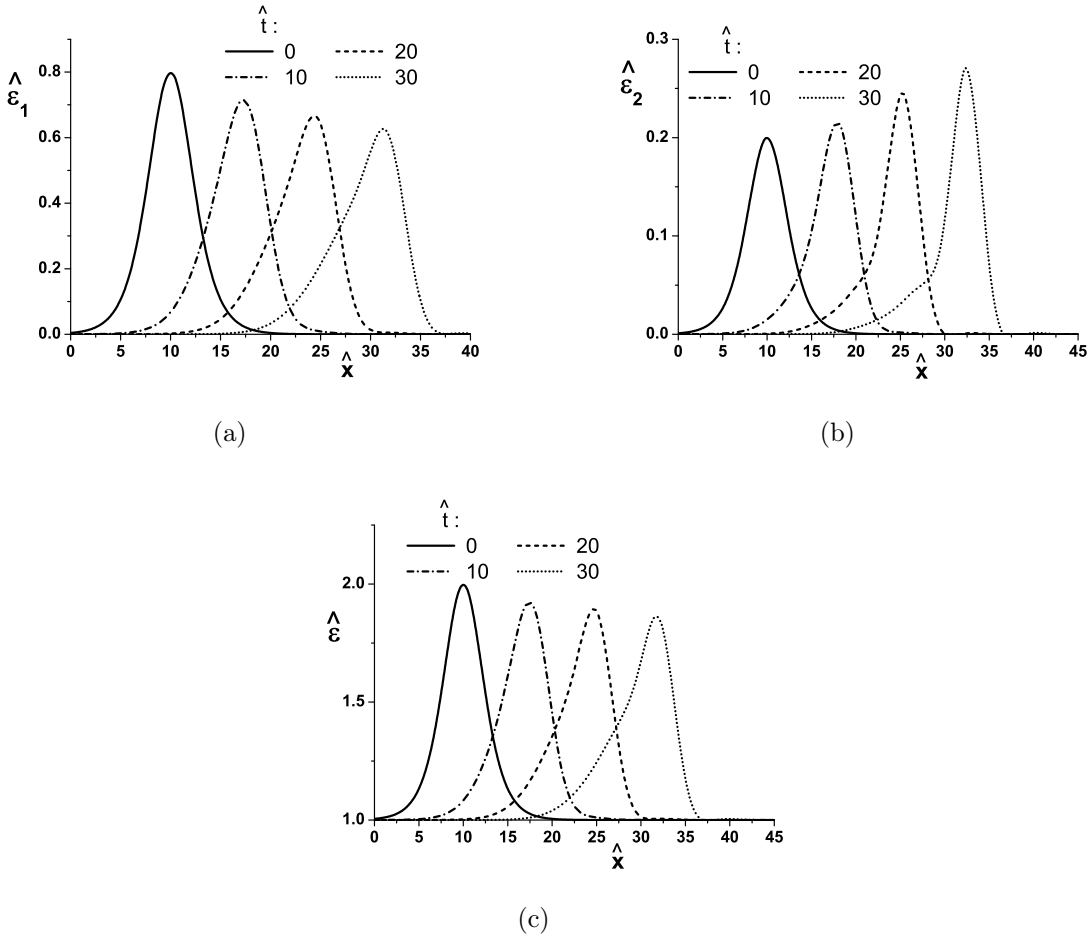

Figure 3.3: *Numerical solutions for the energy density disturbances in the nonlinear regime in Eqs. (3.11) (fig. 3.3(a)) and (3.12) (fig. 3.3(b)) for* $\eta_0/s_0 = 1/(4\pi)$ *and* $\hat{\tau}_\pi = [2 - ln\,2]/(2\pi)$. *The initial conditions are (3.13) and (3.14) with* $A_1 = 0.8$, $A_2 = 0.2$ *and* $B_1 = B_2 = 3$. *In this case the width of the initial pulses is 6 times larger than in Fig. 3.1. The fig. 3.3(c) shows the complete energy density perturbation. The perturbations with these initial profiles mimic soliton behavior.*

unphysical values of relaxation time and large initial spatial gradients. This statement suggests that in physical systems under conditions that are consistent with the hydrodynamic behavior (small gradients), $\hat{\tau}_\pi/(\eta/s)$ should be of order 1 and the effect of the relaxation time on nonlinear wave propagation can be taken to be a small correction.

The differential equations (3.11) and (3.12) are nontrivial alternative approaches to investigate the nonlinear regime of wave propagation in 2nd order conformal hydrodynamics in the Israel-Stewart approximation. However, they are still simple enough to be investigated with simple numerical routines. For this particular type of study, these equations offer a simple (though clearly limited) alternative to the full numerical hydrodynamical equations. We hope that our work can be used both as a motivation for the search for

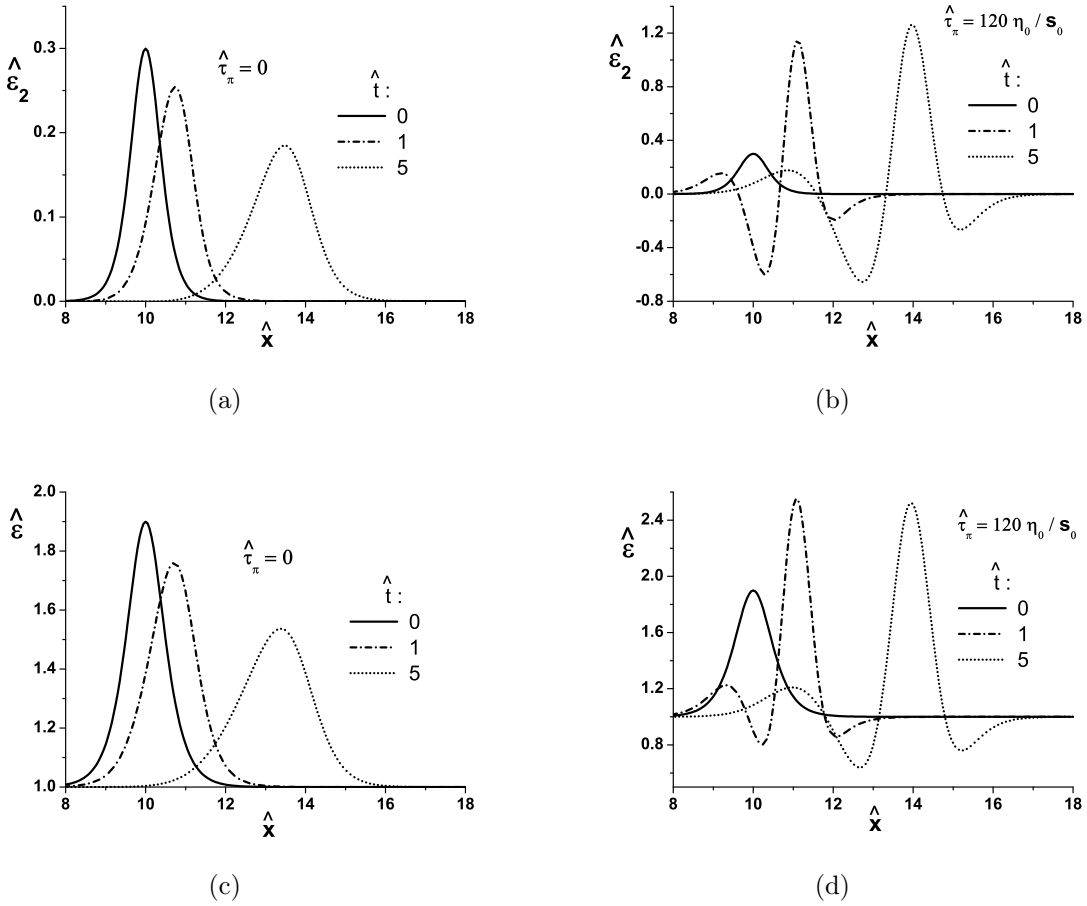

Figure 3.4: *Numerical solutions for the energy density disturbance in the nonlinear regime in Eq. (30) (fig. 3.4(a) and fig. 3.4(b)) for* $\eta_0/s_0 = 1/(4\pi)$ *and two choices of* $\hat{\tau}_\pi$*. The initial conditions are (3.13) and (3.14) with* $A_1 = 0.6$*,* $A_2 = 0.3$*,* $B_1 = 0.7$ *and* $B_2 = 0.5$ *. The fig. 3.4(c) and 3.4(d) shows the complete energy density perturbation. For large values of the relaxation time coefficient, the energy perturbation* $\hat{\varepsilon}_2$ *acquires large amplitude and becomes inconsistent as a small disturbance (note, however, that the initial gradients are large).*

soliton waves in the full Israel-Stewart equations as well as a possible check of precision of numerical hydrodynamic codes, similar to the analytical solutions found in [53, 111, 112].

It would be interesting to generalize the analysis performed here to include effects from bulk viscosity (i.e., by dropping the underlying conformal invariance of the equations) and different equations of state. Moreover, even though the nonlinear terms in 2nd order hydrodynamics do not contribute to the linearized study, they may play an interesting role in the investigation of nonlinear wave propagation in the QGP but we leave this investigation to a future study.

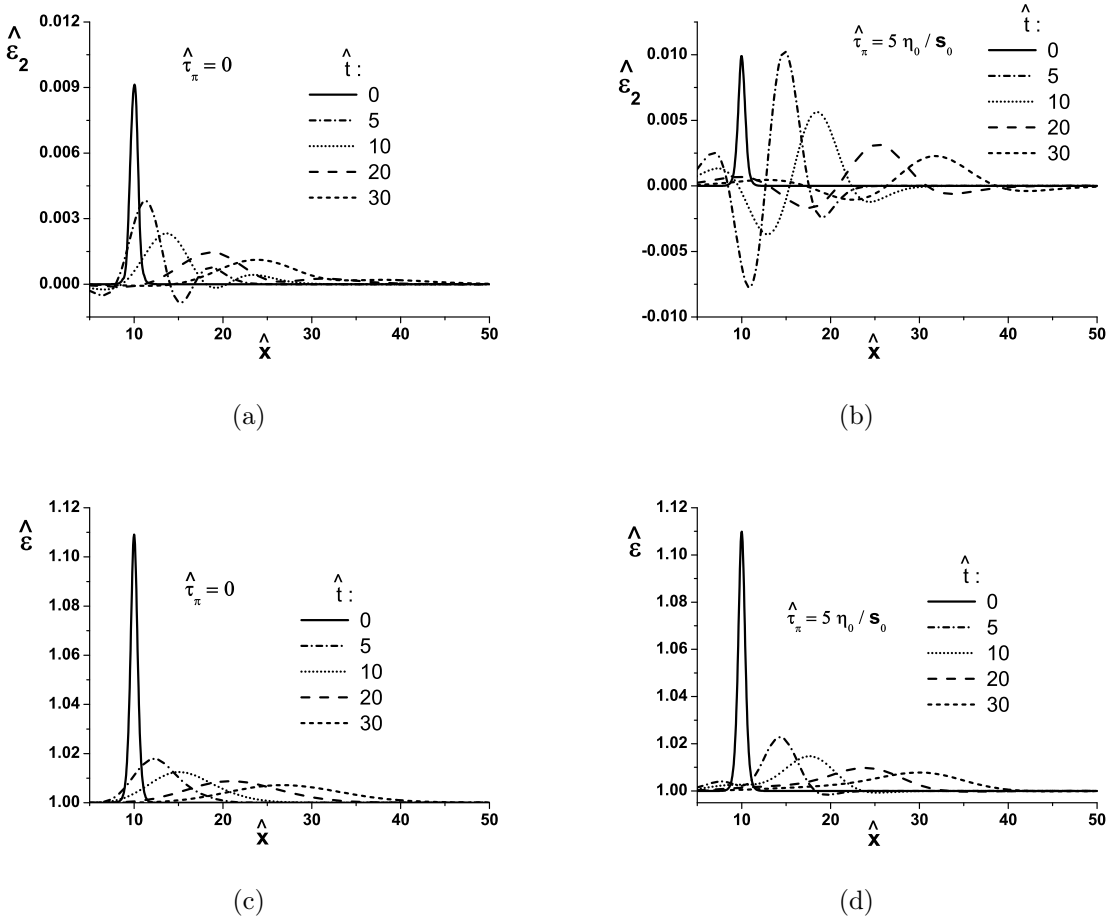

Figure 3.5: *Comparison between the energy density perturbations in Navier-Stokes and Israel-Stewart theory for* $\eta_0/s_0 = 1$ *and* $\hat{\tau}_\pi = 5\,\eta_0/s_0$. *The initial conditions are (3.13) and (3.14) with* $A_1 = 0.1$, $A_2 = 0.01$ *and* $B_1 = B_2 = 0.5$. *The fig. 3.5(a) and fig. 3.5(b) show the numerical solutions for Eq. (3.12) and fig. 3.5(c) and 3.5(d) are the complete energy density perturbation. The relaxation ensures that rarefaction occurs in the tail of the pulse while there is an enhancement in the front of the pulse.*

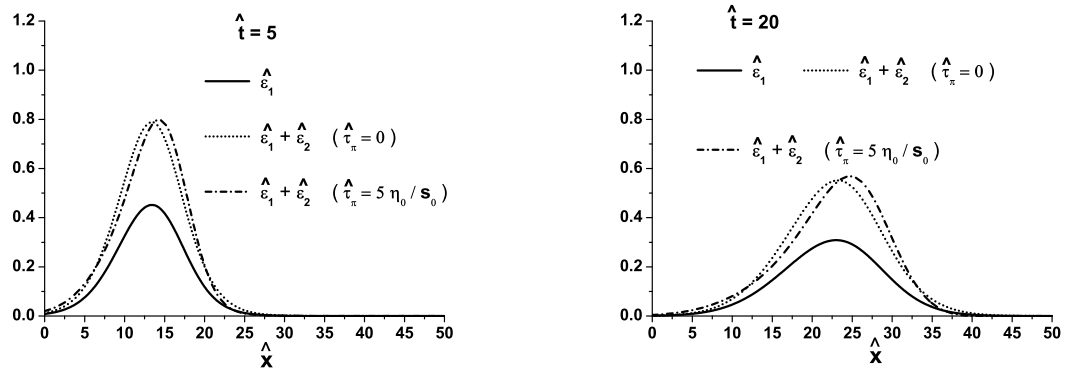

(a) (b)

Figure 3.6: *Comparison between the energy density perturbations in Navier-Stokes and Israel-Stewart theory for $\eta_0/s_0 = 1$ and $\hat{\tau}_\pi = 5\,\eta_0/s_0$ for larger width of the initial pulse. The initial conditions are (3.13) and (3.14) with $A_1 = 0.6$, $A_2 = 0.4$ and $B_1 = B_2 = 4$. Conformal Israel-Stewart hydrodynamics favors the wall front formation.*

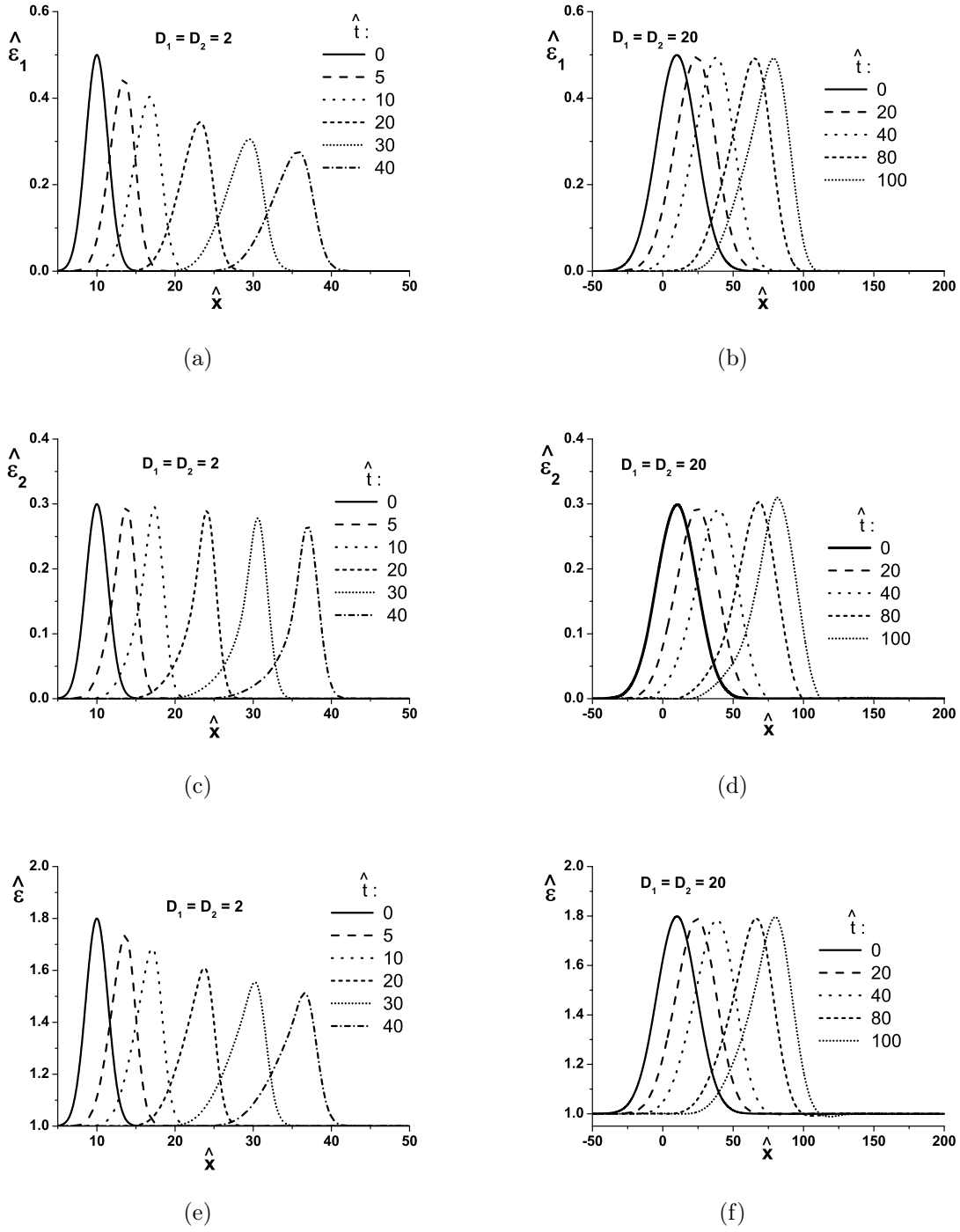

Figure 3.7: *Stability is found by increasing the initial width of the initial gaussian profiles (3.15) and (3.16) with* $C_1 = 0.5$ *and* $C_2 = 0.3$ *. The plots are the numerical solutions in the nonlinear regime in Eqs. (3.11) (3.7(a) and 3.7(b)), and (3.12) (3.7(c) and 3.7(d)) for* $\eta_0/s_0 = 1/(4\pi)$ *and* $\hat{\tau}_\pi = [2 - ln\, 2]/(2\pi)$*. In 3.7(e) and 3.7(f): the complete energy density perturbation* $\hat{\varepsilon} = 1 + \hat{\varepsilon}_1 + \hat{\varepsilon}_2$*. The perturbations survive despite the dissipative effects.*

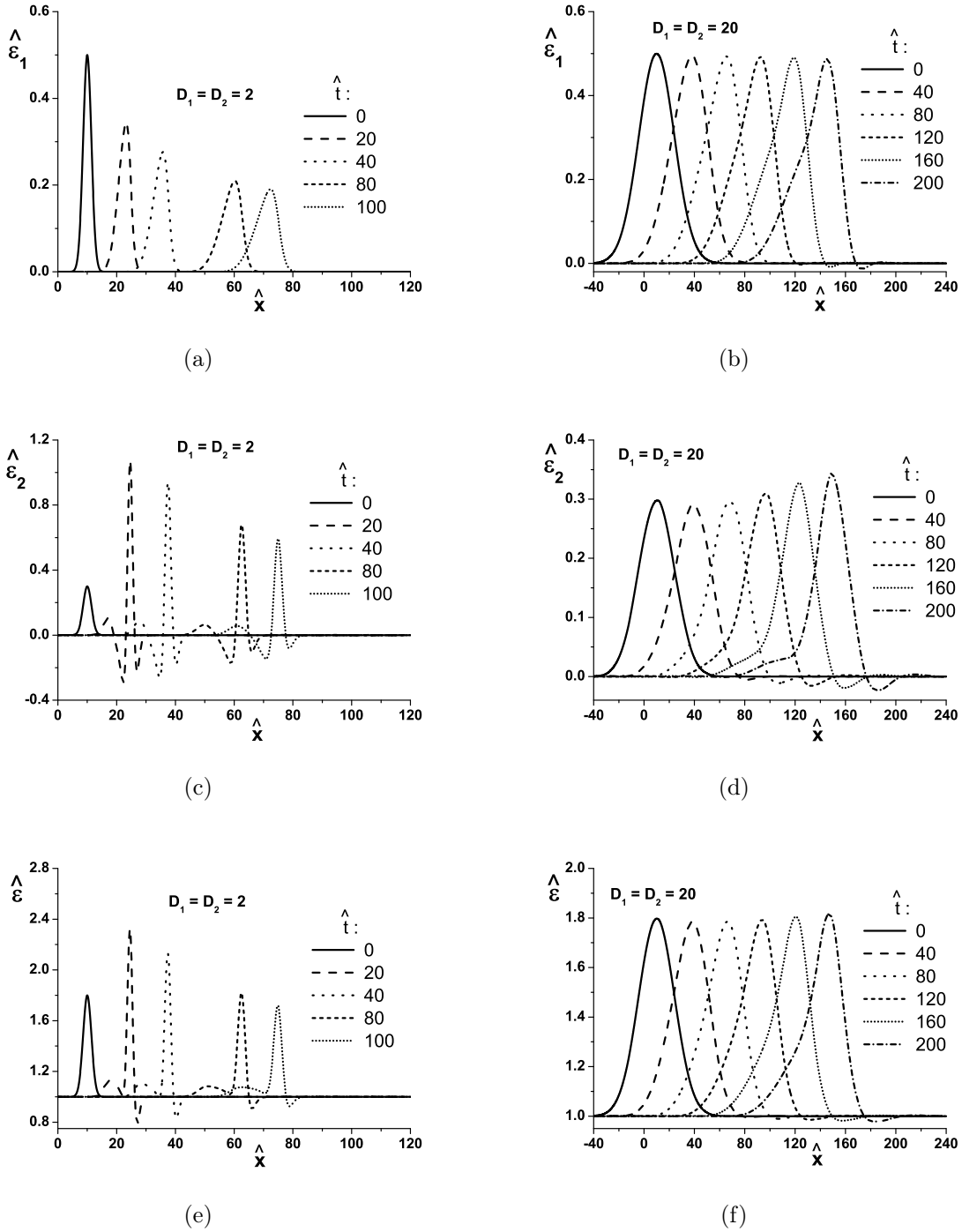

Figure 3.8: *Stability is found by increasing the width of the initial gaussian profiles (3.15) and (3.16) with $C_1 = 0.5$ and $C_2 = 0.3$, even for large values of the relaxation time. The plots are the numerical solutions in the nonlinear regime in Eqs. (29) (3.8(a) and 3.8(b)), and (30) (3.8(c) and 3.8(d)) for $\eta_0/s_0 = 1/(4\pi)$ and $\hat{\tau}_\pi = 200\eta_0/s_0$. In 3.8(e) and 3.8(f): the complete perturbation. The perturbations survive despite the dissipative effects.*

Chapter 4

Breakdown of the gradient expansion formalism under linear perturbations

Hydrodynamics is understood as the effective low-energy excitation theory of collective behavior. In this chapter we argue that some dissipative theories are ill defined and see clearly indications of the advantage of the Israel-Stewart [49, 50] formalism over the gradient expansion. The majority of this chapter will appear in an upcoming paper [60], and a small part of it is based on the fluid dynamics discussions in [38].

The idea of this chapter is to throughly investigate the structure of linear perturbations on dissipative relativistic hydrodynamics. In the sense of effective theory, the slowest degrees of freedom accessible in the fluid are the temperature and flow velocity and in the gradient expansion approach the hydrodynamic equations involve only derivatives of these quantities. It is then natural to assume that the inclusion of more and more derivatives in the gradient expansion description of a relativistic fluid can only alter the description of short wavelength phenomena. More specifically, consider for instance the sound mode, $\omega_{sound}(k)$, of a relativistic fluid. The hydrodynamic expansion corresponds to an expansion in powers of momentum k, i.e., $\omega_{sound}(k) = c_s k + \mathcal{O}(k^2)$, where c_s is the speed of sound and $\mathcal{O}(k^2)$ denotes the dissipative contributions associated with higher order gradients. In order to allow for meaningful applications in physical systems, the equations of dissipative relativistic hydrodynamics should be stable at least against small perturbations around a well defined equilibrium state and, more importantly, the inclusion of higher order derivatives must not affect the low k properties of the fluid.

Following the seminal work of Hiscock and Lindblom [41–43], recently a few groups have returned to the questions regarding the stability and causality properties of linear disturbances in relativistic fluids [58, 74, 113]. While it is known that first-order relativistic hydrodynamics is generically unstable [41–43], to the best of our knowledge, a similar study has not been carried out at second and third order in gradients. Since Israel-Stewart

(IS) theories are related to second order gradient expansion theories and the IS equations can be causal and stable [41, 74], one may be tempted to conclude that the stability problems that plague relativistic NS theory are already removed at second order in gradients.

In this chapter we show that this is not true. We study the properties of *linear* disturbances associated with shear viscosity in the sound and shear channels of a relativistic dissipative fluid defined by a 3rd-order gradient expansion. At weak coupling such a theory could be derived, for instance, by implementing the relativistic version of the Chapman-Enskog program [114] while at strong coupling one may employ the fluid/gravity correspondence [39] (Chapter 5). We investigate the structure of the sound and shear dispersion relations in a covariant manner and show that the number of modes in a moving fluid is always larger than that found in a fluid at rest. After revisiting the case of relativistic NS theory, we move on to second order in gradients and show that the sound disturbances around a static background are linearly unstable below a certain wavelength (this is also true in the case of a moving background). Moreover, we explicitly demonstrate that the hydrodynamic series within the gradient expansion becomes problematic at third order because both the sound and shear disturbances around a static background have a mode that goes as $\sim 1/k^2$. Thus, the addition of more derivatives in the gradient expansion does not necessarily improve the short wavelength description of the fluid. Rather, at third order the homogeneous limit of sound and shear disturbances is lost.

It is straightforward to generalize our results taking into account bulk viscosity effects. However, in this thesis we shall focus solely on the viscous effects that stem from shear viscosity and leave this generalization to a future study. However, we we show the results of stability with bulk viscosity in Appendix E.

Throughout this chapter we adopt the mostly negative metric $g_{\mu\nu} = \text{diag}(+,-,-,-)$ and natural units.

4.1 Relativistic dissipative fluid dynamics under Linear Perturbations

In this section we consider the equations of relativistic fluid dynamics in flat spacetime in the absence of conserved currents (such as baryon number) and take into account only effects from shear viscosity, though the fluid may not be conformal.

The conservation of energy and momentum $\nabla_\mu T^{\mu\nu} = 0$ leads to the following equations, repeated here for convenience

$$D\varepsilon + (\varepsilon + p)\theta - \pi^{\mu\nu}\,\sigma_{\mu\nu} = 0 \tag{4.1}$$

$$(\varepsilon + p)Du^\alpha - \nabla_\perp^\alpha p + \Delta_\nu^\alpha \partial_\mu \pi^{\mu\nu} = 0 \tag{4.2}$$

the simplified set of the conformal IS equations [68] that defines the dynamics of the shear stress tensor $\pi^{\mu\nu}$ used here are [53]

$$\tau_\pi \left(\Delta_\alpha^\mu \Delta_\beta^\nu D\pi^{\alpha\beta} + \frac{4}{3}\pi^{\mu\nu}\theta \right) + \pi^{\mu\nu} = 2\eta\sigma^{\mu\nu} \tag{4.3}$$

and the gradient expansion conformal equation up to second order

$$\pi^{\mu\nu} = 2\eta\sigma^{\mu\nu} + 2\eta\tau_\pi \left(D\sigma^{<\mu\nu>} + \frac{\theta}{3}\sigma^{\mu\nu} \right) , \tag{4.4}$$

The holographic transport coefficients are also rewritten here for convenience [68]

$$\frac{\eta}{s} = \frac{1}{4\pi} , \qquad \tau_\pi T = \frac{2 - \ln 2}{2\pi} , \qquad \frac{\lambda_1 T}{s} = \frac{1}{2\pi}\frac{\eta}{s} . \tag{4.5}$$

Following [41–43] we now linearize these equations around a uniform background described by ε_0, P_0, and u_0^μ and take the plane wave Ansatz for the disturbances

$$\varepsilon \to \varepsilon_0 + \delta\varepsilon\, e^{-ik_\nu x^\nu} \qquad u^\mu \to u_0^\mu + \delta u^\alpha\, e^{-ik_\nu x^\nu} \qquad \pi^{\alpha\beta} \to \delta\pi^{\alpha\beta}\, e^{-ik_\nu x^\nu} . \tag{4.6}$$

The corresponding equations for the disturbances can be written in a covariant form after defining

$$\Omega = u_{0\,\mu} k^\mu , \qquad \kappa^\nu = \Delta_{0\,\alpha}^\nu k^\alpha \tag{4.7}$$

(note that $\kappa_\mu \kappa^\mu = -\kappa^2$ and, by construction, $u_0^\mu \kappa_\mu = 0$) and the following projector in momentum space

$$\Delta_\kappa^{\mu\nu} = g^{\mu\nu} + \frac{\kappa^\mu \kappa^\nu}{\kappa^2} . \tag{4.8}$$

This allows us to write $\delta u^\mu = \delta u_\parallel \kappa^\mu/\kappa + \delta u_\perp^\mu$ where

$$\delta u_\parallel = -\frac{\kappa_\nu \delta u^\nu}{\kappa} , \qquad \delta u_\perp^\mu = \Delta_\kappa^{\mu\nu}\delta u_\nu , \tag{4.9}$$

are the components of the background velocity in the direction of k^μ and perpendicular to it, respectively. With these definitions, the covariant equations for the fluctuations become

$$\Omega\, \delta\varepsilon - (\varepsilon_0 + P_0)\kappa\, \delta u_\parallel = 0 , \tag{4.10}$$

$$(\varepsilon_0 + P_0)\Omega\, \delta u_\parallel - \kappa\, c_s^2 \delta\varepsilon - \frac{\kappa_\mu \kappa_\nu}{\kappa}\delta\pi^{\mu\nu} = 0 , \tag{4.11}$$

$$(\varepsilon_0 + P_0)\Omega\, \delta u_\perp^\mu + \kappa_\nu \delta\pi^{\mu\nu} + \kappa^\mu \frac{\kappa_\alpha \kappa_\beta}{\kappa^2}\delta\pi^{\alpha\beta} = 0 , \tag{4.12}$$

where $c_s^2 = dP_0/d\varepsilon_0$.

The first two equations above are the ones needed to investigate the structure of the modes in the sound (i.e., longitudinal) channel while third equation defines the shear channel. One may rewrite the equations for the sound and shear channels as follows

$$\left(\Omega^2 - c_s^2\kappa^2\right)\delta u_\parallel - \Omega\,\kappa\,\delta\bar{\pi}_\parallel = 0\,, \tag{4.13}$$

$$\Omega\,\delta u_\perp^\mu - \kappa\,\delta\bar{\pi}_\parallel^\mu = 0 \tag{4.14}$$

where $\delta\bar{\pi}_\parallel = \frac{\kappa_\mu\kappa_\nu}{\kappa^2}\delta\pi^{\mu\nu}/(\varepsilon_0{+}P_0)$ and $\delta\bar{\pi}_\parallel^\mu = -\left(\Delta_\kappa\right)_\alpha^\mu \frac{\kappa_\beta}{\kappa}\delta\pi^{\alpha\beta}/(\varepsilon_0{+}P_0)$. In order to determine the spectrum of the sound and shear modes one needs to know the general expression for $\delta\bar{\pi}_\parallel$ and $\delta\bar{\pi}_\parallel^\mu$ in Eqs. (4.13) and (4.14) according to the gradient expansion. This will be discussed in the next section.

4.2 Gradient expansion approach for linearized shear disturbances

While writing down the full nonlinear expansion of the shear stress tensor with N derivatives is a daunting task[1], expressions for $N = 2$ [30, 39, 68] and $N = 3$ have been proposed [117, 118]. The main difficulty comes from the inclusion of nonlinear terms in the gradients of flow and energy density. Within kinetic theory, it is possible use the Chapman-Enskog approach to find the nonlinear expression for the shear stress tensor that describes the gradient expansion at high orders. In this method, comoving derivatives of the particle distribution function are converted into transverse derivatives at each order using the conservation laws and the final expression for $\pi^{\mu\nu}$ possesses only spatial gradients of the hydrodynamic variables

However, in our case we are only interested in the *linear* terms and the most general linear expression for the shear stress tensor disturbance can be easily written in terms of the hydrodynamic variables up to third order in gradients,

[1]Even for $N = 2$ there are several forms to write the expansion that are equivalent at that order, as discussed in [68] for the case of a conformal fluid (see also [115]). See, however, the "tour-de-force" performed in [116] where the shear stress tensor for the case of a boost-invariant, Bjorken expanding strongly coupled $\mathcal{N} = 4$ supersymmetric Yang-Mills plasma was determined up to 240 derivatives.

$$\delta\pi^{\mu\nu} = \Delta^{\mu\nu}_{\alpha\beta}\Big(2\eta_0\,\delta\sigma^{\alpha\beta} + \mathcal{C}_1\nabla^\alpha_\perp\nabla^\beta_\perp\delta\epsilon - 2\eta_0\tau_\pi D_0\delta\sigma^{\alpha\beta} + \mathcal{C}_2\nabla^\alpha_\perp\nabla^\beta_\perp\delta\theta + \mathcal{C}_3\nabla^\alpha_\perp\nabla^\beta_\perp D_0\delta\epsilon + \mathcal{C}_4\nabla^\lambda_\perp\nabla_{\perp\lambda}\delta\sigma^{\alpha\beta} + \mathcal{C}_5 D_0^2\delta\sigma^{\alpha\beta}\Big)\,. \tag{4.15}$$

We included all the possible contributions from derivatives of the energy density and flow that respect rotational invariance. Under linear perturbation, there is an exact relation between the energy density and the parallel 4-velocity due to energy conservation,

$$\delta\varepsilon = (\varepsilon_0 + P_0)\,\frac{\kappa}{\Omega}\,\delta u_\parallel\,. \tag{4.16}$$

The same is true for the expansion rate $\delta\theta$, as it only adds contributions to the parallel direction. The shear tensor contributes both to the parallel and perpendicular equation as follows

$$\begin{aligned}\delta\bar\sigma_\parallel &= \frac{\kappa_\mu\kappa_\nu}{\kappa^2}\delta\sigma^{\mu\nu} = -\frac{2\,i\,\kappa}{3}u_\parallel\,,\\ \delta\bar\sigma^\mu_\perp &= -(\delta_\kappa)^\mu_\alpha\frac{\kappa_\beta}{\kappa}\delta\sigma^{\alpha\beta} = -\frac{i\kappa}{2}\delta u^\mu_\perp\,.\end{aligned} \tag{4.17}$$

The dissipative tensor can be decomposed as

$$\begin{aligned}\delta\bar\pi_\parallel &= \frac{\kappa_\mu\kappa_\nu}{\kappa^2(\varepsilon_0+P_0)}\delta\pi^{\mu\nu}\,,\\ \delta\bar\pi^\mu_\perp &= -(\Delta_\kappa)^\mu_\alpha\frac{\kappa_\beta}{\kappa(\varepsilon_0+P_0)}\delta\pi^{\alpha\beta}\,.\end{aligned} \tag{4.18}$$

We find using Eq. (4.15) in Fourier space in the parallel direction

$$\delta\bar\pi_\parallel = \left(-\frac{4}{3}i\frac{\eta_0}{s_0T_0}\kappa - \frac{2}{3}\mathcal{C}_1\frac{\kappa^3}{\Omega} + \frac{4}{3}\frac{\eta_0\tau_\pi}{s_0T_0}\Omega\kappa - \frac{2}{3}i\frac{\mathcal{C}_2}{s_0T_0}\kappa^3 + \frac{2}{3}i\mathcal{C}_3\kappa^3 - \frac{2}{3}i\frac{\mathcal{C}_4}{s_0T_0}\kappa^3 + \frac{2}{3}i\frac{\mathcal{C}_5}{s_0T_0}\Omega^2\kappa\right)\delta u_\parallel\,, \tag{4.19}$$

and the perpendicular component

$$\delta\bar\pi^\mu_\perp = \left(-i\frac{\eta_0}{s_0T_0}\kappa + \frac{\eta_0\tau_\pi}{s_0T_0}\Omega\kappa - \frac{i}{2}\frac{\mathcal{C}_4}{s_0T_0}\kappa^3 + \frac{i}{2}\frac{\mathcal{C}_5}{s_0T_0}\Omega^2\kappa\right)\delta u^\mu_\perp\,. \tag{4.20}$$

We adopt the convention that the dispersion relations are dimensionless, i.e., an appropriate factor of temperature was absorbed either by the extra factors of Ω and κ, or

by the transport coefficient. Also, we redefine the ratio of a transport coefficient with the equilibrium entropy background s_0 as

$$\frac{\eta_0}{s_0} \to \Gamma\,, \qquad\qquad \frac{\mathcal{C}_i}{s_0} \to c_i\,. \tag{4.21}$$

The parallel dispersion (sound mode) resulting from the third order dissipative theory (4.15) is then

$$\begin{aligned}&\Omega^2 - \frac{1}{3}\kappa^2 + \frac{4}{3}i\,\Gamma\,\Omega\kappa^2 + \frac{2}{3}\,\mathcal{C}_1\,\kappa^4 - \frac{4}{3}\,\Gamma\tau_\pi\,\Omega^2\kappa^2 + \\ &\frac{2}{3}i\,c_2\,\Omega\kappa^4 - \frac{2}{3}i\,\mathcal{C}_3\,\Omega\kappa^4 + \frac{2}{3}i\,c_4\,\Omega\kappa^4 - \frac{2}{3}i\,c_5\,\Omega^3\kappa^2 = 0\ ,\end{aligned} \tag{4.22}$$

and the perpendicular equation (shear mode)

$$\Omega + i\Gamma\,\kappa^2 - \Gamma\tau_\pi\,\Omega\kappa^2 + \frac{i}{2}\,c_4\,\kappa^4 - \frac{i}{2}\,c_5\,\Omega^2\kappa^2 = 0\ . \tag{4.23}$$

Notice that the terms with c_2, $\mathcal{C}_3$ and c_4 contribute the same way to the sound dispersion relation. However, only the term with c_4 is nonzero in the shear dispersion. Navier-Stokes theory corresponds to take only Γ as nonzero. It is easy to see that, after linearization, the second order theory studied in [68] corresponds to taking Γ and τ_π as the only nonzero coefficients in the expansion. In general, apart from $\Gamma > 0$ to recover the correct NS limit, one does not know a priori the sign of the higher order transport coefficients. Also, they may have a complicated temperature dependence if the fluid is not conformal.

In the case where the background is static, i.e., $u_0^\mu = (1,0,0,0)$, we obtain for the sound mode

$$\begin{aligned}&\omega^2 - \frac{1}{3}k^2 + \frac{4}{3}i\,\Gamma\,\omega k^2 + \frac{2}{3}\,\mathcal{C}_1\,k^4 - \frac{4}{3}\,\Gamma\tau_\pi\,\omega^2k^2 + \\ &\frac{2}{3}i\,c_2\,\omega k^4 - \frac{2}{3}i\,\mathcal{C}_3\,\omega k^4 + \frac{2}{3}i\,c_4\,\omega k^4 - \frac{2}{3}i\,c_5\,\omega^3k^2 = 0\ ,\end{aligned} \tag{4.24}$$

and the perpendicular shear mode becomes

$$\omega + i\Gamma\,k^2 - \Gamma\tau_\pi\,\omega k^2 + \frac{i}{2}\,c_4\,k^4 - \frac{i}{2}\,c_5\,\omega^2k^2 = 0\ . \tag{4.25}$$

where $k^\mu = \left(\omega, \vec{k}\right)$ and $k^2 = \vec{k}^2$. The sound and shear modes for a static background are found by solving each of the equations above for $\omega = \omega(k)$ at a given order in the derivative expansion.

One interesting contribution to Eqs. (4.22) and (4.23) comes from the operator related to c_5. For instance, one can see that for $N \leq 2$ there are two modes in the sound channel and only one mode in the shear channel. However, for $N > 2$ one has N modes in the sound channel and $N-1$ modes in the shear channel.

For a constantly moving background[2] with velocity $u_0^\mu = \gamma\,(1, \vec{v})$ and $\gamma = 1/\sqrt{1-v^2}$ [41, 42], one can use (4.13) and (4.14) to find the general dispersion relations we substitute $\Omega = \gamma\,(\omega - kv)$ and $\kappa = \gamma\,(k - \omega v)$, in which for simplicity we take $\vec{k}$ parallel to $\vec{v}$.

One can easily see that already for $N = 1$ (NS) the sound channel has three modes and the shear has two modes if $v \neq 0$, which shows that there are mode modes in a moving background in comparison to the case where the fluid is at rest. In general, for $N \geq 2$ the sound mode has $N+2$ modes while the shear has $N+1$ modes for a moving fluid.

This analysis suggests that it is impossible to have a dissipative theory constructed using the gradient expansion that displays the same degrees of freedom (at the linear level) both in the case where the fluid is at rest and also when the fluid is moving. In the next sections we explore in detail the structure of the dispersion relations under these conditions for different theories obtained via the gradient expansion.

4.3 N=1, Relativistic Navier-Stokes theory

For the sake of completeness, we first consider the already well-known [41, 42] relativistic Navier-Stokes theory, which corresponds to the case where $N = 1$ in the gradient expansion in the case of a static background. The sound dispersion relation is

$$\omega^2 + \frac{4}{3} i\Gamma\omega k^2 - k^2 c_s^2 \;=\; 0\,. \tag{4.26}$$

where $\Gamma = \eta_0/(s_0)$ and s_0, T_0 are the background entropy density and temperature, respectively. This is a simple second order polynomial and one can write the general solution of the modes in the following form

$$\omega\,(k) = -\frac{2}{3} i\Gamma k^2 \pm \sqrt{k^2 c_s^2 - \frac{4}{9}\Gamma^2 k^4}\,.$$

It is straightforward to show that the imaginary part of the modes defined above are always negative and, consequently, the solution is always stable in the linear regime. Also, one can show that for all wavenumbers above $k_c = 3c_s/\,(2\Gamma)$ the modes become purely imaginary (though still stable), i.e., there is no propagation of sound.

[2] This should be taken of course as an approximation to describe the situation in which the flowing background vary in space and time in scales much longer than those corresponding to the fluctuations. Mathematically, this is equivalent to a boost.

Note that, in the limit of small and large wave-number, $k \to 0$ and $k \to \infty$, respectively, the modes can be written as

$$\begin{aligned} \omega(k) &= \pm c_s k - \frac{2}{3} i\Gamma k^2 + \mathcal{O}\left(k^3\right), \\ \omega(k) &= -\frac{2}{3} i\Gamma k^2 (1 \mp 1) \pm \frac{3}{4} \frac{i}{\Gamma} \frac{c_s^2}{} + \mathcal{O}\left(\frac{1}{k^4}\right). \end{aligned}$$

For the moving background the dispersion relation becomes

$$(\omega - kv)^2 + \frac{4}{3} i\gamma\,\Gamma(\omega - kv)(k - \omega v)^2 - (k - \omega v) \tag{4.27}$$

This is now a polynomial of order three and, therefore, it must have one additional mode that did not exist in the static background case. For this case, we consider to be enough to write the general form of the solution in the homogeneous limit when $k \to 0$. For this purpose we expand each mode in a Taylor series $\omega(k) = \chi_0 + \chi_1 k + O(k^2)$, insert this expression into the dispersion relation derived above, and keep only the leading terms. The result is

$$\chi_0^2 \left[1 - v^2 c_s^2 + \frac{4}{3} i\Gamma\gamma v^2 \chi_0\right] = 0\,. \tag{4.28}$$

One can see that two modes remain hydrodynamical, i.e., they satisfy $\chi_0 = 0$, while one mode will be non-hydrodynamical (i.e., $\lim_{k\to 0} \omega_{\text{non-hydro}}(k) \neq 0$)

$$\chi_0 = i\frac{3}{4}\left(\frac{1 - v^2 c_s^2}{\Gamma\gamma v^2}\right).$$

Note that this mode did not exist when $v = 0$. Also, in the limit where $v \to 0$, this mode diverges instead of becoming zero indicating that the number of modes is not necessarily a continuous function of v. Finally, since $v^2 c_s^2$ is always smaller than 1, χ_0 will always be a positive purely imaginary number, showing that this mode is linearly unstable.

We illustrate these results in Fig. (4.1). Notice that for small background velocities, there is one unstable and acausal mode. This problem persists for any value of k, therefore it is also an infrared problem and should be relevant to the hydrodynamical regime.

For the shear channel in the static case the solution is simply $\omega(k) = -i\Gamma k^2$, which illustrates that Γ controls the diffusion of momentum. For a moving background the dispersion relation is

$$(\omega - kv) + i\Gamma\,\gamma(k - \omega v)^2 = 0\,. \tag{4.29}$$

This is now a second order polynomial and there thus two modes in the shear channel. In the homogeneous limit one of the modes remains hydrodynamical while the other one is non-hydrodynamical $\omega(k \to 0) \to i/(\Gamma\gamma v)$. Therefore, the extra mode in the shear channel

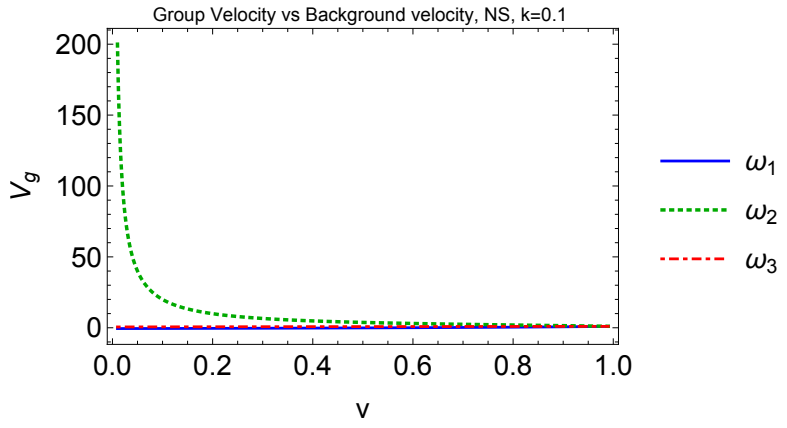

(a)

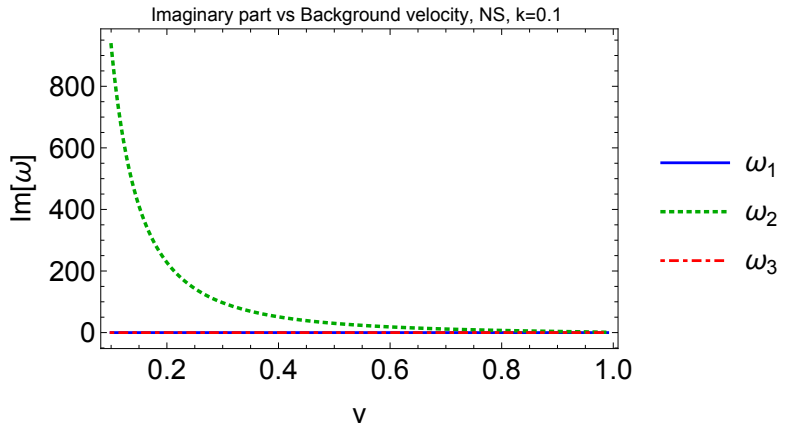

(b)

Figure 4.1: *Group velocity and the imaginary part for Navier-Stokes theory as a function of the background velocity, fixed at a small k of 0.1. The transport coefficient is calculated from $\mathcal{N} = 4$ SYM (4.5), $\eta/s = 1/(4\pi)$. This is unstable for positive imaginary values.*

is linear unstable and also diverges when $v \to 0$. Thus, the relativistic NS equations for a moving fluid contains unstable non-hydrodynamical modes.

These results are well-known and were studied with great detail by several authors [41–43]. Below we study some of the properties of the sound and shear channels in the gradient expansion taking $N = 2$.

4.4 Relativistic Burnett theory

When $N = 2$ one obtains the linearized version of relativistic Burnett theory. In this case one truncates the operators of the dissipative tensor at second order,

$$\delta\pi^{\mu\nu} = \Delta^{\mu\nu}_{\alpha\beta}\Big(2\eta_0\,\delta\sigma^{\alpha\beta} + \mathcal{C}_1\nabla^{\alpha}_{\perp}\nabla^{\beta}_{\perp}\delta\epsilon - 2\eta_0\tau_\pi D_0\delta\sigma^{\alpha\beta}\Big) = 0\ . \tag{4.30}$$

which gives the sound and shear channels

$$\Omega^2 - c_s^2\kappa^2 + \frac{4}{3}i\Omega\kappa^2\Gamma\left(1+i\tau_\pi\Omega\right) + \frac{2}{3}\mathcal{C}_1\,\kappa^4 = 0\,, \tag{4.31}$$

$$\Omega + i\kappa^2\Gamma\left(1+i\tau_\pi\Omega\right) = 0\,. \tag{4.32}$$

4.4.1 Sound dispersion

The sound dispersion relation for a static background is

$$\omega^2\left(1-\frac{4}{3}\tau_{\pi 0}\Gamma k^2\right) + \frac{4}{3}i\Gamma k^2\omega - c_s^2k^2 + \frac{2}{3}\mathcal{C}_1\,k^4 = 0\,. \tag{4.33}$$

Therefore, similarly to the NS theory, there are only two hydrodynamical modes that are now given by the solution for ω

$$\omega\left(k\right) = -\frac{2i\,\Gamma k^2}{3}\frac{1}{\left(1-\frac{4}{3}\Gamma\tau_{\pi\,0}k^2\right)}\left[1\pm\sqrt{1-\frac{3c_s^2}{4k^2\Gamma^2}\left(3c_s^2-2\mathcal{C}_1\right)\left(1-\frac{4}{3}\Gamma\tau_{\pi\,0}k^2\right)}\right].$$

However, in contrast to the NS case, the imaginary part of the modes above can become positive for nonzero k. Here, there is also a critical wavenumber, k_c, above which the mode is always purely imaginary and there is no propagation of sound (for simplicity given the conformal case $\mathcal{C}_1 = 0$)

$$k_c = \frac{3c_s}{2\sqrt{\Gamma^2 + 3c_s^2\Gamma\tau_{\pi 0}}}.$$

Note that, taking $\tau_{\pi 0}\to 0$, one recovers the same critical wavenumber obtained for Navier-Stokes theory. However, assuming that $\tau_{\pi 0}$ is positive, the critical wavenumber for the absence of sound in the Burnett system is always smaller than that found in Navier-Stokes theory.

As it is well-known, the solution up to $\mathcal{O}(k^2)$ is the same as the one found in Navier-Stokes theory

$$\omega\left(k\right) = \pm c_s k - \frac{2}{3}i\Gamma k^2 \mp \frac{2\Gamma}{9c_s}\left(\Gamma - 3c_s^2(\tau_\pi - \frac{3}{2}\frac{\mathcal{C}_1}{\Gamma})\right)k^3 - \frac{8}{9}i\Gamma^2\tau_\pi k^4 + \mathcal{O}\left(k^5\right)\ . \tag{4.34}$$

This happens because the gradient expansion at this order corrects only moderately large wavenumbers and, in this case, one only see corrections involving τ_π at order $\mathcal{O}\left(k^3\right)$

and higher. If one is left to truncate the theory at order $\mathcal{O}(k^3)$, the coefficient $\mathcal{C}_1$ can be absorbed redefining the coefficient τ_π. This is not true however for all orders, since the k^4 term already breaks this argument. Naturally, the solution for large wavenumbers significantly differs from the one found for Navier-Stokes theory,

$$\omega(k) = \frac{i}{2\tau_\pi} \pm \sqrt{\frac{\mathcal{C}_1}{2\Gamma\tau_\pi}}\,.$$

If τ_π is positive (as it is the case of strongly coupled $\mathcal{N}=4$ Supersymmetric Yang-Mills theory [68]), in this limit one of the modes will have a positive imaginary part and, as mentioned above, the theory becomes linearly unstable[3].

We show the behavior of the sound modes for the conformal coefficients $\eta/s = 1/(4\pi)$ and $T\,\tau_\pi = \frac{2-ln\,2}{2\pi}$ (and since it lacks a holographic calculation of the coefficient $\mathcal{C}_1$, $\mathcal{C}_1 = 0$) in Figs. 4.2 and 4.3. There are instabilities and the group velocity diverges near this critical k_c.

The sound dispersion in a moving background becomes

$$\begin{aligned}(\omega - kv)^2 - c_s^2(k-\omega v)^2 + \\ +\frac{4\gamma}{3}i(\omega-kv)(k-\omega v)^2\Gamma\left(1+i\gamma\tau_\pi(\omega-kv)\right) + \frac{2\gamma^2}{3}\mathcal{C}_1\left(k-\omega v\right)^4 &= 0\,,\end{aligned} \tag{4.35}$$

or explicitly writing the highest powers of ω,

$$\begin{aligned}\cdots + \frac{4}{3}\left(2\mathcal{C}_1 kv^3\gamma^4 + iv^2\gamma^3\Gamma - 2kv\gamma^4\Gamma\tau_\pi - 2kv^3\gamma^4\Gamma\tau_\pi\right)\omega^3 + \\ \frac{2}{3}\left(\mathcal{C}_1 v^4\gamma^4 - 2v^2\gamma^4\Gamma\tau_\pi\right)\omega^4 = 0\,.\end{aligned} \tag{4.36}$$

Since this is complicated to explicitly solve, there is a more appropriate method to analyse the properties of the roots. We use the Vieta's formula to study the sum of the roots, or more precisely: For a polynomial $a_n z^n + a_{n-1}z^{n-1} + \cdots + a_0 = 0$, for complex coefficients and variables, the sum of the roots r_i is

$$\mathcal{S} \equiv \sum_{i=1}^{n} r_i = -\frac{a_{n-1}}{a_n}\,. \tag{4.37}$$

[3]We remark that the coefficient τ_π that appears at second order in the gradient expansion does not need to be necessarily positive. In fact, a recent study [119] in a strongly coupled model has found $\tau_{\pi\,0} < 0$. In this case, there is no linear instability.

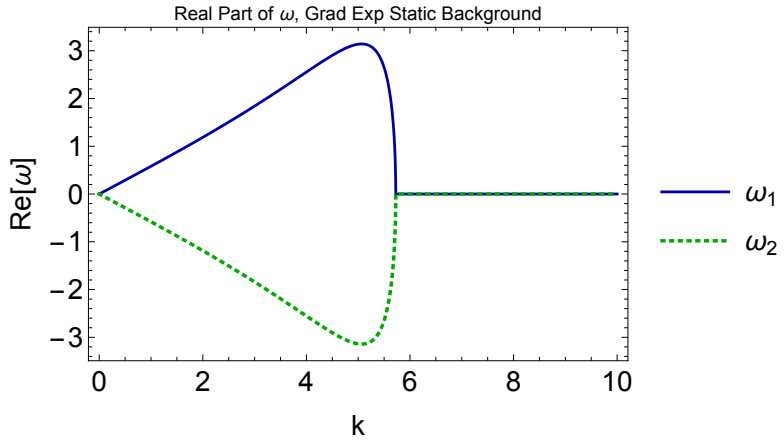

(a)

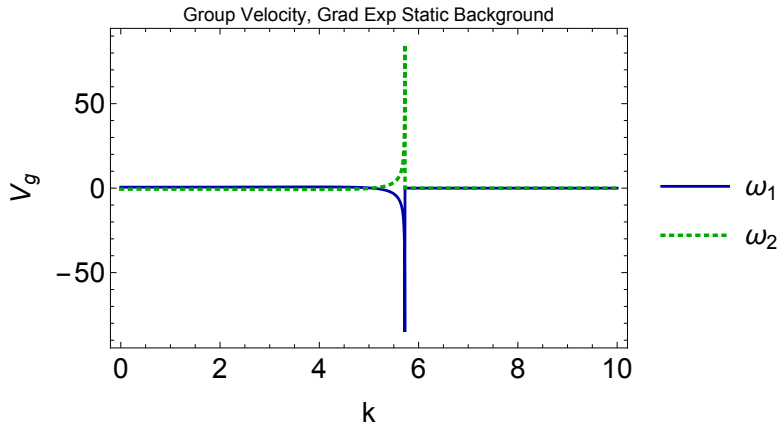

(b)

Figure 4.2: *Group velocity and the real part of sound modes for static background. The transport coefficients are $\mathcal{N}=4$ SYM (4.5), $\eta/s = 1/(4\pi)$ and $\tau_\pi T = \frac{(2-\ln 2)}{2\pi}$.*

Therefore, for Eq. (4.36) the sum of roots are

$$\mathcal{S}(k,v) = \frac{4\mathcal{C}_1 k v + 2i\Gamma}{\gamma(2\tau_\pi\Gamma - \mathcal{C}_1 v^2)} - \frac{4k(1+v^2)\tau_\pi\Gamma}{v(2\tau_\pi\Gamma - \mathcal{C}_1 v^2)} \ . \tag{4.38}$$

Even though we do not know the sign of $\mathcal{C}_1$, for small v this expression has a positive imaginary number. Therefore, at least one of the roots need to have a positive imaginary part, which translates to instabilities.

It is clear from Eq. (4.38) that the two coefficients $\mathcal{C}_1$ and τ_π contribute differently to the overall behavior of the modes. However, it is not immediately clear that one can differentiate them if the expansion is truncated up to terms in k to the third power.

It is possible to solve Eq. (4.35) taking $k \to 0$ and using $\omega(k) \to \chi_0 + \chi_1 k + O(k^2)$ and

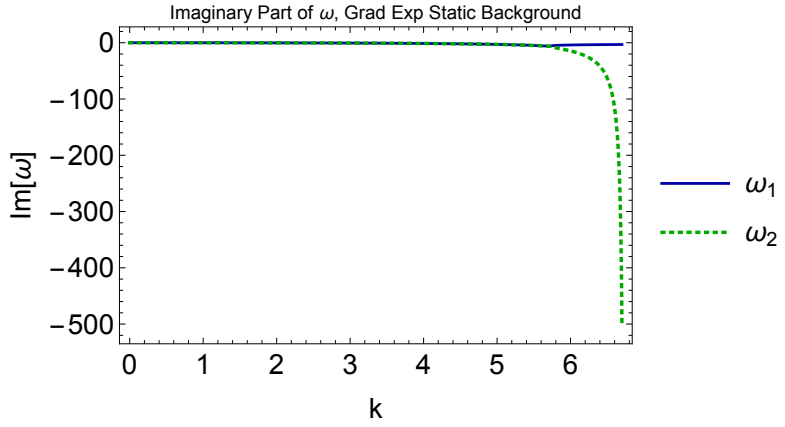

(a)

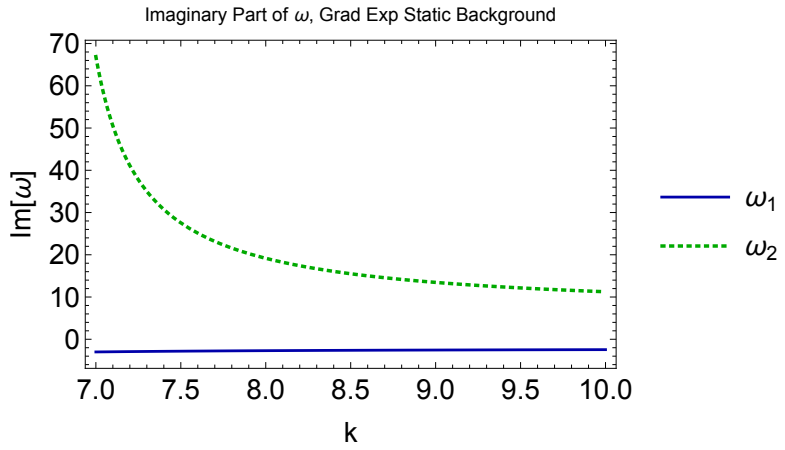

(b)

Figure 4.3: *Imaginary part of sound modes for static background. The transport coefficients are* $\mathcal{N} = 4$ *SYM (4.5),* $\eta/s = 1/(4\pi)$ *and* $\tau_\pi T = \frac{(2-\ln 2)}{2\pi}$*. This is unstable for positive imaginary values.*

keeping only the leading terms one finds

$$\chi_0^2\left[1 - v^2c_s^2 + i\frac{4}{3}\Gamma\,\gamma v^2\chi_0 - \frac{4}{3}\Gamma\tau_\pi\,\gamma^2v^2\chi_0^2 + \frac{2}{3}\mathcal{C}_1v^4\chi_0^2\right] = 0\,. \tag{4.39}$$

As it happened in Navier-Stokes theory, two modes will be hydrodynamical, i.e., they satisfy $\chi_0 = 0$, while the remaining modes will be non-hydrodynamical

$$\chi_0 = \frac{i\Gamma}{\gamma(2\Gamma\tau_\pi - \mathcal{C}_1v^2)}\left[1 \pm \sqrt{1 - \frac{3}{2v^2\Gamma^2}(1 - c_s^2v^2)(2\Gamma\tau_\pi - \mathcal{C}_1v^2)}\right]\,.$$

Both these modes did not exist when $v = 0$. Also, as it occurred in Navier-Stokes theory, they diverge in the limit where $v \to 0$. Finally, since $v^2c_s^2 < 1$ and assuming that τ_π is positive, both nontrivial solutions for χ_0 will have positive imaginary parts and the system

is, thus, linearly unstable.

4.4.2 Shear dispersion

The general covariant shear dispersion is

$$\Omega + i\Gamma\kappa^2 - \Gamma\tau_\pi\,\Omega\kappa^2 = 0\ . \tag{4.40}$$

In the static background, the shear dispersion relation to second order is

$$\omega + i\Gamma\,k^2 - \Gamma\tau_\pi\,\omega k^2 = 0\ . \tag{4.41}$$

It is easy to see that for the shear channel in a static background the solution is

$$\omega(k) = -\frac{ik^2\Gamma}{1-\tau_\pi\Gamma k^2} \tag{4.42}$$

and this becomes linearly unstable when $k > 1/\sqrt{\tau_{\pi\,0}\Gamma}$, but at that scale the sound channel has already developed an instability as showed before. For a moving background one finds the dispersion relation

$$(\omega - kv) + i(k-\omega v)^2\gamma\Gamma\left[1 + i\tau_\pi\gamma(\omega - kv)\right] = 0 \tag{4.43}$$

with which is easy to show that the sum of the modes is

$$\mathcal{S}(k,v) = kv\left(1+\frac{2}{v^2}\right) + \frac{i}{\gamma\tau_\pi} \tag{4.44}$$

and, hence, this system is linearly unstable. In fact, one can show that when $k \to 0$ one of the modes is hydrodynamical while the other two are non-hydrodynamical and linearly unstable if $\tau_\pi > 0$

$$\chi_0 = \frac{i}{2\tau_\pi\gamma}\left(1 \pm \sqrt{1 - \frac{4\tau_\pi}{v^2\Gamma}}\right)\ . \tag{4.45}$$

Up to the third power of k, there is no dependence on the second order coefficients. The same is true in the moving background dispersion for the hydrodynamical mode. This mode depends on v as

$$\omega = -vk - \frac{i}{\gamma^3}\Gamma k^2 - \frac{2v}{\gamma^4}\Gamma^2 k^3 + \mathcal{O}(k^4)\ . \tag{4.46}$$

This claim does not hold for higher powers of k or for the other non-hydrodynamical modes that appear in the theory. Moreover, the non hydrodynamical modes are sensitive to the coefficient τ_π (but not $\mathcal{C}_1$). These claims are evident from the structure of the sum

Eq. (4.44).

Therefore, we see that by going to second order in gradients the problems of the first order theory are not resolved. Rather, in this case the system is linearly unstable even when the background is static (the instability for a moving fluid also persisted). Next, we will show that the inclusion of one more derivative makes this situation much worse. In this case, the inclusion of a third derivative renders the system not only unstable but also also leads one to question hydrodynamical expansion.

4.5 Breakdown of the hydrodynamic expansion at third order in gradients?

We wrote a general expression that includes all relevant operators under linear perturbations up to third order of gradient expansion ($N = 3$), i.e., the dissipative theory Eq. (4.15). The resulting dispersion relations are written in covariant notation in Eqs. (4.22) and (4.23).

4.5.1 Sound Dispersion

In the static case, the sound channel is defined by

$$\omega^2 - \frac{1}{3}k^2 + \frac{4}{3}i\,\Gamma\,\omega k^2 + \frac{2}{3}\mathcal{C}_1\,k^4 - \frac{4}{3}\,\Gamma\tau_\pi\,\omega^2 k^2 + \\ \frac{2}{3}i\,c_2\,\omega k^4 - \frac{2}{3}i\,\mathcal{C}_3\,\omega k^4 + \frac{2}{3}i\,c_4\,\omega k^4 - \frac{2}{3}i\,c_5\,\omega^3 k^2 = 0\ , \tag{4.47}$$

The sum of the three modes $\omega(k)$ is

$$\mathcal{S}(k,v) = -\frac{3i}{2c_5\,k^2} + \tau_\pi\Gamma\,\frac{2i}{c_5}\ , \tag{4.48}$$

which shows that there are terms that go as $\sim 1/k^2$ in the modes (alternatively, note that taking $k = 0$ in the dispersion relation changes the order of the polynomial). In fact, one can solve the equation for the modes and show that in the low momentum limit one finds

$$w(k) = \pm c_s k - \frac{2}{3}ik^2\Gamma + \mathcal{O}(k^3)\,, \qquad \omega(k) = -\frac{3}{2}\frac{i}{c_5 k^2} + \frac{2i}{c_5}\Gamma\tau_{\pi\,0} + \frac{4}{3}ik^2\Gamma + \mathcal{O}(k^4)\,. \tag{4.49}$$

There are two hydrodynamic modes and one non-hydrodynamic mode but this theory is linearly unstable for any value of k. In fact, one can see that the hydrodynamic expansion breaks down due to the $\sim 1/k^2$ term in the third mode. This theory is pathological

since the additional derivative with respect to $N = 2$ case affects not only the short wavelength behavior of the modes but it also destroys the infrared of the theory making the homogeneous limit of the sound channel ill-defined.

4.5.2 Shear Dispersion

Eq. (4.23) in a static background is a simple second order polynomial,

$$\omega + i\Gamma\, k^2 - \Gamma\tau_\pi\, \omega k^2 + \frac{i}{2}\, c_4\, k^4 - \frac{i}{2}\, c_5\, \omega^2 k^2 = 0\ . \tag{4.50}$$

In the shear channel one can solve the dispersion equation directly to find that there are now one hydrodynamic mode and also an additional non-hydrodynamic mode

$$\omega(k) = -i\Gamma k^2 + \mathcal{O}(k^4)\,, \qquad \omega(k) = -\frac{2i}{c_5}\frac{1}{k^2} + \frac{2i}{c_5}\Gamma\tau_\pi + i\Gamma k^2 + \mathcal{O}(k^4)\,. \tag{4.51}$$

Once more, the system is unstable and the homogeneous limit of the shear channel does not exist anymore. A more thorough analysis may be performed to find the properties of this third order system in a moving fluid. However, given the serious issue regarding the absence of the homogeneous limit found already in the case of perturbations around the static background we leave such an analysis to a future study.

4.5.3 Sound mode without Second Comoving Derivative of Shear Tensor

We briefly investigate the behavior of third order sound dispersion relation Eq. (4.22) if we neglect a contribution from the second comoving derivative of the shear tensor, i.e., $c_5 = 0$.

In the covariant notation, the equation is then

$$\begin{aligned}&\Omega^2 - \frac{1}{3}\kappa^2 + \frac{4}{3}i\,\Gamma\,\Omega\kappa^2 + \frac{2}{3}\,\mathcal{C}_1\,\kappa^4 - \frac{4}{3}\,\Gamma\tau_\pi\,\Omega^2 k^2 + \\ &\frac{2}{3}i\,c_2\,\Omega k^4 - \frac{2}{3}i\,\mathcal{C}_3\,\Omega k^4 + \frac{2}{3}i\,c_4\,\Omega k^4 = 0\ .\end{aligned} \tag{4.52}$$

For the usual choice $\Omega = \gamma(\omega - kv)$ and $\kappa = \gamma(k - \omega v)$ in a moving fluid, the sum of the 5 roots of the 5^{th} order polynomial is

$$\mathcal{S}(k, v) = \frac{i}{\gamma}\frac{\mathcal{C}_1}{(c_2 - \mathcal{C}_3 + c_4)} - 4\frac{k}{v} - kv - \frac{2\,i}{\gamma\, v^2}\frac{\Gamma\tau_\pi}{(c_2 - \mathcal{C}_3 + c_4)}\,. \tag{4.53}$$

There are modes with divergence for small v as well, which results in group velocities

that scale as $1/v$. The sign of the imaginary part depends on the details of the coefficients that are not known in principle, and that is also a problem with such an approach. The third order coefficients should be a small correction to the dynamics of the system and, therefore, it is odd that any small deviation of such value would imply infinitely large instabilities (as it scales as $1/v^2$).

However, if one neglects the contribution of the second comoving derivative of the shear tensor, the infrared inconsistencies of modes depending on the inverse of the wavenumber are absent.

4.6 Linearized second order Israel-Stewart theory

In this section we analyse the behavior of Israel-Stewart Eq. (3.4) under linear perturbations, in which the dissipative tensor becomes

$$\tau_\pi D_0 \delta\pi^{<\mu\nu>} + \delta\pi^{\mu\nu} = 2\eta_0 \delta\sigma^{\mu\nu} \,. \tag{4.54}$$

Therefore, the sound and shear covariant dispersion relations are

$$(\Omega^2 - \frac{1}{3}\kappa^2)(1 - i\tau_\pi\Omega) + \frac{4}{3}i\Gamma\Omega\kappa^2 = 0 \,, \tag{4.55}$$

$$\Omega(1 - i\tau_\pi\Omega) + i\Gamma\kappa^2 = 0 \,. \tag{4.56}$$

4.6.1 Sound Modes

In the static background, the dispersion relation is a third order polynomial,

$$(\omega^2 - \frac{1}{3}k^2)(1 - i\tau_\pi\omega) + \frac{4}{3}i\Gamma\omega k^2 = 0 \,. \tag{4.57}$$

We show the results in Figs. 4.4 and 4.5.

The group velocity is always bounded and well-behaved, and the imaginary part is always negative, which indicates stability. The theory is mathematically well-defined at any k, differently from the behavior of second order gradient expansion theory in Figs. 4.2 and 4.3.

Another feature of the Israel-Stewart theory is that there are always the same number of modes for any background velocities: two hydrodynamical and one non-hydrodynamical. The gradient expansion theory had emerging non-hydrodynamical modes for non-zero v, which lead to instabilities and $1/v$ behavior. Therefore, it is interesting to investigate the Israel-Stewart modes for a moving background, Eq. 4.55 with the usual $\Omega = \gamma(\omega - kv)$

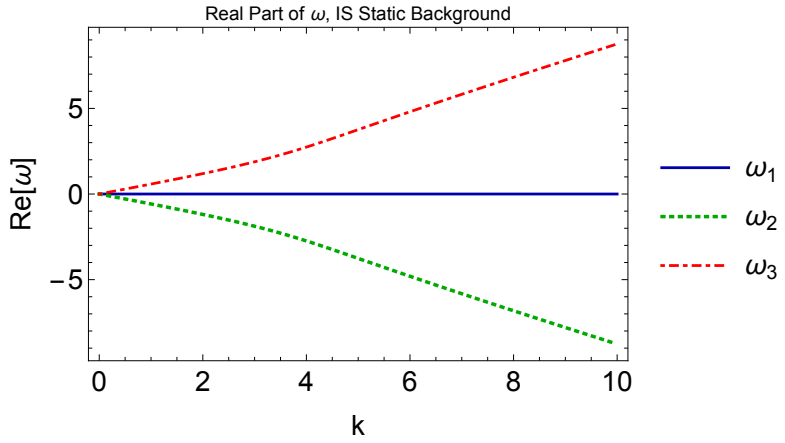

(a)

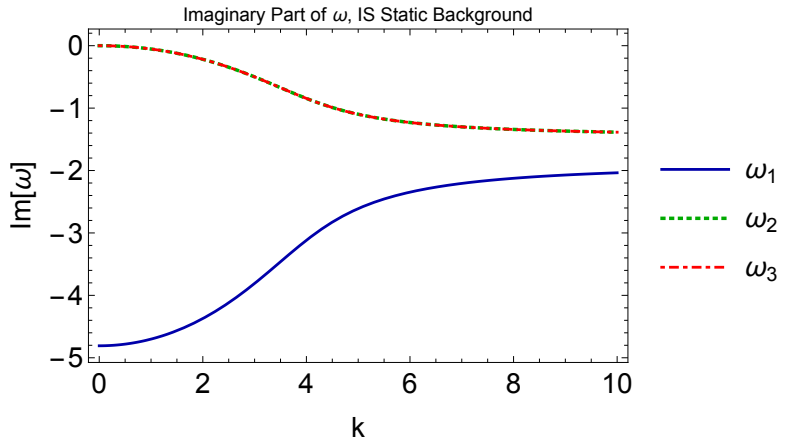

(b)

Figure 4.4: *Real and imaginary part of sound modes for static background, Israel-Stewart theory. The transport coefficients are $\mathcal{N} = 4$ SYM (4.5), $\eta/s = 1/(4\pi)$ and $\tau_\pi T = \frac{(2-\ln 2)}{2\pi}$. Negative imaginary values correspond to stable dynamics.*

and $\kappa = \gamma(k - \omega v)$. The third order polynomial roots can be solved in general, but we focus on the structure for small k and v.

The sound and shear hydrodynamical modes in Israel-Stewart theory are equivalent to the ones in the gradient expansion theory up to k^3. This statement holds even in a moving background. The sound modes are

$$\omega_{1,2} = -\frac{2v \pm \sqrt{3}(1-v^2)}{3-v^2}\, k - \frac{2i}{\gamma^3}\frac{9 \mp v\left(9\sqrt{3} \mp v\left(9 \mp \sqrt{3}v\right)\right)}{(3-v^2)^3}\Gamma\, k^2 + \left[\pm\frac{2\sqrt{3}}{9}\left(\Gamma - \tau_\pi\right) + \frac{8}{9}\left(\tau_\pi - 2\Gamma\right)v + \mathcal{O}(v^2)\right]\Gamma k^3 + \mathcal{O}(k^4)\ , \tag{4.58}$$

The non-hydrodynamical modes are different for Israel-Stewart and Burnett theories.

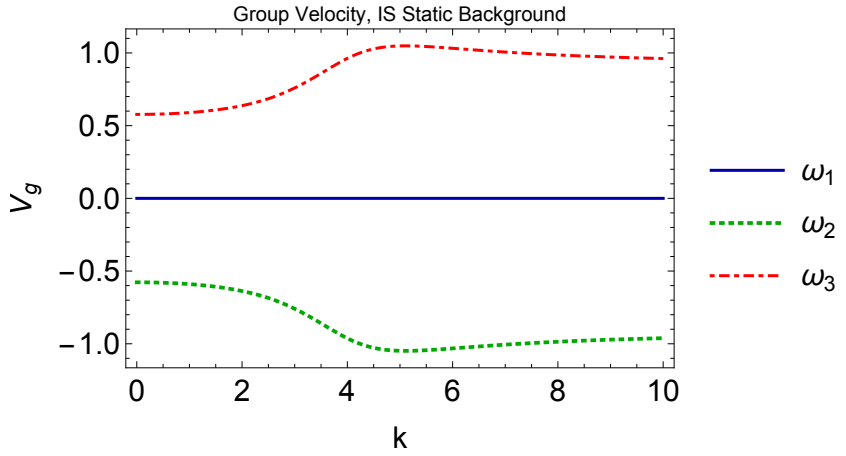

Figure 4.5: *Group velocity and the real part of sound modes for static background, Israel-Stewart theory. The transport coefficients are $\mathcal{N} = 4$ SYM (4.5), $\eta/s = 1/(4\pi)$ and $\tau_\pi T = \frac{(2-\ln 2)}{2\pi}$.*

In particular, the IS one is always stable and causal under linear perturbation given τ_π is larger than a critical value.

The non-hydrodynamical mode in Israel-Stewart theory is

$$\omega_3 = -\frac{\gamma\, i\, (3-v^2)}{3\tau_\pi - v^2(\tau_\pi + 4\Gamma)} + \left[\left(\frac{8}{3\tau_\pi}\Gamma - 1\right) v + \mathcal{O}(v^3)\right] k + \\ + \left[\frac{4\,i}{3}\Gamma - \frac{i}{3}\,(10\Gamma - \tau_\pi)\, v + \mathcal{O}(v^4)\right] k^2 + \mathcal{O}(k^3)\ . \tag{4.59}$$

If $\tau_\pi > 2\Gamma$, it is guaranteed from Eq. (4.59) that this mode is always stable for any background velocity [59, 74].

4.6.2 Shear Modes

The dispersion relation of shear modes in Israel-Stewart theory, given by Eq. (4.56), has two modes for every background velocity. We solve $\omega(k)$ for small k and a generic background velocity,

$$\omega_1 = -vk - \frac{i}{\gamma^3}\Gamma k^2 - \frac{2v}{\gamma^4}\Gamma^2 k^3 + \mathcal{O}(k^4)\ , \\ \omega_2 = -\frac{i}{\gamma(\tau_\pi - v^2\Gamma)} - \frac{(v(\tau_\pi - 2\Gamma) + v^3\Gamma)}{\tau_\pi - \Gamma} k + \mathcal{O}(k^2)\ . \tag{4.60}$$

Notice that the non-hydrodynamical mode is once again stable if τ_π is large enough compared to Γ. Also, the hydrodynamical mode agrees with the second order gradient expansion theory (4.46).

4.7 Improving the short wavelength behavior through resummation

Let us return to the sound dispersion relation in the second order theory (the same argument done below is also valid for the shear channel). As shown before, the sound modes are defined by

$$\Omega^2 - c_s^2\kappa^2 + \frac{4}{3}i\Omega\kappa^2\Gamma\left(1 + i\tau_\pi\Omega\right) = 0\,. \tag{4.61}$$

To lowest order in frequency and momenta, one may use the substitution [68]

$$\frac{1}{1 - i\tau_\pi\Omega} = 1 + i\tau_\pi\Omega + \mathcal{O}(\Omega^2) \tag{4.62}$$

and find a new dispersion relation that is of Israel-Stewart type

$$\Omega^2 - c_s^2\kappa^2 + \frac{4}{3}i\Omega\kappa^2\Gamma\frac{1}{1 - i\tau_\pi\Omega} = 0\,. \tag{4.63}$$

In terms of the equations of motion, this resummation is equivalent to impose that $\pi^{\mu\nu}$ obeys a first-order, relaxation-like equation such as that found, for instance, in kinetic theory through the moments method [30].

The results from this “resummed" theory agree with those from the gradient expansion up to the order of validity of Burnett's theory. In fact, for a static background this dispersion relation becomes

$$(\omega^2 - c_s^2k^2)(1 - i\tau_\pi\omega) + \frac{4}{3}i\omega k^2\Gamma = 0\,, \tag{4.64}$$

which is a polynomial of order three and has, thus, three modes given by

$$\omega(k) = \pm c_s k - \frac{2}{3}i\Gamma k^2 \mp \frac{2\Gamma}{9c_s}(\Gamma - 3c_s^2\tau_\pi)k^3 + \mathcal{O}\left(k^4\right) \tag{4.65}$$

$$\omega(k) = -\frac{i}{\tau_\pi} + \mathcal{O}(k^2)\,. \tag{4.66}$$

The first two hydrodynamic modes are the same as those found in (4.34) up to order k^3. The third mode is non-hydrodynamical (though stable) and it decouples from the spectrum if k is sufficiently small. Therefore, in the case of disturbances around a static background, in the hydrodynamic limit the resummed dispersion relation (4.63) and the gradient expansion (4.33) describe essentially the same physics and one can “bypass" the instability found in the sound channel of Burnett's theory by effectively using the modes of the Israel-Stewart-like theory for all values of $k < 1/\tau_\pi$ (with this restriction the additional

non-hydrodynamical mode does not contribute to the effective theory).

As we previously showed, in the case of a moving fluid Burnett's theory has four modes in the sound channel, two of which are hydrodynamical while the others are non-hydrodynamical and intrinsically linearly unstable even in the limit of $k \to 0$. However, the IS-like theory in (4.63) does not change the number of modes when going from a static background to a moving fluid. Once more, the two hydrodynamic modes found in this case agree with those of Burnett's theory up to $\mathcal{O}(k^4)$ but the non-hydrodynamic mode of this theory is stable (see [74] for the conditions on the value of τ_π in Israel-Stewart theory that must be met to guarantee linear stability). Therefore, even in the case of a moving fluid, the replacement (4.33) $\to$ (4.63) does not alter the low momentum properties of the system and it changes only the short wavelength, non-hydrodynamic behavior. Clearly, a necessary condition for the use of this type of resummation is that the infrared, hydrodynamic properties of the system are maintained and only the short wavelength physics is affected.

One may then wonder if the infrared problem found at third order in gradients already in the case of a static background can be "cured" by a similar resummation. In this case, the sound channel of the resummed theory would be (with $\mathcal{C}_1 = 0$ and the other contributions rescaled to c_4)

$$\Omega^2 - c_s^2\kappa^2 + \frac{4}{3}i\Omega\kappa^2\Gamma\,\frac{1+d_1(-i\Omega)}{1-i(\tau_\pi+d_1)\Omega + c_4\frac{\kappa^2}{2\Gamma} + c_5\frac{\Omega^2}{2\Gamma}} \;=\; 0\,. \tag{4.67}$$

where d_1 is a new coefficient that can appear at this order. Note that this equation agrees with (4.22) when Ω and κ are small. In terms of equations of motion, this dispersion relation corresponds to the case where the shear stress tensor obeys an independent differential equation of second order in derivatives, as explained in [29, 120]. For a static background one finds that the sum of the four modes is

$$\mathcal{S} = \frac{2i}{c_5}\Gamma(d_1+\tau_\pi)\,. \tag{4.68}$$

While the stability properties of such a theory depends on the values (and the signs!) of its various transport coefficients, one can immediately see that the $\sim 1/k^2$ contribution found for the third order gradient theory is not present. Therefore, one can safely take the $k \to 0$ limit to find

$$\chi_0^2\left[1 - i(\tau_\pi+d_1)\chi_0 + c_5\frac{\chi_0^2}{2\Gamma}\right] = 0\,, \tag{4.69}$$

which shows that there are two hydrodynamic modes (as expected) and also two non-

hydrodynamic modes

$$\chi_0 = i\frac{\Gamma}{c_5}\left[\tau_\pi + d_1 \pm \sqrt{(\tau_\pi + d_1)^2 + \frac{2c_5}{\Gamma}}\right] . \tag{4.70}$$

If $c_5 > 0$ the homogenous limit of these modes is linearly unstable while stability requires $c_5 < 0$. In fact, in this case for $|c_5| < \Gamma(\tau_\pi + d_1)^2/2$ no conditions on the sign of $\tau_\pi + d_1$ are need while if $|c_5| > \Gamma(\tau_\pi + d_1)^2/2$ one needs $\tau_\pi + d_1 > 0$ for homogeneous stability. A full stability analysis of this theory for nonzero k requires the knowledge of the several transport coefficients involved in the equations. The value of these coefficients can be found, in the context of kinetic theory, using the formalism developed in [29] but this is beyond the scope of this thesis. Also, it is possible to check that the shear channel in the static fluid is also free of $1/k^2$ terms in this resummed theory (the corresponding analysis for a moving fluid is very cumbersome though straightforward but we will not study it here since it does not bring any new aspect into the problem).

This resummed theory has two hydrodynamic modes that agree with those of the $N = 3$ gradient theory at low momentum but the two non-hydrodynamic modes in this case are well defined (and can be stable) in the homogeneous limit of the perturbations. Therefore, the resummation is not really equivalent to the $N = 3$ gradient expansion theory since the hydrodynamic expansion in powers of momentum works in the former but fails for the latter.

4.7.1 Expansion in derivatives of $\pi^{\mu\nu}$

We now argue that the resummation argument from the last section is connected to a truncation of an expansion in derivatives of $\pi^{\mu\nu}$. Since the differential equation involves a larger number of initial conditions, it seems reasonable to assume that the new initial conditions on $\pi^{\mu\nu}$ represent some resummed microscopic degree of freedom and then the tensor $\pi^{\mu\nu}$ is an effective emergent degree of freedom. This behavior was evident for the Israel-Stewart semi-analytical solutions for the Bjorken and Gubser flows, discussed in Chapter 2.

We propose the general expansion of the dissipative tensor up to third order of comoving derivatives of dissipative tensor, which we will call third order Israel-Stewart (only linear contributions are relevant for this discussion),

$$\begin{aligned}&\mathcal{B}_{3,2}D_0\nabla_\perp^2\delta\pi^{<\mu\nu>} + \mathcal{B}_{3,1}D_0^3\delta\pi^{<\mu\nu>} + \mathcal{B}_{2,2}\nabla_\perp^2\delta\pi^{<\mu\nu>} + \\ &\mathcal{B}_{2,1}D_0^2\delta\pi^{<\mu\nu>} + \mathcal{B}_1 D_0\delta\pi^{<\mu\nu>} + \delta\pi^{\mu\nu} = 2\eta_0\delta\sigma^{\mu\nu} + \cdots .\end{aligned} \tag{4.71}$$

where on the right hand side we considered the gradient expansion terms of Eq. (4.30). In the covariant momentum space, the contribution of the dissipative tensor to the sound and shear modes are modified as (GE stands for gradient expansion),

$$\delta\pi^{\mu\nu}_{IS} = \frac{1}{1 - i\mathcal{B}_1\Omega - \mathcal{B}_{2,1}\Omega^2 - \mathcal{B}_{2,2}\kappa^2 + i\mathcal{B}_{3,1}\Omega^3 + i\mathcal{B}_{3,2}\Omega\kappa^2}\,\delta\pi^{\mu\nu}_{GE}\ . \tag{4.72}$$

Furthermore, we can write the general sound and shear dispersion relation for this Israel-Stewart-like theory as

$$\begin{aligned}&(\Omega^2 - \frac{1}{3}\kappa^2)(1 - i\mathcal{B}_1\Omega - \mathcal{B}_{2,1}\Omega^2 - \mathcal{B}_{2,2}\kappa^2 + i\mathcal{B}_{3,1}\Omega^3 + i\mathcal{B}_{3,2}\Omega\kappa^2) + \frac{4}{3}i\Gamma\Omega\kappa^2 + \\ &\frac{2}{3}\mathcal{C}_1\kappa^4 - \frac{4}{3}\Gamma\tau_\pi\Omega^2\kappa^2 + \frac{2}{3}ic_2\Omega\kappa^4 - \frac{2}{3}i\mathcal{C}_3\Omega\kappa^4 + \frac{2}{3}ic_4\Omega\kappa^4 - \frac{2}{3}ic_5\Omega^3\kappa^2 = 0\ .\end{aligned} \tag{4.73}$$

And the shear dispersion becomes

$$\begin{aligned}&\Omega(1 - i\mathcal{B}_1\Omega - \mathcal{B}_{2,1}\Omega^2 - \mathcal{B}_{2,2}\kappa^2 + i\mathcal{B}_{3,1}\Omega^3 + i\mathcal{B}_{3,2}\Omega\kappa^2) + \\ &i\Gamma\kappa^2 - \Gamma\tau_\pi\Omega\kappa^2 + \frac{i}{2}c_4\kappa^4 - \frac{i}{2}c_5\Omega^2\kappa^2 = 0\ .\end{aligned} \tag{4.74}$$

It is very hard task to make general statements about stability and causality as we do not know from first principles which microscopic model would generate such macroscopic theory, nor we know the full parameter space of these many coefficients. However, we notice one interesting feature of such polynomials: there is always the same number of degrees of freedom in the static as well as in the moving background. The number of modes is clearly the same as the sound dispersion contains the term Ω^5 and the shear dispersion contains Ω^4. Therefore, we do not expect the non-hydrodynamical modes to scale as $1/v$ as the gradient expansion theories. If we analyze Eq. (4.73) in a static background, the Vieta formula for the sum of the roots is simply

$$\mathcal{S} = -\frac{i\mathcal{B}_{2,1}}{\mathcal{B}_{3,1}}\,, \tag{4.75}$$

which is free of the IR divergence $1/k^2$.

Therefore, we can use fourth order Israel-Stewart to "define" the third order gradient expansion, similarly to using second order Israel-Stewart to "define" Navier-Stokes equation.

4.8 Conclusions of the Chapter

The causality and stability properties of linear perturbations in the sound channel of a dissipative fluid constructed using an N^{th} order gradient expansion are nontrivial but still tractable in some important limits, such as the hydrodynamical limit of small momenta k. We showed that at the linear level (which is the adequate limit concerning sound waves) there is violation of causality and there is also at least one (linearly) unstable mode in the sound channel up to third order in the derivative expansion for small background flow velocities. The problems of stability and causality were translated into a mathematical investigation of the properties of the roots of the polynomial defined by the sound dispersion relation. We believe that such identification was crucial to investigate the idea that a relativistic theory constructed using the gradient expansion has generally unstable modes in its spectrum[4]. Our results are consistent with Ref. [42] where instabilities were found to be a generic property of 1st-order Navier-Stokes theories.

We note that the higher order terms in Israel-Stewart were introduced in order to avoid the divergences in small v and small k of the third order theory in the gradient expansion. One non-trivial connection to the non-equilibrium physics is through the quasi-normal (QN) modes obtained from a microscopic theory; for instance, systems described by the Boltzmann equation or AdS/CFT. In holography, the structure of QN modes implies that the dissipative tensor should generally obey at least a second order differential equation. The effective hydrodynamical theory that emerges from holography should be directly connected to the microscopical degrees of freedom of the plasma. Therefore, not only it should contain the known hydrodynamical excitations, but it should also include non-equilibrium physics encoded in non-hydrodynamical modes. Well defined nonlinear relativistic theories should not contain divergences, instabilities, and causality issues. It is crucial the role of non-linearity in this scenario, as propagation beyond the linearized regime will mix the modes seen in a linear treatment nontrivially.

In the next section we review the fluid/gravity duality, which is based on thegradient expansion, and suggest further investigation in order to find the holographic dual of a consistent dissipative relativistic fluid theory.

[4]A general background flow should have regions where the velocity is small and, thus, we expect that the linear instability found here should be a common problem in these theories.

Chapter 5

Overview of the Fluid-Gravity Correspondence

We overview some aspects of the fluid-gravity correspondence [39, 61, 62] and its implications to non-equilibrium physics in this final chapter. Since this is still a work in progress, the approach is quite different from the rest of the thesis: we limit ourselves to overview some aspects found in the literature and outline future research directions.

In the context of the fluid-gravity correspondence, a gradient expansion approach has already been consolidated. However, as we throughly discussed through this thesis, it is not expected that the dissipative relativistic hydrodynamics constructed in this manner to produce well-behaved solutions, whether analytically and semi-analytically (Chapter 2) or that are stable under linear perturbations (Chapter 4). Therefore, a natural question is whether there is a rigorous construction that is mathematically well-behaved for different background velocities and wavelengths at strong coupling while it also describes the well-stablished properties of the quasinormal (QN) modes of AdS/CFT for late times. In fact, the goal would be to find whether there is an effective nonlinear theory that connects both hydrodynamical and non-hydrodynamical modes within the Fluid-Gravity correspondence, in analogy to the truncation through the moments method [30] of the Boltzmann equation.

We use natural units and the mostly plus metric signature in this chapter, $g_{\mu\nu} = \text{diag}(-1, 1, 1, 1)$, as well as natural units.

5.1 The Fluid-Gravity construction

An exciting consequence of the AdS/CFT correspondence is that the dynamics of gravity in $(d + 1)$ dimension asymptotically Anti-de Sitter spacetime is dual to fluid dynamics in its d dimensional conformal boundary [62].

The classical limit of a strongly interacting many-body quantum field theory is supposed to be described by collective dynamics, a relativistic strongly interacting fluid that rapidly thermalizes. Recent experimental results corroborate this picture [7], and heavy ion collisions are believed to produce the Quark Gluon Plasma, a strongly interacting fluid with origin in the many-body properties of non-Abelian gauge theory, QCD. QCD at low-energies is strongly interacting and so far the methods to successfully address its non-perturbative behavior, such as lattice-QCD, are not appropriate to describe real-time phenomena and consequently the calculations of transport coefficients and hydrodynamics behavior.

Despite $\mathcal{N} = 4$ Super Yang-Mills being a very different quantum field from QCD(there is no confinement and the beta function vanishes) it seems that its hydrodynamical regime reveals some kind of universal behavior. Therefore, it is natural to consider the framework of AdS/CFT (and holography in general) as a useful tool to access the non-equilibrium physics. For a recent review of holography and some phenomenological applications of strongly coupled gauge theories, see for instance Ref. [31].

If the fluid picture is the appropriate dynamics of long wavelength excitations of a hot quantum plasma, then its solutions should be connected somehow to the dynamics of gravity in one higher dimension, by the principles of AdS/CFT. The early efforts [121–125] to understand such mappings were connected to the Bjorken symmetry, throughly discussed in Chapter 2. The question was which dual spacetime described the scaling Bjorken analytic solution. Since fluid dynamics is an effective, long wavelength coarse-grained description of a microscopic theory and its related fields, it seems reasonable to assume some sort of truncation on Einstein's equation should lead to the correct map.

It is crucial at this point to notice that the construction of dissipative hydrodynamics is not unique. In the previous chapters we analyzed very different implementations of dissipative hydrodynamics at second order in gradients, the relaxation type Israel-Stewart theory and the gradient expansion Burnett theory. For instance, the microscopic origins of both theories can be traced back to kinetic theory; however, the assumptions about truncation are responsible for the final structure of the theory.

For instance, the gradient expansion approach involves a truncation on all the perfect fluid variables as a series controlled by a small parameter, such as the mean free path ($\lambda_{\rm mfp}$) of quasiparticle excitations [40]. In such scenario, we have

$$\pi^{\mu\nu} \approx \frac{\lambda_{\rm mfp}}{l}\,\mathcal{O}_1^{\mu\nu} + \frac{\lambda_{\rm mfp}^2}{l^2}\,\mathcal{O}_2^{\mu\nu} + \cdots\,, \tag{5.1}$$

where $\mathcal{O}_j^{\mu\nu}$ stands for a class of nonlinear operators of order j in derivatives that respects the system's symmetry and l is the typical length of the gradient. This ratio $\mathrm{Kn} \equiv \lambda_{\rm mfp}/l$ is known as the Knudsen number.

The Israel-Stewart approach can be obtained from kinetic theory/Boltzmann equation using the moments method [30]. This method involves expanding the collision term of the Boltzmann equation in momentum space, through an irreducible and complete basis. Each moment of the Botzmann distribution function is a new dynamical field, and the truncation of this series depends on a different dimensionless variable in the theory. The usual solution is to consider a truncation in the inverse Reynolds number, which relates the dissipative tensor $\mu\nu$ to the equilibrium pressure p_0 as $R_\pi^{-1} \equiv |\pi^{\mu\nu}|/p_0$, and is a measure of how far from equilibrium the system is.

The picture is very clear: the higher moments of the Boltzmann distribution describe higher energy excitations, which probe shorter distances/lengths. Therefore, the truncation in momentum space for the inverse Reynolds number just implies an effective long wavelength theory, just what is expected of hydrodynamics. However, such theories have also excitations other than the hydrodynamical modes, which we showed in the last chapter are necessary to ensure causality and stability for the whole spectrum of wavenumber and velocities. It is true that we expect these very high-energetic modes to be suppressed otherwise the validity of the hydrodynamical approximation is broken, but nonetheless they are necessarily present to ensure mathematical consistency of the infrared theory. One example is general relativity, even though at short distances there should be the new degrees of freedom of quantum gravity, the long wavelength classical approximation of general relativity is not only mathematically consistent, but its own definition is that locally spacetime should become Minkowskian!

The so called Fluid-Gravity correspondence is a long wavelength approximation of Einstein's equation with negative cosmological constant where the dynamical variables are truncated order by order, and the boundary fluid theory is exactly the Burnett gradient expansion theory. In a sense, the current fluid/gravity map is the strong coupling analog of the Chapman-Enskog theory [114], commonly used in kinetic theory [40].

In the following sections, we shall study some properties of AdS space and black brane solutions, while giving an introduction to holographic methods. Then, we review the Fluid-Gravity in the case of Navier-Stokes theory.

5.2 The geometry of AdS

To investigate the geometrical properties of AdS spaces, we follow the references [33, 126, 127] closely. Consider the Lorentzian curve in $\mathbb{R}^{p+1,2}$,

$$\eta_{ab}X^aX^b = -L^2\,,$$
$$-X_0^2 + \sum_{i=1}^{p+1} X_i^2 - X_{p+2}^2 = -L^2\,. \tag{5.2}$$

The metric on this embedded space is simply

$$ds^2 = -dX_0^2 + \sum_{i=1}^{p+1} dX_i^2 - dX_{p+2}^2\,. \tag{5.3}$$

This embedding of the AdS_{p+2} makes the isometry $SO(2,p+1)$ manifest. For instance, it is no surprise then that should there be a relation between AdS_5 and the conformal group in four dimensions $SO(2,4)$.

We can write the metric in global coordinates through the identification [1]

$$X_0 = L\cosh\rho\cos\tau\,,$$
$$X_i = L\sinh\rho\,\Omega_i\,,$$
$$X_{p+2} = L\cosh\rho\sin\tau\,. \tag{5.4}$$

and $\sum_{i=1}^{p+1}\Omega_i$. The global metric then becomes

$$ds^2 = L^2\left(-\cosh^2\rho\,d\tau^2 + d\rho^2 + \sinh^2\rho\,d\Omega_p^2\right)\,. \tag{5.5}$$

This metric has the rotational symmetry $SO(p+1)$ explicit from $d\Omega_p^2$, and from the coordinate transformations there is a rotation symmetry $SO(2)$ for $\tau \to \tau + a$. The coordinates $\rho \geq 0$ and $0 \leq \tau \leq 2\pi$ cover the hyperboloid once. We represent this geometry in Fig. 5.1.

5.2.1 Asymptotic Flatness

We want to briefly study the causal structure of $\mathbb{R}^{1,p}$. The causal structure is preserved under Weyl transformations, as light rays ($\eta_{ab}X^aX^b = 0$) are invariant under such operations. We call the flat space of interest ds_1^2, and in order to study its causal structure we study the following operations [33],

[1] We also study global coordinates of de Sitter space in Appendix C .

$$ds_1^2 = -dt^2 + dr^2 + r^2 d\Omega_{p-1}^2 \,,$$
$$ds_1^2 = -du_+ u_- + \frac{1}{4}(u_+ - u_-)^2 d\Omega_{p-1}^2 \,, \tag{5.6}$$

where the coordinates $u_\pm = t \pm r$ are the lightcone trajectories. Now we can bring spatial infinity to finite coordinates with the following operations and identifications, $u_\pm = \tan\tilde{u}_\pm$, and writing in more usual coordinates $\tilde{u}_\pm = (\tau \pm \theta)/2$. The metric is then

$$ds_1^2 = \frac{1}{4\cos^2\tilde{u}_+ \cos^2\tilde{u}_-} \left(-d\tau^2 + d\theta^2 + \sin^2\theta \, d\Omega_{p-1}^2\right) . \tag{5.7}$$

This maps a fixed point on the sphere S_{p-1} to triangular regions in τ and θ. It can be analytically continued outside the triangle to make manifest the symmetry of the spacetime, $0 \leq \theta \leq \pi$ and $-\infty < \tau < \infty$. Notice that for $\tau = 0$, $\theta = 0$ and $\theta = \pi$ map spatial infinity, or the north and south pole of the sphere S^p. The boundary of this spacetime then has topology of $\mathbb{R} \times S^p$. We represent its Penrose diagram in Fig. 5.2.

5.2.2 Asymptotic AdS

For small ρ, the metric (5.5) becomes a closed timelike curve with radius L, as $\cosh\rho \to 1$, with topology $S^1 \times \mathbb{R}^{p+1}$. For physical descriptions this is clearly a problem and the appropriate AdS metric should "unwrap" the time coordinate, which means finding the universal cover of the hyperboloid. Before doing so, it is interesting to check the boundary of AdS though a conformal transformation. Suppose we have [33]

$$\tan\theta = \sinh\rho \,,$$
$$ds^2 = \frac{L^2}{\cos^2\theta} \left(-d\tau^2 + d\theta^2 + \sin^2\theta d\Omega_p^2\right) , \tag{5.8}$$

with the range of the new coordinate as $0 \leq \theta \leq \pi/2$. The conformal metric that preserves the causal structure is then

$$ds'^2 = \left(-d\tau^2 + d\theta^2 + \sin^2\theta d\Omega_p^2\right) . \tag{5.9}$$

The topology of the boundary of this spacetime is then $\mathbb{R} \times S^p$, with a boundary at $\theta = \pi/2$. Spacetimes that can be conformally mapped to such asymptotic structure are called asymptotic Anti-de Sitter spaces, and they need a boundary condition to have a well posed Cauchy problem at $\theta = \pi/2$. The map of the asymptotic Anti-de Sitter space is exactly half of the conformal compactification of $\mathbb{R}^{1,p}$, which corroborates the

idea in holography that AdS_{p+2} and $\mathbb{R}^{1,p}$ have similar boundaries. We represent a Penrose diagram of AdS space in Fig. 5.3.

5.2.3 Poincaré Patch

Finally, we want to "unwrap" the time coordinate of the global AdS space in order to study its physical properties. Such construction is called the universal covering of the space. It can be achieved through the coordinate parametrizations $(r, t, \vec{x})$ and $0 < u, \vec{x} \in \mathbb{R}^p$). The following substitution then covers half of the hyperboloid [33],

$$\begin{aligned} X_0 &= \frac{1}{2r}\left(1 + r^2(L^2 + \vec{x}^2 - t^2)\right) , \\ X^{p+1} &= \frac{1}{2r}\left(1 - r^2(L^2 - \vec{x}^2 + t^2)\right) , \\ X^i &= Lrx^i \quad (i = 1, \cdots, p) , \\ X_{p+2} &= Lrt . \end{aligned} \tag{5.10}$$

And the resulting metric is the familiar construction

$$ds^2 = L^2\left(\frac{dr^2}{r^2} + r^2(-dt^2 + d\vec{x}^2)\right) , \tag{5.11}$$

where the boundary is at $r \to \infty$.

The explicit isometries are the Poincaré group $ISO(1, p)$, and the hyperbolic symmetry $SO(1, 1)$, which is related to dilatation of the coordinates $(t, \vec{x}, r) \to (\lambda t, \lambda\vec{x}, r/\lambda)$ and $\lambda > 0$. The combination of isometries still matches the ones from the conformal group, as $SO(2, p + 1) \to ISO(1, p) \times SO(1, 1)$.

Another useful notation is to write Eq. (5.11) as $r = \frac{1}{z}$, therefore moving the boundary to $z = 0$, we have the metric

$$ds^2 = \frac{L^2}{z^2}\left(dz^2 - dt^2 + d\vec{x}^2\right) , \tag{5.12}$$

which makes manifest that every slice of constant z looks like Minkowski space!

The relevant Einstein equations are simply Einstein gravity with a negative cosmological constant, which we write as

$$E_{MN} = R_{MN} - \frac{1}{2}g_{MN}R - \Lambda g_{MN} = 0 , \tag{5.13}$$

where the cosmological constant is related to the AdS radius as $\Lambda = -(p+1)(p+2)/2L^2$. We use Latin indices (M, N) for the objects in the $d + 1$ manifold, and Greek indices for

the d boundary (μ, ν), where $d = p + 1$. Eq. (5.13) is simply a vacuum equation, and admits the solution of AdS_{p+2} Eq. 5.12.

5.2.4 Extracting the energy-momentum tensor from holography

Our goal is just to convey the idea of how to extract the stress-energy tensor at the boundary from the gravitational theory in the bulk.

The core idea is the need to add counterterms in the supergravity action, just as a usual QFT has short wavelengths divergences. Therefore, the idea of the holographic renormalization is to relate the infrared infinities of the supergravity action to the ultraviolet infinities of the CFT, which is a strict test of the consistency of the AdS/CFT duality [128].

First, there is the Brown-York construction of the "quasilocal stress tensor" [129], which is defined locally in the boundary of a region of spacetime. Therefore, as a functional of the induced boundary metric $\gamma_{\mu\nu}$, it is defined as

$$T^{\mu\nu} = \frac{2}{\sqrt{-\gamma}} \frac{\delta S_{\text{grav}}}{\delta \gamma_{\mu\nu}} , \tag{5.14}$$

which diverges if the boundary is at infinity. If the divergences are identifies as the UV divergencies of the CFT in the AdS/CFT map, then it uniquely determines local counterterms in the boundary to make the action finite. As in any QFT, the bare quantities should be renormalized in order to obtain physically sound results.

The Brown-York formula for achieving renormalization is by considering the induced metric $\gamma_{\mu\nu}$ on a hyper-surface $r = r_c$, where r is the AdS radius with boundary at ∞. The normal vector to this surface is

$$n_M = \frac{\nabla_M r}{\sqrt{g^{MN} \nabla_M r \nabla_N r}} . \tag{5.15}$$

and the induced metric

$$\gamma_{MN} = g_{MN} - n_M n_N . \tag{5.16}$$

Then the extrinsic curvature can be calculated as

$$K_{MN} = -\nabla_M n_N . \tag{5.17}$$

The quantities in 5 dimensions can be expressed as boundary tensors as

$$A_{\mu\nu} = A_{MN} \left(\frac{\partial x^M}{\partial x^\mu} \right) \left(\frac{\partial x^N}{\partial x^\nu} \right) . \tag{5.18}$$

Then, the prescription is that the stress-energy tensor should be [61]

$$T^{\mu\nu} = \lim_{r_c\to\infty} \frac{r_c^2}{16\pi G_N^5}\left[K^{\mu\nu} - K\gamma^{\mu\nu} - 3\gamma^{\mu\nu} - \frac{1}{2}\left(R^{\mu\nu} - \frac{1}{2}R\gamma^{\mu\nu}\right)\right], \tag{5.19}$$

where the Ricci tensor and scalar are constructed by the induced metric $\gamma_{\mu\nu}$.

Another possible approach involves considering the bulk metric written in the Fefferman-Graham form, similar to Eq. (5.12) [128],

$$ds^2 = \mathcal{G}_{MN}dx^M dx^N = \frac{L^2}{z^2}(dz^2 + g_{\mu\nu}(x,z)dx^\mu dx^\nu)\,, \tag{5.20}$$

$$g(x,z) = g_{(0)} + z^2 g_{(2)} + \cdots + z^n g_{(n)} + h_{(n)}\, z^n \log z^2 + \mathcal{O}(z^{n+1})\,. \tag{5.21}$$

The logarithm appears in even dimensions and is related to curved spacetime in the boundary and Weyl anomaly. There are only even powers up to order (n+1). The power of Eq. (5.20) is that any asymptotically AdS metric can be written in such manner near the boundary. The metric stress-tensor is then related to the coefficient $g_{(d)}$ in the near boundary expansion as [128]

$$g_{\mu\nu}(x,z) \approx \eta_{\mu\nu} + \sum_{n=4}^{\infty} g_{(n)\mu\nu}\, z^n\,, \tag{5.22}$$

for $d = 4$ flat spacetime at the boundary $\eta_{\mu\nu}$. If we rescale the stress-energy tensor as $\hat{T}_{\mu\nu}(x) = T_{\mu\nu}(x)/\kappa$, with $\kappa = N_C^2/(2\pi^2)$, one finds

$$< \hat{T}_{\mu\nu}(x) >= g_{(4)\mu\nu}\,. \tag{5.23}$$

The difficult part left is to solve the full non-linear Einstein equations. Also, if one is interested in deep infrared phenomena, as well as black holes dynamics, then the Fefferman-Graham formalism may develop true singularities and yield unphysical results. It is natural since the Fefferman-Graham description is appropriate for describing near boundary behavior. In the next section we discuss one possible formalism to investigate hydrodynamical properties and non-equilibrium phenomena in holography.

5.3 Boosted Black Branes

One very important application of holographic methods is to further investigate thermal phenomena of strongly coupled quantum matter. Thermal states in the boundary should be dual to black hole geometries in the bulk, which is an implementation of the holographic hypothesis. Entropy in gravitational degrees of freedom scales as the area,

while in quantum field theories it scales with the volume. Therefore, the entropy of a thermal QFT should be related to the entropy of a gravitational theory in a higher dimension. The correspondence AdS/CFT gives a precise map and a regime of validity for this claim.

The black brane solution in AdS_5 is [34, 126, 130]

$$ds^2 = \frac{L^2}{z^2}\left(-f(z)dt^2 + d\vec{x}^2 + \frac{dz^2}{f(z)}\right), \qquad f(z) = 1 - \frac{z^4}{z_m^4}. \tag{5.24}$$

If $f(z) = 1$, then we recover the Fefferman-Graham AdS_5 metric (5.12). Therefore, the black hole and the black hole horizon are deep infrared phenomena. There is an origin from supergravity and near horizon limit of a stack of black $D3$ branes, but we skip this discussion as it is out of scope of this thesis [130]. We treat Eq. (5.24) as a higher dimensional classical solution of a black hole in asymptotically AdS spacetime.

The relation to thermodynamical quantities can be calculated through the black hole area law. The analytically continued near horizon limit of (5.24) is, by the usual definition $\rho^2 = 4z_m(z_m - z)$, $t = -it_E$ and $\psi = t_E/2\psi$ [126, 127]

$$ds^2 \approx \kappa_s^2\rho^2 d\psi^2 + d\rho^2 + \frac{L^2}{z_m^2}d\vec{x}^2, \tag{5.25}$$

where $\kappa_s = 2/z_m$. Periodicity then let us identify the Hawking temperature as

$$T = \frac{\kappa_s}{2\pi} = \frac{1}{\pi z_m}. \tag{5.26}$$

We can also compute the entropy density for the $\mathcal{N} = 4$ SYM discussed in Chapter 2 using Eq. (2.38). The area of the black brane at the horizon, and for a fixed time is simply [127]

$$A(t = \text{fixed}, z = z_m) = \int \sqrt{\left(\frac{L}{z_m}\right)^{2\times 3}} d^3x = \left(\frac{L}{z_m}\right)^3 V_3 \ . \tag{5.27}$$

The area formula for entropy is (with $\frac{L^3}{4G_5} = \frac{N_c^2}{2\pi}$) [10, 34]

$$S = \frac{A}{4G_5} = \frac{L^3}{4G_5}\frac{V_3}{z_m^3} = \frac{\pi^2}{2}N_c^2 V_3 T^3. \tag{5.28}$$

5.3.1 Eddington-Finkelstein coordinates for Schwarzschild Black Holes

The black brane metric in Fefferman-Graham construction (5.24) has a coordinate singularity at the horizon, which indicates that the metric is appropriate for very far observers to study its dynamics. Here we introduce the Eddington-Finkelstein coordinate system [127], but first we develop it for Schwarzschild black holes in 4 dimensions and asymptotically flat spacetimes, which is the Schwarzschild solution

$$\begin{aligned} ds^2 &= -\left(1-\frac{r_s}{r}\right)dt^2 + \left(1-\frac{r_s}{r}\right)^{-1}dr^2 + r^2 d\Omega \\ ds^2 &= -\left(\frac{r-r_s}{r}\right)\left(dt+\frac{r}{r-r_s}dr\right)\left(dt-\frac{r}{r-r_s}dr\right) + r^2 d\Omega\,. \end{aligned} \tag{5.29}$$

They are both the same Schwarzschild metric, but in the second line we appropriately separated the radius and time coordinates. For the substitution $dv = dt + \frac{r}{r-r_s}dr$, which consequently means $dt - \frac{r}{r-r_s}dr = dv - \frac{2r}{r-r_s}dr$. Therefore, the metric in these coordinates becomes

$$ds^2 = -\left(\frac{r-r_s}{r}\right)dv^2 + 2dvdr + r^2 d\Omega\,. \tag{5.30}$$

The metric is now off-diagonal, but it has the advantage that the coordinate singularity of the horizon has vanished. The geodesics of light rays can be easily calculated equating $ds^2 = 0$,

$$\begin{aligned} dp &= 0\,, \\ \frac{dr}{dp} &= \left(\frac{r-r_s}{2r}\right)\,. \end{aligned} \tag{5.31}$$

The first equality denotes ingoing light rays, while the second is outgoing for $r > r_s$ and ingoing $r < r_s$. Therefore, there is no outgoing light rays originating from behind the horizon, as expected. The advantage of the Eddington-Finkelstein coordinates is that the regularity of the black hole is manifest. The disadvantage of the metric, apart from its off-diagonal term, is that the identification of asymptotically far observer's time is tangled with the radial coordinate. This fact is crucial when the system is analyzed in the AdS black brane setup.

It is possible to integrate dv, and then it is related to the other coordinates as

$$v = t + r + r_s \ln \frac{|r - r_s|}{r_s} \,. \tag{5.32}$$

5.3.2 Setup of Boosted Black Brane

We start by changing the Fefferman-Graham coordinates to Eddington-Finkelstein in the black brane solution. We write Eq. (5.24) but with inverse AdS radius coordinate $r = 1/z$,

$$ds^2 = L^2 \left[-\left(\frac{r^4 - r_m^4}{r^2}\right)\left(dt + \frac{r^2}{r^4 - r_m^4} dr\right)\left(dt - \frac{r^2}{r^4 - r_m^4} dr\right) + r^2 d\vec{x}^2 \right] . \tag{5.33}$$

Now, with the coordinate transformation

$$dv \equiv dt + \frac{r^2}{r^4 - r_m^4} dr \,, \tag{5.34}$$

the black brane in Eddington-Finkelstein coordinates becomes ($L = 1$)

$$ds^2 = 2\, dv dr - r^2 f(r) dv^2 + r^2 d\vec{x}^2 \,, \tag{5.35}$$

where $f(r) = 1 - (r_m/r)^4$.

The isometries of the conformal group in four dimensions allow for a rigid boost of such metric. Recall that when we discussed the Poincaré patch of the AdS metric we noticed that the isometries were the usual Poincaré group in 4 dimensions and an extra dilatation. Rotations and translations leave the solution invariant, while the dilatation generates temperature [2], and the boosts a unique normalized four-vector. The covariant result of these symmetries is then the so called boosted black brane solution [39],

$$ds^2 = -2u_\mu dx^\mu dr - r^2 f(br) u_\mu u_\nu dx^\mu dx^\nu + r^2 \Delta_{\mu\nu} dx^\mu x^\nu \,. \tag{5.36}$$

The Greek indices indicate contractions with the boundary metric, which is the minkowski metric $\eta_{\mu\nu}$. The four-vector u^μ is identified as the usual fluid velocity four-vector, and its norm is unity $u_\mu u^\mu = -1$. We set $r_m = 1$, AdS radius L to unity and then the parameter b is related to the Hawking temperature as $b = 1/(\pi T)$. We rewrite the definition of the four-velocity orthogonal projector $\Delta^{\mu\nu} = \eta^{\mu\nu} + u^\mu u^\nu$. In the next section we review the Fluid/Gravity correspondence for the Navier-Stokes theory, which consists of implementing the gradient expansion on a boosted black brane solution. We show the Penrose and

[2] Since if one rescales the fifth coordinate, it effectively changes the black hole temperature defined by the function f(r), while the boundary coordinates can just absorb the rescaling factor.

Kruskall-Szekeres diagrams of an extended AdS planar black hole solution in Figs. 5.4 and 5.5.

5.4 Fluid-Gravity correspondence and the gradient expansion

The rigid boosted black brane Eq. (5.36) is an exact solution of Einstein's Eq. (5.13). However, if we promote the four-velocity and the inverse temperature b as functions of the boundary coordinates x^μ, there are very complicated constraints on the exact form of the functions $u^\mu(x^\mu)$ and $b(x^\mu)$. The argument of the fluid-gravity correspondence is that if the deviations from equilibrium are truncated order by order by a small parameter, then Einstein's equation can also be truncated order by order on the boundary coordinates. We represent this construction in the Penrose diagram Fig. 5.6. What is interesting about this construction is that the integral over the AdS radius r is not approximated, it is just truncated order by order. Therefore, up to a certain order of expansion δx^μ, the renormalization group interpretation of the fifth coordinate then implies that at each order the whole towering of ultraviolet and infrared operators are taken under consideration.

We follow the original notation [39] and then parametrize the four-velocity as $u^\mu = (\frac{1}{\sqrt{1-\beta_i^2}}, \frac{\beta_i}{\sqrt{1-\beta_i^2}})$. The ansatz metric is then

$$ds^2 = -2u_\mu(x^\alpha)dx^\mu dr - r^2 f(b(x^\alpha)r)u_\mu(x^\alpha)u_\nu(x^\alpha)dx^\mu dx^\nu + r^2\Delta_{\mu\nu}(x^\alpha)dx^\mu x^\nu\,. \tag{5.37}$$

and the boundary values vary slowly in a gradient expansion (as it is the case of the known Chapman-Enskog construction in kinetic theory)

$$\beta_i(x^\alpha) = \beta_i^{(0)} + \epsilon\,\beta_i^{(1)}(x^\alpha) + \mathcal{O}(\epsilon^2)\,, \tag{5.38}$$

$$b(x^\alpha) = b^{(0)} + \epsilon\, b^{(1)}(x^\alpha) + \mathcal{O}(\epsilon^2)\,. \tag{5.39}$$

and we are interested in a gradient expansion solution to Einstein's equation,

$$G = G^{(0)}(\beta_i, b) + \epsilon G^{(1)}(\beta_i, b) + \epsilon^2 G^{(2)}(\beta_i, b) + \mathcal{O}(\epsilon^3)\,, \tag{5.40}$$

where $G^{(0)}(\beta_i, b)$ is Eq. (5.37). The solution order by order is supposed to hold if gradients are not large compared to a local temperature, i.e., $\partial u^\mu/T$ and $\partial \log T/T$ are of comparable to $\epsilon \ll 1$.

There is gauge redundancy and we adopt the one used in the original calculation of the background field, which implies [39]

$$G_{rr} = 0\,, \qquad G_{rv} \propto u^{\mu}\,, \qquad \mathrm{Tr}\left((G^{(0)})^{-1}G^{n}\right)\ \forall\, n > 0\,. \tag{5.41}$$

The constraint equations consist of solving first order equations on r, which result from a projection of Eq. (5.13) in the radial direction, the one form $\xi_N = dr$,

$$E_{MN}\xi^{N} = 0\,, \tag{5.42}$$

On the other hand, the dynamical equations can be solved taking advantage of the rotational symmetry $SO(3)$ of the boosted black brane in AdS_5. The dynamical equations then consist of finding the scalar, vector, and tensor corrections at a given order to the metric. This will be the procedure used in order to find the Navier-Stokes dual. Ref. [39] exposes a general form of the radial operator and the existence of a source term order by order, but since we only wish to solve for Navier-Stokes in this thesis, we refer the reader to the references for such discussions.

5.4.1 Construction of the Navier-Stokes dual

In order to find a truncated solution to Einstein's equation, we use the expansion Eq. (5.40) up to first order. It is possible for simplify to solve it when the background is simply $b^{(0)} = 1$ and $\beta_i^{(0)} = 0$, then use the symmetries to boost and dilate to a general temperature and four-velocity. For the perturbations of temperature and velocity of first order,

$$\beta_i^0 \to x^{\mu}\partial_{\mu}\beta_i^{(0)}(x^{\alpha}) + \mathcal{O}(\epsilon^2)\,, \qquad b^0 \to 1 + x^{\mu}\partial_{\mu}\, b^{(0)} + \mathcal{O}(\epsilon^2)\,. \tag{5.43}$$

For such expansion of temperature and velocity, the metric Eq. (5.37) becomes up to first order of derivatives of the boundary coordinate

$$\begin{aligned} ds^2_{(0)} &= 2\,dv\,dr\ - r^2\,f(r)\,dv^2 + r^2\,dx_i dx^i \\ -2x^{\mu}\,\partial_{\mu}\beta_i^{(0)}\,dx^i dr - 2x^{\mu}\partial_{\mu}\beta_0^{(1)} r^2(1-f(r))\,dx^i dv &- 4\frac{x^{\mu}\partial_{\mu}b^{(0)}}{r^2}dv^2\,. \end{aligned} \tag{5.44}$$

We follow the notation of Ref. [39] and then add the following first order correction to truncate Einstein's equation,

$$ds^2_{(1)} = -3h_1(r)\,dv\,dr\ + r^2 h_1(r) dx_i\,dx^i + \frac{k_1(r)}{r^2}dv^2 + \frac{2j_i^{(1)}(r)}{r^2}dvdx^i + r^2\alpha_{ij}^{(1)}dx^i\,dx^j\,. \tag{5.45}$$

Scalars

First, we solve for the scalar degrees of freedom. They only involve the functions h_1 and k_1 (5.45), which were constructed respecting the system's gauge condition.The first interesting constraint equation $E_{MN}\xi^N$ is then the temporal component of such, $E_{vN}\xi^N$,

$$r^2 f(r) E_{rv} + E_{vv} = 0\,. \tag{5.46}$$

The solution is simply the energy conservation equation

$$\partial_v b^{(0)} = \frac{\partial \beta_i^{(0)}}{3}\,. \tag{5.47}$$

The second constraint involves the scalar functions $h_1(r)$ and $k_1(r)$ and it is the AdS radial direction of the constraint equation, $r^2 f(r) E_{rr} + E_{vr} = 0$. After some calculations, one finds the equality

$$2r^2\partial_i\beta_i^{(0)} + 12\,r^3 h_1(r) + (3r^4 - 1)\,h_1'(r) - k_1'(r) = 0\,. \tag{5.48}$$

There is non-uniqueness in an extra constraint necessary to solve the equation above. However, such can always be resolved by redefining the physical fields β_i and b, therefore there is not an inconsistency in this freedom. We follow Ref. [39] and write the extra constraint as

$$5h_i'(r) + r h_1''(r) = 0\,. \tag{5.49}$$

The function $h_1(r)$ is then an homogeneous excitation, and the integrated results are

$$h_1(r) = s + \frac{t}{r^4}\,, \qquad\qquad k_1(r) = \frac{2r^3\partial_i\beta_i^{(0)}}{3} + 3r^4 s - \frac{t}{r^4} + u\,. \tag{5.50}$$

The integrated constants s, t and u may be set to zero due to boundary conditions, radial symmetry and orthogonality of the energy-momentum tensor to the boundary four-velocity, as explained in [39]. Therefore, the non-trivial metric contribution of the scalar

sector is then

$$ds^2_{(1)} = \frac{2r\partial_i\beta_i^{(0)}}{3}\, dv^2 + \cdots . \tag{5.51}$$

Vector

The vector constraint equation is any i^{th} equation $r^2 f(r) E_{ri} + E_{vi} = 0$. The resulting conservation is the ideal momentum equation

$$\partial_i b^{(0)} = \partial_v \beta_i^{(0)} . \tag{5.52}$$

We solve the dynamical equation $E_{ri} = 0$ for the vector function parametrized as $\frac{2j_i^{(1)}(r)}{r^2} dv dx^i$, which results in

$$r\frac{d^2}{d\,r^2} j_i^{(1)}(r) - 3\frac{d}{d\,r} j_i^{(1)}(r) = -3r^2 \partial_v\, \beta_i^{(0)} , \tag{5.53}$$

with solution

$$j_i^{(1)}(r) = \partial_v \beta_i^{(0)}\, r^3 + A_1 \frac{r^4}{4} + B_1 . \tag{5.54}$$

The integration constants can be set to zero, as A_1 is non-renormalizable and the boundary condition imposes such, and B_1 is effectively a shift in the boundary velocity only (compare to Eq. (5.36)). Therefore, the vector contribution is

$$ds^2_{(1)} = \cdots + 2r\partial_v \beta_i^{(0)}\, dv\, dx^i + \cdots . \tag{5.55}$$

Tensor

Finally, we can solve the tensorial degree of freedom. Einstein's Equation E_{ij} leads to the following condition for the first order function $r^2 \alpha_{ij}^{(1)} dx^i\, dx^j$,

$$\frac{d}{d\,r}\left(r^5\, f(r)\, \frac{d}{d\,r} \alpha_{ij}^{(1)} \right) = -6r^2 \sigma_{ij}^{(0)} , \tag{5.56}$$

where the shear tensor obeys its usual definition $\sigma_{\mu\nu} = \Delta^{\mu\nu\alpha\beta}\partial_\alpha u_\beta$. The resulting integral is

$$\alpha_{ij}^{(1)} = C_2 + C_1 \ln\left[\frac{r^4(1-r)}{(1+r)(1+r^2)}\right] - \frac{\sigma_{ij}^{(0)}}{4}\left[4\arctan(r) + \ln\frac{(1-r^2)}{(1+r^2)}\right] . \tag{5.57}$$

Requiring that the solution is regular at the horizon (in these calculations at $r = 1$),

and choosing the appropriate constants of integration, we recover the function encountered in [39], with the tensorial contribution being

$$r^2\alpha_{ij}^{(1)}dx^i\,dx^j = 2r^2F(r)\sigma_{ij}^{(0)}dx^i\,dx^j = \lim_{r\to\infty} 2\left(r-\frac{1}{4r^2}\right)\sigma_{ij}^{(0)}dx^i\,dx^j \tag{5.58}$$

And the function is

$$F(r) = \frac{1}{4}\left[\pi - 2\arctan(r) + \ln\frac{(1+r^2)(1+r)^2}{r^4}\right]. \tag{5.59}$$

Navier-Stokes dual metric

Finally, we can write the total metric that solves Einstein's equation to first order in gradient expansion.

$$\begin{aligned} ds^2 = 2\,dv\,dr\; - r^2\,f(r)\,dv^2 + r^2\,dx_i dx^i \\ -2x^\mu\,\partial_\mu\beta_i^{(0)}\,dx^i dr - 2x^\mu\partial_\mu\beta_0^{(1)}r^2(1-f(r))\,dx^i dv - 4\frac{x^\mu\partial_\mu b^{(0)}}{r^2}dv^2\,. \\ +2r^2F(r)\sigma_{ij}^{(0)}dx^i\,dx^j + \frac{2}{3}r\partial_i\beta_i^{(0)}dv^2 + 2r\partial_v\beta_i^{(0)}dvdx^i\,. \end{aligned} \tag{5.60}$$

We write the above metric in a boundary-covariant manner using the notation in [52]

,

$$\begin{aligned} &ds^2 = -2u_\mu dx^\mu(dr + r\mathcal{A}_\nu) + r^2\eta_{\mu\nu}dx^\mu dx^\nu + \frac{1}{b^4r^2}u_\mu u_\nu dx^\mu dx^\nu + 2br^2F(br)\sigma_{\mu\nu}dx^\mu dx^\nu\,, \\ &\mathcal{A}_\mu = D\,u_\mu - \frac{1}{3}\theta\,u_\mu\,,\quad b = \frac{1}{\pi T}\,. \end{aligned} \tag{5.61}$$

The stress-energy tensor at the boundary is then obtained using Eq.(5.19) ,

$$T^{\mu\nu} = \frac{1}{b^4}(4u^\mu u^\nu + \eta^{\mu\nu}) - \frac{2}{b^3}\sigma^{\mu\nu}\,, \tag{5.62}$$

If we recover the factors of N_c, gives the famous holographic calculation of the shear viscosity coefficient over the entropy density Eq. (5.28)of $\mathcal{N}=4$ SYM [10],

$$\frac{\eta}{s} = \frac{1}{4\pi}\,. \tag{5.63}$$

This procedure has been done for higher orders of gradient expansion and other asymptotically AdS_5 metrics [39, 61, 62].

Throughout this thesis, we showed many inconsistencies of the relativistic Navier-Stokes theory, as well as the higher order corrections constructed by the gradient expansion

truncation. For instance, the temperature becomes negative, which means that at some point it has to be zero. Therefore, this is equivalent to reaching the black brane singularity at $r = 0$, which is a big inconsistency. Of course, the problem lies in the regime of validity: Navier-Stokes and the general gradient expansion theories have a very limited applicability to phenomena very close to equilibrium and at very large times. Therefore, if one wants to access the true dynamics connected to more rapidly flow patterns, hydrodynamics constructed via the gradient expansion is definitely not the right effective theory.

The natural question is whether it is possible to write an effective theory that generalizes the gradient expansion approach, as the Israel-Stewart formalism did in kinetic theory. We do not know how to answer such a question, but we discuss some future guidelines in the next section.

5.5 Connection to Quasinormal Modes and effective theory?

We briefly overview the results of the literature on numerical relativity methods to study real-time holographic phenomena [44, 45], as well as the physics of the quasinormal modes and implications to hydrodynamics. These topics are very rich and should be studied with proper care. Here we only sketch some results and discuss how future work could be done in that direction.

5.5.1 Brief exposure to numerical setup up

Suppose we want to write a very general metric in asymptotically AdS_5 space with Eddington-Finkelstein coordinates, i.e., everywhere regular. We could use for instance the ansatz [44]

$$ds^2 = dv(-Adv + 2dr + 2F_i dx^i) + S^2 h_{ij} dx^i dx^j \,, \tag{5.64}$$

where A, F_i, S, h_{ij} are generic functions of all the coordinates and it is imposed that $\det[h_{ij}] = 1$. This ansatz has been used for evolution of numerical simulation in AdS_5 [44].

It is necessary to have an initial condition for $h_{ij}(v = 0, r, x^i)$ and boundary conditions for A and F_i at infinity. The rest is fixed by the dynamics of Einstein's equations. The biggest complication of not using some sort of truncation method is that Einstein's equations are highly non-linear and despite having few variables and functions, the problem easily becomes intractable.

One simplification is to work the homogeneous relaxation scenario, where every variable is either a function of the time v and the AdS radius r. This problem is intimately

connected via coordinate transformation to the case discussed in [44]. This is a future problem to tackle, but we only present here for completeness.

In reference, the investigated solution is homogeneous in the boundary coordinates $x^i = (x_L, \vec{x}_T)$, but there is a time dependent anisotropy in the boundary stress-energy tensor, $T_{x_L x_L}(v) \neq T_{x_T x_T}(v)$. The authors then used the following ansatz for their metric tensor,

$$ds^2 = 2dvdr - Adv^2 + S^2 e^{-2B} dx_L^2 + S^2 e^B dx_T^2 \,, \tag{5.65}$$

and A, S and B are functions of the AdS radial coordinate and time v. The authors considered the holographic renormalization in this coordinate system to lead the following near boundary expansion,

$$A = (r + \xi(v))^2 - 2\partial_v \xi(v) + \frac{a_4}{r^2} + \cdots \,, \tag{5.66}$$

$$B = \frac{b_4(v)}{r^4} + \frac{\partial_v b_4(v) - 4 b_4(v)\xi(v)}{r^4} + \cdots \,, \tag{5.67}$$

$$S = r + \xi(v) - \frac{b_4(v)^2}{7r^7} \,. \tag{5.68}$$

The symmetry $\xi(v)$ is a residual gauge symmetry. The details of such constructions can be found in references. The authors identified the normalizable modes with the coefficients a_4 and b_4 [44],

$$\epsilon = p_L(v) + 2p_T(v) = -\frac{3a_4}{4} \,, \qquad \Delta p = p_L(v) - p_T(v) = 3b_4(v) \,. \tag{5.69}$$

and the stress-energy tensor is simply $< T^{\mu\nu} >= \frac{N_c^2}{2\pi^2}\, \mathrm{diag}[\epsilon, p_L(v), p_T(v), p_T(v)]$.

It is convenient to write Einstein's equations in a form that makes the symmetries of the problem manifest. For this construction, Einstein's equations are simply written as [44, 45]

$$S'' + \frac{1}{2}B'^2 S = 0\,, \tag{5.70}$$

$$S(\dot{S})' + 2S'\dot{S} - 2S^2 = 0\,, \tag{5.71}$$

$$S(\dot{B})' + \frac{3}{2}\left(S'\dot{B} + B'\dot{S}\right) = 0\,, \tag{5.72}$$

$$A'' + 3B'\dot{B} - 12\frac{S'\dot{S}}{S^2} + 4 = 0\,, \tag{5.73}$$

$$\ddot{S} + \frac{1}{2}\left(\dot{B}^2 S - A'\dot{S}\right) = 0\,. \tag{5.74}$$

with the definition of derivatives

$$h' \equiv \partial_r h\,, \qquad\qquad \dot{h} \equiv \partial_t h + \frac{1}{2}A\partial_r h\,. \tag{5.75}$$

The goal for a near future project is then to understand how the near-boundary expansion Eq. (5.68) can be achieved from different metric ansatz and symmetries, as well as the relevant Einstein equations in the form (5.74) (another construction can be found in Ref. [45]). This is the next step to understand non-equilibrium physics in holography and a different regime from the fluid-gravity correspondence. The simplest example is then homogeneous relaxation, where all spatial gradients are zero and the only non-trivial differential equation is

$$\mathcal{O}(D, D^2, \nabla_\perp^2, \cdots)\,\pi^{\mu\nu}(v) = 0\,, \tag{5.76}$$

where we do not know exactly the operator $\mathcal{O}$. It is however interesting to note that the complicated non-linear dynamics of this numerical setup is directly connected to the quasinormal modes. In fact, studies showed that the late time behavior approximates well the lowest quasinormal modes dynamics [119, 131].

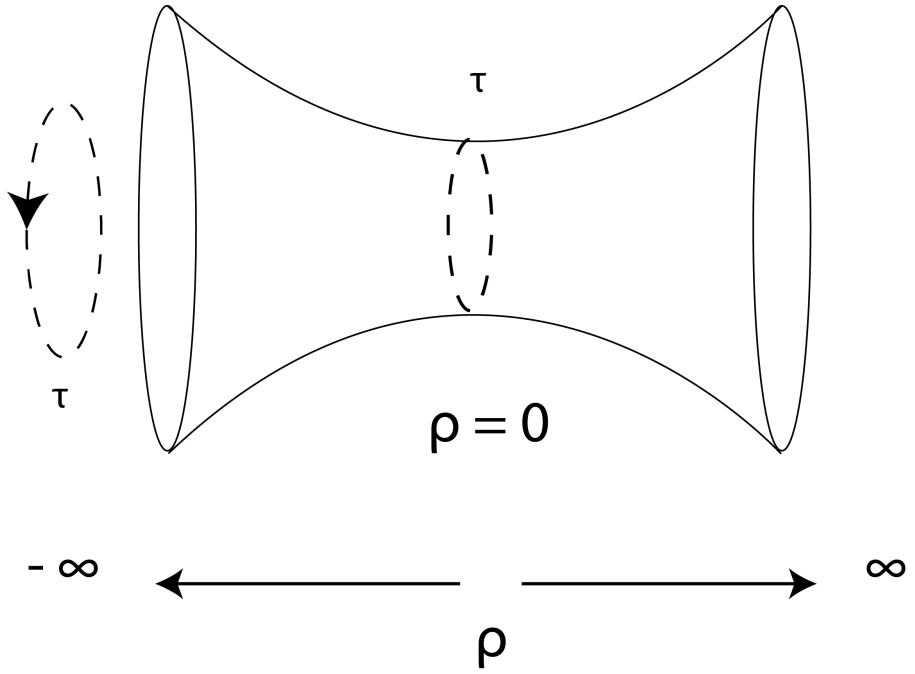

Figure 5.1: *A representation of Anti-de Sitter space as the embedded hyperboloid given by Eq. (5.2). Notice the closed timelike curves in the τ direction.*

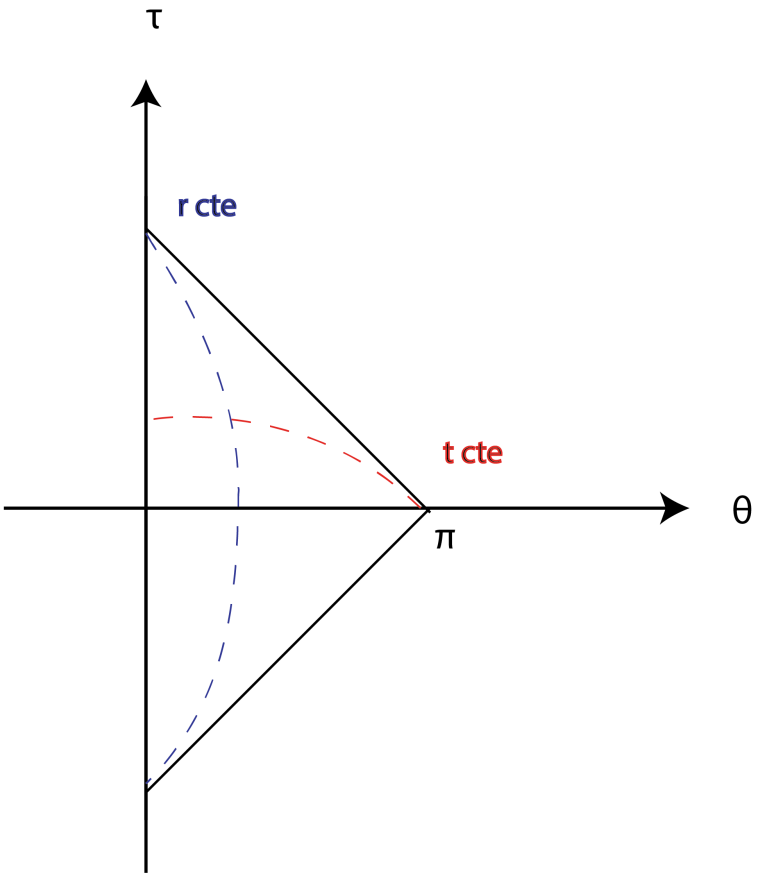

Figure 5.2: *A Penrose diagram of Minkowski space $\mathbb{R}^{1,p}$ for $p > 1$. Each point in the plane represents a fixed point in the sphere S^{p-1}. This space can be analytically continued outside the triangle, which results in the geometry of Einstein static universe with topological structure $\mathbb{R}\otimes S^p$.*

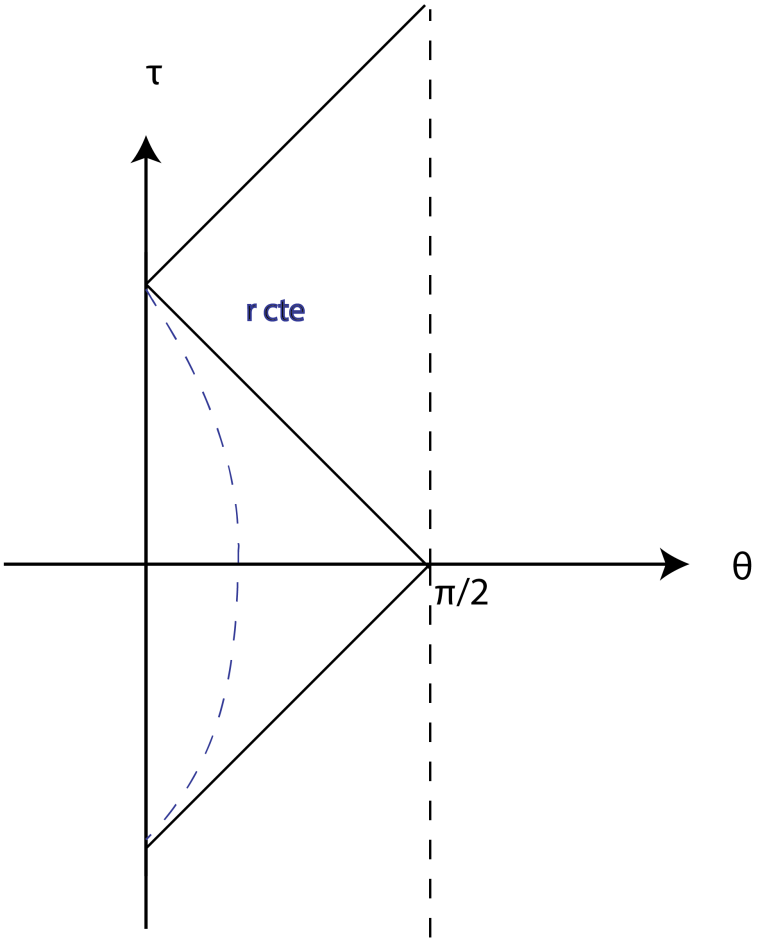

Figure 5.3: *A Penrose diagram of Anti-de Sitter space AdS_{p+2}. Each point in the plane represents a fixed point in the sphere S^p. The geometry is half of the Einstein static universe $(0 < \theta < \pi/2)$ and topological structure $\mathbb{R} \otimes S^p$. AdS space has a timelike boundary.*

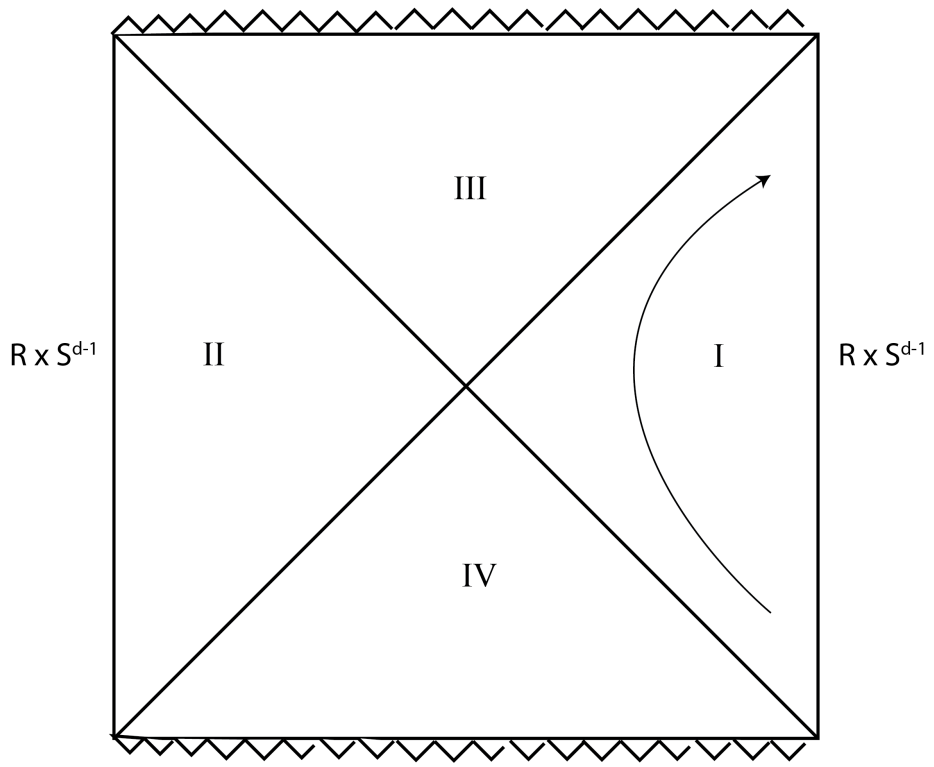

Figure 5.4: *A Penrose diagram for an extended AdS planar black hole solution. The spacetime of this extended solution has four regions and two AdS boundaries. Region I covers the outside of black hole as measured by a distant observer, region II is just an identical copy. Regions III and IV contain spacelike singularities. [1].*

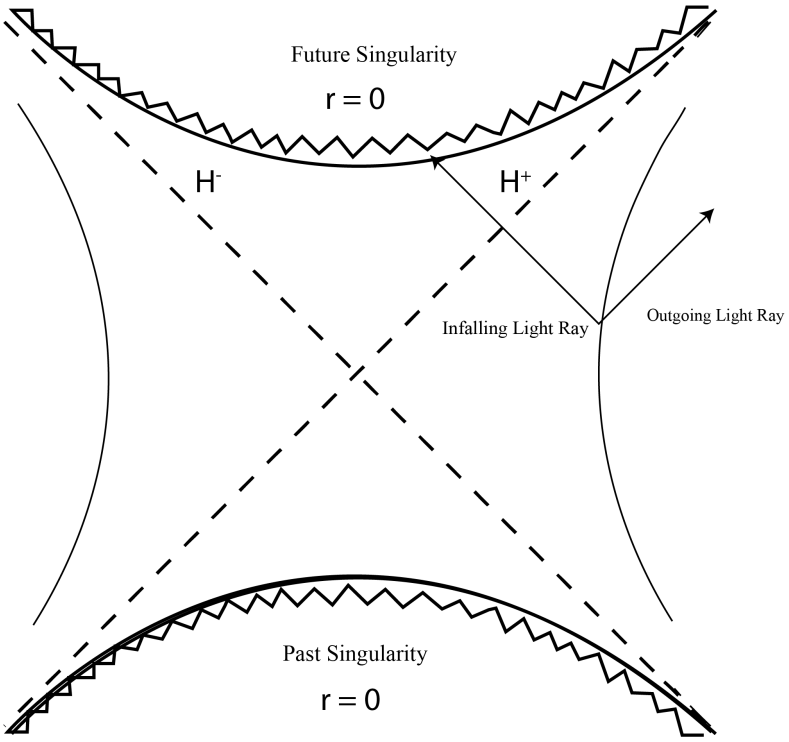

Figure 5.5: *Kruskall-Szekeres diagram for an extended AdS planar black hole solution. We represent an in falling radial light ray that crosses the horizon H^+ and hits the singularity, as well as an outgoing radial light ray that is originated outside the horizon H^+.*

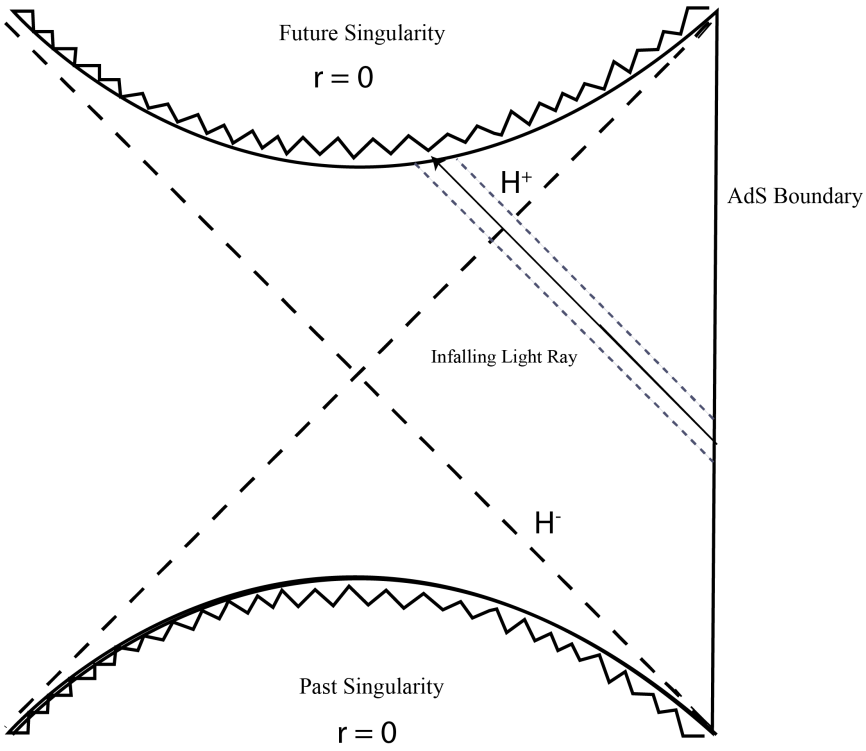

Figure 5.6: *Penrose diagram for an extended AdS planar black hole solution in the Fluid-Gravity construction. We represent an infalling radial light ray that originates from the boundary, crosses the future horizon H^+ and hits the singularity. The Fluid-Gravity construction is the tubewise approximation represented by the two dashed lines around the ingoing light ray.*

Chapter 6

Conclusion and Outlook

The main goal of this thesis was to investigate the structure of the relativistic dissipative hydrodynamics in several contexts.

In Chapter 2 we found for the first time a radially expanding and time evolving causal and consistent semi-analytical solution of dissipative relativistic hydrodynamics in the conformal approximation. One immediate advantage of such is that it provides a test for numerical hydrodynamics simulations. There has been an increasing effort towards a state-of-art simulation of the hydrodynamical phase of QGP for comparison to data; therefore, the need for a rigorous and "simple" check of numerical codes is clearly of relevance. Another property of solutions investigated is the influence of the initial condition for the dissipative tensor. The choice of an appropriate initial condition guarantees that the second law of thermodynamics holds for the whole spacetime. In all the analytic and semi-analytic cases studied, the gradient expansion theories contained regions with instabilities, violation of physics laws, and negative temperatures.

In the next chapter, the focus shifted to study the influence of the second order coefficient of relaxation time, τ_π, in nonlinear wave propagation. The conclusion was that relaxation time amplifies the solitonic behavior of pulses in a toy $1+1$ model, but the consistency of the study depended on the initial profile. For very steep gradients, our solution grew larger and the perturbative method should not be trusted. The main lesson is that hydrodynamic truncations may not give the appropriate effective theory for very steep and irregular initial conditions.

The structure of linear perturbations of relativistic dissipative fluids was the main focus in Chapter 4. We reviewed the existing literature, as well as introduced a covariant formalism that revealed much of the structure of the higher order corrections. We showed how gradient expansion theories of second and third order were generally and inherently unstable. We associated the different degrees of freedom for different background velocities as one of the main sources of inconsistencies, which is generally cured by trun-

cating derivatives of $\pi^{\mu\nu}$ in a similar way to Israel-Stewart theory. Of course, for higher derivatives the solution should be spurious and is expected to fail, therefore it seems that the appropriate strategy is to look for non-equilibrium physics instead of truncating an asymptotic series.

The spirit of chapter 5 was to introduce the fluid/gravity correspondence and the associated higher dimensional gravity solutions to fluid dynamics in the boundary. There is an existing map of such solutions, which is the holographic implementation of the Chapman-Enskog method [40]. Since the gradient expansion theory contains instabilities, it should be possible to find another consistent low-energy theory that corrects such behavior, similar to what Israel-Stewart theory did in kinetic theory. We discussed how the truncation of Einstein's equations beyond the linear quasinormal modes is a very non-trivial problem, which involves global regularity and deep infrared problems in the bulk.

6.1 Future Directions

The study of the full nonlinear Einstein's equations in order to understand homogeneous relaxation is the first step to understand the non-hydrodynamical behavior of fluids in AdS/CFT. It is possible that in the structure of the bulk's dynamical equations there is a logical infrared truncation of the dissipative tensor. However, it seems that if non-linearity is taken into account, the whole tower of modes should be integrated. One advantage of the gradient expansion method is that there is naturally a truncation of Einstein's equation order by order, the boundary variables and their gradients, but homogeneous relaxation possesses none of these.

Another interesting question that requires a full study of Einstein's equations is the role played by irregular initial conditions on late time evolution. If there is a significant deviation, then hydrodynamics should literally be taken as the effective theory only when all quantities are very well-behaved and deep in the infrared regime.

Appendix A

The Conformal Group

We briefly sketch the properties of the conformal group in this Appendix. We followed the discussion in Ref. [48, 126, 130]. For this appendix, we use the metric signature $g_{\mu\nu} = \mathrm{diag}(-1, 1, 1, 1)$.

A conformal transformation has the properties of preserving angles upon a Weyl transformation $ds^2 \to \Omega(x)^2 ds^2$. The Poincaré algebra is just the special case $\Omega(x)^2 = 1$. For instance, for two vector u^μ and v^μ, we have

$$\cos\theta = \frac{u^\mu\, v_\mu}{\sqrt{u^\nu\, v_\nu}\sqrt{u^\lambda\, v_\lambda}} \to \frac{u'^\mu\, v'_\mu}{\sqrt{u'^\nu\, v'_\nu}\sqrt{u'^\lambda\, v'_\lambda}} = \cos\theta' = \cos\theta\,. \tag{A.1}$$

In order to find its generators, consider the following infinitesimal transformation

$$x^\mu \to x^\mu + \epsilon^\mu(x)\,, \qquad\qquad g_{\mu\nu} \to \eta_{\mu\nu} - (\partial_\mu\epsilon_\nu + \partial_\nu\epsilon_\mu)\,. \tag{A.2}$$

For the transformation to be just an overall factor of the metric, we need to impose that

$$(\partial_\mu\epsilon_\nu + \partial_\nu\epsilon_\mu) = f(x)\eta_{\mu\nu}\,, \tag{A.3}$$

If we take the trace ($\eta^{\mu\nu}$) of Eq. (A.3), we have the definition of the function in terms of the infinitesimal transformation,

$$f(x) = \frac{2}{d}\partial_\rho\epsilon^\rho\,. \tag{A.4}$$

Then we can rewrite Eq. (A.3) as

$$(\partial_\mu\epsilon_\nu + \partial_\nu\epsilon_\mu) = \frac{2}{d}\partial_\rho\epsilon^\rho\eta_{\mu\nu}\,, \tag{A.5}$$

If we differentiate the left hand side of the equation above with respect to μ, and with the usual box definition $\partial^\mu\partial_\mu \equiv \Box$,

$$\Box\epsilon_\nu + (1 - \frac{2}{d})\partial_\nu\partial_\rho\epsilon^\rho = 0\,. \tag{A.6}$$

In two dimensions, the conformal algebra is the class of holomorphic functions of complex variables (because of identity $\Box\epsilon_\nu = 0$).

For $d > 2$, we do the following operations: box Eq. (A.5) and take a derivative with index ∂_μ Eq. (A.6). Then, we have the identity involving three derivatives,

$$(2 - d)\partial_\mu\partial_\nu\partial_\rho\epsilon^\rho = \Box\,\partial_\rho\epsilon^\rho\,\eta_{\mu\nu}\,, \tag{A.7}$$

and its trace implies that

$$\partial_\mu\partial_\nu\partial_\rho\epsilon^\rho(x) = 0\,. \tag{A.8}$$

Therefore, the infinitesimal transformation is a most a quadratic function of the coordinates x. We identify the following symmetries then,

$$\text{Translation}: \quad \epsilon^\mu = a^\mu\,, \tag{A.9}$$

$$\text{Dilatation}: \quad \epsilon^\mu = \lambda x^\mu\,, \tag{A.10}$$

$$\text{Rotation}: \quad \epsilon^\mu = \omega^\mu_\nu x^\nu\,, (\omega_{\mu\nu} = -\omega_{\nu\mu})\,, \tag{A.11}$$

$$\text{Special Conformal Transformation}: \quad \epsilon^\mu = b^\mu\vec{x}\cdot\vec{x} - 2(\vec{x}\cdot\vec{b})x^\mu\,. \tag{A.12}$$

We can also write the generators of the following symmetries. Following the convention in [48], we have

$$x^{\mu'} = x^\mu + \epsilon^\mu(x) = x^\mu + \theta_a\frac{\delta\,x^\mu}{\delta\,\theta_a}\,, \tag{A.13}$$

$$\Phi'(x') = \Phi(x) + \theta_a\frac{\delta\mathcal{F}(x)}{\delta\theta_a}\,, \tag{A.14}$$

where θ_a is just a parametrisation of the infinitesimal symmetries, and $\mathcal{F}(\Phi) \equiv \Phi'(x')$ is the appropriate operation of a general field transformation in such a manifold. The generator is the symmetry transformation at the same point,

$$\delta_\theta \Phi(x) = \Phi^{'}(x) - \Phi(x) \equiv= -i\theta_a G_a \phi(x)\,, \tag{A.15}$$

$$iG_a\Phi = \frac{\delta x^\mu}{\delta\theta_a}\partial_\mu\Phi - \frac{\delta\mathcal{F}}{\delta\theta_a}\,. \tag{A.16}$$

We write here the generators for these infinitesimal symmetries,

$$\text{Translation}: \quad P_\mu = -i\partial_\mu\,, \tag{A.17}$$

$$\text{Dilatation}: \quad D = -ix^\mu\partial_\mu\,, \tag{A.18}$$

$$\text{Rotation}: \quad L_{\mu\nu} = i(x_\mu\partial_\nu - x_\nu\partial_\mu)\,, \tag{A.19}$$

$$\text{Special Conformal Transformation (SCT)}: \quad K_\mu = -i(x^2\partial_\mu - 2x_\mu x^\nu\partial_\nu)\,. \tag{A.20}$$

and the generators of the conformal algebra

$$[D, P_\mu] = iP_\mu\,, \tag{A.21}$$

$$[D, K_\mu] = iK_\mu\,, \tag{A.22}$$

$$[D, L_{\mu\nu}] = 0\,, \tag{A.23}$$

$$[K_\mu, P_\nu] = -2i(\eta_{\mu\nu}D - L_{\mu\nu})\,, \tag{A.24}$$

$$[K_\rho, L_{\mu\nu}] = -i(\eta_{\rho\mu}K_\nu - \eta_{\rho\nu}K_\mu)\,, \tag{A.25}$$

$$[P_\rho, L_{\mu\nu}] = i(\eta_{\rho\mu}P_\nu - \eta_{\rho\nu}P_\mu)\,, \tag{A.26}$$

$$[L_{\mu\nu}, L_{\rho\sigma}] = i(\eta_{\nu\rho}L_{\mu\sigma} + \eta_{\mu\sigma}L_{\nu\rho} - \eta_{\mu\rho}L_{\nu\sigma} - \eta_{\nu\sigma}L_{\mu\rho})\,, \tag{A.27}$$

The generators can be recombined in the form

$$M_{\mu\nu} = L_{\mu\nu}\,, \quad M_{\mu\,d} = \frac{1}{2}(K_\mu - P_\mu)\,, \quad M_{\mu\,(d+1)} = \frac{1}{2}(K_\mu + P_\mu)\,, \quad M_{d\,(d+1)} = D\,. \tag{A.28}$$

The Lorentz group in $d = p+q$ dimensions labeled as (p, q), $SO(p, q)$, is related to the conformal group $SO(p+1, q+1)$, just like the redefinition of the above generators made it explicit. So, for $d = 4$, the Lorentz group $SO(3, 1)$ with the inclusion of dilatation and special conformal transformations is related to the conformal group $SO(4, 2)$. We have used this fact many times when discussing symmetries of the conformal group in Chapter 2, as well as the isometry group of AdS in Chapter 5.

The integrated special conformal transformation symmetry can be achieved by a

change of variables $\vec{y} = \frac{\vec{x}}{x^2}$, and integrating $d\vec{x}/d\lambda = b^\mu \vec{x} \cdot \vec{x} - 2(\vec{x} \cdot \vec{b})x^\mu$, which gives

$$x^\mu \to \frac{x^\mu + b^\mu \vec{x}^2}{1 + 2\vec{x} \cdot \vec{b} + \vec{x}^2 \vec{b}^2} \,. \tag{A.29}$$

Another way to write the SCT is

$$\frac{x'^\mu}{\vec{x}' \cdot \vec{x}'} = \frac{x^\mu}{\vec{x} \cdot \vec{x}} + b^\mu \,. \tag{A.30}$$

This form makes it exploit its relation to translations and inversions. The transformation consists of an inversion, then a translation, and then again an inversion. The SCT relation to translations and as a symmetry in the conformal group was the motivation for substituting the translation symmetry in the Bjorken flow to a special conformal symmetry, which resulted in the Gubser flow, and was explored in Chapter 2 to solve analytically and semi-analytically dissipative conformal hydrodynamic theories.

Appendix B

Hydrodynamics and Weyl transformations

Many results in this thesis depend on the assumption of conformal symmetry, so in this Appendix we overview how hydrodynamics behave under Weyl transformations on the metric. One advantage of carefully discussing these issues is that it makes the symmetry argument more explicit. In Appendix A we reviewed briefly the properties of the conformal group. In this Appendix we follow references [52, 132] and use the metric signature $g_{\mu\nu} = \text{diag}(-1, 1, 1, 1)$.

First, we want to show that the equations of hydrodynamics that we constructed are conformally invariant. For such, we want to study how the several variables of interest change upon a metric transformation,

$$g_{\mu\nu} \to e^{2\,\Omega(x)}\, \hat{g}_{\mu\nu}\,. \tag{B.1}$$

The first important remark is that a conformal transformation is not a simple coordinate transformation. For instance, there are several curved spacetimes that are conformally mapped to Minkowski, in fact we investigated one of such when we analyzed the Gubser flow. Conformal transformations may relate two spacetimes described by the same coordinate charts, but with different curvature. It is a rather special assumption, and theories that are conformally invariant are very restrictive and symmetric.

We say that a quantity has weight w if under Eq. (B.1) it transforms as

$$X \to e^{-w\,\Omega(x)}\, \hat{X}\,. \tag{B.2}$$

If we use Gubser's notation [52], where $[X]$ denotes the conformal weight of such variable, we have that the covariant and contravariant metric tensors transform as

$$[g_{\mu\nu}] = 2, \qquad [g^{\mu\nu}] = -2\,. \tag{B.3}$$

The stress-energy tensor is calculated from the metric and the partition function. When the theory is conformally anomaly-free, which happens only on higher orders, the partition function is conformally invariant. Also, the conformal weight of the determinant of the metric is

$$\sqrt{-g} \to \sqrt{e^{d\,2\Omega(x)}\hat{g}} \to e^{d\,\Omega(x)}\sqrt{-\hat{g}}\,, \qquad \left[\sqrt{-g}\right] = -d\,. \tag{B.4}$$

Therefore, the definition of the stress-energy tensor implies that

$$\langle T^{\mu\nu}\rangle = \frac{2}{\sqrt{-g}}\frac{\delta \ln Z}{\delta g_{\mu\nu}}\,, \tag{B.5}$$

which results in

$$[T^{\mu\nu}] = d+2\,, \qquad [T_{\mu\nu}] = d-2\,. \tag{B.6}$$

The four-velocity has invariant norm, $g_{\mu\nu}u^\mu u^\nu = g^{\mu\nu}u_\mu u_\nu = -1$, which implies that the conformal weights are $[u^\mu] = 1$ and $[u_\mu] = -1$. From Eq. (2.5), we conclude that the conformal weight of the energy density is $[\varepsilon] = d$, which is 4 in our examples. Finally, it follows that the conformal weight of temperature is simply $[T] = 1$.

In [132], the author defines a covariant derivative which takes the natural time-like normalized vector in hydrodynamics, the quadrivelocity, and induce a special connection in a manifold with conformal structure. We will enunciate its form, but we find an explicit construction didactic and illustrative. In order to simply the notation, we will drop that $\Omega(x)$ is a function of the coordinates, we leave that meaning implicit.

First, the expansion rate has the following transformation rule

$$\theta = \nabla_\mu u^\mu = \frac{\partial_\mu(\sqrt{-g}\,u^\mu)}{\sqrt{-g}} \to e^{-\Omega}\left(\hat{\theta} + (d-1)\hat{D}\Omega\right)\,, \tag{B.7}$$

where the notation upper-hat means $\hat{D} \equiv \hat{u}^\mu\partial_\mu$ and $\hat{\theta} \equiv \hat{\nabla}_\mu\hat{u}^\mu$. The expansion rate by itself is clearly not conformal invariant. However, it is fundamental in our constructions. For instance, we analyze the simplest scenario under conformal transformations, the derivative of the temperature. The combination that appears in the conservation of energy (2.20) is

a conformal covariant, as

$$DT + \frac{T\theta}{d-1} \to e^{-2\Omega}\left(\hat{D}\hat{T} + \frac{\hat{T}\hat{\theta}}{d-1}\right) , \tag{B.8}$$

in which the contributions that depend on the derivative of the function Ω cancel identically. The general structure is however more complicated, as it involves derivatives of four vectors and tensors. Therefore, we need to write down the transformation rule of the Levi-Civita connection, which is a straightforward calculation from its definition,

$$\begin{aligned} \Gamma^{\alpha}_{\mu\nu} &= \frac{1}{2} g^{\alpha\beta}\left(\partial_\mu g_{\nu\beta} + \partial_\nu g_{\mu\beta} - \partial_\beta g_{\mu\nu}\right) , \\ \Gamma^{\alpha}_{\mu\nu} &\to \hat{\Gamma}^{\alpha}_{\mu\nu} + \left(\delta^{\alpha}_{\nu}\partial_\mu\Omega + \delta^{\alpha}_{\mu}\partial_\nu\Omega - \hat{g}_{\mu\nu}\hat{g}^{\alpha\beta}\partial_\beta\Omega\right) . \end{aligned} \tag{B.9}$$

It is possible to find the transformation of the derivative of the four-velocity, which is

$$\nabla_\mu u^\nu \to e^{-\Omega}\left(\hat{\nabla}_\mu \hat{u}^\nu + \delta^{\nu}_{\mu}\hat{D}\Omega - \hat{u}_\mu \hat{g}^{\nu\lambda}\partial_\lambda\Omega\right) . \tag{B.10}$$

It follows from Eq. (B.10) that the calculation of the shear tensor, which is also conformal covariant, gives

$$\sigma^{\mu\nu} \to e^{-3\Omega}\hat{\sigma}^{\mu\nu} . \tag{B.11}$$

The derivative of the shear tensor is necessary in the second order gradient expansion theory (2.16), and the derivative of the shear tensor in the Israel-Stewart (2.17). Even though they have a different weight under conformal transformation, both are symmetric, traceless and orthogonal to the four-velocity vectors. Therefore, it is easier to calculate the derivative of a general tensor with conformal weight ω, i. e., $\mathcal{B}_{\mu\nu} \to e^{-\omega\Omega}\hat{\mathcal{B}}_{\mu\nu}$, and the same properties of being symmetry, traceless and orthogonal to u^μ. This is a long but direct calculation involving the the Levi-Civita connection transformation (B.9),

$$\begin{aligned} D\mathcal{B}_{\mu\nu} &\to e^{-(\omega+1)\Omega}\left(\hat{D}\hat{\mathcal{B}}_{\mu\nu} - (\omega+2)\hat{\mathcal{B}}_{\mu\nu}\hat{D}\Omega + \hat{u}_\mu\hat{\mathcal{B}}^{\alpha}_{\nu}\partial_\alpha\Omega + \hat{u}_\nu\hat{\mathcal{B}}^{\alpha}_{\mu}\partial_\alpha\Omega\right) , \\ D\mathcal{B}^{<\mu\nu>} &\to e^{-(\omega+5)\Omega}\left(\hat{D}\hat{\mathcal{B}}^{<\mu\nu>} - (\omega+2)\hat{\mathcal{B}}^{\mu\nu}\hat{D}\Omega\right) . \end{aligned} \tag{B.12}$$

The procedure to eliminate the dependence on the derivative of the conformal factor is analogous to the temperature case,

$$\left(D\mathcal{B}^{<\mu\nu>} + \frac{(\omega+2)}{d-1}\theta\mathcal{B}\right) \to e^{-(\omega+5)\Omega}\left(\hat{D}\hat{\mathcal{B}}^{<\mu\nu>} + \frac{(\omega+2)}{d-1}\hat{\theta}\hat{\mathcal{B}}\right) . \tag{B.13}$$

Finally, as $[\sigma_{\mu\nu}] = -1$ and $[\pi_{\mu\nu}] = 2$,

$$\left(D\sigma^{<\mu\nu>} + \frac{1}{d-1}\,\theta\,\sigma^{\mu\nu}\right) \to e^{-4\Omega}\left(\hat{D}\hat{\sigma}^{<\mu\nu>} + \frac{1}{d-1}\,\hat{\theta}\,\hat{\sigma}^{\mu\nu}\right), \tag{B.14}$$

and

$$\left(D\pi^{<\mu\nu>} + \frac{4}{d-1}\,\theta\,\pi^{\mu\nu}\right) \to e^{-7\Omega}\left(\hat{D}\hat{\pi}^{<\mu\nu>} + \frac{4}{d-1}\,\hat{\theta}\,\hat{\pi}^{\mu\nu}\right), \tag{B.15}$$

which are exactly the contributions in Eqs. (2.16) and (2.17).

It is straightforward then to conclude that the other contributions are conformal covariants, as there are no other terms containing derivatives. This whole discussion should resemble general arguments in constructing gauge theories and local gauge symmetry. It is no coincidence that this mathematical structure is known from Weyl [133], whose early efforts were related to a geometrical unified theory of electromagnetism and general relativity. In the work of Loganayagam, the covariant derivative and gauge theory structure are more evident. Even though we already explicitly calculated the relevant terms for this thesis under conformal transformation, we present the so called Weyl derivative for completeness. We define the following derivatives related to the four-velocity,

$$\begin{aligned}
\theta \equiv \nabla_\mu u^\nu &\to e^{-\Omega}\left(\hat{\theta} + (d-1)\hat{D}\Omega\right), \\
a^\nu \equiv Du^\nu &\to e^{-2\Omega}\left(\hat{a}^\nu + \hat{\Delta}^{\nu\sigma}\partial_\sigma\Omega\right), \\
\mathcal{A}_\nu \equiv a_\nu - \frac{\theta}{d-1}u_\nu &\to \hat{\mathcal{A}}_\nu + \partial_\nu\Omega\,.
\end{aligned} \tag{B.16}$$

And for a tensorial field $T^{\mu\cdots}_{\nu\cdots} \to e^{-\omega\Omega}\,\hat{T}^{\mu\cdots}_{\nu\cdots}$, with conformal weight ω, its Weyl derivative $\mathcal{D}$ will also transform with the same weight, $\mathcal{D}_\lambda T^{\mu\cdots}_{\nu\cdots} \to e^{-\omega\Omega}\,\hat{\mathcal{D}}_\lambda\hat{T}^{\mu\cdots}_{\nu\cdots}$ for the following

$$\begin{aligned}
\mathcal{D}_\lambda T^{\mu\cdots}_{\nu\cdots} &\equiv \nabla_\lambda T^{\mu\cdots}_{\nu\cdots} + \omega\mathcal{A}_\lambda T^{\mu\cdots}_{\nu\cdots} \\
&+\left(g_{\lambda\alpha}\mathcal{A}^\mu - \delta^\mu_\lambda\mathcal{A}_\alpha - \delta^\mu_\alpha\mathcal{A}_\lambda\right)T^{\alpha\cdots}_{\nu\cdots} + \cdots \\
&-\left(g_{\lambda\nu}\mathcal{A}^\alpha - \delta^\alpha_\lambda\mathcal{A}_\nu - \delta^\alpha_\nu\mathcal{A}_\lambda\right)T^{\mu\cdots}_{\alpha\cdots} - \cdots\,.
\end{aligned} \tag{B.17}$$

Notice that these definitions are consistent with the explicit results we calculated in this section. There is a geometrical motivation for constructing such derivatives, as for a manifold with a conformal structure, there is a general class of one-forms we can specify the conformal connection for conformal equivalent sets of metric. The choice of the Weyl derivative is related to the more general concept in differential geometry of Weyl

connection, and by construction, $\mathcal{D}_\lambda g_{\mu\nu} = 0$. The one-form is uniquely fixed by requiring zero comoving derivative $u^\mu \mathcal{D}_\mu u^\nu = 0$ and the expansion rate $\mathcal{D}_\mu u^\mu = 0$.

Appendix C

The de Sitter space

The Gubser solution carefully discussed in Chapter 2 is manifestly more powerful when analyzed in the curved space with global coordinates in $dS_3 \otimes \mathbb{R}$. We expose in this appendix some properties of de Sitter spacetime that is relevant to obtain some geometric intuition. This appendix is based on Refs. [127, 134].

Suppose the following embedding in $(d+1)$ Minkowski space

$$\eta_{MN} X^M X^N = -(X^0)^2 + (X^1)^2 + \cdots + (X^d)^2 = L^2 \,. \tag{C.1}$$

We call this geometrical object the dS_d de Sitter spacetime. One simple interpretation of time slices is that for every fixed X^0, the remaining coordinates form a sphere S^{d-1} with radius $\sqrt{L^2 + (X^0)^2}$. The topology of this spacetime is then $\mathbb{R} \otimes S^{d-1}$. Also, notice that the minimum radius of the sphere is L, and of course infinity corresponds to $X^0 = \pm\infty$.

The symmetry group of dS_d is the Lorentz group $O(1,d)$, and this is a maximally symmetric space, which implies a constant curvature. Also, dS_d is a solution of Einstein's equation with positive cosmological constant,

$$R_{MN} - \frac{R}{2} g_{MN} + \Lambda g_{MN} = 0 \,, \qquad \Lambda = \frac{(d-2)(d-1)}{2L^2} \,. \tag{C.2}$$

The differential form of Eq. (C.1) is simply

$$-X^0 dX^0 + X^1 dX^1 + \cdots + X^d dX^d = 0 \,. \tag{C.3}$$

The $d-1$ sphere is parametrized with $d-1$ as usual [134],

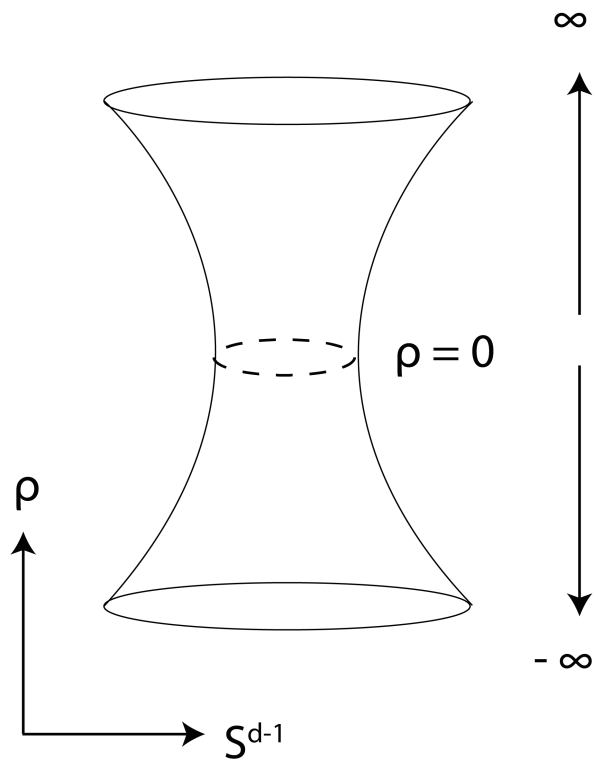

Figure C.1: *Pictorial representation of de Sitter space, with the horizontal direction representing the sphere S^{d-1}. Notice that the sphere has a minimum nonzero size at $\rho = 0$ (global coordinates).*

$$\begin{aligned}
\omega^1 &= \cos\theta_1\,, \\
\omega^2 &= \sin\theta_1 \cos\theta_2\,, \\
&\vdots \\
\omega^{d-1} &= \sin\theta_1 \cdots \sin\theta_{d-2} \cos\theta_{d-1}\,, \\
\omega^d &= \sin\theta_1 \cdots \sin\theta_{d-2} \sin\theta_{d-1}\,.
\end{aligned} \tag{C.4}$$

The angles are limited by $0 \leq \theta_i < \pi$ if $1 \leq d-1$, but $0 \leq \theta_{d-1} < 2\pi$. By definition, it sums up to unity, $\sum_{i=1}^{d} (\omega^i)^2 = 1$. The metric on the sphere S^{d-1} with unit radius is then

parametrized as

$$d\Omega_{d-1}^2 = \sum_{i=1}^{d} (d\omega^i)^2 = d\theta_1^2 + \sin^2\theta_1 d\theta_2^2 + \cdots + \sin^2\theta_1 \cdots \sin^2\theta_{d-2} d\theta_{d-1}^2 \,. \tag{C.5}$$

It clearly reduces to the usual angular part of spherical coordinates for $d = 2$. The global coordinates of de Sitter is then obtained by the following coordinate parametrization

$$\begin{aligned} X^0 &= L \sinh\rho \,, \\ X^i &= L\,\omega^i \cosh\rho \,, \quad i = 1, \cdots, d \,. \end{aligned} \tag{C.6}$$

Notice how the angles ω^i make the isometry S^{d-1} manifest and the parameter ρ ranges from $-\infty < \rho < \infty$. The topology of the space is then $\mathbb{R} \otimes S^{d-1}$. Hyperbolic functions are necessary as we need $\cosh^2\rho - \sinh^2\rho = 1$ in order to satisfy Eq. (C.1). Inserting these definitions in Eq. (C.3), we finally have the induced metric on dS_d on global coordinates becomes (setting $L = 1$)

$$ds^2 = -d\rho^2 + \cosh^2\rho \, d\Omega_{d-1}^2 \,. \tag{C.7}$$

Due to the cosh factor, it follows that the minimum radius of the S^{d-1} sphere is unity (for $L = 1$).

For the Gubser flow, we had the factor dS_3, which is then simply

$$ds^2 = -d\rho^2 + \cosh^2\rho \, (d\theta^2 + \sin\theta^2 + d\phi^2) \,, \tag{C.8}$$

which agrees with Eq. (2.53) apart from the extra direction $\mathbb{R}$, consequence of boost invariance in the Gubser flow.

Appendix D

The RPM method in Israel-Stewart Hydrodynamics

Here we focus on the detailed calculations involved in Chapter 3. The RPM method is used in the simplest conformal relativistic Israel-Stewart hydrodynamics equations (3.2), (3.3) and (3.4).

From the property of the dissipative tensor $u_\mu \pi^{\mu\nu} = 0$ we can write

$$\pi^{tt} = v^2 \pi^{xx} \qquad \text{and} \qquad \pi^{tx} = \pi^{xt} = v\pi^{xx} \,. \tag{D.1}$$

Notice that even though the RPM perturbative scheme does take into consideration nonlinearities, we can the general form of the flow, $u_\mu = (\gamma, -\gamma v, 0, 0)$, to write all the possible contributions of the shear tensor components. Since it is traceless, its diagonal components are related as

$$\begin{aligned} g_{\mu\nu}\pi^{\mu\nu} = \pi^{tt} - \pi^{xx} - \pi^{yy} - \pi^{zz} = 0 \,, \\ \pi^{\perp} \equiv \pi^{yy} = \pi^{zz} \,, \\ \pi^{\perp} = \frac{(v^2-1)}{2}\pi^{xx} \,. \end{aligned} \tag{D.2}$$

Using the conservation of energy, the term that contains the dissipative tensor in Eq. (3.2) can be written as a function of the x coordinate (using the previous relations)

$$\pi^{\mu\nu}\sigma_{\mu\nu} = \left(\frac{3}{2} - v^2 + \frac{3}{2}v^4\right)\pi^{xx}\sigma_{xx} \,. \tag{D.3}$$

The same can be done for the dissipative contribution in the momentum equation Eq. (3.3):

$$\Delta^x_\mu \partial_\nu \pi^{\mu\nu} = v\partial_t \pi^{xx} + \partial_x \pi^{xx} \,. \tag{D.4}$$

Now, for more general flow patterns the relaxation equation Eq. (3.4) will couple the different components of the dissipative tensor. However, in our particular case regarding this $1+1$ flow pattern, different components do not couple and the relevant term simply becomes

$$\Delta^x_\alpha \Delta^x_\beta D\pi^{\alpha\beta} = \gamma^4 (1-v^2)^2 D\pi^{xx} = D\pi^{xx}\,. \tag{D.5}$$

Therefore, our analysis is consistent (and simple) and does not require any further approximation regarding the mixing of different shear stress tensor components.

Using $\varepsilon_0/\kappa {T_0}^4 = 3/4$ and (D.1) in (3.2), (3.3) and (3.4), performing the operations (a) to (c), we find:

$$\sigma\left\{ -\frac{\partial \varepsilon_1}{\partial X} + \frac{4}{3}\frac{\partial v_1}{\partial X}\right\} + \sigma^2\left\{ -\frac{\partial \varepsilon_2}{\partial X} + \frac{4}{3}\frac{\partial v_2}{\partial X} + \frac{\partial \varepsilon_1}{\partial Y} + v_1\frac{\partial \varepsilon_1}{\partial X} - \frac{4}{9}v_1\frac{\partial v_1}{\partial X} + \frac{1}{3}\pi_1^{xx}\frac{\partial v_1}{\partial X}\right\}$$

$$+\sigma^3\left\{ -\frac{\partial \varepsilon_3}{\partial X} + \frac{\partial \varepsilon_2}{\partial Y} + v_1\frac{\partial \varepsilon_2}{\partial X} + v_2\frac{\partial \varepsilon_1}{\partial X} - \frac{4}{9}v_1\frac{\partial v_2}{\partial X} - \frac{4}{9}v_2\frac{\partial v_1}{\partial X} + \frac{4}{9}v_1\frac{\partial v_1}{\partial Y} + \frac{4}{3}\frac{\partial v_3}{\partial X} + \frac{4}{9}{v_1}^2\frac{\partial v_1}{\partial X}\right.$$

$$\left. -\frac{1}{9}\pi_1^{xx}v_1\frac{\partial v_1}{\partial X} + \frac{1}{3}\pi_1^{xx}\frac{\partial v_2}{\partial X} + \frac{1}{3}\pi_2^{xx}\frac{\partial v_1}{\partial X}\right\} = 0\,, \tag{D.6}$$

$$\sigma\left\{ \frac{\partial \varepsilon_1}{\partial X} - \frac{4}{3}\frac{\partial v_1}{\partial X} + \frac{\partial \pi_1^{xx}}{\partial X}\right\} + \sigma^2\left\{ -\frac{4}{3}\frac{\partial v_2}{\partial X} + \frac{\partial \varepsilon_2}{\partial X} + \frac{4}{3}\frac{\partial v_1}{\partial Y} + \frac{4}{3}v_1\frac{\partial v_1}{\partial X} - \frac{1}{3}v_1\frac{\partial \varepsilon_1}{\partial X}\right.$$

$$\left. -\frac{1}{3}v_1\frac{\partial \pi_1^{xx}}{\partial X} - \frac{1}{3}\pi_1^{xx}\frac{\partial v_1}{\partial X} + \frac{\partial \pi_2^{xx}}{\partial X}\right\} + \sigma^3\left\{ -\frac{4}{3}\frac{\partial v_3}{\partial X} + \frac{4}{3}\frac{\partial v_2}{\partial Y} + \frac{4}{3}v_1\frac{\partial v_2}{\partial X} + \frac{4}{3}v_2\frac{\partial v_1}{\partial X} - \frac{4}{9}{v_1}^2\frac{\partial v_1}{\partial X}\right.$$

$$\left. -\frac{1}{3}v_2\frac{\partial \varepsilon_1}{\partial X} - \frac{1}{3}v_1\frac{\partial \varepsilon_2}{\partial X} + \frac{1}{3}v_1\frac{\partial \varepsilon_1}{\partial Y} + \frac{\partial \varepsilon_3}{\partial X} + \frac{\partial \pi_3^{xx}}{\partial X} - \frac{1}{3}{v_1}^2\frac{\partial \pi_1^{xx}}{\partial X} - \frac{1}{3}v_1\frac{\partial \pi_2^{xx}}{\partial X}\right.$$

$$\left. -\frac{1}{3}v_2\frac{\partial \pi_1^{xx}}{\partial X} + \frac{1}{3}v_1\frac{\partial \pi_1^{xx}}{\partial Y} + \frac{1}{3}v_1\frac{\partial \pi_1^{xx}}{\partial Y} - \frac{1}{3}\pi_1^{xx}\frac{\partial v_2}{\partial X} - \frac{1}{3}\pi_1^{xx}v_1\frac{\partial v_1}{\partial X} - \frac{1}{3}\pi_2^{xx}\frac{\partial v_1}{\partial X}\right\} = 0 \tag{D.7}$$

and

$$\sigma^{1/2}\left\{ L\sqrt{3}\,\pi_1^{xx}\right\} + \sigma^{3/2}\left\{ -\tilde{\tau}_\pi\frac{\partial \pi_1^{xx}}{\partial X} + \frac{4}{3}\frac{\tilde{\eta}}{p_0}\frac{\partial v_1}{\partial X} + L\sqrt{3}\,\pi_2^{xx}\right\}$$

$$+\sigma^{5/2}\left\{ -\tilde{\tau}_\pi\frac{\partial \pi_2^{xx}}{\partial X} + \tilde{\tau}_\pi\frac{\partial \pi_1^{xx}}{\partial Y} + \tilde{\tau}_\pi v_1\frac{\partial \pi_1^{xx}}{\partial X} + \frac{4}{3}\tilde{\tau}_\pi\pi_1^{xx}\frac{\partial v_1}{\partial X} - \frac{4}{9}\frac{\tilde{\eta}}{p_0}v_1\frac{\partial v_1}{\partial X}\right.$$

$$+\frac{4}{3}\frac{\tilde{\eta}}{p_0}\frac{\partial v_2}{\partial X}+L\sqrt{3}\,\pi_3^{xx}-\frac{L}{\sqrt{3}}\,\pi_1^{xx}v_1\Bigg\}=0 \tag{D.8}$$

respectively. The pressure p_0 is the background pressure. As described in the step (d), from the $\mathcal{O}(\sigma^{1/2})$ term in (D.8) we have:

$$\pi_1^{xx}=0\ . \tag{D.9}$$

From $\mathcal{O}(\sigma)$ terms of (D.6) and (D.7) (and using (D.9)) we find:

$$v_1=\frac{3}{4}\,\varepsilon_1\ . \tag{D.10}$$

Applying (D.9) and (D.10) to the $\mathcal{O}(\sigma^{3/2})$ term of (D.8), we find:

$$\pi_2^{xx}=-\frac{\tilde{\eta}}{p_0}\frac{1}{L\sqrt{3}}\frac{\partial\varepsilon_1}{\partial X}\ . \tag{D.11}$$

Similarly, applying (D.9), (D.10) and (D.11) to the $\mathcal{O}(\sigma^2)$ terms of (D.6) and (D.7) we find respectively:

$$\frac{4}{3}\frac{\partial v_2}{\partial X}-\frac{\partial\varepsilon_2}{\partial X}=-\frac{\partial\varepsilon_1}{\partial Y}-\frac{1}{2}\,\varepsilon_1\frac{\partial\varepsilon_1}{\partial X} \tag{D.12}$$

and

$$\frac{4}{3}\frac{\partial v_2}{\partial X}-\frac{\partial\varepsilon_2}{\partial X}=\frac{\partial\varepsilon_1}{\partial Y}+\frac{1}{2}\,\varepsilon_1\frac{\partial\varepsilon_1}{\partial X}-\frac{\tilde{\eta}\sqrt{3}}{3Lp_0}\frac{\partial^2\varepsilon_1}{\partial X^2}\ . \tag{D.13}$$

Inserting (D.9), (D.10) and (D.11) into the $\mathcal{O}(\sigma^{5/2})$ term of (D.8) we obtain:

$$\frac{4}{3}\frac{\tilde{\eta}}{p_0}\frac{\partial v_2}{\partial X}+L\sqrt{3}\,\pi_3^{xx}-\frac{\tilde{\eta}}{4p_0}\,\varepsilon_1\frac{\partial\varepsilon_1}{\partial X}+\tilde{\tau}_\pi\frac{\tilde{\eta}}{L\sqrt{3}\,p_0}\frac{\partial^2\varepsilon_1}{\partial X^2}=0\ . \tag{D.14}$$

Equating (D.12) with (D.13) we find the following Burgers' equation for $\varepsilon_1(X,T)$:

$$\frac{\partial\varepsilon_1}{\partial Y}+\frac{1}{2}\,\varepsilon_1\frac{\partial\varepsilon_1}{\partial X}=\frac{\tilde{\eta}\sqrt{3}}{6Lp_0}\frac{\partial^2\varepsilon_1}{\partial X^2}\ . \tag{D.15}$$

The $\mathcal{O}(\sigma^3)$ terms of (D.6) and (D.7) provide, after using (D.9), (D.10) and (D.11) the following results:

$$\frac{4}{3}\frac{\partial v_3}{\partial X}-\frac{\partial\varepsilon_3}{\partial X}+\frac{\partial\varepsilon_2}{\partial Y}+\frac{3}{4}\,\varepsilon_1\frac{\partial\varepsilon_2}{\partial X}+\frac{2}{3}\,v_2\frac{\partial\varepsilon_1}{\partial X}-\frac{1}{3}\,\varepsilon_1\frac{\partial v_2}{\partial X}$$

$$+\frac{1}{4}\,\varepsilon_1\frac{\partial\varepsilon_1}{\partial Y}+\frac{3}{16}\,{\varepsilon_1}^2\frac{\partial\varepsilon_1}{\partial X}-\frac{\tilde{\eta}}{4Lp_0\sqrt{3}}\left(\frac{\partial\varepsilon_1}{\partial X}\right)^2=0 \tag{D.16}$$

and

$$\frac{\partial\varepsilon_3}{\partial X}-\frac{4}{3}\frac{\partial v_3}{\partial X}+\frac{4}{3}\frac{\partial v_2}{\partial Y}-\frac{1}{4}\varepsilon_1\frac{\partial\varepsilon_2}{\partial X}+\frac{2}{3}v_2\frac{\partial\varepsilon_1}{\partial X}+\varepsilon_1\frac{\partial v_2}{\partial X}+\frac{1}{4}\varepsilon_1\frac{\partial\varepsilon_1}{\partial Y}-\frac{3}{16}{\varepsilon_1}^2\frac{\partial\varepsilon_1}{\partial X}$$

$$+\frac{\tilde{\eta}}{4Lp_0\sqrt{3}}\left(\frac{\partial\varepsilon_1}{\partial X}\right)^2+\frac{\partial\pi_3^{xx}}{\partial X}+\frac{\tilde{\eta}}{4Lp_0\sqrt{3}}\varepsilon_1\frac{\partial^2\varepsilon_1}{\partial X^2}=0\ . \tag{D.17}$$

Isolating π_3^{xx} in (D.14) and $\partial\varepsilon_3/\partial X$ in (D.16), and then substituting these two results into (D.17) we obtain the following equation for $\varepsilon_2(X,T)$ and $v_2(X,T)$ (considering ε_1 previously known from (D.15)) :

$$\frac{\partial\varepsilon_2}{\partial Y}+\frac{4}{3}\frac{\partial v_2}{\partial Y}+\frac{1}{2}\varepsilon_1\frac{\partial\varepsilon_2}{\partial X}+\frac{4}{3}v_2\frac{\partial\varepsilon_1}{\partial X}+\frac{2}{3}\varepsilon_1\frac{\partial v_2}{\partial X}$$

$$+\frac{1}{2}\varepsilon_1\frac{\partial\varepsilon_1}{\partial Y}+\frac{\tilde{\eta}}{4Lp_0\sqrt{3}}\varepsilon_1\frac{\partial^2\varepsilon_1}{\partial X^2}+\frac{\tilde{\eta}}{4Lp_0\sqrt{3}}\left[\left(\frac{\partial\varepsilon_1}{\partial X}\right)^2+\varepsilon_1\frac{\partial^2\varepsilon_1}{\partial X^2}\right]$$

$$-\tilde{\tau}_\pi\frac{\tilde{\eta}}{3L^2p_0}\frac{\partial^3\varepsilon_1}{\partial X^3}-\frac{4\sqrt{3}\tilde{\eta}}{9Lp_0}\frac{\partial^2 v_2}{\partial X^2}=0\ . \tag{D.18}$$

We have thus a system of wave equations: (D.12), (D.15) and (D.18) for the three variables: $\varepsilon_1(X,T)$, $\varepsilon_2(X,T)$ and $v_2(X,T)$. In order to solve it, we shall return to the Cartesian (x,t) space using the (3.6) and (3.7) as described in the step (d) of the RPM. So, (D.12), (D.15) and (D.18) are rewritten as:

$$\frac{4}{3}\frac{\partial}{\partial x}\hat{v}_2-\frac{\partial}{\partial x}\hat{\varepsilon}_2=-\sqrt{3}\frac{\partial}{\partial t}\hat{\varepsilon}_1-\frac{\partial}{\partial x}\hat{\varepsilon}_1-\frac{1}{2}\hat{\varepsilon}_1\frac{\partial}{\partial x}\hat{\varepsilon}_1\ , \tag{D.19}$$

$$\frac{\partial}{\partial t}\hat{\varepsilon}_1+\frac{1}{\sqrt{3}}\frac{\partial}{\partial x}\hat{\varepsilon}_1+\frac{1}{2\sqrt{3}}\hat{\varepsilon}_1\frac{\partial}{\partial x}\hat{\varepsilon}_1=\frac{\eta}{6p_0}\frac{\partial^2}{\partial x^2}\hat{\varepsilon}_1 \tag{D.20}$$

and

$$\frac{\partial}{\partial t}\hat{\varepsilon}_2+\frac{1}{\sqrt{3}}\frac{\partial}{\partial x}\hat{\varepsilon}_2+\frac{4}{3}\frac{\partial}{\partial t}\hat{v}_2+\frac{4}{3\sqrt{3}}\frac{\partial}{\partial x}\hat{v}_2+\frac{1}{2\sqrt{3}}\hat{\varepsilon}_1\frac{\partial}{\partial x}\hat{\varepsilon}_2+\frac{4}{3\sqrt{3}}\hat{v}_2\frac{\partial}{\partial x}\hat{\varepsilon}_1+\frac{2}{3\sqrt{3}}\hat{\varepsilon}_1\frac{\partial}{\partial x}\hat{v}_2$$

$$+\frac{1}{2}\hat{\varepsilon}_1\frac{\partial}{\partial t}\hat{\varepsilon}_1+\frac{1}{2\sqrt{3}}\hat{\varepsilon}_1\frac{\partial}{\partial x}\hat{\varepsilon}_1+\frac{\eta}{4p_0}\hat{\varepsilon}_1\frac{\partial^2}{\partial x^2}\hat{\varepsilon}_1+\frac{\eta}{4p_0}\left[\left(\frac{\partial}{\partial x}\hat{\varepsilon}_1\right)^2+\hat{\varepsilon}_1\frac{\partial^2}{\partial x^2}\hat{\varepsilon}_1\right]$$

$$-\tau_\pi\frac{\eta}{3\sqrt{3}\,p_0}\frac{\partial^3}{\partial x^3}\hat{\varepsilon}_1-\frac{4\eta}{9p_0}\frac{\partial^2}{\partial x^2}\hat{v}_2=0\ . \tag{D.21}$$

The three equations above are for the dimensionless variables $\hat{\varepsilon}_1 \equiv \sigma\varepsilon_1$, $\hat{\varepsilon}_2 \equiv \sigma^2\varepsilon_2$ as defined in (3.8) and $\hat{v}_2 \equiv \sigma^2 v_2$ from (3.9). Inserting (D.20) into (D.19) we obtain:

$$\frac{\partial}{\partial x}\hat{v}_2 = \frac{3}{4}\frac{\partial}{\partial x}\hat{\varepsilon}_2 - \frac{\eta\sqrt{3}}{8p_0}\frac{\partial^2}{\partial x^2}\hat{\varepsilon}_1 \tag{D.22}$$

which, considering the constant of integration equals to zero yields the the following relation:

$$\hat{v}_2 = \frac{3}{4}\hat{\varepsilon}_2 - \frac{\eta\sqrt{3}}{8p_0}\frac{\partial}{\partial x}\hat{\varepsilon}_1 \ . \tag{D.23}$$

Calculating the spatial derivative of (D.20) we have:

$$\frac{\partial}{\partial t}\frac{\partial}{\partial x}\hat{\varepsilon}_1 = -\frac{1}{\sqrt{3}}\frac{\partial^2}{\partial x^2}\hat{\varepsilon}_1 - \frac{1}{2\sqrt{3}}\left[\left(\frac{\partial}{\partial x}\hat{\varepsilon}_1\right)^2 + \hat{\varepsilon}_1\frac{\partial^2}{\partial x^2}\hat{\varepsilon}_1\right] + \frac{\eta}{6p_0}\frac{\partial^3}{\partial x^3}\hat{\varepsilon}_1 \tag{D.24}$$

Substituting (D.23) and (D.24) in (D.21) we find:

$$\frac{\partial}{\partial t}\hat{\varepsilon_2} + \frac{1}{\sqrt{3}}\frac{\partial}{\partial x}\hat{\varepsilon}_2 + \frac{1}{2\sqrt{3}}\hat{\varepsilon}_1\frac{\partial}{\partial x}\hat{\varepsilon}_2 - \frac{\eta}{6p_0}\frac{\partial^2}{\partial x^2}\hat{\varepsilon}_2 + \frac{1}{2\sqrt{3}}\hat{\varepsilon}_2\frac{\partial}{\partial x}\hat{\varepsilon}_1$$

$$+\frac{\eta}{12p_0}\hat{\varepsilon}_1\frac{\partial^2}{\partial x^2}\hat{\varepsilon}_1 + \frac{1}{4}\hat{\varepsilon}_1\frac{\partial}{\partial t}\hat{\varepsilon}_1 + \frac{1}{4\sqrt{3}}\hat{\varepsilon}_1\frac{\partial}{\partial x}\hat{\varepsilon}_1 + \frac{\eta}{6p_0}\left[\frac{\eta\sqrt{3}}{12p_0} - \frac{\tau_\pi}{\sqrt{3}}\right]\frac{\partial^3}{\partial x^3}\hat{\varepsilon}_1 = 0 \ . \tag{D.25}$$

Finally, the set of equations for the small perturbations in energy density: $\hat{\varepsilon}_1$ and $\hat{\varepsilon}_2$ as described by (3.8), is given by the Burgers' equation (D.20) and the equation (D.25).

Using the dimensionless variables $\hat{x} = x\,T_0$, $\hat{t} = t\,T_0$, $\hat{\tau}_\pi = T_0\,\tau_\pi$ and recalling to the Gibbs relation $p_0 = T_0 s_0/4$, we rewrite (D.20) and (D.25) as:

$$\frac{\partial}{\partial\hat{t}}\hat{\varepsilon}_1 + \frac{1}{\sqrt{3}}\frac{\partial}{\partial\hat{x}}\hat{\varepsilon}_1 + \frac{1}{2\sqrt{3}}\hat{\varepsilon}_1\frac{\partial}{\partial\hat{x}}\hat{\varepsilon}_1 = \frac{\chi}{2}\frac{\partial^2}{\partial\hat{x}^2}\hat{\varepsilon}_1 \tag{D.26}$$

and

$$\frac{\partial}{\partial\hat{t}}\hat{\varepsilon_2} + \frac{1}{\sqrt{3}}\frac{\partial}{\partial\hat{x}}\hat{\varepsilon}_2 + \frac{1}{2\sqrt{3}}\hat{\varepsilon}_1\frac{\partial}{\partial\hat{x}}\hat{\varepsilon}_2 - \frac{\chi}{2}\frac{\partial^2}{\partial\hat{x}^2}\hat{\varepsilon}_2 + \frac{1}{2\sqrt{3}}\hat{\varepsilon}_2\frac{\partial}{\partial\hat{x}}\hat{\varepsilon}_1 + \frac{\chi}{4}\hat{\varepsilon}_1\frac{\partial^2}{\partial\hat{x}^2}\hat{\varepsilon}_1$$

$$+\frac{1}{4}\hat{\varepsilon}_1\frac{\partial}{\partial\hat{t}}\hat{\varepsilon}_1 + \frac{1}{4\sqrt{3}}\hat{\varepsilon}_1\frac{\partial}{\partial\hat{x}}\hat{\varepsilon}_1 + \frac{\chi}{2}\left[\frac{\chi\sqrt{3}}{4} - \frac{\hat{\tau}_\pi}{\sqrt{3}}\right]\frac{\partial^3}{\partial\hat{x}^3}\hat{\varepsilon}_1 = 0\,. \tag{D.27}$$

Appendix E

Linear instability of the gradient expansion at 2nd order with bulk viscosity

In this Appendix we investigate the *linear stability* properties of a fluid described by the 2nd order gradient expansion theory with bulk viscosity in flat spacetime around static equilibrium. It is based on our paper [38], and we use the mostly plus flat spacetime metric $g_{\mu\nu} = \mathrm{diag}(-1,1,1,1)$ and natural units. Consider the following theories [68, 73]

$$\begin{aligned}
\pi^{\mu\nu} &= -\eta\sigma^{\mu\nu} + \eta\tau_\pi\left(D\sigma^{\langle\mu\nu\rangle} + \frac{\theta}{3}\sigma^{\mu\nu}\right) + \kappa\left(\mathcal{R}^{\langle\mu\nu\rangle} - 2u_\alpha u_\beta\mathcal{R}^{\alpha\langle\mu\nu\rangle\beta}\right) \\
&+ \lambda_1\sigma_\lambda^{\langle\mu}\sigma^{\nu\rangle\lambda} + \lambda_2\sigma_\lambda^{\langle\mu}\Omega^{\nu\rangle\lambda} - \lambda_3\Omega_\lambda^{\langle\mu}\Omega^{\nu\rangle\lambda} \\
&+ 2\kappa^*\, u_\alpha u_\beta\mathcal{R}^{\alpha\langle\mu\nu\rangle\beta} + \eta\tau_\pi^*\,\sigma^{\mu\nu}\,\frac{\theta}{3} + \lambda_4\nabla^{\langle\mu}\ln s\,\nabla^{\nu\rangle}\ln s\,, \qquad \text{(E.1)}
\end{aligned}$$

and

$$\begin{aligned}
\Pi &= -\zeta\theta + \zeta\tau_\Pi\, D\theta + \xi_1\sigma_{\mu\nu}\sigma^{\mu\nu} + \xi_2\,\theta^2 \\
&+ \xi_3\Omega_{\mu\nu}\Omega^{\mu\nu} + \xi_4\nabla_\mu^\perp\ln s\,\nabla_\perp^\mu\ln s + \xi_5\mathcal{R} + \xi_6 u^\mu u^\nu\mathcal{R}_{\mu\nu}\,, \qquad \text{(E.2)}
\end{aligned}$$

Also, we need the conservation equations for momentum and energy,

$$\begin{aligned}
u_\nu\nabla_\mu T^{\mu\nu} &= D\,\varepsilon + (\varepsilon + p)\,\theta + \Pi^{\mu\nu}\nabla_{\perp(\mu}u_{\nu)} = 0\,, \\
\Delta^\alpha_\nu\nabla_\mu T^{\mu\nu} &= (\varepsilon+p)Du^\alpha + \nabla^\alpha_\perp p + \Delta^\alpha_\nu\nabla_\mu\Pi^{\mu\nu} = 0\,. \qquad \text{(E.3)}
\end{aligned}$$

In a linear analysis, the relevant linear terms involving the dissipative part of the

energy-momentum tensor are

$$\begin{aligned} \pi^{\mu\nu} &= -\eta\sigma^{\mu\nu} + \eta\tau_\pi D\sigma^{<\mu\nu>} \ , \\ \Pi &= -\zeta\theta + \zeta\tau_\Pi D\theta \ . \end{aligned} \tag{E.4}$$

We follow [41–43, 59] and consider linear perturbations around a static background. In order to investigate the stability of the sound channel, it is sufficient to study the effect of the perturbations

$$\begin{aligned} \varepsilon &= \varepsilon_0 + \delta\varepsilon(t,x) \ , \\ P &= P_0 + \delta P(t,x) \ , \\ u^\mu_{sound} &= (1,0,0,0) + (0,\delta u^x(t,x),0,0) \ , \\ \eta &= \eta_0 + \delta\eta(t,x) \ , \ \tau_\pi = \tau_{\pi,0} + \delta\tau_\pi(t,x) \ , \\ \zeta &= \zeta_0 + \delta\zeta(t,x) \ , \ \tau_\Pi = \tau_{\Pi,0} + \delta\tau_\Pi(t,x) \ . \end{aligned} \tag{E.5}$$

In this case, the relevant terms for linear perturbations are

$$\begin{aligned} \theta &= \partial_x \delta u^x \ , \\ \sigma^{xx} &= \frac{4}{3}\partial_x \delta u^x + \mathcal{O}(\delta^2) \ , \\ \pi^{xx} &= -\frac{4}{3}\eta_0 \partial_x \delta u^x + \frac{4}{3}\eta_0\tau_{\pi,0}\partial_x\partial_t \delta u^x + \mathcal{O}(\delta^2) \ , \\ \Pi &= -\zeta_0 \partial_x \delta u^x + \zeta_0\tau_{\Pi,0}\partial_t\partial_x \delta u^x + \mathcal{O}(\delta^2) \ . \end{aligned} \tag{E.6}$$

Using these results in the conservation equations E.3, one obtains the following differential equation for the sound disturbance[1]

$$\left[\partial_t^2 - c_{s,0}^2\partial_x^2 - \left(\frac{4}{3}\frac{\eta_0}{s_0} + \frac{\zeta_0}{s_0}\right)\partial_x^2\partial_t + \left(\frac{4}{3}\frac{\eta_0}{s_0}\tau_{\pi,0} + \frac{\zeta_0}{s_0}\tau_{\Pi,0}\right)\partial_x^2\partial_t^2\right]\delta u^x(t,x) = 0 \ , \tag{E.7}$$

where $s_0T_0 = \varepsilon_0 + P_0$. In Fourier space, for $\delta u^x(t,x) = \delta u^x_0\, e^{i(kx-\omega t)}$, one finds the dispersion relation

$$\omega^2 - c_{s,0}^2 k^2 + \left(\frac{4}{3}\frac{\eta_0}{s_0} + \frac{\zeta_0}{s_0}\right) i\omega k^2 - \left(\frac{4}{3}\frac{\eta_0}{s_0}\tau_{\pi,0} + \frac{\zeta_0}{s_0}\tau_{\Pi,0}\right)\omega^2 k^2 = 0 \ . \tag{E.8}$$

While the equation above can be solved exactly, when it comes to the stability properties of these modes it is sufficient to look at the sum of the roots [60], Chapter 4. For the

[1] Note that we use dimensionless variables $t \to t\,T_0$ and $x \to xT_0$ and, correspondingly, $\omega \to \omega/T_0$ and $k \to k/T_0$.

polynomial corresponding to sound disturbances, the sum of the two roots gives

$$\omega_1 + \omega_2 = \frac{i\left(\frac{4}{3}\frac{\eta_0}{s_0} + \frac{\zeta_0}{s_0}\right)}{\left(\frac{4}{3}\frac{\eta_0}{s_0}\tau_{\pi,0} + \frac{\zeta_0}{s_0}\tau_{\Pi,0}\right)k^2 - 1} \,. \tag{E.9}$$

Notice that for k larger than a critical wavenumber k_c^{sound} defined by

$$k_c^{sound} = \frac{1}{\sqrt{\frac{4}{3}\frac{\eta_0}{s_0}\tau_{\pi,0} + \frac{\zeta_0}{s_0}\tau_{\Pi,0}}} \,, \tag{E.10}$$

the sum of the roots adds up to a positive imaginary number. Therefore, for $k > k_c^{sound}$ one of the modes has a positive imaginary part and is, thus, unstable.

Note that in the limit when $\tau_{\pi,0}\,, \tau_{\Pi,0} \to 0$ one finds that k_c^{sound} diverges, which is in agreement with the fact that NS theory is stable against small perturbations in a fluid at rest [41–43]. Clearly, for a moving fluid the stability properties become more involved but it is possible to show that the same type of problems that appears in NS theory also appear in this case [60]. However, we remark that hydrodynamics is only expected to be valid in the low frequency, large wavelength limit. Nevertheless, the instability found here at finite wavenumber motivates the search for a UV completion of this theory that is linearly stable and can, therefore, be safely used in numerical simulations.

A larger critical wavenumber, k_c^{shear}, appears in the shear channel. Linear stability of shear modes can be studied by choosing a flow disturbance of the kind $u^\mu_{shear} = (1,0,0,0) + (0,0,\delta u^y(t,x),0)$ while the other relations in (E.6) remain valid (see [67]). This leads to the following dispersion relation

$$\omega\left(1 - \frac{\eta_0}{s_0}\tau_{\pi_0}k^2\right) + i\frac{\eta_0}{s_0}k^2 = 0 \,, \tag{E.11}$$

which can be easily solved to give

$$\begin{aligned} \omega(k) &= \frac{i\,\frac{\eta_0}{s_0}k^2}{\frac{\eta_0}{s_0}\tau_{\pi,0}k^2 - 1} \,, \\ k_c^{shear} &= \frac{1}{\sqrt{\frac{\eta_0}{s_0}\tau_{\pi,0}}} > k_c^{sound} \,. \end{aligned} \tag{E.12}$$

Bibliography

[1] J. M. Maldacena, "Eternal black holes in anti-de Sitter," *JHEP* **0304** (2003) 021, arXiv:hep-th/0106112 [hep-th]. x, 123

[2] M. Eckert, *The Dawn of Fluid Dynamics: A Discipline Between Science and Technology*. Wiley-VCH; 1 edition, 2006. 2

[3] M. Gyulassy and L. McLerran, "New forms of QCD matter discovered at RHIC," *Nucl.Phys.* **A750** (2005) 30–63, arXiv:nucl-th/0405013 [nucl-th]. 2

[4] U. Heinz and R. Snellings, "Collective flow and viscosity in relativistic heavy-ion collisions," *Ann.Rev.Nucl.Part.Sci.* **63** (2013) 123–151, arXiv:1301.2826 [nucl-th]. 2, 33

[5] **BRAHMS Collaboration** Collaboration, I. Arsene *et al.*, "Quark gluon plasma and color glass condensate at RHIC? The Perspective from the BRAHMS experiment," *Nucl.Phys.* **A757** (2005) 1–27, arXiv:nucl-ex/0410020 [nucl-ex]. 2

[6] **PHENIX Collaboration** Collaboration, K. Adcox *et al.*, "Formation of dense partonic matter in relativistic nucleus-nucleus collisions at RHIC: Experimental evaluation by the PHENIX collaboration," *Nucl.Phys.* **A757** (2005) 184–283, arXiv:nucl-ex/0410003 [nucl-ex]. 2

[7] **ATLAS Collaboration** Collaboration, G. Aad *et al.*, "Measurement of the azimuthal anisotropy for charged particle production in $\sqrt{s_{NN}} = 2.76$ TeV lead-lead collisions with the ATLAS detector," *Phys.Rev.* **C86** (2012) 014907, arXiv:1203.3087 [hep-ex]. 2, 24, 102

[8] **CMS Collaboration** Collaboration, C. Collaboration, "Azimuthal anisotropy harmonics in ultra-central PbPb collisions at $\sqrt{s_{NN}} = 2.76$ TeV," CMS-PAS-HIN-12-011. 2, 24

[9] L. D. Landau and Lifshitz, *Fluid Mechanics, Volume 6 (Course of Theoretical Physics)*. Butterworth-Heinemann; 2 edition, 1987. 2, 9, 11, 13, 61, 63

[10] P. Kovtun, D. T. Son, and A. O. Starinets, "Viscosity in strongly interacting quantum field theories from black hole physics," *Phys.Rev.Lett.* **94** (2005) 111601, arXiv:hep-th/0405231 [hep-th]. 2, 5, 20, 34, 109, 116

[11] M. Gell-Mann, "A Schematic Model of Baryons and Mesons," *Phys.Lett.* **8** (1964) 214–215. 2

[12] O. Greenberg, "Spin and Unitary Spin Independence in a Paraquark Model of Baryons and Mesons," *Phys.Rev.Lett.* **13** (1964) 598–602.

[13] M. Han and Y. Nambu, "Three Triplet Model with Double SU(3) Symmetry," *Phys.Rev.* **139** (1965) B1006–B1010.

[14] A. Halzen, Francis; Martin, *Quarks and Leptons: An Introductory Course in Modern Particle Physics*. John Wiley and Sons, 1984. 2, 3

[15] D. J. Gross and F. Wilczek, "Ultraviolet Behavior of Nonabelian Gauge Theories," *Phys.Rev.Lett.* **30** (1973) 1343–1346. 2

[16] H. D. Politzer, "Reliable Perturbative Results for Strong Interactions?," *Phys.Rev.Lett.* **30** (1973) 1346–1349. 2

[17] J. Greensite, *An Introduction to the Confinement Problem*. Springer, 2011. 2

[18] W. Greiner, *Quantum Chromodynamics*. Springer, 1995. 3

[19] M. L. Miller, K. Reygers, S. J. Sanders, and P. Steinberg, "Glauber modeling in high energy nuclear collisions," *Ann.Rev.Nucl.Part.Sci.* **57** (2007) 205–243, arXiv:nucl-ex/0701025 [nucl-ex]. 3

[20] T. Hirano, U. W. Heinz, D. Kharzeev, R. Lacey, and Y. Nara, "Hadronic dissipative effects on elliptic flow in ultrarelativistic heavy-ion collisions," *Phys.Lett.* **B636** (2006) 299–304, arXiv:nucl-th/0511046 [nucl-th]. 3

[21] T. Lappi and L. McLerran, "Some features of the glasma," *Nucl.Phys.* **A772** (2006) 200–212, arXiv:hep-ph/0602189 [hep-ph]. 3

[22] S. Durr, Z. Fodor, J. Frison, C. Hoelbling, R. Hoffmann, *et al.*, "Ab-Initio Determination of Light Hadron Masses," *Science* **322** (2008) 1224–1227, arXiv:0906.3599 [hep-lat]. 3

[23] Y. Aoki, G. Endrodi, Z. Fodor, S. Katz, and K. Szabo, "The Order of the quantum chromodynamics transition predicted by the standard model of particle physics," *Nature* **443** (2006) 675–678, arXiv:hep-lat/0611014 [hep-lat]. 3, 62

[24] S. Borsanyi, Z. Fodor, C. Hoelbling, S. D. Katz, S. Krieg, *et al.*, "Full result for the QCD equation of state with 2+1 flavors," *Phys.Lett.* **B730** (2014) 99–104, arXiv:1309.5258 [hep-lat]. 3, 62

[25] P. de Forcrand and O. Philipsen, "The QCD phase diagram for small densities from imaginary chemical potential," *Nucl.Phys.* **B642** (2002) 290–306, arXiv:hep-lat/0205016 [hep-lat]. 3

[26] W. A. van Leewen, S. R. de Groot, and C. G. van Weert, *Relativistic Kinetic Theory: principles and applications*. Elsevier North-Holland, 1980. 3

[27] C. Cercignani and G. M. Kremer, *The relativistic Boltzmann Equation: Theory and Applications*. Birkhauser Verlag (Basel, Switzerland), 2002. 3

[28] G. Denicol, T. Koide, and D. Rischke, "Dissipative relativistic fluid dynamics: a new way to derive the equations of motion from kinetic theory," *Phys.Rev.Lett.* **105** (2010) 162501, arXiv:1004.5013 [nucl-th]. 3, 5, 19, 21, 34

[29] G. S. Denicol, J. Noronha, H. Niemi, and D. H. Rischke, "Origin of the Relaxation Time in Dissipative Fluid Dynamics," *Phys.Rev.* **D83** (2011) 074019, arXiv:1102.4780 [hep-th]. 66, 97, 98

[30] G. Denicol, H. Niemi, E. Molnar, and D. Rischke, "Derivation of transient relativistic fluid dynamics from the Boltzmann equation," *Phys.Rev.* **D85** (2012) 114047, arXiv:1202.4551 [nucl-th]. 3, 5, 7, 14, 19, 21, 34, 66, 80, 96, 101, 103

[31] A. Adams, L. D. Carr, T. Schafer, P. Steinberg, and J. E. Thomas, "Strongly Correlated Quantum Fluids: Ultracold Quantum Gases, Quantum Chromodynamic Plasmas, and Holographic Duality," *New J.Phys.* **14** (2012) 115009, arXiv:1205.5180 [hep-th]. 4, 5, 102

[32] J. M. Maldacena, "The Large N limit of superconformal field theories and supergravity," *Int.J.Theor.Phys.* **38** (1999) 1113–1133, arXiv:hep-th/9711200 [hep-th]. 4

[33] O. Aharony, S. S. Gubser, J. M. Maldacena, H. Ooguri, and Y. Oz, "Large N field theories, string theory and gravity," *Phys.Rept.* **323** (2000) 183–386, arXiv:hep-th/9905111 [hep-th]. 4, 5, 103, 104, 105, 106

[34] A. V. Ramallo, "Introduction to the AdS/CFT correspondence," arXiv:1310.4319 [hep-th]. 109

[35] H. Nastase, "Introduction to AdS-CFT," arXiv:0712.0689 [hep-th]. 4, 5

[36] L. Susskind, "The World as a hologram," *J.Math.Phys.* **36** (1995) 6377–6396, arXiv:hep-th/9409089 [hep-th]. 5

[37] J. Casalderrey-Solana, H. Liu, D. Mateos, K. Rajagopal, and U. A. Wiedemann, "Gauge/String Duality, Hot QCD and Heavy Ion Collisions," arXiv:1101.0618 [hep-th]. 5

[38] S. I. Finazzo, R. Rougemont, H. Marrochio, and J. Noronha, "Hydrodynamic transport coefficients for the non-conformal quark-gluon plasma from holography," *Accepted for publication in JHEP* (2014) , arXiv:1412.2968 [hep-ph]. 5, 7, 14, 77, 145

[39] S. Bhattacharyya, V. E. Hubeny, S. Minwalla, and M. Rangamani, "Nonlinear Fluid Dynamics from Gravity," *JHEP* **0802** (2008) 045, arXiv:0712.2456 [hep-th]. 5, 7, 78, 80, 101, 111, 112, 113, 114, 116

[40] C. Cercignani, *Mathematical Methods in Kinetic Theory*. Springer, 1969. 6, 14, 102, 103, 127

[41] W. Hiscock and L. Lindblom, "Stability and causality in dissipative relativistic fluids," *Annals Phys.* **151** (1983) 466–496. 6, 7, 14, 77, 78, 79, 83, 85, 146, 147

[42] W. A. Hiscock and L. Lindblom, "Generic instabilities in first-order dissipative relativistic fluid theories," *Phys.Rev.* **D31** (1985) 725–733. 83, 100

[43] W. A. Hiscock and L. Lindblom, "Linear plane waves in dissipative relativistic fluids," *Phys.Rev.* **D35** (1987) 3723–3732. 6, 7, 14, 77, 79, 85, 146, 147

[44] W. van der Schee, "Gravitational collisions and the quark-gluon plasma," arXiv:1407.1849 [hep-th]. 6, 117, 118

[45] P. M. Chesler and L. G. Yaffe, "Numerical solution of gravitational dynamics in asymptotically anti-de Sitter spacetimes," *JHEP* **1407** (2014) 086, arXiv:1309.1439 [hep-th]. 6, 117, 118, 119

[46] H. Georgi, *Lie Algebras In Particle Physics: from Isospin To Unified Theories*. Westview Press, 1999. 6

[47] S. Coleman, *Aspects of Symmetry*. Cambridge University Press, 1988. 6

[48] P. Francesco and P. Mathieu, *Conformal Field Theory*. Springer, 1999. 6, 128, 129

[49] W. Israel, "Nonstationary irreversible thermodynamics: A Causal relativistic theory," *Annals Phys.* **100** (1976) 310–331. 6, 14, 22, 77

[50] W. Israel and J. Stewart, "Transient relativistic thermodynamics and kinetic theory," *Annals Phys.* **118** (1979) 341–372. 6, 14, 22, 23, 77

[51] S. S. Gubser, "Symmetry constraints on generalizations of Bjorken flow," *Phys.Rev.* **D82** (2010) 085027, arXiv:1006.0006 [hep-th]. 6, 9, 16, 23, 24, 25, 27, 28

[52] S. S. Gubser and A. Yarom, "Conformal hydrodynamics in Minkowski and de Sitter spacetimes," *Nucl.Phys.* **B846** (2011) 469–511, arXiv:1012.1314 [hep-th]. 6, 9, 14, 23, 24, 25, 26, 27, 28, 116, 132

[53] H. Marrochio, J. Noronha, G. S. Denicol, M. Luzum, S. Jeon, and C. Gale, "Solutions of conformal israel-stewart relativistic viscous fluid dynamics," *Phys. Rev. C* **91** (Jan, 2015) 014903. http://link.aps.org/doi/10.1103/PhysRevC.91.014903. 7, 9, 14, 29, 32, 36, 64, 72, 79

[54] R. C. Davidson, *Methods in Nonlinear Plasma Theory*. Academic Press (February 1972), 1972. 7, 62, 64

[55] H. Washimi and T. Taniuti, "Propagation of ion-acoustic solitary waves of small amplitude," *Phys. Rev. Lett.* **17** (Nov, 1966) 996–998. http://link.aps.org/doi/10.1103/PhysRevLett.17.996.

[56] H. Leblond, "The reductive perturbation method and some of its applications," *Journal of Physics B: Atomic, Molecular and Optical Physics* **41** no. 4, (2008) 043001. http://stacks.iop.org/0953-4075/41/i=4/a=043001. 7, 62, 64

[57] D. Fogaca, H. Marrochio, F. Navarra, and J. Noronha, "Nonlinear waves in second order conformal hydrodynamics," *Nuclear Physics A* **934** no. 0, (2015) 18 – 40. http://www.sciencedirect.com/science/article/pii/S0375947414006265. 7, 61

[58] G. Denicol, T. Kodama, T. Koide, and P. Mota, "Stability and Causality in relativistic dissipative hydrodynamics," *J.Phys.* **G35** (2008) 115102, arXiv:0807.3120 [hep-ph]. 7, 28, 77

[59] S. Pu, T. Koide, and Q. Wang, "Causality and stability of dissipative fluid dynamics with diffusion currents," *AIP Conf.Proc.* **1235** (2010) 186–192. 7, 95, 146

[60] H. Marrochio, D. Fogaca, J. Noronha, and G. S. Denicol, "Breakdown of gradient expansion approach under linear perturbations." Work in Progress. 7, 14, 77, 146, 147

[61] M. Rangamani, "Gravity and Hydrodynamics: Lectures on the fluid-gravity correspondence," *Class.Quant.Grav.* **26** (2009) 224003, arXiv:0905.4352 [hep-th]. 7, 101, 108, 116

[62] V. E. Hubeny, S. Minwalla, and M. Rangamani, "The fluid/gravity correspondence," arXiv:1107.5780 [hep-th]. 7, 101, 116

[63] J. Bjorken, "Highly Relativistic Nucleus-Nucleus Collisions: The Central Rapidity Region," *Phys.Rev.* **D27** (1983) 140–151. 9, 17, 36

[64] B. Schenke, S. Jeon, and C. Gale, "(3+1)D hydrodynamic simulation of relativistic heavy-ion collisions," *Phys.Rev.* **C82** (2010) 014903, arXiv:1004.1408 [hep-ph]. 9, 36, 37

[65] B. Schenke, S. Jeon, and C. Gale, "Higher flow harmonics from (3+1)D event-by-event viscous hydrodynamics," *Phys.Rev.* **C85** (2012) 024901, arXiv:1109.6289 [hep-ph].

[66] B. Schenke, S. Jeon, and C. Gale, "Elliptic and triangular flow in event-by-event (3+1)D viscous hydrodynamics," *Phys.Rev.Lett.* **106** (2011) 042301, arXiv:1009.3244 [hep-ph]. 9, 36, 37, 61

[67] P. Romatschke, "New Developments in Relativistic Viscous Hydrodynamics," *Int.J.Mod.Phys.* **E19** (2010) 1–53, arXiv:0902.3663 [hep-ph]. 9, 13, 61, 147

[68] R. Baier, P. Romatschke, D. T. Son, A. O. Starinets, and M. A. Stephanov, "Relativistic viscous hydrodynamics, conformal invariance, and holography," *JHEP* **0804** (2008) 100, arXiv:0712.2451 [hep-th]. 14, 18, 19, 64, 66, 79, 80, 82, 87, 96, 145

[69] G. S. Denicol, U. W. Heinz, M. Martinez, J. Noronha, and M. Strickland, "Studying the validity of relativistic hydrodynamics with a new exact solution of the Boltzmann equation," *Phys.Rev.* **D90** no. 12, (2014) 125026, arXiv:1408.7048 [hep-ph]. 14

[70] M. P. Heller and R. A. Janik, "Viscous hydrodynamics relaxation time from AdS/CFT," *Phys.Rev.* **D76** (2007) 025027, arXiv:hep-th/0703243 [HEP-TH]. 18, 19

[71] P. B. Arnold, G. D. Moore, and L. G. Yaffe, "Transport coefficients in high temperature gauge theories. 1. Leading log results," *JHEP* **0011** (2000) 001, arXiv:hep-ph/0010177 [hep-ph]. 19

[72] P. B. Arnold, G. D. Moore, and L. G. Yaffe, "Transport coefficients in high temperature gauge theories. 2. Beyond leading log," *JHEP* **0305** (2003) 051, arXiv:hep-ph/0302165 [hep-ph]. 19

[73] P. Romatschke, "Relativistic Viscous Fluid Dynamics and Non-Equilibrium Entropy," *Class.Quant.Grav.* **27** (2010) 025006, arXiv:0906.4787 [hep-th]. 19, 145

[74] S. Pu, T. Koide, and D. H. Rischke, "Does stability of relativistic dissipative fluid dynamics imply causality?," *Phys.Rev.* **D81** (2010) 114039, arXiv:0907.3906 [hep-ph]. 28, 36, 77, 78, 95, 97

[75] L.-G. Pang, Y. Hatta, X.-N. Wang, and B.-W. Xiao, "Analytical and numerical Gubser solutions of the second-order hydrodynamics," arXiv:1411.7767 [hep-ph]. 34

[76] M. Luzum and J.-Y. Ollitrault, "Extracting the shear viscosity of the quark-gluon plasma from flow in ultra-central heavy-ion collisions," *Nucl.Phys.* **A904-905** (2013) 377c–380c, arXiv:1210.6010 [nucl-th]. 34

[77] T. Csorgo, F. Grassi, Y. Hama, and T. Kodama, "Simple solutions of relativistic hydrodynamics for longitudinally and cylindrically expanding systems," *Phys.Lett.* **B565** (2003) 107–115, arXiv:nucl-th/0305059 [nucl-th]. 36

[78] T. Csorgo, L. Csernai, Y. Hama, and T. Kodama, "Simple solutions of relativistic hydrodynamics for systems with ellipsoidal symmetry," *Heavy Ion Phys.* **A21** (2004) 73–84, arXiv:nucl-th/0306004 [nucl-th].

[79] T. Csorgo, M. Nagy, and M. Csanad, "A New family of simple solutions of perfect fluid hydrodynamics," *Phys.Lett.* **B663** (2008) 306–311, arXiv:nucl-th/0605070 [nucl-th]. 36

[80] D. H. Rischke, Y. Pursun, and J. A. Maruhn, "Relativistic hydrodynamics for heavy ion collisions II. Compression of nuclear matter and the phase transition to the quark - gluon plasma," *Nucl.Phys.* **A595** (1995) 383–408, arXiv:nucl-th/9504021 [nucl-th]. 36

[81] Y. Akamatsu, S.-i. Inutsuka, C. Nonaka, and M. Takamoto, "A new scheme of causal viscous hydrodynamics for relativistic heavy-ion collisions: A Riemann solver for quark-gluon plasma," *J.Comput.Phys.* **256** (2014) 34–54, arXiv:1302.1665 [nucl-th].

[82] I. Bouras, E. Molnar, H. Niemi, Z. Xu, A. El, *et al.*, "Investigation of shock waves in the relativistic Riemann problem: A Comparison of viscous fluid dynamics to kinetic theory," *Phys.Rev.* **C82** (2010) 024910, arXiv:1006.0387 [hep-ph]. 36

[83] A. Kurganov and E. Tadmor, "New high-resolution central schemes for nonlinear conservation laws and convectionâdiffusion equations," *Journal of Computational Physics* **160** no. 1, (2000) 241 – 282. http://www.sciencedirect.com/science/article/pii/S0021999100964593. 36

[84] R. Naidoo and S. Baboolal, "Application of the kurganovâlevy semi-discrete numerical scheme to hyperbolic problems with nonlinear source terms," *Future Generation Computer Systems* **20** no. 3, (2004) 465 – 473. http://www.sciencedirect.com/science/article/pii/S0167739X03001870. Selected numerical algorithms. 36

[85] J. Kapusta, B. Muller, and M. Stephanov, "Relativistic Theory of Hydrodynamic Fluctuations with Applications to Heavy Ion Collisions," *Phys.Rev.* **C85** (2012) 054906, arXiv:1112.6405 [nucl-th]. 61

[86] R. Andrade, F. Grassi, Y. Hama, T. Kodama, and J. Socolowski, O., "On the necessity to include event-by-event fluctuations in experimental evaluation of elliptical flow," *Phys.Rev.Lett.* **97** (2006) 202302, arXiv:nucl-th/0608067 [nucl-th]. 61

[87] R. Andrade, F. Grassi, Y. Hama, T. Kodama, and W. Qian, "Importance of Granular Structure in the Initial Conditions for the Elliptic Flow," *Phys.Rev.Lett.* **101** (2008) 112301, arXiv:0805.0018 [hep-ph].

[88] J. Takahashi, B. Tavares, W. Qian, R. Andrade, F. Grassi, *et al.*, "Topology studies of hydrodynamics using two particle correlation analysis," *Phys.Rev.Lett.* **103** (2009) 242301, arXiv:0902.4870 [nucl-th].

[89] E. Shuryak, "The Cone, the Ridge and the Fate of the Initial State Fluctuations in Heavy Ion Collisions," *Phys.Rev.* **C80** (2009) 054908, arXiv:0903.3734 [nucl-th].

[90] P. Staig and E. Shuryak, "The Fate of the Initial State Fluctuations in Heavy Ion Collisions. II The Fluctuations and Sounds," *Phys.Rev.* **C84** (2011) 034908, arXiv:1008.3139 [nucl-th].

[91] S. Floerchinger and U. A. Wiedemann, "Fluctuations around Bjorken Flow and the onset of turbulent phenomena," *JHEP* **1111** (2011) 100, arXiv:1108.5535 [nucl-th].

[92] R. Andrade and J. Noronha, "Di-hadron angular correlation function in event-by-event ideal hydrodynamics," *Phys.Rev.* **C88** no. 3, (2013) 034909, arXiv:1305.3098 [nucl-th]. 61

[93] H. Stoecker, "Collective flow signals the quark gluon plasma," *Nucl.Phys.* **A750** (2005) 121–147, arXiv:nucl-th/0406018 [nucl-th]. 61

[94] J. Casalderrey-Solana, E. Shuryak, and D. Teaney, "Conical flow induced by quenched QCD jets," *J.Phys.Conf.Ser.* **27** (2005) 22–31, arXiv:hep-ph/0411315 [hep-ph].

[95] A. Chaudhuri and U. Heinz, "Effect of jet quenching on the hydrodynamical evolution of QGP," *Phys.Rev.Lett.* **97** (2006) 062301, arXiv:nucl-th/0503028 [nucl-th].

[96] B. Betz, J. Noronha, G. Torrieri, M. Gyulassy, I. Mishustin, *et al.*, "Universality of the Diffusion Wake from Stopped and Punch-Through Jets in Heavy-Ion Collisions," *Phys.Rev.* **C79** (2009) 034902, arXiv:0812.4401 [nucl-th].

[97] B. Betz, M. Gyulassy, J. Noronha, and G. Torrieri, "Anomalous Conical Di-jet Correlations in pQCD vs AdS/CFT," *Phys.Lett.* **B675** (2009) 340–346, arXiv:0807.4526 [hep-ph].

[98] J. Noronha, M. Gyulassy, and G. Torrieri, "Di-Jet Conical Correlations Associated with Heavey Quark Jets in anti-de Sitter Space/Conformal Field Theory Correspondence," *Phys.Rev.Lett.* **102** (2009) 102301, arXiv:0807.1038 [hep-ph].

[99] B. Betz, J. Noronha, G. Torrieri, M. Gyulassy, and D. H. Rischke, "Universal Flow-Driven Conical Emission in Ultrarelativistic Heavy-Ion Collisions," *Phys.Rev.Lett.* **105** (2010) 222301, arXiv:1005.5461 [nucl-th]. 61

[100] S. Weinberg, *Gravitation and Cosmology: Principles and Applications of the General Theory of Relativity.* Wiley, New York [et al.], 1972. 61

[101] J.-Y. Ollitrault, "Relativistic hydrodynamics for heavy-ion collisions," *Eur.J.Phys.* **29** (2008) 275–302, arXiv:0708.2433 [nucl-th]. 61

[102] D. Fogaca, F. Navarra, and L. Ferreira Filho, "Viscosity, wave damping and shock wave formation in cold hadronic matter," *Phys.Rev.* **C88** no. 2, (2013) 025208, arXiv:1305.0798 [nucl-th]. 62, 63, 64, 66

[103] S. Borsanyi, G. Endrodi, Z. Fodor, A. Jakovac, S. D. Katz, *et al.*, "The QCD equation of state with dynamical quarks," *JHEP* **1011** (2010) 077, arXiv:1007.2580 [hep-lat]. 62

[104] M. Cheng, S. Ejiri, P. Hegde, F. Karsch, O. Kaczmarek, *et al.*, "Equation of State for physical quark masses," *Phys.Rev.* **D81** (2010) 054504, arXiv:0911.2215 [hep-lat]. 62

[105] D. Fogaca, F. Navarra, and L. Ferreira Filho, "On the radial expansion of tubular structures in a quark gluon plasma," *Nucl.Phys.* **A887** (2012) 22–41, arXiv:1201.0943 [hep-ph]. 62, 63

[106] D. Fogaca, F. Navarra, and L. F. Filho, "Nonlinear waves in strongly interacting relativistic fluids," arXiv:1212.6932 [nucl-th]. 64

[107] D. Fogaca, F. Navarra, and L. Ferreira Filho, "KdV solitons in a cold quark gluon plasma," *Phys.Rev.* **D84** (2011) 054011, arXiv:1106.5959 [hep-ph]. 63

[108] N. Antar, "The korteweg-de vries-burgers hierarchy in fluid-filled elastic tubes," *International Journal of Engineering Science* **40** no. 11, (2002) 1179 – 1198. http://www.sciencedirect.com/science/article/pii/S0020722502000113. 64

[109] R. Saeed and A. Shah, "Nonlinear korteweg-de vries-burger equation for ion acoustic shock waves in a weakly relativistic electron-positron-ion plasma with thermal ions," *Physics of Plasmas (1994-present)* **17** no. 3, (2010) –. http://scitation.aip.org/content/aip/journal/pop/17/3/10.1063/1.3328805. 64

[110] M. Luzum and P. Romatschke, "Conformal Relativistic Viscous Hydrodynamics: Applications to RHIC results at $\sqrt{s_{NN}} = 200$ GeV," *Phys.Rev.* **C78** (2008) 034915, arXiv:0804.4015 [nucl-th]. 70

[111] Y. Hatta, J. Noronha, and B.-W. Xiao, "Exact analytical solutions of second-order conformal hydrodynamics," *Phys.Rev.* **D89** no. 5, (2014) 051702, arXiv:1401.6248 [hep-th]. 72

[112] Y. Hatta, J. Noronha, and B.-W. Xiao, "A systematic study of exact solutions in second-order conformal hydrodynamics," *Phys.Rev.* **D89** no. 11, (2014) 114011, arXiv:1403.7693 [hep-th]. 72

[113] Y. Minami and Y. Hidaka, "General conditions ensuring relativistic causality in an effective field theory based on the derivative expansion," arXiv:1401.0006 [hep-ph]. 77

[114] S. Chapman and T. G. Cowling, *The Mathematical Theory of Non-Uniform Gases*. Cambridge University Press, 1970. 78, 103

[115] G. Denicol, J. Noronha, H. Niemi, and D. Rischke, "Determination of the Shear Viscosity Relaxation Time at Weak and Strong Coupling," *J.Phys.* **G38** (2011) 124177, arXiv:1108.6230 [nucl-th]. 80

[116] M. P. Heller, R. A. Janik, and P. Witaszczyk, "Hydrodynamic Gradient Expansion in Gauge Theory Plasmas," *Phys.Rev.Lett.* **110** no. 21, (2013) 211602, arXiv:1302.0697 [hep-th]. 80

[117] A. El, Z. Xu, and C. Greiner, "Third-order relativistic dissipative hydrodynamics," *Phys.Rev.* **C81** (2010) 041901, arXiv:0907.4500 [hep-ph]. 80

[118] A. Jaiswal, "Relativistic third-order dissipative fluid dynamics from kinetic theory," *Phys.Rev.* **C88** (2013) 021903, arXiv:1305.3480 [nucl-th]. 80

[119] T. Schaefer, "Viscosity spectral function of a scale invariant nonrelativistic fluid from holography," *Phys.Rev.* **D90** no. 10, (2014) 106008, arXiv:1408.4503 [hep-th]. 87, 119

[120] J. Noronha and G. S. Denicol, "Transient Fluid Dynamics of the Quark-Gluon Plasma According to AdS/CFT," arXiv:1104.2415 [hep-th]. 97

[121] R. A. Janik and R. B. Peschanski, "Asymptotic perfect fluid dynamics as a consequence of Ads/CFT," *Phys.Rev.* **D73** (2006) 045013, arXiv:hep-th/0512162 [hep-th]. 102

[122] R. A. Janik and R. B. Peschanski, "Gauge/gravity duality and thermalization of a boost-invariant perfect fluid," *Phys.Rev.* **D74** (2006) 046007, arXiv:hep-th/0606149 [hep-th].

[123] S. Nakamura and S.-J. Sin, "A Holographic dual of hydrodynamics," *JHEP* **0609** (2006) 020, arXiv:hep-th/0607123 [hep-th].

[124] S. Bhattacharyya, S. Lahiri, R. Loganayagam, and S. Minwalla, "Large rotating AdS black holes from fluid mechanics," *JHEP* **0809** (2008) 054, arXiv:0708.1770 [hep-th].

[125] R. A. Janik, "Viscous plasma evolution from gravity using AdS/CFT," *Phys.Rev.Lett.* **98** (2007) 022302, arXiv:hep-th/0610144 [hep-th]. 102

[126] J. McGreevy, "Holographic duality with a view toward many-body physics," *Adv.High Energy Phys.* **2010** (2010) 723105, arXiv:0909.0518 [hep-th]. 103, 109, 128

[127] A. Zee, *Einstein Gravity in a Nutshell*. Princeton University Press, 2013. 103, 109, 110, 137

[128] S. de Haro, S. N. Solodukhin, and K. Skenderis, "Holographic reconstruction of space-time and renormalization in the AdS / CFT correspondence," *Commun.Math.Phys.* **217** (2001) 595–622, arXiv:hep-th/0002230 [hep-th]. 107, 108

[129] V. Balasubramanian and P. Kraus, "A Stress tensor for Anti-de Sitter gravity," *Commun.Math.Phys.* **208** (1999) 413–428, arXiv:hep-th/9902121 [hep-th]. 107

[130] E. Kiritsis, *String Theory in a Nutshell*. Princeton University Press, 2007. 109, 128

[131] R. A. Janik, "AdS/CFT for the early stages of heavy ion collisions," *Nucl.Phys.* **A931** (2014) 176–184, arXiv:1409.7571 [hep-ph]. 119

[132] R. Loganayagam, "Entropy Current in Conformal Hydrodynamics," *JHEP* **0805** (2008) 087, arXiv:0801.3701 [hep-th]. 132, 133

[133] H. Weyl, "Reine infinitesimalgeometrie," *Mathematische Zeitschrift* **2** no. 3-4, (1918) 384–411. http://dx.doi.org/10.1007/BF01199420. 135

[134] M. Spradlin, A. Strominger, and A. Volovich, "Les Houches lectures on de Sitter space," arXiv:hep-th/0110007 [hep-th]. 137